EPRI

Prediction of the Environmental Mobility of Arsenic

Evaluation of a Mechanistic Approach to Modeling Water-Rock Partitioning

Technical Report

Prediction of the Environmental Mobility of Arsenic

Evaluation of a Mechanistic Approach to Modeling Water-Rock Partitioning

1000547

Final Report, September 2000

EPRI Project Manager
M.E. McLearn

DISCLAIMER OF WARRANTIES AND LIMITATION OF LIABILITIES

THIS DOCUMENT WAS PREPARED BY THE ORGANIZATION(S) NAMED BELOW AS AN ACCOUNT OF WORK SPONSORED OR COSPONSORED BY THE ELECTRIC POWER RESEARCH INSTITUTE, INC. (EPRI). NEITHER EPRI, ANY MEMBER OF EPRI, ANY COSPONSOR, THE ORGANIZATION(S) BELOW, NOR ANY PERSON ACTING ON BEHALF OF ANY OF THEM:

(A) MAKES ANY WARRANTY OR REPRESENTATION WHATSOEVER, EXPRESS OR IMPLIED, (I) WITH RESPECT TO THE USE OF ANY INFORMATION, APPARATUS, METHOD, PROCESS, OR SIMILAR ITEM DISCLOSED IN THIS DOCUMENT, INCLUDING MERCHANTABILITY AND FITNESS FOR A PARTICULAR PURPOSE, OR (II) THAT SUCH USE DOES NOT INFRINGE ON OR INTERFERE WITH PRIVATELY OWNED RIGHTS, INCLUDING ANY PARTY'S INTELLECTUAL PROPERTY, OR (III) THAT THIS DOCUMENT IS SUITABLE TO ANY PARTICULAR USER'S CIRCUMSTANCE; OR

(B) ASSUMES RESPONSIBILITY FOR ANY DAMAGES OR OTHER LIABILITY WHATSOEVER (INCLUDING ANY CONSEQUENTIAL DAMAGES, EVEN IF EPRI OR ANY EPRI REPRESENTATIVE HAS BEEN ADVISED OF THE POSSIBILITY OF SUCH DAMAGES) RESULTING FROM YOUR SELECTION OR USE OF THIS DOCUMENT OR ANY INFORMATION, APPARATUS, METHOD, PROCESS, OR SIMILAR ITEM DISCLOSED IN THIS DOCUMENT.

ORGANIZATION(S) THAT PREPARED THIS DOCUMENT

Miller Water Associates

ORDERING INFORMATION

Requests for copies of this report should be directed to the EPRI Distribution Center, 207 Coggins Drive, P.O. Box 23205, Pleasant Hill, CA 94523, (800) 313-3774.

Electric Power Research Institute and EPRI are registered service marks of the Electric Power Research Institute, Inc. EPRI. ELECTRIFY THE WORLD is a service mark of the Electric Power Research Institute, Inc.

CITATIONS

This report was prepared by

Miller Water Associates
1711-G El Camino Real
Socorro, New Mexico 87801

Principal Investigator
G.P. Miller

This report describes research sponsored by EPRI.

The report is a corporate document that should be cited in the literature in the following manner:

Prediction of the Environmental Mobility of Arsenic: Evaluation of a Mechanistic Approach to Modeling Water-Rock Partitioning, EPRI, Palo Alto, CA: 2000. 1000547.

REPORT SUMMARY

Arsenic chemistry is important to the drinking water, waste management, and energy industries because of its potential health effects from low levels of exposure, breadth of occurrence, and expense of current treatment and disposal technologies. Since predicting arsenic behavior and mobility in the environment is currently not well developed, this project was undertaken to increase knowledge by testing and evaluating a mechanistic model for arsenic water-mineral partitioning.

Background
Environmental managers need cost-effective methods to restore contaminated sites to productive use while meeting regulatory and programmatic requirements. Computerized models are often used to evaluate the effect of a selected action because they indicate probable outcomes before pilot studies or field demonstrations. Currently, there are two modes used to constrain environmental models, empirical and mechanistic. Though empirical determinations can be highly accurate, they are limited because they are only truly applicable to the specific media or site evaluated. In theory, mechanistic approaches do not suffer from this limitation because they are based on fundamental chemical and physical principles that are controlled by measurable parameters such as temperature or contaminant concentration. However, fundamental relationships that govern a mechanistic surface complexation approach may be poorly understood. A mechanistic modeling effort—which is an important part of a complete solution— is impossible without detailed understanding of these relationships. For arsenic, the relationships have been developed to the point where mechanistic modeling is a practical part of the solution.

Objectives
To test arsenic field separation and preservation techniques by quantifying arsenic species in select natural and contaminated waters, and to evaluate mechanistic modeling approaches for sources of error while determining arsenic partitioning in the environment.

Approach
The study began by selecting field sites in Rio Salado, Mexico, and northwestern Florida, where arsenic-bearing sediments and waters could be easily collected for analysis. To determine if bulk sample wet extraction methods would support arsenic surface complexation modeling, the project team selected several extraction techniques that are in common use. They chose public domain geochemical models to increase the generality and reproducibility of the study. Within these geochemical models, there are a number of surface complexation models available that differ in their mechanistic assumptions. The team selected the generalized two-layer model because of its broad citation in the literature and because availability of supporting data for the model was greater than for any other mathematical formulation for surface complexation.

Following data collection and validation, they evaluated the mechanistic surface complexation approach and determined sources and magnitude of error. Since the scientific consensus is that the arsenic species generally present in water include two inorganic and several organic species, the project team used a speciation-based approach when evaluating environmental impacts.

Results

The evaluation at Rio Salado, Mexico, offered a natural analog for testing the mechanistic approach to modeling inorganic arsenic attenuation. The project's capability to model the total concentration of arsenic present on Rio Salado sediments to within $\pm$ 50% was very successful. The approach was then applied to water-mineral partitioning of arsenic in soils and sediments from Florida that were arsenic-impacted due to releases from nearby contaminated sites. The model fit in Florida was not quite as good as in Rio Salado. It is highly probable that the model fit for Florida and other sites can be substantially improved with additional development of the current mechanistic approach.

EPRI Perspective

Geochemical modeling is generally recognized to be a developing science. The ability of the mechanistic model to describe the partitioning of arsenic in these different hydrogeologic settings is a major step in applying the approach to environmental assessment and restoration. Continued development of this modeling approach could result in a practical tool that can be used by managers, scientists, and engineers to guide data collection efforts in support of arsenic modeling and management; develop mechanistic modeling approaches to risk assessment and feasibility studies; provide the modeling parameters necessary to implement a mechanistic approach to arsenic mobility modeling; establish a framework for evaluating the validity of conceptual models; provide an error evaluation for use in risk assessment; and, propose and defend a mechanistic modeling approach for arsenic in a stakeholder setting.

Keywords

Arsenic
Contaminated soil
Groundwater
Fate and transport

ABSTRACT

Arsenic chemistry is important to environmental managers because of its potential health effects from low levels of exposure, breadth of occurrence, and cost of treating and removing. This project was undertaken to increase knowledge by testing and evaluating a mechanistic model for arsenic water-mineral partitioning. The project team tested arsenic field separation and preservation techniques by quantifying arsenic species in select natural and contaminated waters. They also evaluated mechanistic modeling approaches for sources of error while determining arsenic partitioning in the environment. The scientific consensus is that the arsenic species generally present in water include two inorganic and several organic species; therefore, the project team used a speciation-based approach when evaluating environmental impacts. The evaluation at the test site in Rio Salado, Mexico, offered a natural analog for testing the mechanistic approach to modeling inorganic arsenic attenuation. The project's capability to model the total concentration of arsenic present on Rio Salado sediments to within $\pm$ 50% was very successful. The approach was then applied to water-mineral partitioning of arsenic in soils and sediments from northwestern Florida that were arsenic-impacted due to releases from nearby contaminated sites. The model fit in Florida was not quite as good as in Rio Salado. It is highly probable that the model fit for Florida and other sites can be substantially improved with additional development of the current mechanistic approach. Continued development of this modeling approach could result in a practical tool that can be used by managers, scientists, and engineers to guide data collection efforts in support of arsenic modeling and management and to propose and defend a mechanistic modeling approach for arsenic in a stakeholder setting.

ACKNOWLEDGMENTS

EXECUTIVE SUMMARY

Many arsenic-contaminated sites exist. More conservative environmental standards for arsenic have been proposed. Arsenic chemistry in natural systems is complex. The prediction of arsenic behavior and mobility in the environment is currently not well developed. Factors indicate that research on arsenic geochemical behavior is needed.

Environmental managers seek cost-effective methods to restore contaminated sites to productive use while meeting regulatory and programmatic requirements. Given the complexity of the decision-making process, computerized models are often used to evaluate the effect of a selected action. Models allow evaluation of the probable outcome of a selected action before pilot studies or field demonstrations. This lowers costs by culling alternatives that show potential for unsatisfactory results. In order to support and explain selection of a particular alternative to stakeholders, the modeling process used needs to be scientifically supportable.

The precision and accuracy of the models, and thereby stakeholder acceptance of the predictions made, are dependent on the ability to quantitatively describe the underlying chemical and physical relationships that govern the behavior of the contaminants of interest. The standard used by stakeholders to determine the merit of model-supported findings moves in step with the development of better approaches. The overall success an environmental action is sensitive to stakeholder perception of how well the system of interest is understood. Consideration of these factors indicates that environmental managers need increasingly accurate and defensible modeling approaches to attain their goals.

There are two modes used to constrain environmental models, empirical and mechanistic. Empirical relationships do not use fundamental chemical and physical principals to evaluate contaminant behavior; they are based on cause and effect observations developed in the laboratory or at field sites. Empirical determinations can be highly accurate and have a successful history of application. However, empiricism is limited because the relationships are only truly applicable to the specific media or site evaluated. Empirical model error increases as the physical properties of the system under evaluation diverge from the system where the empirical relationships were developed. The potential error in an empirical modeling approach cannot be evaluated before application and validation of the model. In theory, mechanistic approaches do not suffer from these limitations because they are based on fundamental chemical and physical principles that are controlled by measurable parameters such as temperature, or contaminant concentration. This means that the potential for accuracy and precision is always higher for mechanistic approaches than empirical. Stakeholder concerns regarding model-based decision making are addressed at a higher level using mechanistic approaches than by empiricism. The fundamental relationships that govern a mechanistic surface complexation approach may be poorly understood. A mechanistic modeling effort is impossible without

detailed understanding of these relationships. For arsenic, the relationships have been developed to the point where mechanistic modeling is practical.

The research described here had two areas of interest. The first was concerned with the occurrence and quantification of arsenic species in select natural and contaminated waters. Testing of arsenic field separation and preservation techniques was a necessary component of this focus area. The second focus area was evaluating modeling approaches to determining arsenic partitioning in the environment. The objective was to test mechanistic modeling protocols while assessing sources of error. Reporting the results of testing and evaluation of a mechanistic model for arsenic water-mineral partitioning is the primary subject of this report. Sampling, analysis, and field speciation method development information is contained in the appendices.

A few empirical relationships to predict arsenic mobility in natural systems have been developed and published. These empirical relationships could be used for predictive field work at some unknown error level. However, published information on their implementation is scant. Similarly, the mechanistic approach to evaluating arsenic mobility has been shown to be plausible in a laboratory setting, but details on implementation or the expected error level in application were unknown prior to this effort. This arsenic study is the first published bridge between laboratory based proof-of-principle efforts and practical field implementation that provides a determination of error level and sensitivity to chemical and physical controls. The results of this study can be used by managers, scientists, and engineers to:

- guide data collection efforts in support of arsenic modeling and management;

- develop mechanistic modeling approaches to risk assessment and feasibility studies;

- provide the modeling parameters necessary to implement a mechanistic approach to arsenic mobility modeling;

- establish a framework for evaluation of the validity of conceptual models;

- provide an error evaluation for use in risk assessment; and,

- propose and defend a mechanistic modeling approach for arsenic in a stakeholder setting.

Arsenic currently commands interest in the drinking water, waste management, and energy industries because of its potential health effects from low levels of exposure, breadth of occurrence, and the expense of current treatment and disposal technologies. The consensus is that the arsenic species generally present in water include two inorganic and several organic species. Since the toxicity of these arsenic species spans three orders of magnitude, it is inappropriate to consider only total arsenic concentration when evaluating environmental impacts. A speciation-based approach to arsenic is critical to risk assessment.

The presence of organic arsenic as a small (<10%), but measurable component of high-arsenic natural and contaminated waters was confirmed. A four-species field separation approach was tested in Mexico and found to work well for As^{3+}, As^{5+}, and monomethylarsonic acid (MMAA) but had significant problems in quantifying dimethylarsinic acid (DMAA). The problems with DMAA were resolved and the method tested in Florida along with a two-species method for As^{3+}

and As^{5+}. From the literature, organic arsenic is present in low arsenic (<100 ppb) systems at 5-60% of the total arsenic available. It appears that the presence of organic arsenic can be assumed in high arsenic surface water and shallow groundwater systems as well. Field separation of up to four arsenic species by ion exchange is practical and reproducible.

Water-mineral interaction controls the mobility of inorganic compounds in natural waters. The net result is that water-mineral interaction influences decision making for all arsenic related remedial or waste management alternatives. The mobility of arsenic in the environment is very complex and controlled by a large number of competitive biogeochemical processes. The dominant factor affecting the mobility of arsenic in natural systems is speciation-controlled complexation (partitioning) with the surface of hydrous metal oxides. Development and use of computerized approaches to problem solving (numerical modeling) has been critical to our current understanding of the environmental chemistry of arsenic. Numerical modeling can be the most practical way to simultaneously evaluate the multitude of independent, dependent, and competitive biogeochemical processes that affect the transport and toxicity of arsenic, and the only way to make mechanistic predictions regarding arsenic persistence and mobility in the environment.

Many of the past and current determinations and modeling of the water-mineral partitioning of arsenic have been accomplished through use of empirical soil-water partition coefficients (Kd's). Kd's are generally not transferable from site to site or system to system. Regulatory and academic groups have recognized that a mechanistic modeling approach that specifically addresses sorption mechanisms offers a technical advantage over the Kd approach. However, there has been little testing of this outside of the laboratory.

The study began with selection of field sites where arsenic-bearing sediments and waters could be easily collected for analysis. Sites with natural and anthropogenic arsenic occurrence were chosen. A phased sampling and analysis approach was used. We felt that it would be useful to determine if bulk sample wet extraction methods would support arsenic surface complexation modeling. Currently, these are the only techniques that are practical and cost effective for determination of the surface composition of bulk mineral, rock, or soil samples. Accordingly, several extraction techniques that are in common use by practitioners were selected and implemented. Public domain geochemical models were chosen for use to increase the generality and reproducibility of the study. There are a number of surface complexation models available within these geochemical models that differ in their mechanistic assumptions. We selected the generalized two-layer model for use because of its broad citation in the literature and that the availability of supporting data for the model was greater than for any other mathematical formulation for surface complexation. Following data collection and validation, the mechanistic surface complexation approach was evaluated and sources and magnitude of error determined.

There have been several studies using a surface complexation model to explain and/or predict field relationships of arsenic partitioning. The work here is different from that previously published. Surface complexation constants are not fit to field data, instead laboratory derived constants for pure mineral phases are used. The quality of the fit of modeled to observed arsenic concentration on sediments is assessed for several conceptual models.

This study uses published laboratory-derived constants and a public domain geochemical model to simulate observed sediment arsenic concentrations with the objective of assessing error sources in modeling arsenic partitioning using a surface complexation approach. Chemical and physical data from baseflow sampling of sediment-water pairs from within a small watershed having naturally high levels of arsenic were used. Published two-layer model data for surface complexation of arsenite, arsenate, and a range of competing anions and cations with goethite, amorphous iron oxide, and gibbsite, were used to constrain the model. When necessary, published data were refit to the general two-layer model, estimated from linear free energy relationships, or directly substituted. Sorbing hydrous metal oxide surfaces were determined using operationally defined partial extractions and constrained for the model using stoichiometric relations, porosity, and bulk density. The sensitivity of arsenic partitioning to competition of other sorbing species and other parameters was determined.

The approach was successful at matching the observed arsenic concentration within reasonable error levels. Constraining surface-complexing iron phases as ferrihydrite (amorphous to quasi-crystalline hydrous iron oxide) in the simulations provided a better match to observation than defining the iron phases as goethite (fully crystalline iron oxide). Failure to account for competition for sorbing sites by ions other than arsenic results in gross over-prediction of the adsorbed arsenic concentrations in the watershed.

Geochemical modeling is generally recognized to be a developing science. The Rio Salado was found to offer a natural analog for testing of the mechanistic approach to modeling inorganic arsenic attenuation. The capability developed here to model the total concentration of arsenic present on Rio Salado sediments to within $\pm$ 50% is a great success. The approach was then applied to water-mineral partitioning of arsenic in soils and sediments from Florida that are arsenic-impacted due to releases from nearby contaminated sites. The model fit in Florida was not quite as good as Rio Salado but it is none the less quite useful. It is highly probable that the model fit for Florida and other sites can be substantially improved with limited development of the current mechanistic approach.

The ability of the mechanistic model to describe the partitioning of arsenic in these different hydrogeologic settings is a major step in application of the approach to environmental assessment and restoration. Continued development of the modeling approach presented here could result in a practical tool for the assessment of arsenic risk, remedial approach, and mitigation. Further model testing and development is warranted.

CONTENTS

LIST OF FIGURES

LIST OF TABLES

1
PROBLEM STATEMENT

Many industries have exposure to environmental arsenic issues. The degree of exposure, and the industry's ability to manage contaminated sites appropriately, depends in a large part on the following five issues.

- Environmental standards for arsenic will be substantially more conservative in the near future. This will begin with the scheduled enforcement by the United States Environmental Protection Agency (USEPA) of new lower arsenic standards for drinking water on January 1, 2001. Heightened restriction on arsenic-bearing-waste management standards will presumably follow.

- The prediction of arsenic behavior and mobility in the environment is currently not well defined in approach, precision, or accuracy. Arsenic chemistry in natural systems is complex. The element is present as many different compounds, all with individual environmental behavior and toxicity.

- There is negative public perception of arsenic at any exposure level. The recently recognized role of arsenic in third-world health problems has increased worldwide scrutiny of the occurrence of this element. Environmental arsenic currently commands interest by the public, regulatory agencies and groups in the drinking water, waste management, and energy industries. This is largely because of current concern about potential health effects from low levels of exposure and the expense of treatment and disposal technologies.

- The toxicity of environmentally significant arsenic species may span greater than three orders of magnitude. There is broad consensus that arsenic species generally present in water include two inorganic and several organic species. Consideration of only total arsenic in risk assessment is probably inaccurate. Current standards are based on total-arsenic risk assessments using conservative assumptions.

- Detection and quantification of arsenic is technically difficult. Total arsenic methods are mature, yet still have difficulty achieving low intra and inter-laboratory error levels. This difficulty increases at lower concentrations. Arsenic speciation and species quantification methods are not as mature as methods for total arsenic. This increases the error in species-based weighting of environmental risk. The relatively large, currently acceptable, error in quantification of arsenic fosters higher overall uncertainty than exists for many other environmentally significant compounds.

Society has a real need to be able to accurately predict the aqueous transport, speciation, and partitioning of metals because of their significance to environmental issues, human health, and mineral exploration. The mobility of metals in the environment is very complex and controlled by a large number of competitive biogeochemical processes. In the last 20 years, there has been remarkable progress in our understanding of controlling mechanisms for metal transport

[1, 2, 3, 4, 5, 6, 7]. Development of computerized approaches to problem solving has been critical to this progress. This is the only practical way to evaluate the independent, dependent, and competitive biogeochemical processes that affect the transport and toxicity of metals [6,7, 8, 9, 10, 11, 12, 13]. Much of the work in the past has been accomplished through use of empirical relationships that are generally not transferable from site to site or system to system. Mechanistic modeling of contaminant interactions with the environment has long been preferable to fully empirical methods, but the data necessary has generally been unavailable. The unique environmental properties of arsenic have generally prevented reliable past prediction of its behavior. This has fostered a need for better understanding of the environmental behavior of arsenic than currently exists.

The dominant factor affecting the mobility of most all arsenic species in most natural systems is speciation controlled complexation with the surface of hydrous metal oxides, closely followed by interaction with organic matter [5, 14]. The mechanistic approach to describing arsenic and other oxyanion interactions with hydrous metal oxides has had great success in the laboratory in simple, tightly constrained, experiments. There has been little laboratory testing of this methodology on natural soils, sediments, or aquifer materials, but a recent modeling study of boron oxyanions on soil showed good fits to the observed data [7]. This project has taken a logical step in development of the understanding of arsenic mobility in the environment, by incrementally testing mechanistic modeling approaches against field observation. In completion, this effort advances our capability for metal transport modeling in general, advances the science of surface complexation modeling, and provides a specific and needed evaluation of our current ability to model arsenic environmental behavior.

Mechanistic approaches to evaluating the environmental mobility of chemicals rely on descriptions of behavior at the molecular level [15, 16]. The processes include but are not limited to ion complexation (pairing), precipitation, sorption or surface complexation, oxidation-reduction reactions, gas exchange, ionic strength effects on molecular activity, temperature corrections to thermodynamic parameters, and buffering of reactions by solid phases. In theory, it is possible to mathematically combine and scale many individual processes, allowing their competitive interaction to fully describe the behavior of complex geochemical systems. The study of arsenic attenuation in a watershed should be amenable to this process. Studies of arsenic surface complexation in natural systems are warranted to evaluate the predictive capability of mechanistic models.

Background

The pending revisions in USEPA standards for arsenic will force large capital expenditures for affected industry [17]. The currently proposed drinking water standard of five ppb total arsenic is based on total arsenic concentration. Since MMAA and DMAA are at least 10 times less toxic than As^{3+} or As^{5+}, ingestion of methylated arsenic will reduce true risk as compared to the assumption that arsenic exists only as an inorganic species. Speciation- based assessment of arsenic-related health risk appears to be warranted.

The USEPA can use the arsenic drinking water limit in determining the appropriate standard for arsenic solid waste disposal. The cost increases in solid waste disposal may meet or exceed those for nation-wide drinking water treatment. The potential for solid waste release of arsenic will require revaluation in the near future.

It has been noted that the number of people worldwide that are suffering from arsenic related disease is far greater than previously estimated [18, 19, 20, 21, 22]. There are latent effects from long-term low-level exposures, raising concerns about the protective ability of our current 50 ppb arsenic in drinking water standard. The National Academy of Science has recently reported [23] that the 50 ppb drinking water level for arsenic can cause bladder cancer with lifetime exposure at the rate of 1 in 1000 individuals exposed. Although not a drinking water focus, irrigation can result in the geochemical concentration of arsenic in soils with resultant increases in the arsenic concentration of foodstuffs. Fertilization of soils containing arsenic has been noted to increase the arsenic related toxicity of foods. All of these factors are increasing the general level of public concern regarding the presence of this element, in any form, in all media. With respect to arsenic in the environment, there are many questions for which science does not have ready answers.

Health Hazard and Social Cost

Arsenic is a known class A carcinogen [24, 25, 26] that is toxic when ingested or inhaled. Over the past decade there has been accumulating evidence that arsenic at low levels in drinking water can seriously effect health [24, 25, 26]. Cancerous lesions are associated with waters containing 100's of ppb arsenic. Increased rates of skin cancer, heart disease, infant mortality and birth defects are related to arsenic levels less than 100 ppb. This has prompted the USEPA to reexamine limits of arsenic in drinking water supplies currently set at 50 ppb. It is expected the new USEPA limit, to be enforced January 2001, will be 5 ppb [27]. The World Health Organization recommends that arsenic concentrations be <10 ppb. The American Water Works Association estimates that the US cost of compliance to a 10 ppb arsenic limit will be $6.3 billion dollars the first year of implementation. Environmental arsenic occurs mainly in four forms, the most toxic As^{+3}, less toxic As^{+5}, and the relatively benign organic forms, DMAA and MMAA. USEPA may approach the wide range in arsenic species toxicity as with mercury, whereby the more toxic species are the most closely regulated. The United States has a problem with arsenic in surface water and groundwater. It affects most major cities in New Mexico, including Albuquerque, Los Alamos, and Socorro that have concentrations in some water sources just lower than the United States Environmental Protection Agency limit of 50 µg/L. It is a problem common in the western US [28, 29, 30], where volcanic rocks are common. Mexico, Central America, Asia, and parts of Europe also have problems with high arsenic ground and surface waters. In Bangladesh, there is an environmental catastrophe with an estimated 500,000 dying of arsenic related cancer, and about 1,200,000 persons showing effects of arsenic poisoning [18, 19, 20, 31].

Current Knowledge of Arsenic Geochemistry

The health effects and behavior of arsenic in biologic systems is currently the subject of a large number of research efforts. The objective is to improve the quality of the data used for risk assessment. Data on the physiochemical behavior of arsenic are equally as essential to support risk determinations, loss prevention strategies and mitigation, and environmental restoration. Excellent reviews on arsenic geochemistry are available in the literature. Some specific aspects with strong bearing on the study are outlined here.

Several wells in Albuquerque have been closed because of poorly understood increases in arsenic concentration [28, 29, 30]. The City of Los Angeles is using the results of arsenic geochemistry studies to evaluate its options regarding the siting of water treatment plants, required capacity, and capital cost [32, 28]. Understanding of arsenic geochemistry is critical to the efforts to supply millions of people in Bangladesh with water that is safe to drink. [20]. Radically different geochemical mechanisms for the Bangladesh arsenic exposure have been published, but have not been tested or a quantitative model proposed [18, 198]. The areas of the world most impacted by arsenic in drinking water have, at best, qualitative understanding of the geochemical processes that are governing arsenic occurrence and distribution. Evaluation of arsenic species has been found to be of use in risk assessment [33]. The kinetics of arsenic transformation are also important in evaluating closure of mine tailings sites [10] and municipal water treatment [28].

Arsenic is found in all environments with normal concentrations ranging from 1 to 9 ppm in rocks and soils [34]. In the western United States the concentration of arsenic in soils and rocks is much higher, for example, vast areas of Nevada have been found to contain rocks that have total arsenic concentrations >200 ppm [35]. Arsenic is a minor element whose geochemistry is poorly understood. It may occur at significant concentrations in surface and groundwaters, which poses a major health hazard. Arsenic is present in water and sediments as the inorganic species As^{3+}, As^{5+}, and the organic compounds MMAA and DMAA [36]. These different forms of arsenic each have individual toxicities and environmental pathways. The dominant compounds found in fresh surface and groundwater each have several pH dependant ionic forms.

Because of the large number of interactions and transformations that arsenic will undergo, the environmental pathways are complex [37,38]. Some environmental partitioning data is available; little was located that provides kinetic data that are suitable for use in quantitative analysis of natural systems. There have been problems in the past being able to differentiate between the various arsenic species during analysis, thus confounding the interpretation of the toxicity of arsenic containing waters [37, 39, 40, 41, 42]. There are known kinetic limitations to the inorganic reactions that are not well quantified [10, 43, 44]. Diurnal variation of total arsenic concentrations is reported in contaminated streams [10]. Aqueous species such as sulfate and organic ligands compete for sorption sites [45]. Predicting arsenic geochemical behavior requires knowledge of the rate and degree of achievement of chemical equilibrium. In water-mineral systems, some forms of arsenic may never reach equilibrium. This is a common situation for many elements and compounds.

The majority of the current research on arsenic chemistry is focused on the upcoming USEPA rulemaking process and the occurrence and treatment of inorganic arsenic, particularly As^{5+}. This is appropriate since inorganic arsenic is the dominant fraction found in drinking water. However, there is increasing data indicating the general presence of methylated arsenic compounds in the environment [22, 33, 36, 46, 47, 48, 49, 50, 51, 52, 53, 54, 55, 56, 57, 58, 59, 60]. Methyl arsenic is a major component in the biological arsenic cycle [61, 62]. Depending on the speciation and analytical method used, past work on arsenic in water may reflect methyl arsenic concentrations as part of the analytic determination of As^{3+} and/or As^{5+} concentrations [63]. Treatment technologies for organic arsenic are not well documented. Accurate assessment of human health risk from some metals (e.g. mercury and chromium) has required a speciation-based approach, as will arsenic.

The inorganic arsenic compounds are often in disequilibrium with their environment with respect to redox conditions and precipitation of solid phases, and can be present as particulate and colloidal matter [37, 38, 61]. Current understanding of arsenic geochemistry is not able to accurately predict inorganic or organic arsenic redox condition based on other data [27]. The species As^{3+} and As^{5+} form what is known as a redox couple, oxidation of As^{3+} produces As^{5+} and reduction of As^{5+} produces As^{3+}. The literature indicates that inorganic arsenic redox species in natural waters are generally not in thermodynamic equilibrium. It is possible that this is the most common condition preventing prediction of arsenic speciation using thermodynamics. For most inorganic compounds in natural waters, speciation, sorption, and supersaturation (precipitation) conditions can be successfully predicted using thermodynamic approaches. If the disequilibrium of arsenic is to be investigated in detail, it is necessary to ascertain the general equilibrium state and chemical dynamics of the majority of the inorganic chemistry. In general, reactions between redox couples are rapid as compared to other dynamics, such as groundwater flow rates and lacustrine sedimentation [5]. However, the arsenic inorganic redox couple can transform slowly [101, 117].

Data is needed on the occurrence, concentration, and proportion of organic arsenic present in the environment [31, 46]. These compounds are produced by biologic transformation. There is very little data on their behavior in the non-marine environment, although they have been found to form over half of the total arsenic present in surface water and groundwater [46, 51]. In general, we find that the occurrence of arsenic organic species in fresh water systems has been ignored, or intentionally overlooked, and in general thought to be inconsequential [39, 64]. In contrast, organic arsenic species are accepted as common in the marine environment [36, 46, 51, 56].

The occurrence and concentration of organic arsenic in the environment may be generally underestimated. Researchers have noted that methylated forms of arsenic can be significant, 0-60% of total arsenic in surface water and groundwater, at low total arsenic concentrations (<50 ppb), and are occasionally the dominant arsenic species present. For sites that have arsenic present because of application of some herbicides or disposal practices, organic arsenic compounds may be present, because of either direct introduction or biologic methylation of inorganic species. It is known that bacteria, fungi, plants, and animals all methylate arsenic efficiently in aerobic or occasionally anaerobic conditions. Although the physical and chemical conditions that favor biotic formation of organic arsenic have been explored in the laboratory, field scale data for terrestrial systems is sparse. It is known that abiotic methylation of arsenic is improbable; methylation of arsenic is dependent on living organisms. Bacteria and fungi are known to exist in the subsurface to substantial depths. Methylation of arsenic is not only possible, but also probable, in the many groundwater and surface water environs. Evaluation of methylated arsenic in water is warranted and necessary for effective evaluation of arsenic health risk .

Predictions of total arsenic behavior can be made in simple systems [10, 49] but there have been few attempts to quantitatively predict arsenic speciation or behavior when there are a large number of geochemical variables. The behavior of arsenic in natural waters is not very predictable with our present state of knowledge [65]. Remedial alternative evaluation also requires better understanding of broad arsenic geochemistry, especially aspects related to controls on speciation, sorption, and redox equilibria.

2
APPROACH

Overview

This project was accomplished in phases. We used the observational approach to guide data collection and analysis. The effort started with evaluation of the arsenic speciation and distribution in a watershed with naturally high levels of arsenic due to geothermal influences (Rio Salado, Mexico). The reconnaissance sampling of Rio Salado used field separation methods for arsenic species. The paired water and sediment samples were analyzed for a broad range of physical and chemical parameters. Examination of the data indicated that Rio Salado was near chemical equilibrium when sampled. The data appeared promising for analysis of arsenic partitioning by numerical modeling if a few data gaps were closed. We quantified B, Ba, Br, Sr, Al, and PO_4^{2-} that were not included in the first round of analyses. Outside validation of detected DMAA levels was conducted. These two actions closed the data gaps; data development and modeling of the Rio Salado data ensued.

It was found that arsenic water-mineral partitioning in the Rio Salado could be described by a mechanistic model using practical field and analytical techniques. The data and analysis were presented at recognized symposia. It was determined that testing at other locations would provide needed validation and the opportunity to make additional observations. Two arsenic-contaminated sites in Florida were selected for sampling. The Florida sampling was conducted for the primary reason of providing suitable material for testing of the modeling approach developed with the Rio Salado data. The data generated from chemical analysis of the Florida samples were used in the same numerical simulation employed for Rio Salado. Again, the field data were well represented by the model predictions.

Objectives

The objectives of this effort were to develop a method for prediction and measurement of arsenic speciation and occurrence that is useful for arsenic risk assessment, environmental mitigation, and property management. Specific objectives were to:

- Improve the quantitative understanding of the controls on arsenic movement and availability;

- Conduct reconnaissance sampling for arsenic speciation to validate the field application of a method for separation of arsenic species;

- Observe the reaction kinetics of arsenic species transformation; and,

- Evaluate a molecular-level modeling approach to predicting the partitioning of arsenic between natural water and rock-sediment-soil phases.

The current knowledge of environmental behavior of metals suggests that it is possible to predict arsenic mobility and partitioning over a wide range of environmental conditions based on water-mineral-biological interaction [6, 14, 66, 67, 68, 69]. The surface complexation mechanism is often cited as being responsible for observed arsenic distributions [7, 14, 40, 65, 70, 71] although there has been little field-scale testing of this assumption [7, 71, 72, 73, 74, 75]. There is considerable discussion in the literature on the ubiquitous nature of organic arsenic and its relative abundance in natural systems. Most arsenic studies have been limited to total arsenic, or just the inorganic compounds when speciation studies were conducted.

Field-based study increases the difficulty of investigation and interpretation of results over well-constrained laboratory efforts. However, it does provide a practical test of predictive capability that is not possible in the laboratory, and at an appropriate scale for environmental studies. By careful field site selection and sampling, it is possible to obtain a snapshot of arsenic geochemistry under a range of environmental conditions. By sampling along a chemically and physically intimate flowpath that undergoes chemical evolution, the effect of a large number of variables on arsenic distribution can be evaluated. This data on arsenic distribution and general geochemistry is then used for evaluation of the controlling factors on arsenic partitioning and speciation.

Site Selection - Sampling Design and Execution

Field data on arsenic partitioning and general aqueous and solid phase geochemistry were needed to provide a data set for testing. The field site could be a groundwater or surface water system. Surface water was preferred because groundwater investigations are generally much more costly and have greater uncertainty in sample collection and preservation. A high arsenic concentration in water was desired to simplify sampling and analytical constraints and reduce analytical error. A system with reasonably average chemistry is preferable since much of the past focus on mechanistic modeling of arsenic transport has been in systems contaminated by mine tailings and dominated by acid rock drainage chemistry [10]. Most electric utility arsenic issues will probably not take place in that realm of geochemical interaction. The results from mining sites are probably not easily transferable to other systems. It is desirable that this effort be comparable to a practical but broad range of conditions. A naturally high-arsenic site was desired to provide an analog for use in assessment of arsenic partitioning in waters of average quality.

Rio Salado, Mexico

The upper Rio Salado, Guadalajara, Mexico was selected for consideration after examination of the available data [77, 78, 79, 80]. A site visit in June 1997 revealed a suitable chemical and physical setting. Rio Salado sampling was conducted in January of 1998. The details of the Rio Salado field investigation are contained in Appendix A.

The system had been at base flow for over a month with the primary source of discharge being high-arsenic springs. There was downstream variation in water chemistry that enabled the modeling effort to test sensitivity to pH, temperature, alkalinity, and arsenic concentration. The sediment is dominantly coarse-grained volcanic glass (>95%), essentially hydrous metal oxide-coated glass, a good analog for laboratory systems. The spring discharges provided a

reasonably constant arsenic flux during the sampling event. Arsenic speciation was dominated by As^{5+}. Most of the stream channel was free of algae mats, allowing good potential for rapid sediment-water interaction. Rio Salado waters are of the common sodium bicarbonate type. A geothermal chemical signature is seen in higher than usual temperatures and concentrations of silica, fluorine, and boron. Overall, Rio Salado is an excellent system for evaluating arsenic distribution because it is relatively simple, has had little man-made interference in natural processes, and is easily accessible. Rio Salado is a good example of a system where arsenic attenuation is dominated by inorganic processes.

Florida Sites

Following the success of modeling the Rio Salado data, it was determined that validation of the model at other sites would be quite useful. Two arsenic-contaminated sites in Florida were selected for sampling: Fort Walton and Tyndall Air Force Base. These sites were selected because arsenic applied nearby as a herbicide had migrated to shallow groundwater. In Florida, much of the shallow groundwater system discharges to surface water features. This provides a sampling opportunity similar to that exploited at the Rio Salado surface water setting, that is, sediment-water pairs could be collected synoptically with a minimum of intrusive activity. This was the setting at the Tyndall and Fort Walton substations where arsenic-contaminated groundwater plumes discharged to open drainage swales. Substation associated arsenic was found to be dominantly in the As^{3+} and As^{5+} forms in roughly equal proportions, with approximately 10% of the total arsenic present as the organic arsenic species MMAA and DMAA. The details of the Florida field investigation are contained in Appendix B.

Flowchart of Data Analysis and Modeling Execution

The objective of the flowcharts is to present a graphical overview of the study. Details regarding activities or findings are contained in the report main body and the appendices. The project execution was observational and iterative. Description of the path and progress of the effort is presented using the flowcharts in Figures 2-1, 2-2, and 2-3. A different flowchart is used for each major phase of the study: data collection and empirical analysis; data development and mechanistic modeling; and, analysis of the modeling results. In the diagrams, the items to the left are generally indicative of actions or data sources. Items to right are more representative of decision points or findings.
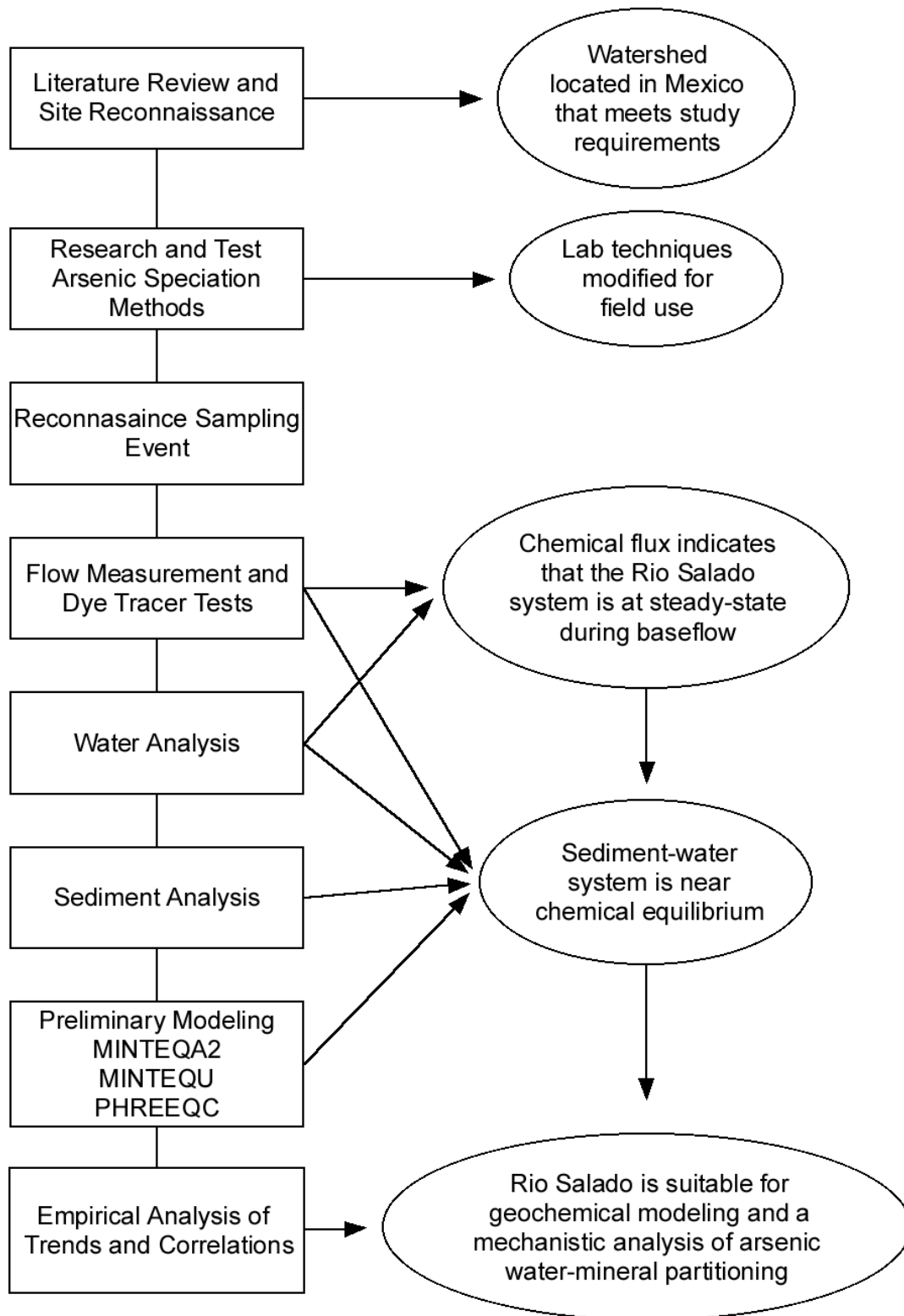
Figure 2-1
Flowchart of Initial Sampling and Analysis Activities that led to Modeling
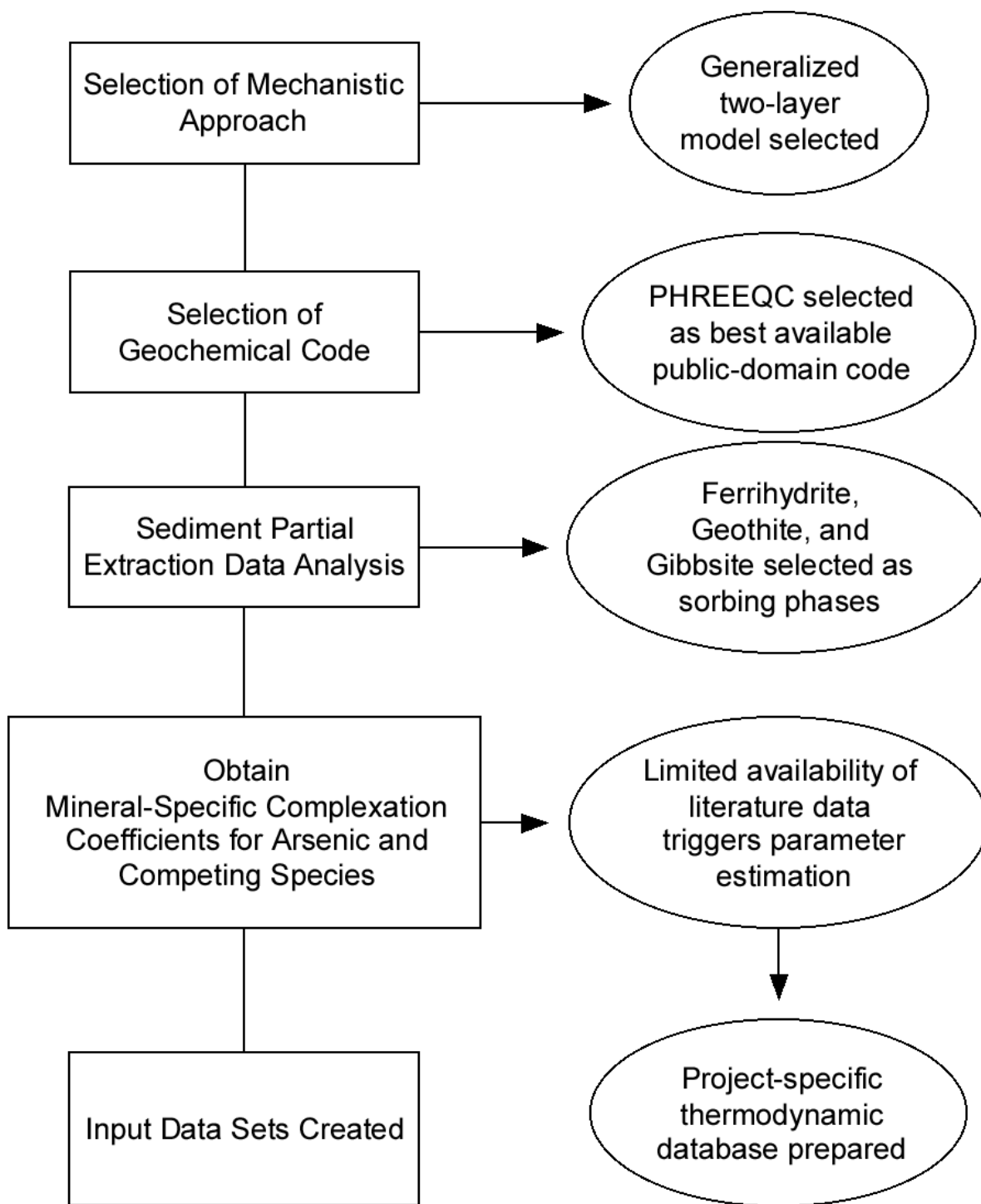
Figure 2-2
Flowchart of Data Development and Model Construction Activities
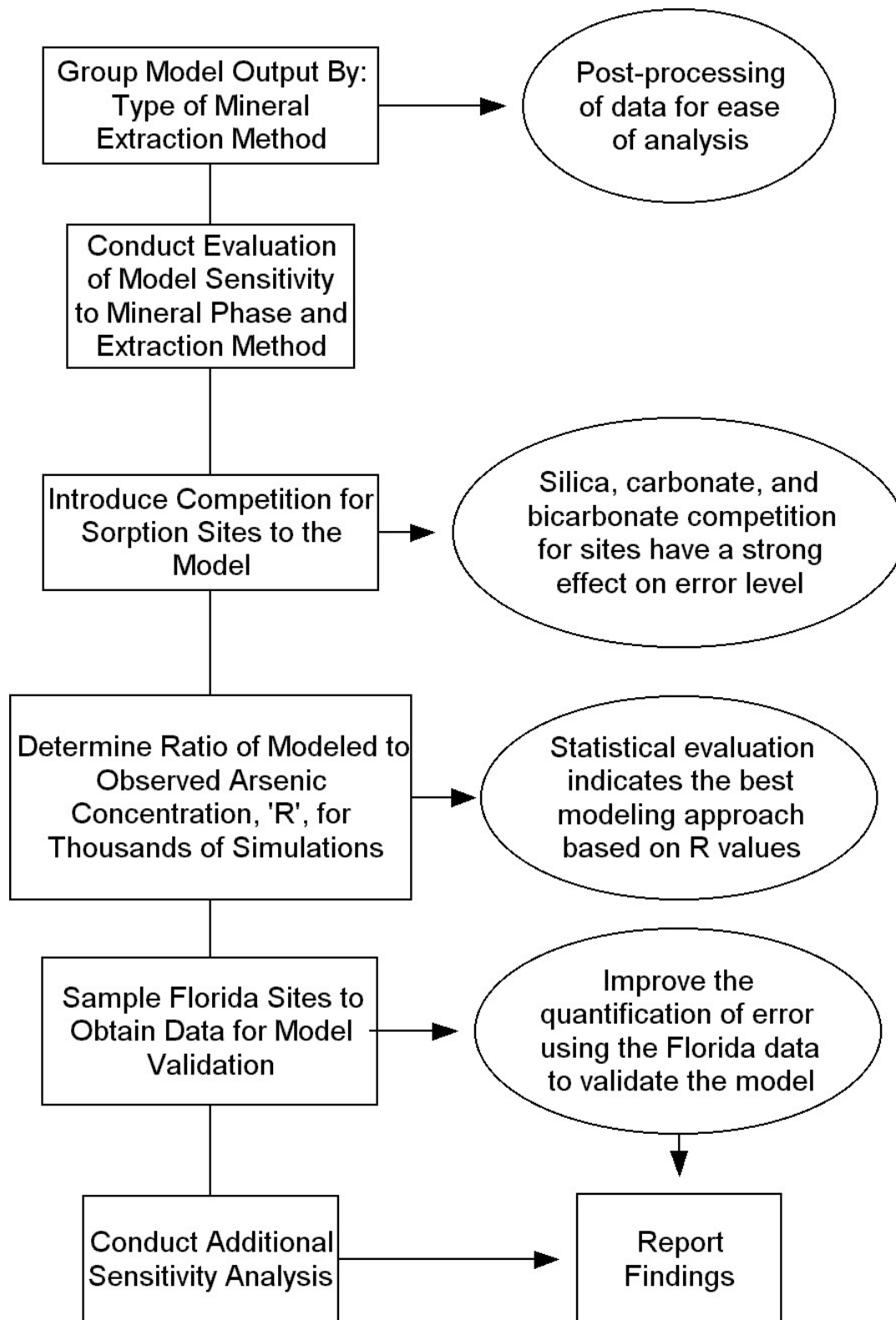
Figure 2-3
Flowchart of Model Output Evaluation

3

MODELING THE SURFACE COMPLEXATION OF ARSENIC

Need for Numerical Modeling

In order to evaluate complex natural chemistry in a mechanistic manner, it was essential to use computer models. The application of competitive, mechanistic, multi-component modeling shows great promise to allow general predictions of metal behavior in the environment. Mechanistic approaches, including thermodynamic, rely on descriptions of metal behavior at the molecular level. The processes include but are not limited to ion complexation (pairing), precipitation, sorption or surface complexation, oxidation-reduction reactions, gas exchange, ionic strength effects on molecular activity, temperature corrections to thermodynamic parameters, and chemical buffering. In theory, it is possible to combine and scale many individual processes, allowing their competitive interaction to fully describe the behavior of complex geochemical systems in a mathematical framework. In reality, there has been little field scale testing of the theory, approach, or practice of mechanistic modeling of metals. Engineering and environmental science needs detailed mechanistic models for metals that have known accuracy and precision. The models must be applicable under a broad range of chemical and physical conditions, have tested and well supported criteria for input data quality, and inexpensive data collection. All of these factors establish the need to be able to simultaneously solve hundreds of equations resulting in an optimized solution. This is only possible using computerized numerical solution methods.

Modeling Approach

We considered simulation of equilibrium inorganic arsenic surface complexation reactions with hydrous metal oxides and competition for sorption sites by ions other than arsenic. The surface complexation simulation is conducted within a multi-component thermodynamic geochemical code, PHREEQC. Surface complexation of ions by hydrous metal oxides is controlled by concentration, pH, temperature, number of available surface sites, ionic strength, chemical speciation (speciation has redox, pH, and biological controls), and feedback between these parameters. The common cations calcium, strontium, barium, magnesium and manganese are allowed to sorb in the simulations. The approach assumes that the dominant ions competing for sorption sites with arsenic sediments are silicic acid, carbonate, bicarbonate, sulfate, borate, and fluoride. The data collection approach assumes that the abundance of hydrous metal oxide sorbing surfaces can be determined by operationally defined chemical extractions of the stream sediments. These operationally defined extractions are practical, have a long history, and have been validated in many media types. There is little published on the use of chemical extractions of natural materials in a surface complexation modeling framework.

Rio Salado - Phase I

The broad objective of the modeling effort was to simulate the equilibrium geochemical behavior of arsenic, compare the simulation with the actual behavior, and explain and quantify the differences. New information on the utility of equilibrium mechanistic modeling as a predictive tool was needed. This began with evaluation of the general geochemistry and equilibrium of Rio Salado (Appendix A). Once this was understood, the controls on arsenic partitioning were explored using surface complexation modeling. Some of the simulations matched the Rio Salado arsenic on sediment data with promising precision and accuracy. Sources of error were evaluated and the results reported at symposia. Development, testing, and reporting of a field-analytical-modeling process for arsenic completed a milestone in the project.

There was backtracking, error trapping, and reiteration as part of the normal modeling process. As such, the list of steps below is more indicative of Rio Salado modeling goals to be accomplished rather than a sequential process. These goals were to:

- Model equilibrium at individual sampling stations accounting for the observed aqueous conditions and concentration and water-mineral interaction as supported by the sediment data. The purpose is to evaluate the degree of attainment of chemical equilibrium at each sample station and look for trends in general geochemistry and arsenic speciation.

- Model chemical changes along stream reaches with multiple stations to examine mechanisms responsible for any systematic downstream variation in the geochemistry of waters and sediments. In combination with mass balance and chemical flux assessment, this will provide increased understanding of geochemical changes that may be kinetically limited.

- Model the mechanistically constrained surface complexation of arsenic on the hydrous metal oxides goethite, gibbsite and ferrihydrite as determined from several sediment extraction techniques that are operationally defined to remove surface active phases.

In order to test the transferability of laboratory surface complexion approaches to the field in a realistic manner, it is important not to oversimplify the system of study. However, there are a large number of complicating factors in evaluating the partitioning of arsenic in natural systems, not all of which can be addressed by this effort. Some of these factors can be assumed negligible in effect but others may prove to be significant. It is difficult to develop a balance between practicality, the need to fully describe the system of interest, and cost and time limitations. The approach is to reduce uncertainty in major areas while looking for indications of secondary effects. The major areas for consideration are equilibrium inorganic arsenic surface complexation reactions with hydrous metal oxides; and, competition for sorption sites by ions other than arsenic.

The major simplifying assumption for Rio Salado is that the system is at a steady state, equilibrium condition. It is generally agreed that arsenic transport in the environment is attenuated primarily by surface complexation as a function of pH and ionic strength. Inorganic arsenic, usually arsenate, is the dominant species to consider. These are assumed to be the two primary factors in arsenic partitioning: speciation and what surface is available for sorption. The particular organic arsenic speciation distribution (MMAA vs. DMAA), kinetically limited reactions, the role of competing ions, organic matter, and biotransformation are generally secondary effects. Organic arsenic was treated as part of the total arsenic concentration used for

model input. Model redox conditions were not used to fix observed As^{3+}/As^{5+} ratios. Complexation kinetics was not modeled in this effort, as the sorption reaction is on the order of 50 ms [81] and the commonly slow, hours to weeks, arsenic species transformation rates are not well known and have poorly defined mechanisms and reactions [82, 83, 84].

The modeling approach assumes that the abundance of hydrous metal oxide sorbing surfaces can be partly determined by chemical extractions. In general, these extractions use acids and/or reducing agents to dissolve the surface oxides in a manner that is aggressive enough to release the metal, but not so aggressive that metal is removed from the substrate. Since these extractions cannot be purely specific for hydrous metal oxides, they are empirical or operationally defined rather than mechanistic. However, these operationally defined extractions are practical, have a long history, and have been validated in many media types.

The assumptions above are not valid for all systems, but may apply to most, and certainly to the relatively simple As^{5+} dominated system at Rio Salado. As such, the test of transferability of laboratory surface complexion approaches to the field will be generally limited to these primary factors, but will remain sensitive to the secondary factors when appropriate. There are some known problems with this approach (i.e. known presence of organic arsenic and organic carbon solid phase sorption phenomena) but it is too difficult and impractical to attack the simulation of all facets of the system, all at once, for all variables.

Published physical and chemical parameters are available that have a proposed chemical mechanism and are describable in terms of mass-action for the surface complexation of ions on mineral surfaces, including arsenate and arsenite on hydrous metal oxides. These published parameters are used in combination with analytical determinations of metal ions on the sediment surface to define the distribution of hydrous metal oxide surfaces in the Rio Salado. PHREEQC is used to bring the observed water chemistry to thermodynamic equilibrium with the sediments. In this manner, the ability to mechanistically model arsenic sorption is tested. Additional details of model construction are contained in following sections.

Florida Sites - Phase II

Following the Rio Salado simulations a second phase was begun to evaluate the data collection and modeling process at a different location. Sediment water pairs were collected from Florida to develop another data set to test the model. Data collection was enhanced by lessons learned from the Rio Salado effort (Appendix A). The level of data analysis with respect to testing of steady state and equilibrium assumptions was not as rigorous for Florida as Rio Salado. The intent was to rapidly develop another data set to test the model (Appendix B). The specific goal of the modeling process was to determine if the successful Rio Salado data collection and modeling process could be directly applied to another site. This is a large step towards validation of the approach in widely different geochemical environments.

Sensitivity Analysis - Phase III

There is some level of error in the analytical data and the constants obtained from the literature. The error can be divided into the experimental error, and the error that results from the

laboratory systems not being a true emulation of nature. It is difficult to assess the true source of error present in this analysis. It is less difficult to determine the effect of a predetermined range of error on the simulation by conducting a sensitivity analysis. In this case, sensitivity analysis is executed by systematically changing the value of input variables to determine the effect on model output. The sensitivity analysis conducted here is biased in that not all parameters are systematically varied but a subjective choice of the variables to alter (pH, Alkalinity, Total Arsenic, Total Silica) has been made. Selection of data sets to model is also subjective. Two sample stations are modeled, one from each sampling locality (Mexico and Florida). The data sets used are for a related simulation, amorphous ferrihydrite, and gibbsite. The stations were selected because the fit to the 'true' value was better than other related simulations. It is recognized that this is not as rigorous as using all sample stations, varying all variables, or conducting evaluations such as a the statistically-based Monte Carlo approach to variable selection common to risk assessment. Although limited in scope and execution, the analysis here identifies first order effects.

It can be said with certainty that the arsenic sorption simulations are quite sensitive to the formulation of the conceptual model. It was our experience that simulations are most sensitive to how the sorbing surface is defined. This includes the surface extraction method, formulation of the mineral surface, the manner in which the amount of hydrous metal oxide surface was calculated, and competition for sorbing sites by other anions. During the first phases of model assessment, input data such as the analytical determinations of elements, pH, temperature and intrinsic sorption constants obtained from the literature were not varied. They were held fixed because it was not the objective to try to obtain a best fit to observed arsenic sorption, but to test the capability of a data collection and modeling procedure to fit the observed data. What required evaluation at this point was the sensitivity of the model to input parameters. What is the quantitative variation in the model output obtained by systematic variation of the input parameters? How much error in data collection is acceptable before the error propagation is noted in the model predictions? What input parameters are the most sensitive, that is, when do small changes in input values cause large changes in model output? All of these questions can be answered by sensitivity analysis.

Selection of Computational Model

The purpose of modeling the data is to evaluate the geochemical information in the broadest possible context. This allows detailed exploration of the geochemistry responsible for the observed phenomena. The modeling effort provided insight into the Rio Salado stream geochemistry that is not readily apparent from the analytical determinations. It was found that arsenic partitioning can be described by a multi-component surface complexation model, and that the system was close to equilibrium and steady state. Computerized mathematical tools are needed to handle the complexities of the required multivariable thermodynamic assessment.

It was desirable that the model used to evaluate the data sets be able to support a broad range of geochemical processes, have a surface complexation subroutine, be current and well documented, and exist in the public domain. Two codes meet these criteria PHREEQC [8] and MINTEQA2. MINTEQA2 was used in some initial comparisons to PHREEQC using the Rio Salado data set and unsatisfactory results were obtained (Appendix A). PHREEQC was used exclusively for the Florida simulations (Appendix B). PHREEQC was selected over MINTEQA2

because of its capabilities, programming language, ease of use in a Windows environment, and reliability [85].

Thermodynamic models for aqueous solutions are of three main types. The first uses Gibbs free energies and sorption parameters to calculate species and solid phase equilibrium, MINTEQA2 is of this type. The second type, represented by PHREEQC and EQ3/6, adds the capability of reaction path simulation, mixing of two waters, addition and removal of reactants, and changing temperature to the capabilities of the first type. A third type of model will handle non-equilibrium conditions, such as kinetic limitations or variable reactant flux in addition to equilibrium conditions. The third type of model has not been located in the public domain and the current goals did not warrant its use.

MINTEQA2

MINTEQA2 holds special distinction among thermodynamic equilibrium models in that it is supported and distributed by the USEPA. MINTEQA2 assumptions and code form the core of some USEPA models that are used to calculate probable consequences of waste disposal. The code calculates equilibrium speciation and a saturation index for solid phases. It uses Eh, pH, temperature and analytical determinations of water chemistry and dissolved gasses as inputs. The code is written in FORTRAN. It has special capabilities in handling theoretical sorption mechanisms.

Errors in MINTEQA2's currently distributed form (USEPA version 3.11) have been reported [85]. Two strategies were attempted for this work to minimize the effect of these errors. First, USEPA contracted to have improvements made to MINTEQA2 that were to be complete in October 1998. Arrangements were made to release the model to this project directly from the subcontractor [11] as a documented beta version (version 4.0 beta) in January 1999. The intent was to test the modeling approach developed using the PHREEQC code against the approved version 4.0 MINTEQA2 by initially using the beta version. Second, corrections for many of the current errors are available [85] and are incorporated into a MINTEQA2 derivative MINTEQU allowing another possible path to avoid errors in version 3.11.

Preliminary testing using these three versions of MINTEQ (A2 3.11, U, and A2 4.0 beta) resulted in re-examination of the relationship of MINTEQ testing to project goals. MINTEQA2 modeling of a subset of stations was to be compared to the primary modeling tool, PHREEQC. MINTEQU and MINTEQA2, version 3.11 and version 4.0 beta, were used for equilibrium and saturation index calculations. It was expected that the MINTEQU and MINTEQA2 version 4.0 beta results would be comparable to PHREEQC results. This was not the case, MINTEQU and PHREEQC results were generally comparable but both of the USEPA versions of MINTEQA2 did not match the MINTEQU and PHREEQC results. For calcite saturation the MINTEQA2 results did not match field observation either, whereas MINTEQU and PHREEQC results did match. MINTEQA2 comparisons to PHREEQC were discontinued at this point.

PHREEQC

PHREEQC [100] is the equilibrium thermodynamic model supported by the United States Geological Survey (USGS). In their early versions, MINTEQA2 was considered superior to PHREEQE for its handling of sorption and mathematical approach. PHREEQE [9] was intended to handle a wider range of problems, such as mixing, but suffered from some simplifying assumptions. PHREEQC has been vastly improved over PHREEQE, surpassing MINTEQA2 in utility, usability and based on the analysis described above, probably accuracy. According to the author of the code,

> "PHREEQC is based on an ion-association aqueous model and has capabilities for (1) speciation and saturation-index calculations, (2) reaction-path and advective-transport calculations involving specified irreversible reactions, mixing of solutions, mineral and gas equilibria, surface-complexation reactions, and ion-exchange reactions, and (3) inverse modeling, which finds sets of mineral and gas mole transfers that account for composition differences between waters, within specified compositional uncertainties."

PHREEQC is a validated public domain chemical reaction and equilibrium code maintained by the USGS that has been subject to peer review for over four years. It is currently configured to use the WATEQ4F database or the MINTEQA2 v3.11 database. The WATEQ4F database was modified to support the surface complexation approach used here. It is written in the C computer language. This provides increased computational capacity over FORTRAN with simpler, more accurate data entry. It operates in a Windows, Mac, or Unix environment. PHREEQC does not require any additional data over that necessary to run MINTEQA2. It supports modeling capabilities germane to the effort that are not available in MINTEQA2. The surface complexation module of PHREEQC was verified against MINTEQA2 by the USGS. PHREEQC forms the geochemical core of much of the USGS research effort in reaction path and reactive transport modeling in groundwater and surface water. PHREEQC was used for calculation of saturation indices, sensitivity, mixing of stream water of different compositions and mechanistic surface complexation of arsenic.

Conceptual Models

As described elsewhere in this report, the Rio Salado conceptual model was built on in-depth observation and several iterations of geochemical modeling. This differs from the Florida simulations, where it is assumed that the conditions present at Rio Salado, that make equilibrium modeling possible, are also present to a substantial degree at the Florida sites. Site-specific elements of the conceptual models are presented below.

Rio Salado

The Rio Salado is a small stream fed by thermal springs. Baseflow discharge during the study was constant at ~0.5 m^3/s. The Rio Salado and smaller tributaries were sampled over 10 km of the river reach. Background on the conceptual model is presented in Appendix A. The following list of concepts are supported by observation and/or the literature on the watershed.

- Rio Salado at baseflow was at steady state with respect to discharge, chemical flux, and chemical equilibria. Known arsenic redox disequilibrium effects on total sorbed arsenic are small.

- The sediment-water system is well mixed due to the coarse nature of the sediments and relatively rapid flow.

- The source of arsenic in the system is constant on the time scale of the sampling event in both flux and concentration, as are other compounds.

- Although there are indications of the presence of organic arsenic, organic solid phases that sorb arsenic, and diurnal fluctuation in speciation, arsenic attenuation in Rio Salado is dominantly an inorganic process and can be modeled as such.

- Stream sediments are dominantly glass with hydrous metal oxide phases present as goethite or ferrihydrite (Fe phase), chalcedony or cristobalite (Si phase), aluminum hydroxide sites as diaspore, gibbsite, amorphous aluminum hydroxide and/or kaolinite, and manganese oxide. The presence of mixed oxides, such as allophane, is minor. There are few clay-sized particles or clay minerals. Of the inorganic sorbants, iron dominates.

Florida - Tyndall AFB

Studies of arsenic in groundwater and soil related to herbicide treatment of a site on Tyndall AFB were conducted. It was determined that a portion of the arsenic-contaminated groundwater discharged to a drainage swale located ~450 ft from the site. Sediment-water pairs were collected ~1 m below the ditch bottom, in the shallow groundwater system up-flow zone. Unlike the purely surface water Rio Salado or Fort Walton investigations, these samples allowed testing the model on a shallow groundwater system. The groundwater discharge was pronounced but at a low rate, possibly on the order of 1-2 L/min·m^2 of ditch surface area. Data collection and analysis methods for the Florida sites are presented in Appendix B. The sediments present in the Tyndall ditch are typical of the aquifer materials of this region. They consist of fine grained quartz sand with a small percentage of heavy minerals, clays, and organic debris. The following assumptions form the conceptual model, some of which have not been tested.

- The sediment-water system in the ditch was at steady state with respect to discharge, chemical flux, and chemical equilibria. Known arsenic redox disequilibrium effects on total sorbed arsenic are small.

- The source of arsenic in the system is constant on the time scale of the sampling event in both flux and concentration, as are other compounds.

- Although there is ~10% organic arsenic and organic solid phases that sorb arsenic, arsenic attenuation in the Tyndall ditch is dominantly an inorganic process and can be modeled as such.

- Sediments are dominantly quartz sand with hydrous metal oxide grain coatings.

- Arsenic sorption on the Tyndall ditch sediments can be modeled in a representative manner using the same methodology as was employed for Rio Salado.

Florida - Fort Walton

The gross characteristics of geologic materials at Fort Walton differ mainly by coarser grain size than found at Tyndall AFB. The Fort Walton samples were also taken from a drainage ditch that receives inflow from arsenic-contaminated groundwater. Total arsenic concentrations in water and sediments are much lower than Rio Salado or Tyndall AFB. The sediments are fine to medium quartz sand with a small percentage of heavy minerals, clays, and organic debris. Oxidized iron staining was noticed on the sediments. In the case of Fort Walton, there was significant flow at the sample locations, approximately $0.010 \text{ m}^3/\text{s}$. With respect to water-mineral interaction, the physical system is more similar to Rio Salado than Tyndall AFB.

- The sediment-water system in the stream was at steady state with respect to discharge, chemical flux, and chemical equilibria. Known arsenic redox disequilibrium effects on total sorbed arsenic are small.

- The sediment-water system is well mixed due to the coarse nature of the sediments and flowing water.

- The source of arsenic in the system is constant on the time scale of the sampling event in both flux and concentration, as are other compounds.

- Although there are organic solid phases that sorb arsenic, arsenic attenuation in the Fort Walton ditch is dominantly an inorganic process and can be modeled as such.

- Fort Walton sediments are dominantly quartz sand with hydrous metal oxide grain coatings.

- Arsenic sorption on the Fort Walton Beach ditch sediments can be modeled in a representative manner using the same methodology as was employed for Rio Salado.

Surface Complexation Theory

The metal sorbing properties of hydrous metal oxides have been studied for over 100 years, mainly by soil scientists [14]. Various theories for this process have been constructed to try to get around the empirical and poorly transferable description of water-mineral interaction of ions using adsorption isotherms [15, 87, 88]. The first of these were the Gouy-Chapman and Stern electric double layer (EDL) theories proposed in the 1940's. EDL sorption is dominated by electrostatic effects. A turning point was made in theory development by Schlindler and Stumm in the late 1960's with their proposal of a surface complexation approach where the sorbing ions specifically interact with definable, functional, surface molecular groups, yet the electrostatic effects in EDL theory are retained. This differs from the approach of EDL theory in that a specific chemical bond is made with the surface at defined sites that are finite in size and number. Since that time, there have been various modifications of the surface complexation theory. Although the number of fitting parameters, required data, and mathematical construct of the models are significantly different they all have certain commonality. Dzomback and Morel (1990) expressed the focus of surface complexation models in the following four statements:

> "Sorption on oxides takes place at specific coordination sites. Sorption reactions on oxides can be described quantitatively via mass law equations. Surface charge results from the sorption reactions themselves. The effect of surface charge on sorption can be taken into account by applying a correction factor derived from the EDL theory to mass law constants for surface reactions."

It should be noted that the fundamental bonding reactions that take place on hydrous metal oxide surfaces are still hotly debated, as are the number and type of functional surface groups available for bonding, the location of the sorbed ions, and the math used for quantification. This results in first-principal differences in how calculations are made in the different models. The concepts behind several models and an excellent review of the current state of surface complexation modeling theory were presented by Goldberg in 1998 [6]. This effort moves out of the laboratory to testing application of the theory in a natural setting. The fundamental principals of arsenic chemisorption by surface complexation will continue to be investigated, and debated, in the years to come. However, there is no reason not to test the current state of the theory against field data. As the theory is revised some of the constants employed here will certainly change, as will the mathematical approach. Given the commonalties in the details of describing surface chemistry, the fundamental approaches used here will remain the same.

Several mathematical formulations of surface complexation models are currently available. The most commonly cited are the:

- Schlindler and Stumm Constant Capacitance Model (CC);

- Dzomback and Morel Generalized Two-Layer or Diffuse Layer Model (DLM);

- Hiemstra and vanRiemsdijk Charge Distribution Multi-Site Complexation One-pK Model (CD-MUSIC); and,

- Triple Layer Model (TLM) of Davis and Leckie.

These models have all been used to fit laboratory derived pure mineral surface complexation data with what has been reported to be equal success. In application, each has limitations requiring that the chemical significance of the approach of each model be evaluated. This effort has been confined to the use of the generally accepted DLM mathematical formulation as contained in PHREEQC.

Surface complexation models use the law of mass action, expressed as an equilibrium constant, to define protonation (K_{S_+}), deprotonation (K_{S_-}), and ion-specific sorption to a surface (K_{int}). To implement surface complexation in PHREEQC these K's must be known for each mineral phase and ion modeled. For sorption of arsenic, and other oxy-anions, the surface complexation process is generally agreed to be covalent bonding.

Central to the surface complexation model approach is that protonation and disassociation reactions and ion specific complexation constants are reversible and apply over a range of pH and ionic strength conditions. The equilibrium constants K_{S-} and K_{S+} are determined for protonation-deprotonation reactions at the oxide surface. CC, DLM and TLM are '2 pK' models in that the protonation reaction with the surface, S, can be described as a two step reversible process where:
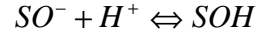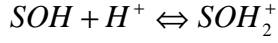
$$SOH + H^+ \Leftrightarrow SOH_2^+ \qquad\qquad SO^- + H^+ \Leftrightarrow SOH$$

$$K_{s+} = \frac{[SOH_2^+]}{[SOH\,][H^+]}\exp\frac{(F\psi_0)}{(RT\,)} \qquad\qquad K_{s-} = \frac{[SO^-][H^+]}{[SOH\,]}\exp\frac{(-F\psi_0)}{(RT\,)}$$

The K_{s-} and K_{s+} constants allow the surface sorbing properties to change with changing pH. Constants for specific sorbing ions that meet these constraints are referred to as "intrinsic constants" or K_{int}. In order to apply these models to surface complexation K_{int} for surface reactions must be known for each surface to be used, each sorbing ion, and each site defined on the surface. To some degree K_{s-}, K_{s+}, and K_{int} values determined for a single mineral may be used interchangeably among the CC, DLM and TLM (single site, 2-pK) models. This requires refitting and corrections for model geometry. Refitting of experimental data to surface complexation models can be accomplished using the FITEQL 4.0 model [89].

The Dzomback and Morel 1990 DLM model uses two populations of sites for sorption of cations, a small number of high affinity sites and a large number of low affinity sites. Dzomback and Morel did not use this method for anions. PHREEQC will properly account for the total number of sites available to anions with database modification. This was done after consultation with the author of the PHREEQC code, David Parkhurst of the USGS. To account for the total number of sites available to anions a dummy K_{int} (equal to the K_{int} weak) was used for the small number of strong sites.

Hiemstra and vanRiemsdijk's CD-MUSIC model is a new approach to surface complexation modeling that has not yet been included in a multicomponent geochemical code. CD-MUSIC constants are not fit from experimental data but are derived from Pauling bond strengths. This is an attempt to predict complexation properties from first principals. It is mentioned here because it has fit the experimental data well in its recent and limited application. In principle, CD-MUSIC is more mechanistic than the CC, DLM, or TLM models. CD-MUSIC is also not confined to the 2-pK assumption. It allows for different K's for different mineral crystal faces, a known issue with CC, DLM, or TLM models [90]. This makes CD-MUSIC currently more difficult to implement. Defining K's for a mineral phase can be quite complex, with 30 published K's needed for mineral face specific goethite protonation-deprotonation reactions alone. Although more complex than CC, DLM, or TLM formulations, CD-MUSIC theory may offer an even more highly mechanistic model for the future. The CD-MUSIC model provides a very close fit to experimental data [90] that is fit equally well by CC, DLM, or TLM models. This indicates that if the CD-MUSIC approach really is superior, the CC, DLM, or TLM models may be more empirical, but not necessarily less accurate or precise.

Surface complexation equilibrium constants used here take the following form, with the example below for arsenate sorbing to a single site, where F is the Faraday constant $(9.65 \times 10^{-4}$ coulomb/mole), ψ_o is the surface potential in volts, R is the universal gas constant, and T is the absolute temperature. This electrostatic term is used to account for the change in surface potential because of the adsorption of the modeled ion.

$$K^1_{As^{5+}_{int}} = \frac{[SH_2AsO_4]}{[SOH\,][H_3AsO_4]} \qquad K^2_{As^{5+}_{int}} = \frac{[SHAsO_4^-][H^+]}{[SOH\,][H_3AsO_4]}\exp\frac{(-F\psi_0)}{(RT\,)} \qquad K^3_{As^{5+}_{int}} = \frac{[SAsO_4^{2-}][H^+]^2}{[SOH\,][H_3AsO_4]}\exp\frac{(-2F\psi_0)}{(RT\,)}$$

The geometry of the models may differ greatly but they all reduce to a set of equations that can be solved numerically. With respect to broad, multicomponent modeling as proposed here, the most important part of this commonality and formulation among the surface complexation models is the universal application of the mass law constraint. The mass law formulation allows the sorption reactions to be used in the existing theoretical and mathematical framework of thermodynamic equilibrium models. Surface complexation reactions become a part of the general mathematical solution of an equilibrium state between an aqueous solution and a solid sorbing phase. In this manner, a single broadly defined geochemical model is used to test several surface complexation approaches.

There are a number of mathematical formulations of these models including constant capacitance, the general two-layer model used here, and the triple-layer model. Goldberg (1998) provides a detailed summary of available data for a number of surface complexation models, the most extensive data being for the constant capacitance model. The general two-layer model was selected for use because of the large number of publications that cite the approach of Dzomback and Morel (1990), the relatively low number of fitting parameters, and the use of the Dzomback and Morel (1990) generalized two-layer model in the PHREEQC code. The two-layer model was selected over the constant capacitance formulation because of the explicit charge balance option available in PHREEQC. This option uses the 1983 method of Borkovec and Westall [133] to account for the composition of the double layer. This method requires artificial charge balancing for convergence of the numerical solution. By accounting for the composition of the double layer it is possible to model the advection of pore fluid away from the system with insignificant changes in the value of chloride ion, a species enabled in PHREEQC as a variable concentration for charge balancing. This is the most realistic way to handle charge balance for these simulations and enhanced model convergence in our model runs.

The K_{s-} and K_{s+} constants allow the surface sorbing properties to change with changing pH and K^1_{int}, K^2_{int} and K^3_{int} provide for surface property changes due to the sorption of arsenic itself. Constants for specific sorbing ions that meet these constraints are referred to as "intrinsic constants" or K_{int}. Lewis acids and bases as well as ion pairs will all have more than one K_{int}. In order to apply PHREEQC to surface complexation K_{int}, for surface reactions must be known for each surface to be used, each sorbing ion, and each site defined on the surface. The K_{s-}, K_{s+}, and K_{int} values used in the simulations are presented in Tables 3-1 through 3-3.

Table 3-1
Surface Complexation Mass-Action Coefficients for Ferrihydrite Surfaces and the Generalized Two-Layer Model

Complex	log K$_{strong}$	log K$_{weak}$		Source
K$_+$	7.29	7.29		Dzomback and Morel, 1990
K$_-$	-8.93	-8.93		Dzomback and Morel, 1990
Ca	4.97	-5.85		Dzomback and Morel, 1990
Sr	5.01	-6.58		Dzomback and Morel, 1990
SrOH	[a]	-17.6		Dzomback and Morel, 1990
Ba	5.46	-7.2		Dzomback and Morel, 1990
Mg	[a]	-4.6		Dzomback and Morel, 1990
Mn	-0.4	-3.5		Dzomback and Morel, 1990
	log Ka$_1$	**log Ka$_2$**	**log Ka$_3$**	
AsO$_4$$^{3-}$$_{strong}$	29.31	23.51	10.58	Dzomback and Morel, 1990
AsO$_4$$^{3-}$$_{weak}$	29.31	23.51	10.58	Dzomback and Morel, 1990
H$_3$AsO$_3$$_{strong}$	5.41			Dzomback and Morel, 1990
H$_3$AsO$_3$$_{weak}$	5.41			Dzomback and Morel, 1990
H$_3$BO$_3$$_{strong}$	0.62			Dzomback and Morel, 1990
H$_3$BO$_3$$_{weak}$	0.62			Dzomback and Morel, 1990
SO$_4$$^-$$_{strong}$	7.78	0.79		Dzomback and Morel, 1990
SO$_4$$^-$$_{weak}$	7.78	0.79		Dzomback and Morel, 1990
F$^-$$_{strong}$	8.7	1.6		Dzomback and Morel, 1990
F$^-$$_{weak}$	8.7	1.6		Dzomback and Morel, 1990
H$_4$SiO$_4$$_{strong}$		4.4	-4.5	Meng and Letterman, 1996, Refit of TLM data
H$_4$SiO$_4$$_{weak}$		4.4	-4.5	Meng and Letterman, 1996, Refit of TLM data
SiO$_3$$^{2-}$$_{strong}$	15.9	8.3		Dzomback and Morel, 1990
SiO$_3$$^{2-}$$_{weak}$	15.9	8.3		Dzomback and Morel, 1990
CO$_3$$^{2-}$$_{strong}$	13.5	6.25		LFER[b]
CO$_3$$^{2-}$$_{weak}$	13.5	6.25		LFER[b]

[a] Linear Free Energy Relationships (LFER) was not derived in Dzomback and Morel 1990.

[b] LFER estimates of K$_{int}$ made using graphics from Dzomback and Morel (1990) and pKa's from VanGeen et al. (1994).

Table 3-2
Surface Complexation Mass-Action Coefficients Used for Goethite Surfaces and the Generalized Two-Layer Model

Complex	log Ka$_1$	log Ka$_2$	log Ka$_3$	Source
K$_+$	7.52			Manning and Goldberg, 1996a
K$_-$	-10.6			Manning and Goldberg, 1996a
Ca	-5.85			Dzomback and Morel, 1990
Sr	-6.58			Dzomback and Morel, 1990
Ba	-7.2			Dzomback and Morel, 1990
Mg	-4.6			Dzomback and Morel, 1990
Mn	-3.5			Dzomback and Morel, 1990
	log Ka$_1$	log Ka$_2$	log Ka$_3$	
AsO$_4$$^{3-}$	9.1	0.0[c]	10.58	Manning and Goldberg, 1996a, Refit from CC data[a]
H$_3$AsO$_3$	5.41			Dzomback and Morel, 1990
H$_3$BO$_3$	0.62			Dzomback and Morel, 1990
SO$_4$$^-$	7.78	0.79		Dzomback and Morel, 1990
F$^-$	8.7	1.6		Dzomback and Morel, 1990
H$_4$SiO$_4$	4.48	-3.43		Goldberg, 1985[d]
CO$_3$$^{2-}$	20.78	12.71		VanGeen et al., 1994

[a] Manning and Goldberg data refit to DLM using FITEQL.

[b] LFER estimates of K$_{int}$ made using graphics from Dzomback and Morel (1990) and pKa's from VanGeen et al. (1994).

[c] Fitting insensitive to the value of this parameter and FITEQL fails to converge if not fixed, set to 0.0.

[d] Constant capacitance parameters for goethite, refitting not possible due to lack of ionic strength data.

Table 3-3
Surface Complexation Mass-Action Coefficients Used for Gibbsite Surfaces and the Generalized Two-Layer Model

Complex	log Ka$_1$	log Ka$_2$	log Ka$_3$	Source
K+	9.1			Manning and Goldberg, 1996a
K-	-10.5			Manning and Goldberg, 1996a
Ca	-5.85			Dzomback and Morel, 1990[a]
Sr	-6.58			Dzomback and Morel, 1990[a]
Ba	-7.2			Dzomback and Morel, 1990[a]
Mg	-4.6			Dzomback and Morel, 1990[a]
Mn	-3.5			Dzomback and Morel, 1990[a]
	log Ka$_1$	log Ka$_2$	log Ka$_3$	
AsO$_4^{3-}$	8.7	1.1	-5.2	Manning and Goldberg, 1996a[b] Refit from CC data
H$_3$AsO$_3$	5.41			Dzomback and Morel, 1990[a]
H$_3$BO$_3$	0.62			Dzomback and Morel, 1990[a]
SO$_4^-$	7.78	0.79		Dzomback and Morel, 1990[a]
F$^-$	8.7	1.6		Dzomback and Morel, 1990[a]
H$_4$SiO$_4$	4.48	-3.43		Goldberg, 1985[a]
CO$_3^{2-}$	20.78	12.71		VanGeen et al., 1994[a]

[a] Direct substitution of ferrihydrite or goethite data from original source for gibbsite.

[b] Manning and Goldberg data refit to DLM using FITEQL.

For sorption of arsenic, the chemical bonding process is generally agreed to be covalent as inner-sphere complexes [87, 91], and the dominant bonding mechanism is bidentate-binuclear, [92, 93]. Most investigations of the surface complexation of arsenic on mineral surfaces has been conducted on simple pure mineral phase systems, with singular sorbing species, in the laboratory. The experimental procedure most often involves the interpretation of pH titrations in the manner of a zero point of charge determination, evaluation of electrophoretic mobility of colloidal sized pure mineral grains, and adsorption experiments over a range of pH and ionic strength [5, 87, 94].

Tables 3-1 through 3-3 contain the mass action coefficients used for the complexation modeling presented here. Whenever possible, published diffuse double layer or general two layer constants were used directly as published in the literature. The PHREEQC database contained the surface complexion constants published in Dzomback and Morel (1990) for hydrous ferrous oxide and a number of ions, dominantly heavy metals. It was necessary to append and modify the supplied database for this study to be able to model the influence of common anions and cations on arsenic complexation. There are many more published coefficients for trace metals than there are for the common anions and cations known to compete for sorbant sites. When necessary, published data was refit to the diffuse layer model in the FITEQL 4.0 [96] or determined using linear free energy relationships (LFER) between the pK$_a$ and K$_{int}$ for an oxyanion [14, 88].

Due to the difficulty in determining sorption and thermodynamic parameters for every system of interest, the geochemical modeling practitioner will generally obtain these constants from the literature. Our approach is the same. In order to extend the simulation to comparison of goethite, ferrihydrite, and gibbsite conceptual models some compromises were made. The significant deviation from principal is where K data had to be substituted between the mineral phases to simulate the competition of specific ions with arsenic for sorption sites, or K estimated using LFER. Surface areas of the hydrous metal oxides and the number of sites per unit area were obtained from the source that supplied the relevant K_-, K_+, and K_{int} data. If double layer model constants were not available in the literature, published data was refit to this model using FITEQL 4.0 [96]. Where complexation data for specific ions of interest could be located only for goethite, or ferrihydrite, direct substitution of K_{int} values between the phases was used. In other cases LFER were estimated from the published data.

Table 3-1 presents the coefficients used in all simulations of ferrihydrite surface complexation. With a few exceptions all parameters are taken from Dzomback and Morel (1990). The Dzomback and Morel (1990) general two-layer model for ferrihydrite uses two sorbing sites, a small number of strong sites and a much larger number of weak sites. The PHREEQC database required modification to use both these strong and weak sites. Other than the surface complexation modifications to the WATEQ4F database supplied with PHREEQC mentioned, no other alterations were made. Goldberg [88] correctly indicates that generalized two-layer model ligand exchange reactions do not require use of strong and weak sites, however, in order to model competition for sorbing sites accurately in the ferrihydrite system these sites were both represented consistently in the database for both anions and cations. Arsenic K_{int} for ferrihydrite were taken from Dzomback and Morel [14]. The data of Meng and Letterman [104] were refit from the triple-layer model to the two-layer model using FITEQL 4.0 [96]. These data were used in preference to the LFER derived relationships for silica of Dzomback and Morel [14] because the Meng and Letterman [104] results are experimental and were conducted in a CO_2 free atmosphere. Published data for carbonate and bicarbonate on ferrihydrite were not located. These coefficients were derived for this study using LFER's and published data.

Tables 3-2 and 3-3 present the mass action coefficients used in simulation of goethite and gibbsite surfaces. K_{S+}, K_{S-}, and arsenic K_{int} for goethite were from Manning and Goldberg (1996b). Manning and Goldberg (1996b) suggest a single sorbing site for arsenic that has two states of protonation for goethite. Accordingly the PHREEQC database was modified so that goethite simulations use a single sorbing site consistently, rather than the two sites used for ferrihydrite [14]. To allow and test competition for sorption sites by divalent cations, and phosphate, sulfate, fluoride, and borate anions, in the goethite and gibbsite simulations, Dzomback and Morel [14] ferrihydrite K_{int} values for these ions were applied to the goethite and gibbsite mineral surfaces. Silica coefficients were applied directly from a constant capacitance model derived from experiments on goethite [97]. The carbonate-bicarbonate K's are from VanGeen et al. [109]. Other than the Manning and Goldberg [91] coefficients for arsenate complexation with gibbsite, all gibbsite coefficients are directly substituted from goethite.

Known Limitations to Approach

Organic Substrates

Arsenic chemisorption is not limited to hydrous metal oxides. Organic substrates such as living and dead plant material, bacteria, and other surface coatings or colloidal organic forms are known to sorb anions and cations. It is recognized that there is an organic substrate effect on arsenic sorption and surface complexation. This has not been factored into the conceptual model or simulations for Florida or Rio Salado. There is also adsorption of dissolved organic compounds such as fulvic and humic acids on hydrous metal oxides that would act in a competitive manner with arsenic. There is some bearing on the findings herein. Given Welch's [108] observed correlation between total organic carbon (TOC) and arsenic in Rio Salado, and the observations for the Florida samples, it is quite probable that some of the observed chemisorption is on organic or biologic material rather than on mineral surfaces. TOC to arsenic correlations were weak for the Florida samples but this fact alone cannot discount probable organic substrate sorption of arsenic.

Organic Arsenic

The organic arsenic concentrations that were detected at Rio Salado and Tyndall AFB are not fully represented in the simulations. Organic arsenic is treated as As^{5+}. Our Rio Salado organic arsenic in water data was hampered by false positives for DMAA attributable to the specific ion exchange separation elution sequence used at that time. MMAA detection was unaffected. Although Rio Salado organic arsenic content is probably less than 10% in water, it is considerably greater in sediments. Florida analysis reveals no organic arsenic at Fort Walton and approximately 10% organic arsenic at Tyndall AFB. Since the K_{int} for MMAA and DMAA are reasonably close to that of As^{5+} [98, 99], the effect is assumed small for the current simulations. To ensure generality of the model, organic arsenic should be rigorously incorporated.

Equilibrium Assumption

The modeling approach assumes that in all cases the system is in chemical equilibrium and is describable without using kinetic constraints. This is probably not completely valid, because arsenite is often present in disequilibrium with the oxidation state of the environment [100, 101, 102, 103] and has significantly different sorption properties than arsenate. It is possible that arsenic redox disequilibrium is the most common aqueous condition. This has also been observed in Rio Salado. The presence of As^{3+} in Rio Salado downstream of the Powerline spring, and subsequent oxidative transport, indicates that the system will move towards equilibria in travel times of tens of minutes over hundreds of meters. Little is known regarding the natural transformation rates of the As^{3+} - As^{5+} redox couple [103]. Redox disequilibria as noted in Welch's [108] sediment extracts and at other sites complicate any interpretation of arsenic mobility based on oxidation state because the As^{3+} - As^{5+} redox equilibria assumption is generally not valid [95]. Redox disequilibria of many metal pairs is due to biogeochemical reactions and the controls imposed by biological terminal electron acceptors and can be modeled using fitted kinetic corrections [74]. The PHREEQC modeling here does not attempt to calibrate the model to observed As^{3+} concentrations. However, we use As^{3+} concentrations predicted to be complexed

with sediments as part of the total arsenic used in model comparisons to field data. The total arsenic mass input as determined from analytical values is accounted for.

In the case of the Florida samples, significant As^{3+} (~50% of the total) was determined to be present at both Fort Walton and Tyndall AFB. Simulations were conducted for relative redox endpoints of the system to evaluate the sensitivity of the modeled sorption to the oxidation state of the arsenic. There were no attempts made to adjust the redox chemistry to simulate the observed arsenic speciation. Based on the discussion above, regarding the prevalence of non-equilibrium conditions for the arsenic redox couple, such simulations are probably meaningless.

Operationally Defined Extractions

Extractions used for determining the hydrous metal oxide surface population on sediment are known and accepted in the scientific community. The hydrous metal oxide surfaces are defined as individual components of a multicomponent site distribution using elemental values determined from the operationally defined extractions. Specifically, iron and aluminum concentrations in sediment extracts are used to back-calculate the amount of hydrous metal oxide that was present on the surface of the sediment grains. The comparison of the amount of arsenic simulated on the sediments is only appropriate when compared to arsenic values from the same extraction. This presents problems in that:

- The amount of arsenic leached may not correspond with the amount of hydrous metal oxide ions that are used to create mineral surfaces for the model, due to preferential leaching of one component over the other;

- The selection of solid phases to represent the extraction data may not be correct;

- The selection of solid phases to simulate and their relative importance is dependent on the specific geochemical reactions controlling the environmental process of interest. This is often poorly understood.

- Explicitly supporting selection of solid phases to simulate is very difficult. This is most often due to the extreme complexity of direct detection and quantification of low concentrations of minerals and amorphous phases in sediments.

- There are questions regarding the theoretical vs. empirical treatment of multiple competing sorbing species and surfaces; and,

- Mixed-mineral-phase complexation behavior may not be additive as compared to the pure-mineral-phase behavior [104].

What is at issue is defining the appropriate extraction method to define mineral phases that result in accurate simulation of environmental processes. Due to the difficulty of defining and quantifying mineral phases directly, we have defined them empirically using operationally defined extractions. Discussion of the validity of this approach was not found in the literature, but there appear to be few alternatives in implementing a mechanistic approach. The result is that the best fitting models are those that provide results that are internally consistent with the ratios of arsenic and hydrous metal oxide forming elements found in the extractions. At best, this is semi-empirical and is certainly not purely mechanistic.

The issues with operationally defined extractions are reflected in comparison of extract to x-ray fluorescence (XRF), or total digestion elemental concentrations. Welch (1999) indicates that the Rio Salado Chao extractions removed 15% of the arsenic detectable using XRF where the HNO_3 extraction removed 85%, and the H_3PO_4 extraction 25%, on average. All extracted iron values were well below (4-21%) the total iron value determined by XRF. XRF provides a measure of the total concentration of an element in the sediments. Similar results were found with the extractions on the Florida sample.

Before the Rio Salado effort it was not known if the extractions would provide meaningful results for use in a surface complexation model. It is possible the extractions would remove the 'correct' surface-active phases responsible for sorbing the arsenic, and the arsenic complexed with those phases, but not support stoichiometric recombination in a surface complexation scheme. We tested that approach here, found it successful, and hope for broader validation of the approach in the future.

Major questions remain regarding the use of sequential extractions in study of the bioavailability of metals. Are the extracted phases physically meaningful as a source of direct toxicity to organisms in the geomedia? Can the technique used here provide consistent results in modeling retardation and attenuation? These questions remain to be investigated but the underlying mechanistic approach appears to be supported by this effort.

The Chao extraction is designed to remove amorphous phases by reductive dissolution. HNO_3 extractions should remove amorphous and crystalline secondary iron, and manganese and aluminum minerals and organic material by oxidation and acid attack. The H_3PO_4 extractions work by acid attack and displacement of complexed arsenic by phosphate. The citrate-bicarbonate-dithionate (CBD) extractions [134] remove amorphous and crystalline secondary iron, manganese and aluminum minerals by reductive dissolution and complexation in a buffered system. These same extractions also provide data on surface silica but with exception of the CBD method, the effectiveness for silica and its complexes is not well described in the literature. The extractions are operationally defined in that they are not as specific for dissolution of mineral types as may be desirable. They may provide data that is not meaningful in the context of surface complexation modeling. This effort provides information on the suitability of the methods to match observation when used for modeling. It does not validate any selective dissolution analysis method as mechanistically correct.

Surface Phase Limitations

Only hydrous metal oxide surfaces for aluminum and iron are used here. No other sorbing phases are simulated or considered directly. Although it is known that carbonates sorb [105], they were omitted due to low abundance. Manganese was observed to be correlated with arsenic in Rio Salado [108] but little data exists to apply these oxides to arsenic attenuation without invoking kinetics [74]. Silica was found in operationally defined extractions, and silica surfaces are probable in the Rio Salado system. The choice of an aluminum oxide as gibbsite was based on the availability of arsenic K_{int} for this phase; another aluminum phase may be more appropriate. Clay minerals are assumed present but not abundant. In order to limit the system simulated to probable first-order sorbing phases only ferrihydrite, goethite and gibbsite phases were used.

Input Data Sets

The PHREEQC input data sets contain solution chemistry, a hydrous metal oxide surface representation, and instructions on how to interact the two. Portions of the surface complexation data are contained in the input data sets and the remainder in the thermodynamic database used by PHREEQC. The water analysis presented in appendices A and B were used for the simulations. Temperature data was extrapolated to fill in for a few missing measurements at Rio Salado. There are only a few cases where the chemical concentration or extraction data were modified from observation. We allowed chloride to make very minor adjustments to maintain charge balance. PHREEQC cannot hold pH or Eh fixed during transport simulations involving surface complexation because these are variables in the iterative numerical solution of the surface complexation equations. In the case of the Florida simulations, the concentration of nitrate (NO_3^-) was high enough to oxidize all of the As^{3+} at simulated equilibrium and cause Eh numerical runaway. This is because the As^{3+} present was not in redox equilibrium. We omitted nitrate from some of the simulations to evaluate the effect. Other than under the above conditions, the chemical concentration or extraction data were not modified to improve model fit.

Aqueous Chemistry

The full water chemistry analysis presented in the appendices was utilized in the modeling. The input data was not modified by "corrections" to improve model fit. Temperature data had to be extrapolated to fill in for the missing measurement at Rio Salado Station 14. In general, the water chemistry data must be very broad in scope and accurate. Since competitive surface complexion is specified in the approach, it is necessary to quantify inorganic compounds that are present at near the concentration of the arsenic species. For Rio Salado, this has meant that any element suspected to be present at even low levels (~1 mg/L) is desirable to evaluate. Many measurements and procedures need to be conducted in the field to make sure that the data is representative of *in-situ* conditions. In order to minimize error in the findings the accuracy and precision of all analyses needs to be high, and quantifiable.

Surface Chemistry

Most surface complexation modeling of arsenic on mineral surfaces has been conducted in simple systems in the laboratory. The experimental procedure most often involves the interpretation of pH titrations in the manner of a zero point of charge determination, evaluation of electrophoretic mobility of colloidal sized pure mineral grains, and adsorption experiments over a range of pH and ionic strength [1, 5, 14]. The primary intent of those efforts has been to obtain K_-, K_+, and K_{int} values using inverse surface complexation models, or trial and error, to fit the observed data. As outlined here, these K's are the heart of the approach to using surface complexation modeling to fit field data. By design, the careful determination of these K's should allow their application in more complex geochemical systems than were tested in the laboratory. In the current literature there are published K_-, K_+, and K_{int} values for arsenate and arsenite surface complexation on the naturally occurring and/or natural analog mineral phases of: amorphous hydrous ferric oxide (HFO), alumina, activated alumina, goethite, gibbsite, kaolinite, montmorillonite, illite, sulfides and others. There are two published papers containing values for

MMAA and DMAA complexation on HFO and activated alumina. Values for the organic arsenic compounds are generally scarce. Through personal communication with several groups it was found that there is broad current effort in defining K_{int} for more mineral surfaces and arsenic compounds using a variety of surface complexation models so new K's are expected soon.

Arsenic K_{int} for HFO were taken from Dzomback and Morel, 1990 and K_{int} for goethite and gibbsite were from Manning and Goldberg, 1996. The corresponding and consistent K_{s-} and K_{s+} data were used from each source. A comprehensive and consistent set of K_{int} values for common anions and cations exists only for HFO [14] and the DLM. The Dzomback and Morel DLM for HFO uses two sorbing sites, a small number of strong sites and a much larger number of weak sites, Manning and Goldberg [91] suggest a single sorbing site for gibbsite and goethite.

Every effort was made to use only actually measured and validated input parameters. There was one significant deviation from that principle in the current effort. In order to allow and test competition for sorption sites by divalent cations, and phosphate, sulfate, fluoride, and borate anions in the goethite and gibbsite simulations, Dzomback and Morel HFO K_{int} values for these ions were substituted for goethite and gibbsite mineral surfaces. It is possible to develop a relationship between laboratory pKa's for many ions, and their K_{int}, for a specific mineral surface and develop K_{int} for untested ions, but that was beyond the scope of this effort.

The K_-, K_+, and K_{int} data used here [14, 91, 107] are mineral-specific and were determined on pure amorphous and crystalline hydrous metal oxide phases. A challenge in applying surface complexation to the field is how to determine what the reactive quantities of these hydrous metal oxides are in natural sediments. This is necessary to constrain the model to field observation. The results are highly dependent on the method used to determine surface composition. Generally, operationally defined wet-chemical digestion methods are used. They are designed to solubilize only certain mineral or organic constituents of a grain surface. In practice the methods can be non-specific and must be used judiciously.

Rio Salado Samples

The iron and aluminum extract values from the samples were used to determine molar masses of hydrous metal oxide phase(s) per kilogram of sediments. Rather than *a priori* selection of a single extraction method as representative, we evaluated several methods to test their ability to produce empirical correlation between iron, manganese, TOC, and operationally defined arsenic extraction and quantification schemes. We then compare the ability of those different extraction methods to support the simulation of arsenic partitioning in Rio Salado. The Rio Salado sediment arsenic and iron data, in combination with later determinations of aluminum in aliquots of the extracts, was used to derive distributions of aluminum and iron hydrous metal oxide sites available for arsenic surface complexation. The sediment extract data used for iron and aluminum surface concentrations was derived from: whole sediment extracts using hot nitric acid (HNO_3 Whole); -80 mesh homogenized sediment extracts using hot nitric acid (HNO_3 Fine); -80 mesh homogenized sediment extracts using hydroxylamine hydrochloride (Chao Reagent); and, -80 mesh homogenized sediment extracts using phosphoric acid (H_3PO_4) as conducted by Welch [108].

The HNO_3 Whole and H_3PO_4 extractions did not have aluminum determined. Aluminum extract values from HNO_3 Fine and Chao Reagent extractions were substituted. Thus, gibbsite values for HNO_3 Whole are equal to HNO_3 Fine, and H_3PO_4 are equal to Chao Reagent. All iron values were independently determined. This provided four input data sets for each sample station, with surface combinations of analytically determined iron and aluminum as ferrihydrite, ferrihydrite + gibbsite, goethite, and goethite + gibbsite. This resulted in 16 combinations of different extraction methods and surface complexation assemblages for each sample station water chemistry determination, or 320 sorbing surface - water chemistry input data sets for modeling. Calculated surface concentrations of hydrous metal oxides are contained in Appendix A.

Florida Samples

Again, the iron and aluminum extract values from the samples were used to determine molar masses of hydrous metal oxide phase(s) per kilogram of sediments. The Florida sediment arsenic and iron data, in combination with later determinations of aluminum in aliquots of the extracts, was used to derive distributions of aluminum and iron hydrous metal oxide sites available for arsenic surface complexation. The sediment extract data used for iron and aluminum surface concentrations was derived from: whole sediment extracts using hot nitric acid (HNO_3); using citrate-bicarbonate-dithionate (CBD); and using hydroxylamine hydrochloride (Chao Reagent); and the Tessier method of partial extractions. Whole sediment extractions using phosphoric acid (H_3PO_4) as conducted by Welch [108] were unsuccessful on the Florida samples, probably due to readsorption of arsenic on other phases during the extraction process.

This provided four input data sets for each sample station, with surface combinations of analytically determined iron and aluminum as ferrihydrite, ferrihydrite + gibbsite, goethite, and goethite + gibbsite. This resulted in 16 combinations of different extraction methods and surface complexation assemblages for each sample station water chemistry determination, or 90 sorbing surface - water chemistry input data sets for modeling.

Water-Mineral Ratio

PHREEQC uses a kilogram of water as its reaction volume requiring that a ratio between the water and sediment surface be set. A sediment porosity of 30% and a density of $2.5 g/cm^3$ was initially assumed for Rio Salado input data sets to establish a fixed water-mineral ratio for the system. Gravimetric determinations of porosity and bulk density were also made on both the Florida and Rio Salado samples. The assumed porosity model is set up so that 1 kg water contacts 2.33 liters of sediments or 5.825 kg, and 1 kg of water reacts with the amount of hydrous metal oxide that is found on 5.825 kg of sediments. The gravimetric porosity data are used to make similar determinations. The model was constrained to simulate the advection of water, a pore volume at a time, of the sampled composition though sediments until the modeled water chemistry matched the observed water chemistry. This simulates the field condition of steady-state flow and chemical equilibrium. After several iterations of model testing 4-10 pore volumes were generally found to be sufficient for model convergence for all input data sets.

Molar surface areas of the hydrous metal oxides and the number of sites per unit area were obtained from the source that supplied the relevant K_-, K_+, and K_{int} data. The analytically

determined Fe and Al values were used to calculate molar masses of hydrous metal oxide phases per kilogram of sediments by unit conversion. Calculated surface concentrations of hydrous metal oxides are contained in Appendix A and B.

4
MODELING RESULTS

The relevant numerical modeling output was in the form of surface concentrations of arsenic complexes with hydrous metal oxides. The input data sets are grouped in major categories of sample location, hydrous metal oxide surface assemblage, and operationally defined extraction method used to derive the surface assemblage. The modeling results were statistically evaluated for the combination of categories that provides the best fit. A perfect simulation of the partitioning of arsenic would reveal all stations having a ratio of unity for modeled to observed arsenic. We refer to this ratio as 'R' herein. The observed arsenic is defined by the extraction method used. Simulations with R less than unity are under-predicting the observed arsenic. Those with R greater than unity are over-predicting. This assumes that the extraction method used removes all arsenic that is associated with the modeled sorbing phases. In order to conduct a numerical evaluation of the modeling, the median and standard deviation of R was calculated for all samples sorted first according to location, second according to the extraction method, and third by the mineral phase(s) used to create the input data set. The median was generally used for comparison, rather than the mean. This was done because the median is more representative of the central tendency in skewed data and is resistant to tails and outliers. Cursory examination of general statistics revealed that most distributions of R are skewed and log-normally distributed. Gaussian distributions of R would have the mean equal to the median.

Surface assemblages of ferrihydrite or ferrihydrite + gibbsite provide the best match of the amount of sorbed arsenic for Rio Salado. Goethite or goethite + gibbsite Rio Salado surface assemblages under-predict the extracted arsenic. Gibbsite complexation of arsenic was not significant as compared to the iron oxide simulations for Rio Salado. This led to the false expectation that similar results would be obtained for the Florida simulations. The role of gibbsite in arsenic attenuation in the Florida simulations was found to be much greater than the contribution of iron oxides. The choice of surface phases is one of the strongest factors affecting the accuracy of the simulations. If an aluminum oxide phase was not included in the Florida simulations, the sorbed arsenic would have been grossly under-predicted.

Extraction method influenced model fit. For the Rio Salado sediments, HNO_3 extractions provided the best results. The Florida best fits were provided by the citrate-bicarbonate-dithionate extractions closely followed by HNO_3 extractions. Phosphate, Total Tessier, and Chao extractions produced results, that even when internally consistent, were not good predictors of the observed arsenic concentrations. The USEPA suggests that SW-846 Method 3050 will extract "…almost all elements that could become "environmentally available"." We used Method 3051; a USEPA approved microwave assisted HNO_3 extraction alternate to Method 3050 that has identical performance. A USEPA recognized extraction method was found suitable for support of the surface complexation modeling presented here.

The absence of simulated competition results in gross over-prediction of the amount of adsorbed arsenic. It was found in all simulations that silica was preferentially sorbed over arsenic on the goethite, ferrihydrite, and gibbsite and occupied more sites than arsenic. This was true even in low silica Florida waters. Carbonate and bicarbonate are preferentially sorbed over arsenic on gibbsite and compete with, but do not overwhelm, arsenic on iron oxide minerals. The role of common oxyanions in arsenic sorption is significant.

The use of filtered samples provides simulations that under-predict arsenic sorption as compared to unfiltered samples. The effect is variable in magnitude depending on the individual differences between the samples. There is some evidence, in the form of Rio Salado saturation index and mass flux calculations (Appendix A), that unfiltered samples are more representative for use in geochemical modeling. The use of measured vs. assumed porosity significantly decreases the error level. Sampling and analysis protocol is a factor in successful mechanistic modeling.

For Rio Salado, it was possible to simplify the conceptual model because of ample evidence that the system was near equilibrium. Over 90% of the arsenic is present as a single specie, As^{5+}. Most of Rio Salado simulations converged with only limited change in redox condition from the input Eh. Redox simulation and measurement can be difficult and error prone. However, the Rio Salado modeling did not require manipulation of measured Eh or "fixing or hard wiring" of redox couples to obtain numerical convergence or meaningful results.

These redox and equilibrium simplifications are not as reasonable for the Florida simulations given the presence of several species of arsenic at significant concentrations. In simulations using raw input, and simulations where redox equilibria were manipulated, charge balance requirements of the diffuse layer simulation caused oxidation of As^{3+} and subsequent sorption of the resultant As^{5+}. In raw data simulations, redox condition became strongly oxidizing due to the reduction of nitrate and other species. Redox manipulations were limited to zeroing input concentrations of redox sensitive NO_3 from the observed 0.0 to 1.4 mg/L. This did not prevent the simulation from oxidizing most of the As^{3+} in solution to As^{5+}, or altering the resultant R value at convergence, but resulted in less As^{3+} oxidation and Eh value at convergence closer to that input. It is probable that an As^{3+} to As^{5+} ratio at convergence can be obtained that matches input values by manipulation of input parameters. The geochemical meaning of such simulations would be questionable for all but the As^{3+}-As^{5+} redox couple.

Rio Salado

The R statistics for Rio Salado are presented in Table 4-1. The standard deviation divided by the median was also calculated as a measure of scatter in results. The standard deviation is used only as a rough estimator of the scatter about the median since it is truly a measure of the spread about the mean and not resistant to outliers. The median is used to rank the results. The mean and standard error of R are listed for comparison purposes.

Table 4-1
Results of Rio Salado Simulations: Summary Statistics of the Ratio of Modeled to Observed Arsenic Concentration on Sediment

Extraction[a]	Mineral Phase	Median	SD	SD/ Median	Mean	Standard Error
H_3PO_4	Goethite	0.001	0.009	1010%	0.005	0.002
H_3PO_4	Goethite and Gibbsite	0.001	0.011	1139%	0.006	0.002
HNO_3 Whole	Goethite	0.003	0.022	811%	0.014	0.005
HNO_3 Fine	Goethite and Gibbsite	0.003	0.031	1131%	0.016	0.007
HNO_3 Whole	Goethite and Gibbsite	0.003	0.029	1008%	0.018	0.006
Chao	Goethite	0.003	0.037	1158%	0.021	0.008
HNO_3 Fine	Goethite	0.003	0.028	883%	0.018	0.006
Chao	Goethite and Gibbsite	0.003	0.042	1301%	0.023	0.009
H_3PO_4	Ferrihydrite	0.245	0.222	90%	0.275	0.050
H_3PO_4	Ferrihydrite and Gibbsite	0.245	0.222	91%	0.275	0.050
HNO_3 Whole	Ferrihydrite	0.737	0.366	50%	0.734	0.082
HNO_3 Whole	Ferrihydrite and Gibbsite	0.744	0.369	50%	0.743	0.082
HNO_3 Fine	Ferrihydrite and Gibbsite	0.762	0.407	53%	0.825	0.091
HNO_3 Fine	Ferrihydrite	0.779	0.402	52%	0.818	0.090
Chao	Ferrihydrite	0.881	0.615	70%	0.963	0.137
Chao	Ferrihydrite and Gibbsite	0.882	0.612	69%	0.963	0.137
Chao NoComp	Goethite	2.413	1.504	62%	2.526	0.336
Chao NoComp	Goethite and Gibbsite	3.746	2.483	66%	4.284	0.555
Chao NCCP	Goethite	4.691	2.662	57%	4.997	0.595
Chao NCCP	Goethite and Gibbsite	7.679	4.976	65%	8.682	1.113
Chao NoComp	Ferrihydrite	19.680	13.734	70%	22.122	3.071
Chao NoComp	Ferrihydrite and Gibbsite	21.546	14.880	69%	24.378	3.327
Chao NCCP	Ferrihydrite	26.720	16.943	63%	29.636	3.789
Chao NCCP	Ferrihydrite and Gibbsite	29.320	18.954	65%	33.307	4.238

[a] All extractions performed on -80 mesh ground and homogenized sediments other than HNO_3 Whole conducted on homogenized <2 mm sediments.

We calculate R for all simulations to evaluate trends in the modeling. Trends indicate non-ideal simulation properties since any deviation from an R of unity is an error in model conceptualization or execution. Evaluation of trends in R allows assessment of the sources and magnitude of model error. The Rio Salado extractable arsenic varies considerably depending on the method used. For any given extraction, R of unity indicates that the extraction can be recombined stoichiometrically within a mechanistic surface complexation approach.

Comparisons have been made between R and temperature, pH, conductivity, redox potential, TOC, total arsenic extracted from sediments, total iron extracted from sediments, total arsenic in water, alkalinity, bulk density, particle density, porosity, the number of sorbing sites in the simulation, and BET N_2 surface area. Trends in R with respect to these variables are summarized in Table 4-2 and examples of trends are plotted in Figures 4-1 through 4-8.

Table 4-2
Trends in R as Compared to Selected Input Parameters for Rio Salado

Component	Trend in R	Nature of Trend[a]	Figure
Distance downstream (sample station)	Yes	Inverse	
BET N_2 surface area	Yes	Inverse	4-1
Total arsenic extracted from sediments	Yes	Inverse	4-2
TOC	Yes	Inverse	4-4
pH	Yes	Inverse	4-6
Porosity	Yes	Inverse	4-8
Temperature	Yes	Proportional	4-5
Conductivity	Yes	Proportional	4-7
The number of sites in the simulation	No		4-1
Total iron extracted from sediments	No		4-3
Total arsenic in water	No		
Alkalinity	No		
Bulk density	No		
Particle density	No		
Redox potential	No		

[a] Inverse trends are where R value decreases as the component value increases

Median R Values

Referring to Table 4-1, it is clear that Rio Salado models using goethite as the hydrous iron phase grossly under-predict the observed arsenic concentration (R of 0.001 to 0.003) and suffer from the greatest proportional scatter in the data between sample stations (SD/Median of 811 to 1301%). Models using ferrihydrite as the hydrous iron phase, neglecting the H_3PO_4 extractions, offer the best predictions with R ranging from 0.737 to 0.882. Of the operational extractions, Chao reagent yields the highest R-values, HNO_3 next, and H_3PO_4 yields the overall lowest R-values for any surface assemblage. The highest R-value indicates the greatest level of internal consistency, not necessarily the greatest predictive ability for the total sorbed arsenic.

The best fit to the measured extractable arsenic data is for Chao reagent with ferrihydrite and gibbsite surfaces with an R of 0.882. Chao extractions should be specific for amorphous iron and manganese phases. This indicates that the Chao extractions and simulations are internally consistent in that 88% of the amount of arsenic extracted can be simulated in a surface complexation framework. The material operationally defined by the Chao extraction as ferrihydrite and gibbsite will accurately recombine with the extracted arsenic, but at levels lower than available arsenic as defined by the HNO_3 extractions. The concentration of arsenic on the modeled surfaces is less than half of that extracted by H_3PO_4 or HNO_3. The Chao extractions were successful for modeling a portion of the surface available arsenic.

The HNO_3 extractions yield arsenic levels that are close to the maximum possible concentration as determined by XRF [108]. The best fit for HNO_3 extractions to the observations is for -80 mesh (HNO_3 Fine) surfaces as ferrihydrite and gibbsite with an R of 0.779. HNO_3 extractions represent arsenic complexed with amorphous and crystalline metal oxides and organic material and offer a good fit to the total arsenic available.

H_3PO_4 extractions are intended to extract arsenic by concentration displacement of sorbed arsenic by phosphate ions. H_3PO_4 extractions yield best match R-values of 0.254 for ferrihydrite and gibbsite. A poor surface complexation recombination is exhibited by this method.

As shown in Table 4-1, the effect of disallowing ion competition for potential arsenic sorption sites is extreme. 'NoComp' refers to simulations where there were no other ions competing for sorption sites other than arsenic. Allowing competition in the Chao extracted goethite systems results in R of 0.001 to 0.003. For the same input data with competition disallowed, R-values range from 2 to 4. The effect is lesser in scale but significant in magnitude for the Chao extracted simulations using ferrihydrite as the iron phase. Here, R from non-competitive models reaches 22 to 24 times the R-values obtained using surface complexation competition. Limited sensitivity analysis indicates that the competition effect on arsenic sorption in Rio Salado was greatest for carbonate-bicarbonate with silica and sulfate having a lesser but similar effect.

In Table 4-1, 'NCCP' refers to NoComp simulations with the additional constraint of constant porosity. The effect of the porosity assumption was less pronounced than neglecting competition, but still significant. Using a fixed porosity resulted in over-prediction because the measured porosity was generally larger than the assumed porosity of 30%. The over-prediction was a factor of 1.4 to 2.1 over all of the Chao extract simulations and mineral phases.

Trends in R as Compared to Select Input Data

Figure 4-1 depicts the relationship of R to the number of sorbing sites contained in the model and the BET surface area. R is not proportional to the number of sorbing sites assigned to the simulation, but a general trend is noted in R vs. BET surface area. A lower R is associated with the larger BET surface area. It is probable that the general relationship for increasing chemical reactivity with increasing solid phase surface area applies here. The sediments with the highest BET surface areas should have the greatest number of potential reaction sites of all possible phases by virtue of substrate surface area. These sediments exhibit the lowest R-values, the inverse of expected. The trend in BET surface area vs. R may indicate that a significant sorbing phase that forms a relatively constant fraction of available sites has not been considered in the conceptual model.

Figure 4-2 depicts the trend in R as compared to arsenic extracted from the sediments using four methods and four definitions of the sorbing surface. Although the goethite simulations do not provide a good match with respect to R, the trend in R for goethite simulations can provide insight into the model behavior and this data is plotted for comparison in most of the figures. Ideally, the graphs would show no variation in R for a given surface and extraction method. What is observed is that there is a tendency for R to decrease in all samples that were prepared as -80 mesh solids for extraction. The HNO_3 extract on whole <2 mm sediments do not clearly show this trend. This trend is also not apparent for iron extracted from the sediments (Figure 4-3). Iron extracted from sediments shows little bias with respect to R-values. The correlation of HNO_3 Whole models to observed arsenic are better than that exhibited by the other three extraction methods. Part of this is probably related to the homogenization process.

Figure 4-4 depicts trends in R as compared to TOC. Although the trend is slight for all extraction methods, and all sorbing mineral surface definitions, R tends to decrease with higher TOC content.

Of similar certainty is the relationship between R and temperature, pH, and conductivity presented in Figures 4-5, 4-6, and 4-7. There are correlations between these parameters and R. Temperature, pH, total arsenic, and conductivity relationships with R may represent a systematic variation that may not be attributable to a particular parameter because they all vary in a systematic downstream. The proportionality of R with porosity (Figure 4-8) applies to the sediments that were processed by grinding and not as much to the HNO_3 Whole samples. In the ground samples as porosity increases there is a tendency for R to decrease.

It is important to acknowledge that all of the trends discussed above are relatively weak. It appears that input parameters, singly or in groups, do not provide good empirical predictors for the quality of model fit. Some inferences can be made from this observation. First, the model is able to make predictions of arsenic sorption that are of equal quality over the moderately high variability in chemistry and sediment characteristics at Rio Salado. Second, since the parameters that R is insensitive to are critical to the mechanistic conceptual and numerical model (e.g. extracted arsenic and iron, pH, alkalinity), the observation helps validate the mechanistic approach. Lastly, the trends that are seen may indicate areas where the model and data should be investigated. This includes determining if the thermodynamic database or conceptual model can be tuned for greater accuracy, and data review for analytical bias that may have propagated in the modeling. Analytical bias is seen in decreasing R values at higher sediment arsenic concentrations for -80 mesh samples and is absent from whole sediment extractions. This type of review is valuable because any trend in R indicates a systematic deviation from the ideal.
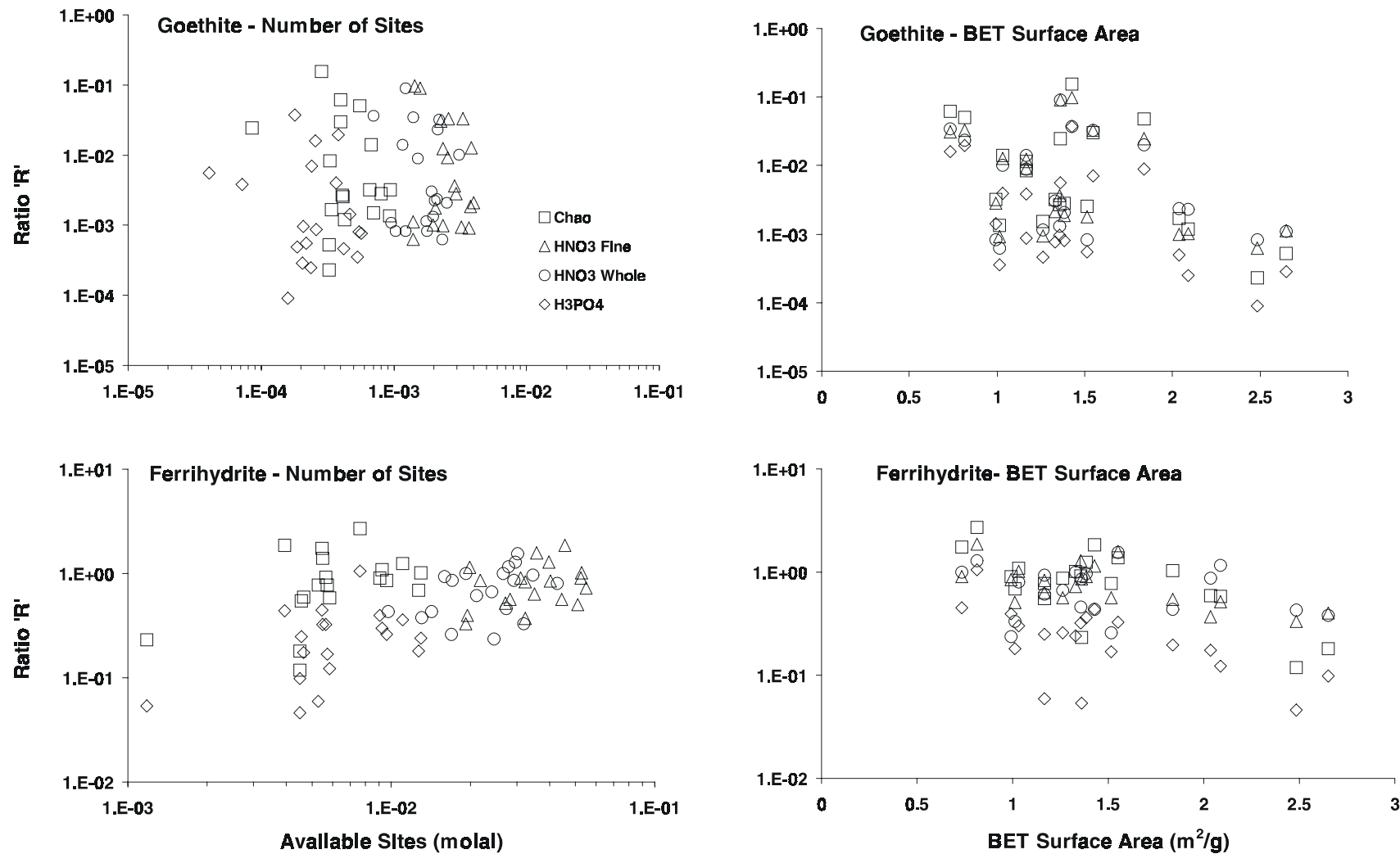
Figure 4-1
Inverse Relationship Between BET Surface Area and Model Fit Factor R vs. Poor Relationship Between the Number of Sites Available and Fit Factor R for Arsenic Extraction Methods
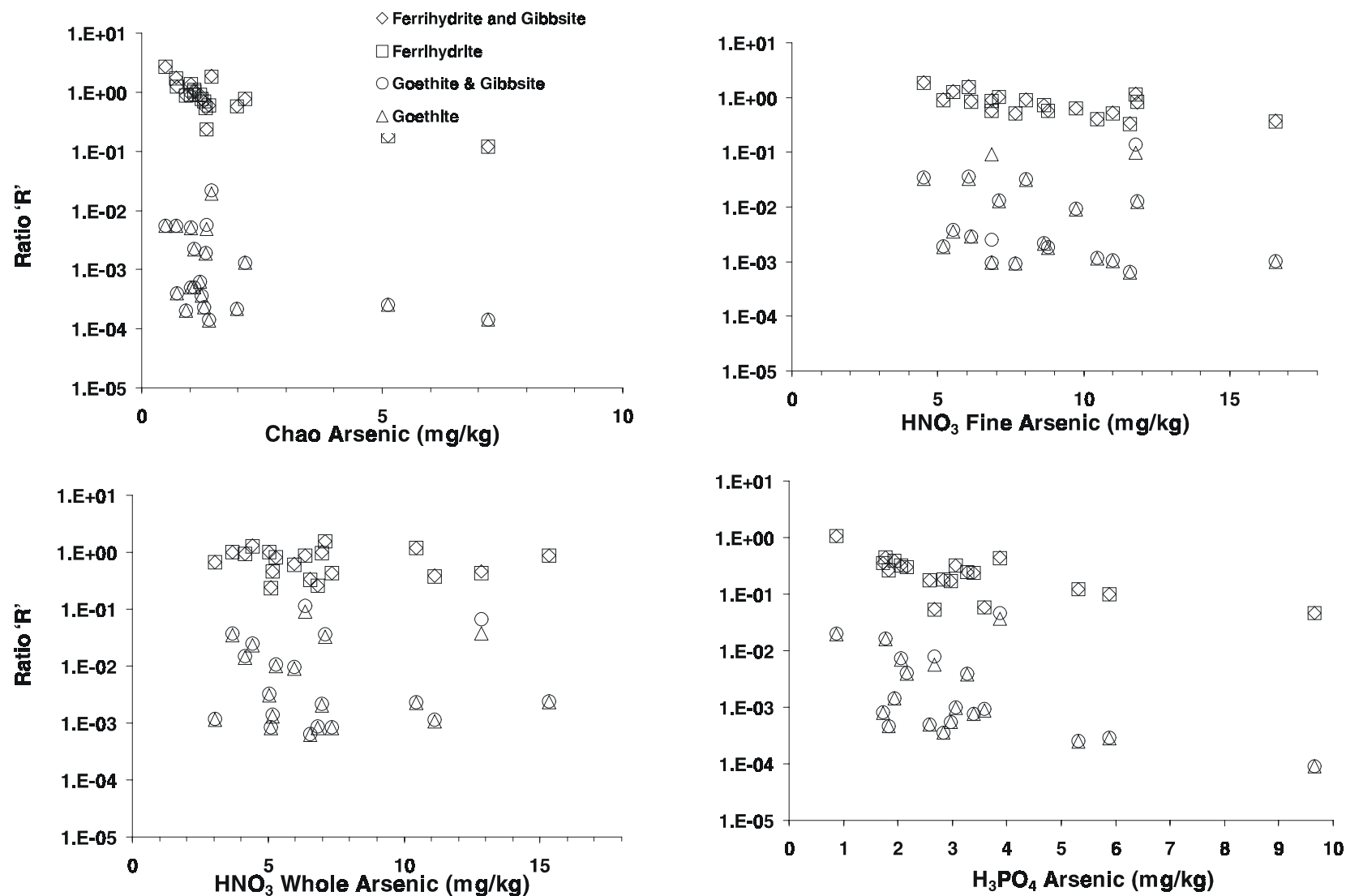
Figure 4-2
Trends in R as Compared to Arsenic Extraction Method and Surface Composition
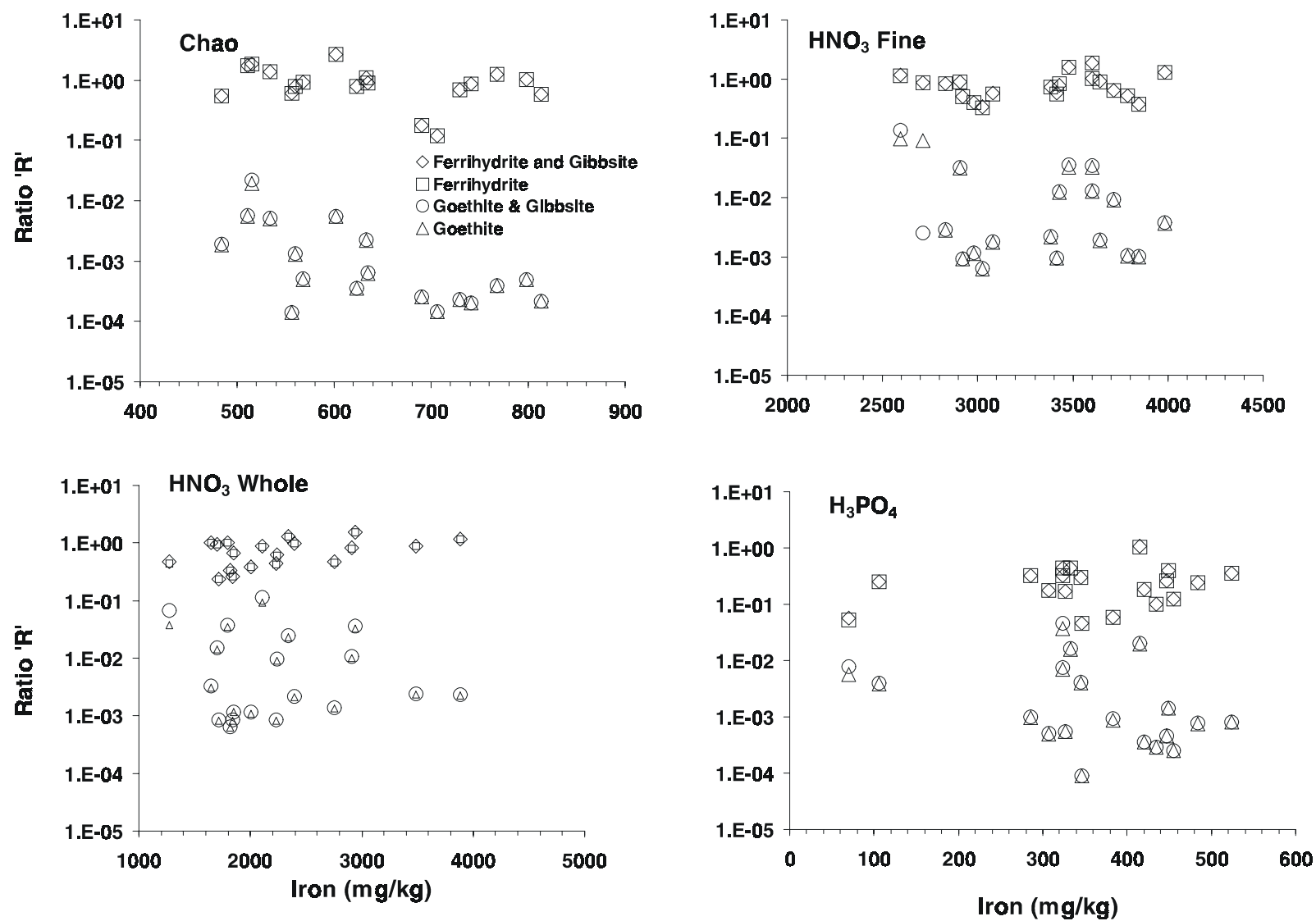
Figure 4-3
Trends in R as Compared to Iron Extraction Method and Surface Composition
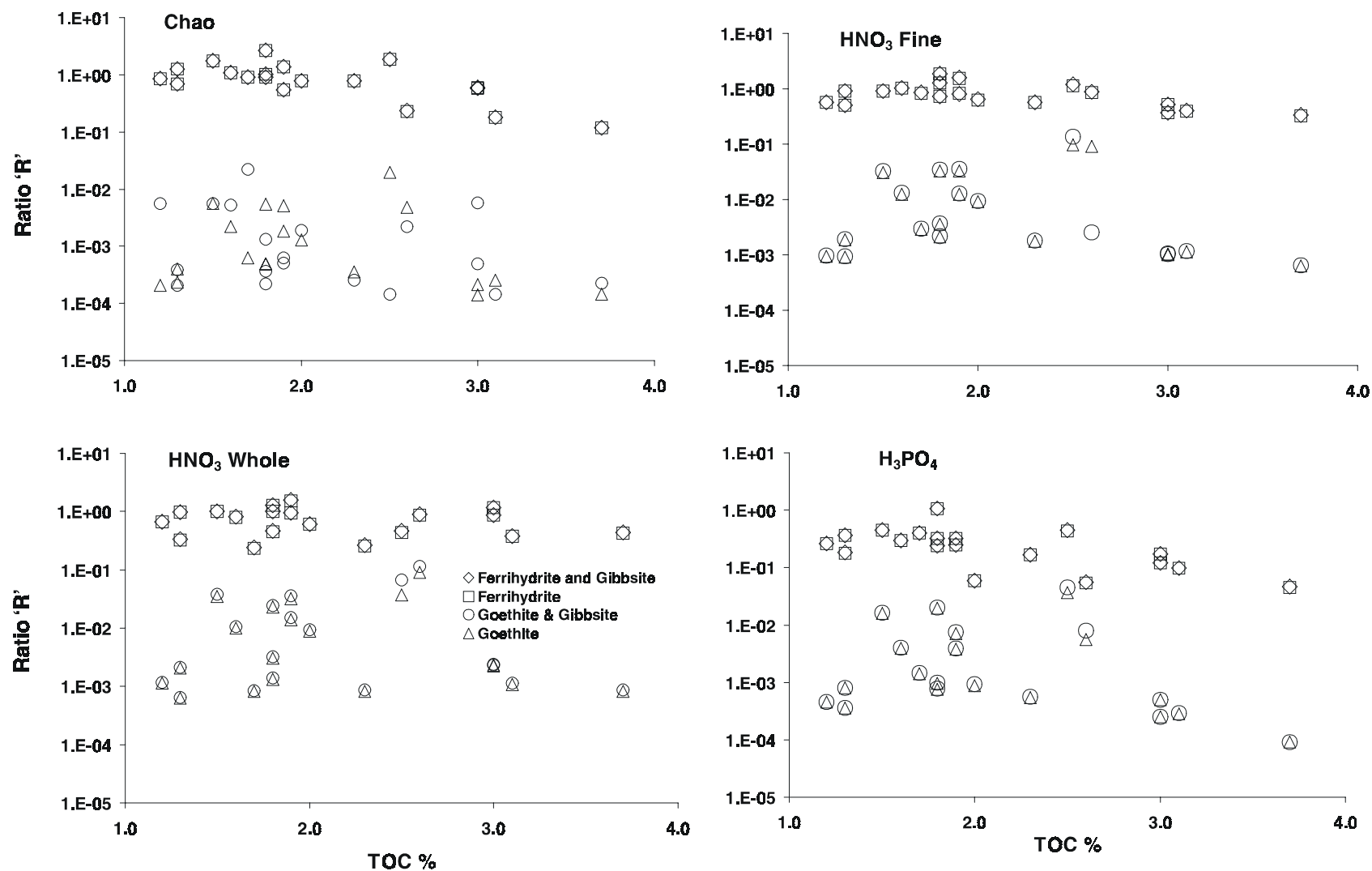
Figure 4-4
Trends in R as Compared to Total Organic Carbon and Surface Composition
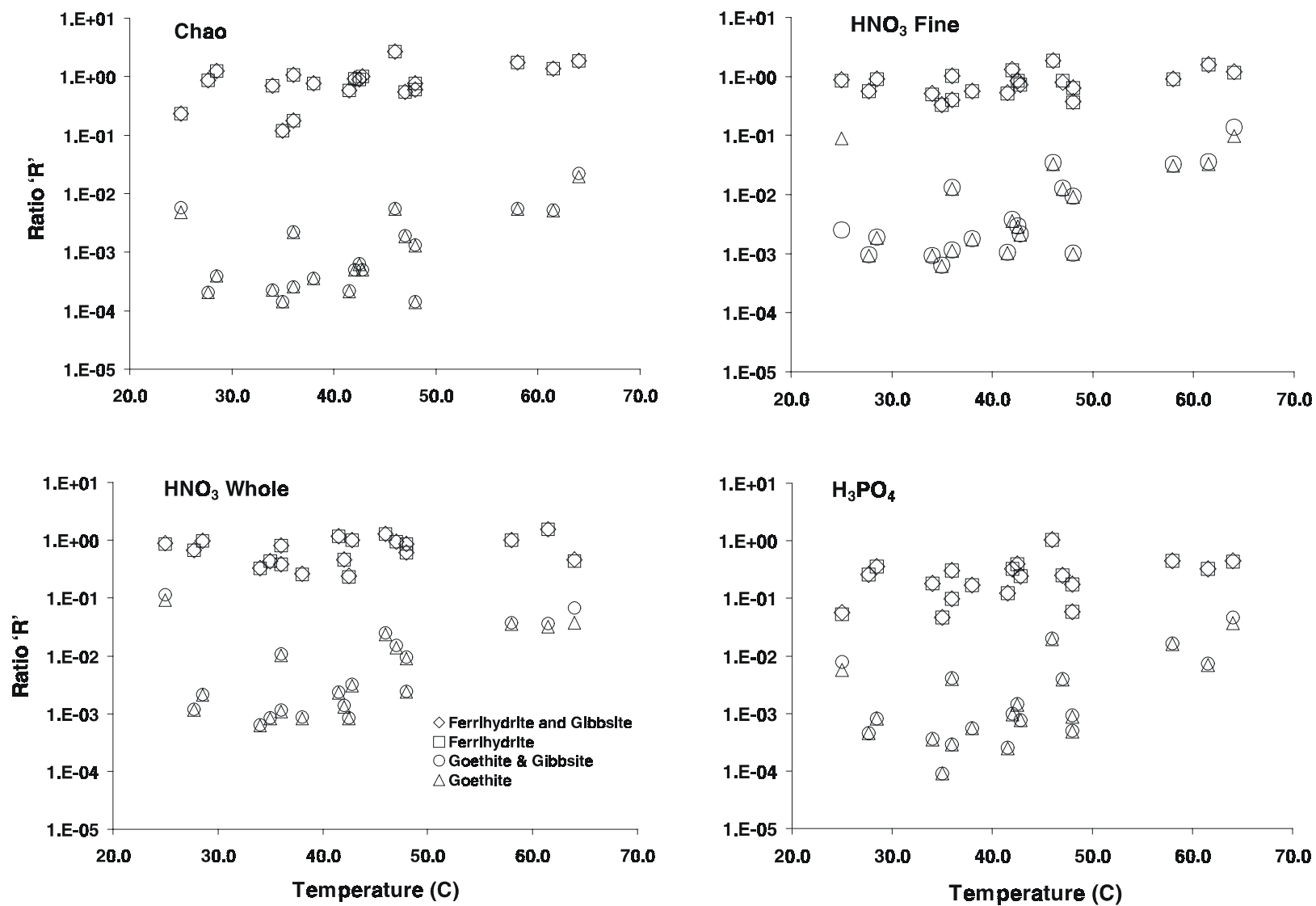
Figure 4-5
Trends in R as Compared to Water Temperature and Surface Composition
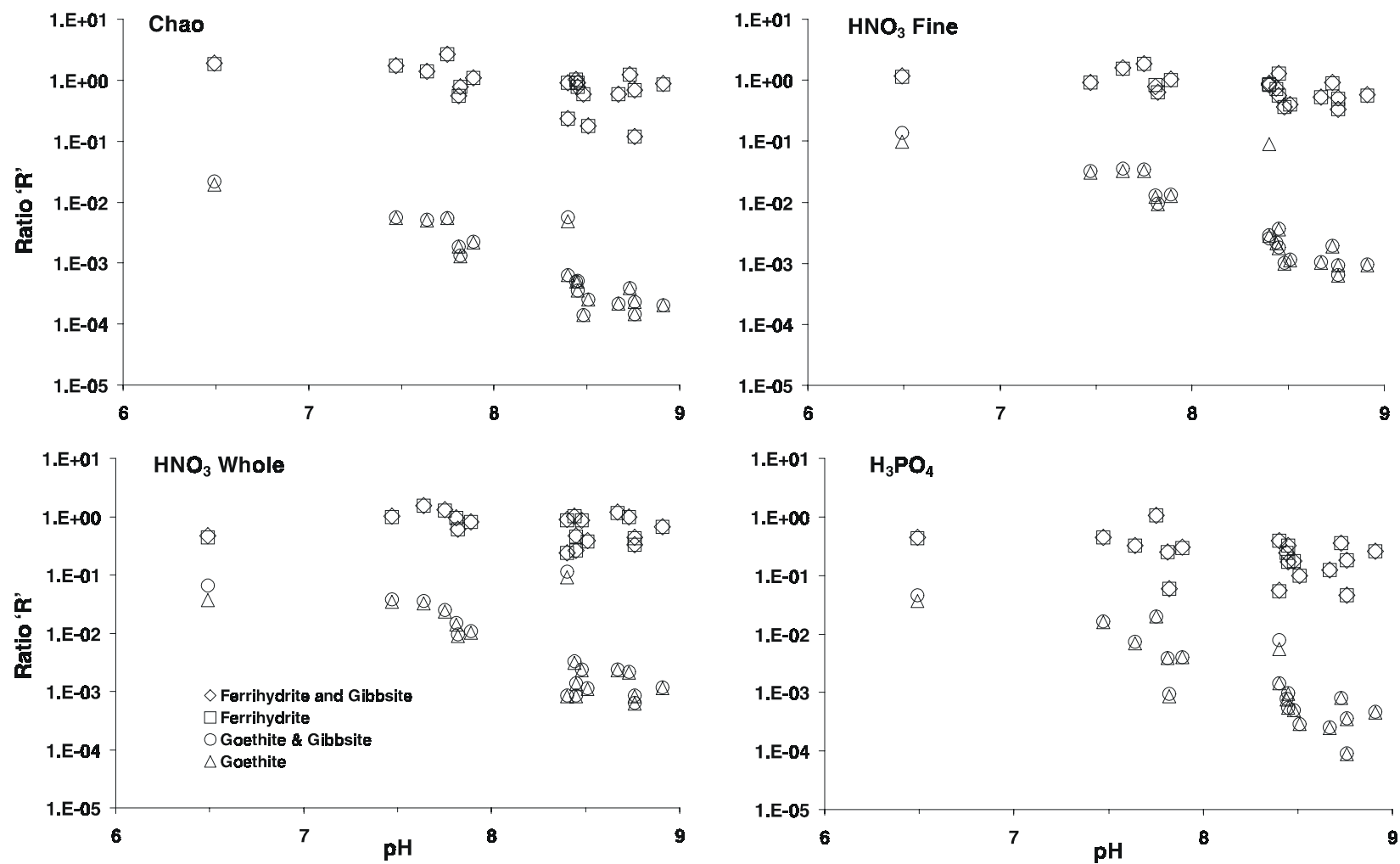
Figure 4-6
Trends in R as Compared to pH and Surface Composition
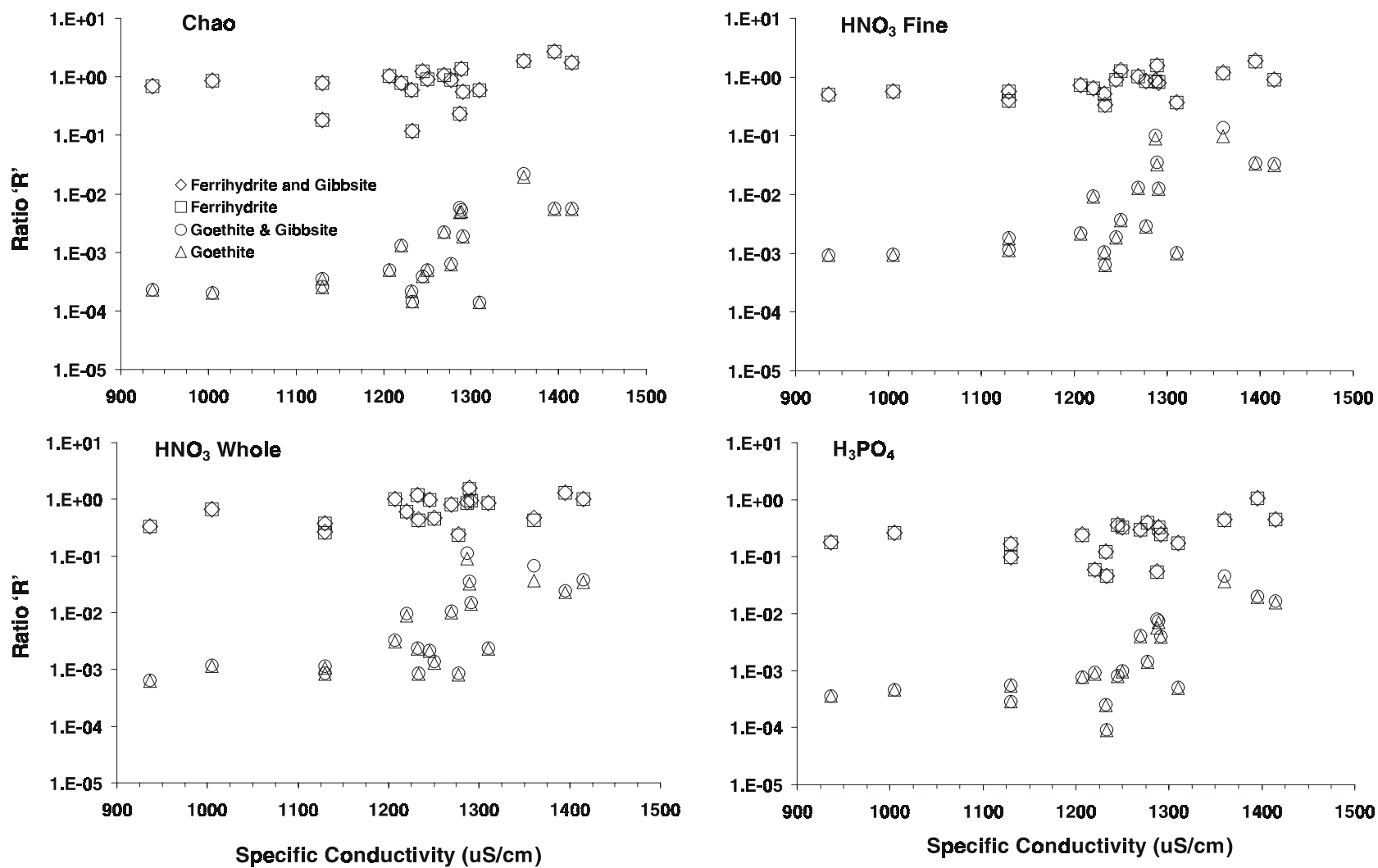
Figure 4-7
Trends in R as Compared to Specific Conductivity and Surface Composition
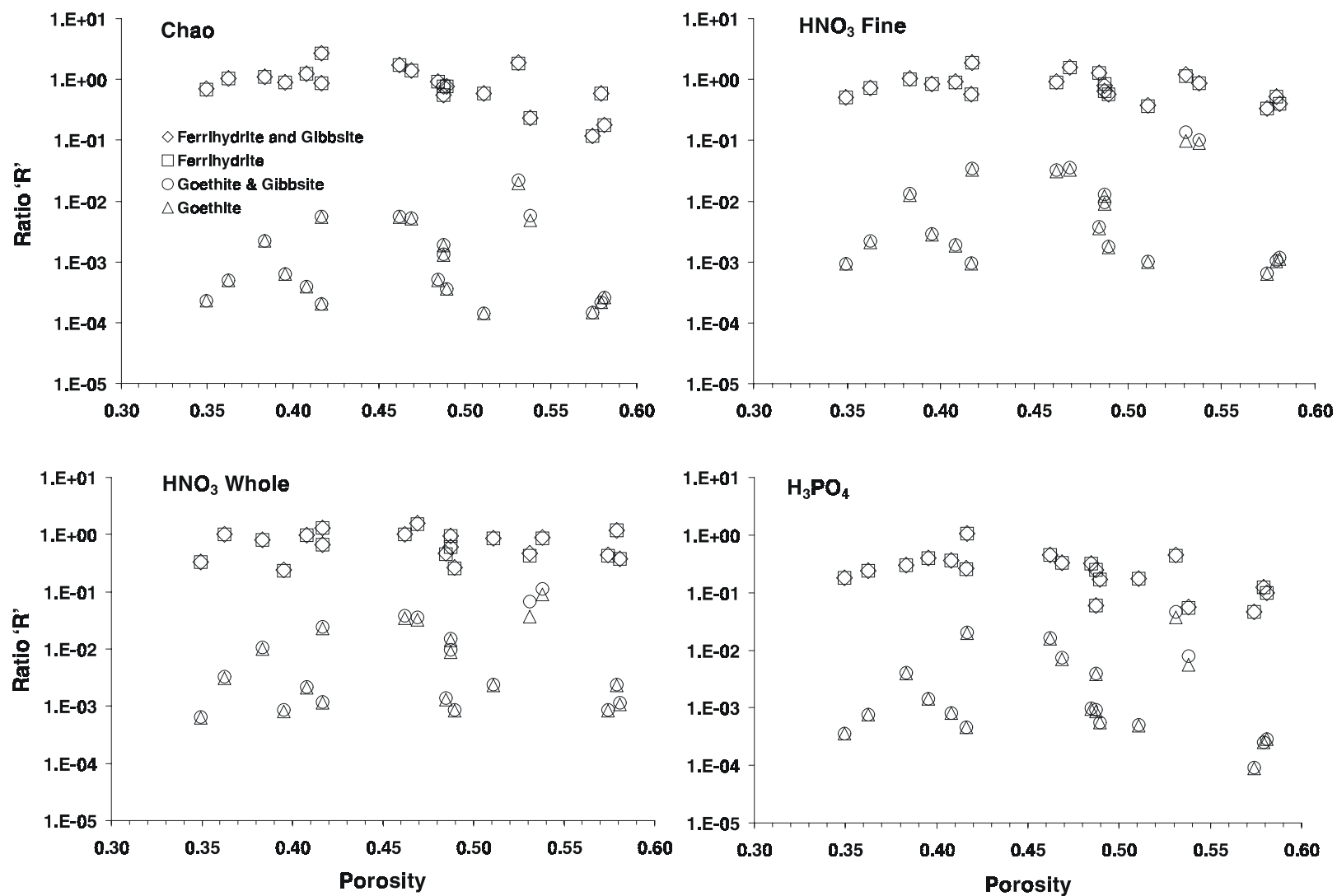
Figure 4-8
Trends in R as Compared to Porosity and Surface Composition

Florida Substations

Table 4-3 presents the R value determinations for the Florida samples. The results are ranked by median value. The standard deviation divided by the median was also calculated as a measure of scatter in results. The standard deviation is used only as a rough estimator of the scatter about the median since it is truly a measure of the spread about the mean and not resistant to outliers. The median is used to rank the results. The mean and standard error of R are listed for comparison purposes.

Table 4-3
Results of Florida Simulations: Summary Statistics of the Ratio of Modeled to Observed Arsenic Concentration on Sediment

Extraction[a]	Mineral Phase	Median	SD	SD/ Median	Mean	Standard Error
CBD	Goethite	0.01	0.0	195%	0.02	0.01
Total Tessier	Goethite	0.02	0.0	135%	0.03	0.01
Chao	Goethite	0.07	6.8	10394%	3.68	1.97
Total Tessier	Goethite and Gibbsite	0.08	0.2	297%	0.20	0.07
CBD	Ferrihydrite	0.15	0.1	84%	0.17	0.04
HNO_3	Goethite	0.18	0.3	163%	0.28	0.09
Total Tessier	Ferrihydrite	0.24	0.6	233%	0.48	0.17
CBD	Goethite and Gibbsite	0.34	0.7	216%	0.62	0.21
Total Tessier	Ferrihydrite and Gibbsite	0.47	0.6	127%	0.63	0.17
HNO_3	Goethite and Gibbsite	0.49	0.6	129%	0.68	0.18
CBD	Ferrihydrite and Gibbsite	0.63	0.8	119%	0.77	0.22
Chao	Ferrihydrite	0.96	37.5	3905%	19.65	10.83
Chao	Goethite and Gibbsite	1.12	19.0	1700%	10.03	5.49
HNO_3	Ferrihydrite	1.16	13.2	1144%	8.10	3.82
Chao	Ferrihydrite and Gibbsite	1.49	49.7	3341%	26.00	14.35
HNO_3	Ferrihydrite and Gibbsite	1.55	13.5	872%	8.49	3.90

[a] All extractions on whole air-dried sediments

Interpretation of the R values contained in Table 4-3 is less straight-forward than for Rio Salado. On initial inspection of the median values of R, there is not an extraction method or mineral that is universally superior to the others, as was the case for HNO_3 extractions on Rio Salado sediments. The Chao extractions have a poor fit as evidenced by the very high values for standard deviation, the ratio of standard deviation to median, and the standard error. Because of the broad scatter in the Chao fits, the extraction is not considered further. By similar process of elimination, the citrate-dithionate-bicarbonate (CBD) extraction as ferrihydrite (HFO) and gibbsite is selected as the superior fit. The R values indicate another significant difference from the Rio Salado samples; gibbsite has a more significant role in sorption of arsenic than hydrous iron oxides, and in some cases dominates the sorption process.

Examination of Figure 4-9 reveals some additional factors for consideration of the best extraction method and surface assemblage. Four surface assemblage's R values are displayed for both filtered and unfiltered water analyses. Three extraction methods HNO_3, CBD, and a summation of the Tessier extractions (TT) are represented. From Figure 4-9 the behavior of sample T-3 is atypical. The varied extraction methods yield uniformly low R values. When T-3 is removed from consideration the match between the HNO_3 and CBD extractions improves as does the model fit. Table 4-4 presents the calculated R values omitting all Chao extractions and T-3 data. CBD extraction as ferrihydrite and gibbsite is clearly the superior fit with a median R almost identical to the mean and very near unity.

Table 4-4
Results of Florida Simulations: Summary Statistics of the Ratio of Modeled to Observed Arsenic Concentration on Sediment with Outliers Censored

Extraction	Mineral Phase	Median	SD	SD/ Median	Mean	Standard Error
CBD	Goethite	0.02	0.02	110%	0.03	0.01
Total Tessier	Goethite	0.03	0.03	100%	0.04	0.01
Total Tessier	Goethite and Gibbsite	0.10	0.23	247%	0.23	0.07
CBD	Ferrihydrite	0.19	0.11	59%	0.20	0.04
HNO_3	Goethite	0.21	0.31	150%	0.32	0.10
Total Tessier	Ferrihydrite	0.31	0.59	190%	0.57	0.19
HNO_3	Goethite and Gibbsite	0.58	0.63	109%	0.79	0.20
Total Tessier	Ferrihydrite and Gibbsite	0.61	0.58	96%	0.75	0.18
CBD	Goethite and Gibbsite	0.69	0.76	110%	0.74	0.24
CBD	Ferrihydrite and Gibbsite	0.97	0.74	76%	0.92	0.23
HNO_3	Ferrihydrite	1.24	14.04	1131%	9.69	4.44
HNO_3	Ferrihydrite and Gibbsite	1.65	14.32	866%	10.14	4.53
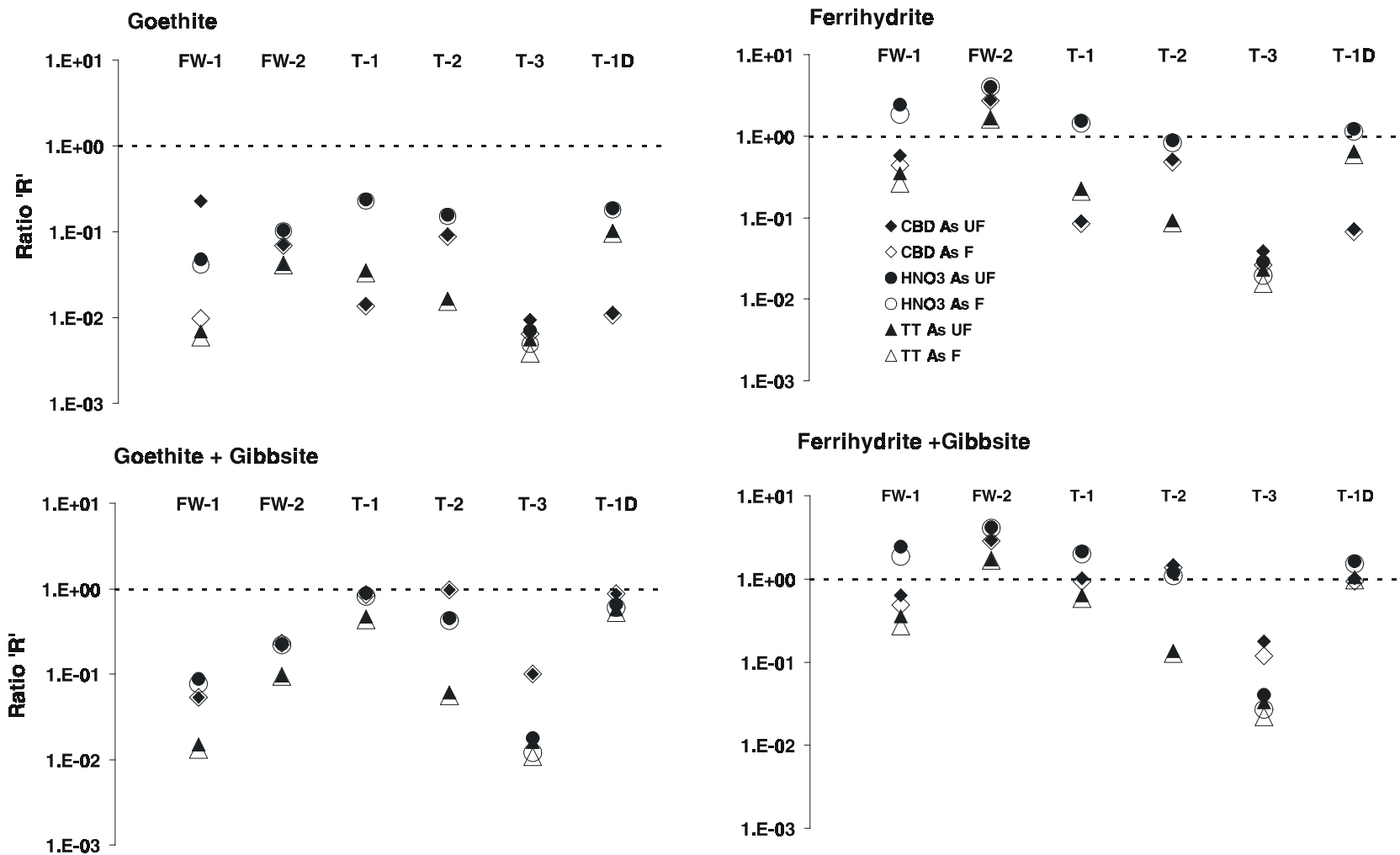
Figure 4-9
Trends in R by Sample Station, Extraction Method, and Surface Assemblage for the Florida Sediments

Sensitivity Analysis

The modeling effort has evaluated the sensitivity of the approach to the operationally defined extraction method, surface assemblage of minerals, competition for sorption sites, and porosity as part of the general modeling effort. As previously presented, the effect of varying approach and assumptions is profound. On the basis of this effort it is known that incorrect assumptions regarding the conceptual model can result in model predictions that are orders of magnitude removed from reality. The effort has demonstrated that the potential for these errors can be controlled by careful consideration of the meaning of field observations and modeling output while defining the conceptual model. This requires an iterative modeling approach.

Iterative modeling of various conceptual models to discover the best model fit provides no information on the effect of errors in the input data on model output. Previous sensitivity analysis points at silica and alkalinity concentrations as factors that will strongly influence sorption of arsenic. It was known that the model would be sensitive to pH and aqueous arsenic concentration. Two sample locations, Tyndall AFB station T-1 and Rio Salado station 12 were selected for use in sensitivity analysis. The ferrihydrite + gibbsite surface assemblage and unfiltered water analysis was used for both stations. We varied alkalinity, total arsenic, pH and total silica concentrations ± 10% from the measured values to simulate the effect of errors in the determinations. The output is then processed in the same manner as previously and the concentration obtained from the altered data set is compared to the original. The results of this analysis are presented in Table 4-5.

Table 4-5
Results of Limited Sensitivity Analysis: Percent Change in the Modeled Sorbed Arsenic Concentration

Tyndall T-1			Rio Salado 12		
Parameter and Baseline	**Variation from Baseline**	**Modeled Arsenic Percent Change**	**Parameter and Baseline**	**Variation from Baseline**	**Modeled Arsenic Percent Change**
Alkalinity	+10%	5.72%	Alkalinity	+10%	0.03%
10 ppm	-10%	0.07%	396 ppm	-10%	1.31%
Total Arsenic	+10%	16.93%	Total Arsenic	+10%	7.09%
211 ppb	-10%	0.03%	983 ppb	-10%	-6.18%
pH	+10%	30.53%	pH	+10%	-11.23%
5.10	-10%	-19.00%	8.44	-10%	26.81%
Total Silica	+10%	5.69%	Total Silica	+10%	-8.28%
3.43 ppm	-10%	0.10%	488 ppm	-10%	11.29%

Reviewing the data above, it is immediately noted that the magnitude of change in output is not equal for equal magnitude but opposite sign changes in input parameters. It is also notable that the magnitude of output change is not directly proportional to the magnitude of change in input. The general reasons for the response to the sensitivity analysis are discernable from the site-specific geochemistry.

Examining the alkalinity and silica results, it is noted that Tyndall and Rio Salado respond to alkalinity and silica changes in different manners. Tyndall waters are poorly buffered with a pH below that optimal for arsenic sorption. Raising alkalinity, or silica, in the Tyndall sample has the effect of increasing arsenic sorption. This is probably due to the associated pH buffering that allows more arsenic to sorb. The increased competitive effects of raising the alkalinity and silica are less than the increased sorption possible in a more highly buffered system. For the same reason lowering the alkalinity and silica has little effect, silica, carbonate, and bicarbonate competition is less important than pH, for the case of Tyndall T-1. The Rio Salado alkalinity response is a bit simpler. The system is highly buffered so raising alkalinity has little effect on sorption, competition by carbonate and bicarbonate is already near a maximum. Lowering the alkalinity does increase sorption, albeit at a small percentage, by reducing competition. The effect of silica competition in Rio Salado is much stronger than Tyndall, as seen in the magnitude of change in the output.

The change in output because of modification of arsenic concentration moves in a manner that is predictable in direction. Although monotonic, the manner of response of Tyndall and Rio Salado is quite interesting. Tyndall simulations indicate that the arsenic sorption is surface controlled rather than controlled by the amount of arsenic in solution, since lowering the aqueous arsenic concentration does not affect sorption while raising the concentration greatly increases the sorbed arsenic. Rio Salado is more balanced, with output magnitude change almost equal for both raising and lowering the arsenic concentration. Rio Salado sorbed arsenic concentration is not fully dominated by the surface.

Changing input pH caused the largest changes in sorption of any of the sensitive parameters presented in Table 4-5. This was not unexpected. The fact that the direction of change is opposite for Rio Salado and Tyndall is explainable by the relative position of solution pH with respect to maximizing sorption. The pH at which maximum sorption takes place is determined by the entire site-specific biogeochemical environment, not by a just a single factor, such as mineral assemblage. It is clear from the results that the Tyndall T-1 system is below the pH of maximum sorption, and that the Rio Salado Station 12 system is above the pH of maximum sorption.

The sensitivity analysis has revealed that small changes in input chemistry will have large changes in model output. Efforts should be made to maximize data quality for sensitive parameters in order to maximize the predictive capability of mechanistic and deterministic methods. The observed difference in magnitude and direction of response from what we expected prior to the simulations does not bode well for alternative modeling approaches that assume linear relationships or Gaussian distributions of the relationships between model input and output. Detailed mechanistic evaluation of surface complexation reveals relationships that will be obscured by other approaches.

5
DISCUSSION

When we attempt to model the mobility of metals in the environment using surface complexation, there are certain decisions that need to be made. An understanding of the solids responsible for sorption must be developed or assumed. This understanding is necessary so that the specific minerals that compose the solid phase can be specified, since each mineral has different complexation properties. Choices must be made as to how the solid phases will be quantified. Here, we quantify the mineral phases using operationally defined wet-chemical extractions. The extractions are 'operationally defined' because past use has indicated that the methods will generally dissolve the mineral of interest, but we can not be certain for all cases that only the mineral of interest will be extracted. This requires that we make choices regarding the best operationally defined extraction for our intended use. Similarly, the breadth of chemical analysis, including the need for arsenic speciation, must be evaluated. All of these requirements for successful mechanistic modeling are driven by project goals and the available data, so it is inevitable that some compromises from the ideal will need to be made.

The successful application of a multi-component mechanistic model to the field distribution of arsenic is demonstrated here. Evaluation of the ratio of modeled to observed arsenic, R, for several conceptual models provides insight into the magnitude and nature of errors in the modeling process. It has been shown that: the conceptual model for field application should consider competitive complexation of carbonate and silica; it is difficult to select an appropriate extraction method prior to modeling the data; and, selection of the appropriate hydrous metal oxides is critical.

The Rio Salado was found to offer a natural analog for testing of mechanistic approaches to the modeling of arsenic attenuation. Detailed information regarding the use of a mechanistic arsenic modeling approach in a natural system was not found in the literature. This makes it difficult to make a quantitative assessment of the precision of the model fit as compared to other work. Detailed geochemical modeling is generally recognized to be a developing science. Therefore, the capability demonstrated here to model the actual concentrations of arsenic present on Rio Salado and Florida sediments to about ± 50% is a success.

Extraction Methods

Care must be used in selection of operationally defined extractions. It is difficult to select which extraction method will be representative of a particular labile or bioavailable arsenic fraction, but the complexation modeling using ferrihydrite was internally consistent. The Chao reagent, hydroxylamine hydrochloride, provided the best results, if arsenic concentration on amorphous surfaces is of interest. The Chao extract simulations, which should represent arsenic complexed with amorphous iron phases, have accounted for less arsenic than found in the extract. This

means that arsenic was preferentially extracted as compared to the amorphous iron oxides. The HNO_3 extractions have been operationally defined as removing surface-active organic, amorphous and crystalline phases. Again, the simulations are internally consistent but about 10% less accurate than the Chao extracts. The HNO_3 extractions provide the best match (85% average) to the total arsenic as defined by XRF. Considering the best match as a combination of prediction of total available arsenic and internal consistency in a surface complexation framework the HNO_3 extractions offer the best match overall.

The HNO_3 Whole extract does not represent the best model based on R approaching unity; that distinction belongs to the Chao extractions. However, it is the case that the HNO_3 Whole extract provides the best model, based on the tendency for HNO_3 Whole R-values to be more resistant to non-ideal behavior. The median values for model fit (Table 4-1) favor the Chao and HNO_3 Fine extractions on ground sediments as the best simulations. The HNO_3 Whole median R of 0.74 under-predicts the observed arsenic by about 25%. The relationships between BET, total sites in the model, and R indicates that the under-prediction is not due to a problem with the numerical simulation. This is probably the result of an underrepresented sorbing phase or a deficiency in the conceptual model. We believe that this is due to complexation by a combination of organic, manganese, silica, and carbonate surfaces that are not represented in the model. The HNO_3 extractions have been used to reconstruct only select iron and aluminum sorbing surfaces. It is known that there is an organic carbon component in the sediments, and that the organic carbon (TOC) is associated with arsenic. The 25% under-prediction of the inorganic HNO_3 model is quite close to the average amount of arsenic in sediments associated with organic material as determined by partial extraction [108]. Based on the magnitude of arsenic in the organic partial extractions, it is probable that the organic fraction of the Rio Salado sediments may account for most of the arsenic 'missing' from the HNO_3 Whole simulations.

Complexation simulation for the Florida sites was also successful. As revealed in the tabular data and graphical analysis, the assumption that the arsenic complexation in Florida would be dominated by iron phases, as it was in Rio Salado, was not correct. Inclusion of aluminum hydrous metal oxide phases resulted in successful representations of the observed arsenic distributions. The testing of CBD extractions on the Florida sediments indicates promise for this operationally defined method. It is suggested that additional development of a standard protocol among practitioners for sample collection and extraction will enhance comparability of data and stakeholder acceptance.

The fact that a commonly used USEPA sanctioned sediment extraction method will work for surface complexation modeling is very promising. Not only could this allow modeling to be supported by standard laboratory methods but also allows assessment of historical data. The HNO_3-based USEPA 3050 and 3051 extraction methods have been used at thousands of hazardous waste sites. Since this data is available, it may be possible to continue the process of model validation using existing data. Overall, through careful geochemical examination and modeling, we can predict the inorganic complexation of arsenic using wet-chemical extractions.

Sorbing Mineral Phase

Examination of Table 4-1 clearly indicates that the choice of sorbing iron oxide phase, goethite vs. ferrihydrite, is one of the most significant factors affecting model fit. The dominant

difference between these two phases with respect to application of surface complexation modeling is the specific surface area of the mineral. Definition of the appropriate mineral phase for use, via separate lines of evidence, has not unambiguously indicated the correct mineral assemblage to use in modeling the Rio Salado arsenic distribution. Evidence for both phases exists. Defining the appropriate mineral assemblage as the one that best fits the modeling is circular with respect to defense of a mechanistic modeling approach, but is used here as a first approximation. The contribution of goethite to arsenic sorption is insignificant as physically defined in the simulation. Ferrihydrite is the appropriate phase to use for Rio Salado.

The ferrihydrite used in the simulations has a surface area over 13 times greater than the goethite. Field evidence for the presence of ferrihydrite, such as iron staining or coating observable with a hand lens, was absent in Rio Salado. Saturation index calculations show goethite to be thermodynamically stable over the entire stream reach and ferrihydrite only partially so. Spectrophotometric detection of goethite was accomplished and goethite was observed petrographically. Partial and operationally defined extractions show the presence of both phases. Based on observation and modeling, the Rio Salado system appears to have mixed iron oxide sorbing surfaces, goethite and ferrihydrite.

Arsenic Speciation to Support Surface Complexation Modeling

Chemical speciation data is useful for risk assessment. Speciation has a direct influence on the environmental availability of chemicals, their behavior over time, and attenuation under transport conditions. In the case of inorganic versus organic arsenic, speciation provides a better quantification of toxicity than use of total arsenic determinations. The data from the Rio Salado and Florida sites, combined with the literature on the occurrence of arsenic species, show that organic arsenic is a common component in natural systems. The presence of organic arsenic as a small (<10%), but measurable component of high-arsenic natural waters was confirmed. A novel field speciation approach was tested and found to work well for As^{3+}, As^{5+}, and MMAA but had significant problems (since resolved) in quantifying DMAA. From the literature, organic arsenic is present in low arsenic (<100 ppb) systems at 5-60% of the total arsenic available. From this work, it appears that the presence of organic arsenic can be assumed in high arsenic surface systems as well.

Our modeling treated organic arsenic as part of the total inorganic concentration. The error resulting from this simplification was not quantified. Organic arsenic species can be separated from inorganic species in water, however, error analysis requires meticulous quantification of sorbed organic arsenic species on sediments. Published K_{int} for MMAA and DMAA are limited to two papers for one mineral phase. We predict that modeling results will be enhanced in the future by specifically addressing organic arsenic complexation, however, much of the fundamental data is not currently published.

Field speciation of arsenic is readily accomplished and inexpensive. When speciation techniques are employed, it eliminates the error in toxicity calculation attributable to the difficulty in preserving arsenic species. The speciation and modeling of inorganic arsenic indicated that when As^{3+} was detected it was generally not in equilibrium with the redox potential of the water. The simulations were not constrained to force redox conditions so that the model would predict the observed As^{3+} concentration. Because As^{3+} is more toxic and more mobile than As^{5+}, it is

important to be able to predict As^{3+} concentrations separately from As^{5+}. Forcing redox conditions in the model is not appropriate because of the unrealistic constraints it imposes on the entire simulation. Based on our observations of in-stream As^{3+} oxidation rate ($t_{1/2}$ of 0.13 hours), and the similar rates in the literature, we believe that As^{3+} modeling will need to be kinetically constrained. Although the approach is more complex than the effort reported here, the most recent versions of PHREEQC support kinetics, and there is a large body of literature on reactive transport simulations. Reactive transport modeling of As^{3+} water-mineral partitioning can be accomplished within the framework presented here, although at an unknown error level.

Competition

Appropriate application of ion competition for sorbing sites is essential to implementation of surface complexation modeling [15, 109]. The comparative results presented here for the Chao extractions, with and without competition, indicate that the error of neglecting competition can be very high. The error can equal or exceed inappropriate choice of mineral phases. Examination of the model output indicates in many cases that silica occupies more sorption sites than any other sorbing compound or ligand. Current research on silica sorption on minerals indicates that silica sorption is probably more complex than simulated here. The published information on carbonate sorption is very limited, presumably due to the experimental difficulty. We found that low error levels depended greatly on the inclusion of common anion competition with arsenic for sorption sites. If sorption competition by common anions and cations, particularly carbonate and bicarbonate from atmospheric interaction, has been neglected in laboratory determinations the parameters produced may be suspect.

Based on our example, field application of surface complexation modeling will rarely be successful if competition is neglected and this simplification should be avoided in model conceptualization. This indicates the need for increasing numbers of laboratory determinations of single-species, single-mineral surface complexation parameters, particularly major anions and cations in natural waters or surrogate solutions. The generality of the approach could be tested more rigorously if there were more complexation parameters available for mineral surfaces and common anions and cations, particularly carbonate-bicarbonate and silica.

Trends in R: The Ratio of Modeled to Observed Arsenic

Several major changes in water chemistry take place as Rio Salado water flows downstream. Correlation of these downstream variables with R allows some assessment of factors controlling the model fit to be made. The water cools, the pH rises, and the specific conductivity of the water decreases downstream. It is not possible to ascertain with certainty whether change of these three processes individually, or in combination, is the cause for the observed downstream trends in R. If it is assumed that pH effects on sorption are well described by the general two layer model, it is possible that temperature effects on the K's are responsible for the slight downstream trend towards lower R-values. The observed trend in R with pH can also be the result of in-situ K_{int}, K_{+}, and K_{-} differing from the values used in the model. Feedback response between all of these parameters and variables cannot be discounted. Although the trends in R are small in magnitude and exhibit low correlation, we feel that additional effort to evaluate the observed trends in R will be rewarded by a more fundamental understanding of the sources of error.

All of the thermodynamic calculations executed in PHREEQC are temperature corrected, with exception of K_-, K_+, K_{int}, and the surface charge calculations. If the slight apparent temperature dependence of R is real, and the practice of surface complexation modeling of field data expands in the direction of using laboratory-derived pure-mineral values; development of complexation temperature dependencies would be useful. It will also be necessary to allow the temperature to vary in the equations that govern surface charging in geochemical codes. Currently, this variable is fixed at a constant 25°C in MINTEQA2 and PHREEQC surface charge calculation algorithms.

Some sediment samples were homogenized to enhance reproducibility between replicates [108]. This should probably be avoided. The total arsenic extracted from sediment is inversely proportional to R (Figure 4-2) in samples that were homogenized using grinding, sieving, and quartering. This trend is not as apparent in the whole sediment samples (HNO_3 Whole). Comparison of the two HNO_3 extract arsenic concentrations shows that the ground sediments are shifted to higher values and show a stronger correlation with R than the whole sediments. Taken together, this indicates that the trend towards lower R with higher arsenic (under-prediction of the analytical concentration obtained from the extraction, and resultant 'true' concentration of sorbed arsenic) may be due to liberation of arsenic that is not normally surface available during grinding. The model would then be predicting lower than observed arsenic concentrations because the observed concentrations are really greater than 'true' values because of a sample preparation and extraction artifact. The above requires that the amount of iron extracted is less enhanced by grinding than the extracted arsenic, otherwise the model would have sufficient sites to use for the increased level of arsenic and there would not be a trend in R. Support is found in the poor correlation found between extracted iron and arsenic for Rio Salado sediments [108], the lack of a relationship between R and iron extracted (Figure 4-3), and that hydrous metal oxides are dominantly found as grain coatings.

The lack of a dependency between R and extracted arsenic, or porosity (Figure 4-8) for the HNO_3 Whole sediments may indicate that the use of whole sediments for HNO_3 extraction is the overall most successful technique that we employed. Common sediment preparation techniques should be evaluated before use to avoid bias in R. Whole grain, air-dried sediment samples are preferred. Use of larger than normal sample aliquots to avoid nugget effects and other bias resulting from inhomogeneity is also appropriate.

General Observations

Surface complexation modeling will be used in the future for prediction of the distribution of trace elements, including arsenic. In order to maximize the consistency and usefulness of future efforts, additional testing of surface complexation modeling in complex but well understood geochemical systems would be useful. Development of relationships for complexation by biological and mixed organic-mineral substrates is critical to the future development of the mechanistic approach. This should be advanced in parallel with the development of protocol for field data collection used in support of geochemical modeling, specifically sediment characterization in support of surface complexation modeling.

In order to expand the use of laboratory-determined sorption parameters to environmental studies, the practice of defining solid phases and sorbed ions on natural materials needs additional development and/or agreement among practitioners. It would be useful to assess the

ability of other extraction schemes to support of the application of complexation modeling. If there is to be general transference of laboratory parameters to field use, it is necessary to build consensus on the appropriate extraction method to use on natural sediments to emulate the laboratory results. Without this consensus, the method for proper application of laboratory results to the field remains ambiguous.

6
IMPLEMENTATION OF THE RESULTS

Before this effort, the potential error in surface complexation modeling of arsenic water-mineral partitioning in natural systems was unavailable in the literature. It is now possible to place some error bounds on modeling of arsenic water-mineral partitioning, at least for the procedures used in this study. Since the modeling effort was conducted without fitting by artificial parameter variation the Rio Salado approach is transferable to other systems. The validation of the approach at the Florida sites indicates suitability for contaminated sites. The general question of how to implement the results of this study to meet arsenic management goals remains.

Determination of the water-mineral partitioning of contaminants is essential to evaluate contaminant transport. Accurate contaminant transport determination forms the underpinnings of risk assessment, remedial design and feasibility studies, and quantification of natural attenuation. The more accurate the assessment, the less uncertainty in cost and the probability of success. Numerical modeling is used to make these determinations. There are mechanistic and empirical strategies to determine a contaminant's transport parameters. The mechanistic strategies would generally employ geochemical modeling and flow-field determination using sequential iteration of the geochemical and the flow code. This is the strategy employed in codes such as UNSATCHEM, HYDROGEOCHEM, and the newer reactive transport formulations of PHREEQC. Although computationally intensive, and requiring expert implementation, mechanistic strategies are intrinsically better than empirical. However, this level of detail may not be required for all decisions.

The PHREEQC modeling approach presented can also be used in a semi-empirical manner. The Rio Salado simulations can be viewed as an example of a semi-empirical strategy. In contaminant transport models, some sort of a retardation or decay factor is used to numerically account for chemical and physical interaction of a contaminant. These interactions cause changes in the aqueous and solid phase distribution of the contaminant over the flow-field. Each of the Rio Salado sampling stations is a point in the surface water flow-field of Rio Salado. The modeled water-mineral partitioning for each station is easily converted into a partition coefficient or retardation factor. These numbers can be used in existing contaminant transport models rather than an estimated or fixed retardation factor. Whether the mechanistic sequential iteration strategy is used, or the semi-empirical approach employed, the data collection and geochemical modeling approach presented here provide guidance on implementation of arsenic surface complexation modeling.

PHREEQC has been shown to be useful as part of predictive toolbox for arsenic environmental management. One of the determinations of this study is that successful implementation of PHREEQC, or any other thermodynamically based approach to model partitioning of arsenic in the environment should consider the following factors.

- Surface complexation modeling requires the conceptual model of the system to be well developed. The conceptual model governs how the numerical model is set up. Geochemical codes like PHREEQC are not readily used in an inverse or parameter estimation mode in the manner of groundwater flow codes. For example, in geochemical codes the differences between the data sets used to calculate water concentrations from initial solid concentrations, and the data sets used to calculate solids concentrations from a known aqueous concentration can be profound. Requirements for data pre- and post-processing can also be substantial. These factors are not limitations, but rather point to the need to clearly understand the questions to be answered before engaging in geochemical modeling. Broad-based exploratory modeling of geochemical data sets rarely produces results useful to environmental management. Phased and structured approaches are the most fruitful.

- Chemical analysis of waters must be broad in order to support the modeling effort. Common compounds such as silica, bicarbonate, and sulfate will strongly effect modeling results. All common anions and cations should be determined. Trace elements (part-per-million and below concentrations) should be included in the analytical program because of the influence they exert on the complexation of part-per-billion concentrations of arsenic in water. Trace element geochemistry in natural and contaminated waters varies enormously. It is premature to discount the influence of trace elements in surface complexation modeling until evidence to the contrary exists. Modeling cannot be successfully conducted if the only parameter available is arsenic concentration.

- The need for arsenic speciation analysis to support the modeling effort will depend on the project goals. It is suggested that, as a minimum, speciation be conducted during the early part of an arsenic assessment. This is to determine if evaluation of As^{3+} transformation kinetics or significant organic arsenic concentrations will be an issue in meeting goals. The geochemical modeling process is linear. Even minor changes in the conceptual model generally require reconstruction of all input data sets and reprocessing of all output data. This makes it virtually impossible to factor in kinetics or additional species into the results obtained from a modeling framework that did not include them from the onset. The determination of the necessity of arsenic speciation should be made before detailed modeling begins.

- The modeling effort revealed the magnitude of some of the potential error sources in applying a mechanistic model. The extraction method used to quantify surface phases and the assumptions used to define those same surfaces are the greatest source of potential error. The error from these two parts of the modeling process can approach orders of magnitude in scale. This indicates the need for detailed assessment of the solid phase. Solid phase mineralogy, assumed or indicated, is essential to constrain the model.

- The role of organic surfaces (TOC in this study) in sediment surface complexation can be major. Competition for sorbing sites by aqueous compounds such as acetate and formate may also be significant in some systems. If reconnaissance sampling solid TOC and dissolved TOC results indicate this is of concern, allowances will need to be made for literature review and fact finding to obtain the necessary parameters for modeling. This is because this area of environmental surface chemistry is in rapid development, but is currently not well understood. However, it has been published that organic substrate and compound partitioning can be determined by mechanistic modeling within a framework such as PHREEQC.

- Site-specific solid phase extractions and physical data are a requirement to minimize model error. We have shown that estimation of sediment porosity and density, assumptions regarding solid-phase surface chemistry, and sensitivity to extraction method have a large affect on model accuracy. Collection of sediment water pairs, with analysis conducted as suggested by the Rio Salado and Florida simulation results, will minimize the potential error. The number of samples required to constrain the model will vary with site complexity. It is suggested, given the sensitivity of the model to sample inhomogeneity, that statistical approaches with replicate samples be employed when the lowest potential error is required.

Geochemical modeling of surface complexation is a developing science. The strategy and considerations developed here are not static. As more field and laboratory studies are conducted, it will be necessary to update the approach to increase accuracy and ensure stakeholder acceptance. Implementation of the approach presented in this report will support arsenic risk assessment, remedial design and feasibility studies, determination of natural attenuation, and allied environmental management goals. Since the approach is mechanistic, it is not only transferable from site to site, but probably suitable for environmental evaluation of any compound that is attenuated by surface complexation. A mechanistic modeling approach can be implemented in support of arsenic environmental management goals using relatively simple field and laboratory techniques, public domain models, and arsenic-specific modeling parameters obtained from the literature.

7
REFERENCE SECTION

1. Stumm, W. 1992. Chemistry of the solid-water interface. John Wiley and Sons, Inc. Wiley-Interscience Publication. New York. 428 pages.

2. Hess, R.E. and R.W. Blanchar. 1976. Arsenic stability in contaminated soils. Soil Sci. Soc. Am. J. 40: 847-852.

3. Hemond, H.F., 1995. Movement and Distribution of Arsenic in the Aberjona Watershed. Environmental Health Perspectives. Vol. 103, Supp. 1, February.

4. Hem, J.D. 1970. Study and interpretation of the chemical characteristics of natural waters. U.S. Geological Survey. Water-Supply Pap. 1473. 363 p.

5. Langmuir, D. 1997. Aqueous Environmental Geochemistry. Prentice Hall, New Jersey.

6. Goldberg, S. 1998. Ion Adsorbtion at the Soil Particle-Solution Interface: Modeling and Mechanisms. in Structure and Surface Reactions of Soil Particles, P.M. Huang ed. pp. 378-408. Wylie and Sons, New York.

7. Goldberg, S. 1999. Prediction of Boron Adsorption in Soils using the Constant Capacitance Model. Presentation at the 27th annual National Meeting of the American Chemical Society.

8. Parkhurst, D.L. 1995. Users Guide to PHREEQC - A Computer Program for Speciation, Reaction-path, Advective-Transport, and Inverse Geochemical Calculations. U.S. Geological Survey Water-Resources Investigations Report 95-4227, 143 p.

9. Parkhurst, D.L., Thorstenson, D.C., and L.N. Plummer. 1980. PHREEQE - A computer program for geochemical calculations. U.S. Geological Survey Water-Resources Investigations 80-96, 210 p.

10. U.S. Geological Survey. 1994. Arsenic contamination in the Whitewood Creek-Belle Fourche River-Cheyenne River System, Western South Dakota, Bibliography of Publications from the Toxic Substances Hydrology Program. U.S. Geological Survey Open-File Report 94-91.

11. HydroGeoLogic, Inc. and Allison Geoscience Consultants, Inc. 1998. MINTEQA2/PRODEFA2, A geochemical assessment model for environmental systems: user manual supplement for version 4.0. Herndon, VA and Flowery Branch, GA.

12. Allison, J.D., D.S. Brown, and K.J. Novo-Gradac. 1991. MINTEQA2/PRODEFA2, A geochemical assessment model for environmental systems: Version 3.0 user's manual. U.S. Environmental Protection Agency Publication EPA/600/3-91/021.

13. Stauffer, R.E. and J.M. Thompson. 1984. Arsenic and antimony in geothermal waters of Yellowstone National Park, Wyoming, U.S.A. Geochimica et Cosmochimica Acta. 48: 2547-2561.

14. Dzomback, D.A. and F.M. M. Morel. 1990. Surface Complexation Modeling: Hydrous Ferric Oxide. John Wylie and Sons, New York.

15. Davis, J.A., Kent, D.B., 1990. Surface complexation modeling in aqueous geochemistry. In: Hochella, M.F., Jr., White, A.F., Ribbe, P.H. (Eds). Reviews in Mineralogy: Mineral-Water Interface Geochemistry, Vol. 23. Mineralogical Society of America, Washington D.C., pp. 177-248 (Chapter 5).

16. Hochella, M.F., Jr., White, A.F, 1990. Mineral-Water Interface Geochemistry: An Overview. In: Hochella, M.F., Jr., White, A.F., Ribbe, P.H. (Eds). Reviews in Mineralogy: Mineral-Water Interface Geochemistry, Vol. 23. Mineralogical Society of America, Washington D.C., pp. 1-15 (Chapter 1).

17. Journal of AWWA. 1994. In search of an arsenic MCL. Journal AWWA. September 1994. p. 43.

18. Bhattacharya, P., A. Sracek, and G. Jacks. 1998. Groundwater arsenic in Bengal delta plains - testing of hypotheses. Dhaka Conference on Arsenic. February, 1998.

19. Bhattacharya, P., M. Larrson, A. Leiss, G. Jacks, A. Sracek, and D. Chatterjee. 1998. Genesis of arseniferous groundwater in the alluvial aquifers of Bengal delta plains and strategies for low-cost remediation. Dhaka Conference on Arsenic. February, 1998.

20. Das, D., G. Samanta, B.K. Mandal, T.R. Chowdhury, C.R. Chanda, P.P. Chowdhury, G.K. Basu and D. Chakraborti. 1996. Arsenic in groundwater in six districts of West Bengal, India. Environmental Geochemistry and Health. 18: 5-15.

21. Del Razo J., L.M., L.H. Hernandez G., G.G. Garcia-Vargas, P. Ostrosky-Wegman, C. Cortinas de Nava, and M.E. Cebrian. 1994. Urinary excretion of arsenic species in a human population chronically exposed to arsenic via drinking water. A pilot study. Arsenic Exposure and Health. Science and Technology Letters. Northwood, pp. 91-101.

22. Smedley, P.L. 1996. Arsenic in rural groundwater in Ghana. Journal of African Earth Sciences. 22(4): 459-470.

23. National Academy of Sciences. March 1999. Arsenic in Drinking Water. Subcommittee on Arsenic in Drinking Water, Committee on Toxicology, Board on Environmental Studies and Toxicology, Commission on Life Sciences, National Research Council. National Academy Press, Washington, D.C.

24. U.S. Environmental Protection Agency. 1992a. Test methods for evaluating solid waste, physical/chemical methods, EPA/SW-846/92.

25. U.S. Environmental Protection Agency. 1998. Arsenic in drinking water: drinking water standards development. Office of Water. http://www.epa.gov/OGWDW/ars/ars2.html.

26. U.S. Environmental Protection Agency. 1998. IRIS substance file: arsenic, inorganic. Integrated Risk Information System. http://www.epa.gov/ngispgm3/iris/subst/0278.htm.

27. Los Angeles Department of Water and Power. 1997. Arsenic removal strategies. LADWP. http://www.ladwp.com/bizserv/water/quality/topics/arsenic/arsenic.htm.

28. Los Angeles Department of Water and Power. 1997. Arsenic general information. LADPW. http://www.ladwp.com/bizserv/water/quality/topics/arsenic/arsenic.htm.

29. Soussan, T. 1997a. Arsenic study nearly finished. Albuquerque Journal, January 21, 1997, Sec. C, p. 1.

30. Soussan, T. 1997b. Arsenic levels in river over Isleta standard. Albuquerque Journal, December 13, 1997, Sec. C, p. 1.

31. Reid, J. 1994. Arsenic occurrence: USEPA seeks a clearer picture. Journal AWWA. September 1994. pp. 44-51.

32. Hering, J.G., and J. Wilkie. 1996. Arsenic geochemistry in source waters of the Los Angeles Aqueduct. Preliminary report to the Water Resources Center, University of California, Davis.

33. Ford, C.J., J.T. Byrd, J.M. Grebmeier, R.A. Harris, R.C. Moore, S.E. Madix, K.A. Newman, and C.D. Rash. 1996. Final project report on arsenic biogeochemistry in the Clinch River and Watts Bar Reservoir, Volume 1 ORNL/ER-206/V1/H3.

34. Turekiann, K.K., 1977, Encyclopedia of Science and Technology, 4th edn., p. 627-630: McGraw-Hill, New York.

35. Shevenell, L., K.A. Conoors, and C.D. Henry. 1999. Controls on pit lake water quality at sixteen open-pit mines in Nevada. Applied Geochemistry, 14(5): 669-687.

36. Cullen, W.R., and K.J. Reimer. 1989. Arsenic speciation in the environment. Chem. Rev. 89: 713-764.

37. Korte, N.E., 1991. Naturally occurring arsenic in the groundwaters of the midwestern United States. Environ. Geol. Water Sci. 18: 137-141.

38. Welch, A.H., M.S. Lico, J.L. Hughs. 1988. Arsenic in the groundwater of the western United States. Ground Water 26(3): 333-347.

39. Eaton, A., H.C. Wang, and J. Northington. 1998. Analytical Chemistry of Arsenic in Drinking Water. AWWA Research Foundation and American Water Works Association, Denver.

40. Korte, N.E. and Q. Fernando. 1991. A review of As(III) in groundwater. Critical Reviews in Environmental Control. 21: 1-39.

41. Miller, G.P., D.M. Welch, D.I. Norman, L.A. Brandvold, and R.M. Prol-Ledesma. 1998a. <u>Arsenic Speciation in a Geothermally Impacted Watershed - Guadalajara, Mexico.</u> Proceedings of the Society of Environmental Geochemistry and Health, Third International Conference on Arsenic in The Environment, San Diego, CA, July 1998.

42. HydroGeoLogic, Inc., Allison Geoscience Consultants, Inc., 1998. MINTEQA2/PRODEFA2, A geochemical assessment model for environmental systems: user manual supplement for version 4.0. Herndon, VA and Flowery Branch, GA.

43. Nimick, D.A. 1998. Arsenic hydrogeochemistry in an irrigated river valley: a reevaluation. Groundwater, v. 36, no. 5, pp. 743-753. September-October, 1998.

44. Wilkie, J.A. and J.G. Hering. 1998. Rapid oxidation of geothermal arsenic(III) in streamwaters of the eastern Sierra Nevada. Environ. Sci. Technol. 32: 657-66.

45. Bowell, R.J. 1994. Sorption of arsenic by iron oxides and oxyhydroxides in soils. Applied Geochemistry 9: 279-286.

46. Anderson, L.C.D. and K.W. Bruland. 1991. Biogeochemistry of arsenic in natural waters: The importance of methylated species. Environ. Sci. Technol. 25: 420-427.

47. Serkiz, S.M., J.D. Allison, E.M. Perdue, H.E. Allen, and D.S. Brown. 1996. Correcting errors in the thermodynamic database for the equilibrium speciation model MINTEQA2. Water Resources 30(8): 1939-1933.

48. Aurillo, A.C., R.P. Mason and H.F. Hemond. 1994. Speciation and fate of arsenic in three lakes of the Aberjona watershed. Environ. Sci. Technol. 28: 577-585.

49. Azcue, J.M. and J.O. Nriagu. 1993. Arsenic forms in mine polluted sediments of Moira Lake, Ontario. Environ Int. 19(4): 405-416.

50. Baker, L.A., T.M. Qureshi, and M.M. Wyman. 1998. Sources and mobility of arsenic in the Salt River watershed, Arizona. Water Resources Research 34(6): 1543-1552.

51. Bowell, R. J. 1992. Supergene gold mineralogy at Ashanti, Ghana: Implications for the supergene behavior of gold. Mineralogical Magazine 56: 545-560.

52. Braman, R.S. and C.C. Foreback. 1973. Methylated forms of arsenic in the environment. Science 182: 1247-1249.

53. Gailer, J. and K.J. Irgolic. 1994. The Ion-chromatographic Behavior of Arsenite, Arsenate, Methylarsonic Acid and Dimethylarsinic Acid on the Hamilton PRP-X100 Anion-exchange Column. Applied Organometallic Chemistry. Vol. 8, p. 129-140.

54. Hasegawa, H., M. Masakazu, S. Okamura, M. Hojo, N. Iwasaki, and Y. Sohrin. 1999. Arsenic Speciation Including 'Hidden' Arsenic. Applied Organometallic Chemistry. Vol. 13, p. 113-119.

55. Hasegawa, H., Y.S. Sohrin, M. Matsui, M. Hojo, and M. Kawashima. 1994. Speciation of Arsenic in Natural Waters by Solvent Extraction and Hydride Generation Atomic Absorption Spectrometry. Analytical Chemistry, Vol. 66, No. 19, pp. 3247-3252.

56. Howard, A.G., M.H. Arbab-Zavar, and S. Apte. 1982. Seasonal variability of biological arsenic methylation in the estuary of the river Beaulieu. Marine Chemistry. 11: 493-498.

57. Maher, W.A. 1981. Determination of inorganic and methylated arsenic species in marine organisms and sediments. Analytica Chimica Acta. 126: 157-164.

58. Maher, W.A. 1984. Mode of Occurrence and Speciation of Arsenic in some Pelagic and Estuarine Sediments. Chemical Geology, 47(1984/1985) 333-345.

59. Millward, G.E., H.J. Kitts, L. Ebdon, J.I. Allen, and A.W. Morris. 1997. Arsenic in the Humber Plume, U.K. Continental Shelf Research, Vol. 17, No. 4, pp. 435-454.

60. Millward, G.E., H.J. Kitts, S.D.W. Comber, L. Ebdon, and A.G. Howard. 1996. Methylated arsenic in the southern north sea. Estuarine, Coastal and Shelf Science. 43: 1-18.

61. Nriagu, J.O. and J. M. Azcue. 1989. Food contamination with arsenic in the environment. National Water Research Institute. Burlington, Ontario, Canada. February, 1989.

62. Welch, A.H. and M.S. Lico. 1998. Factors controlling As and U in shallow ground water southern Carson Desert, Nevada. Applied Geochemistry 13: 521-539.

63. Cullen, W.R. and K.J. Reimer.1989. Arsenic speciation in the environment. Chem. Rev. 89: 713-764.

64. Sadiq, M. 1997. Arsenic chemistry in soils: an overview of thermodynamic predictions and field observations. Water, Air, and Soil Pollution 93: 117-136.

65. Deuel, L.E., and A.R. Swoboda. 1972. Arsenic Solubility in a reduced environment. Soil Sci. Soc. Amer. Proc. 36: 276-278.

66. Elkhatib, E.A., O.L. Bennett, and R.J. Wright. 1984. Kinetics of arsenite sorption in soils. Soil Sci. Soc. Am. J. 48: 758-762.

67. Forstner, U. and I. Haase. 1998. Geochemical demobilization of metallic pollutants in solid wasted-implications for arsenic in waterworks sludges. Journal of Geochemical Exploration, v. 62, pp. 29-36.

68. Kimball, A.K., R.E. Broshears, K.E. Bencala, and D.M. McKnight. 1994. Coupling of hydrologic transport and chemical reactions in stream affected by acid mine drainage. Environ. Sci. Technol., v. 28, no. 12, pp. 2065-2073.

69. Livesey, N.T. and P.M. Huang. 1981. Adsorption of arsenate by soils and its relation to selected chemical properties and anions. Soil Sci. 131: 88-94.

70. Belzile, N. and A. Tessier. 1990. Interactions between arsenic and iron oxyhydroxides in lacustrine sediments. Geochimica et Cosmochimica Acta 54: 103-109.

71. Kimball, A.K., Broshears, R.E., Bencala, K.E., McKnight, D.M., 1994. Coupling of hydrologic transport and chemical reactions in stream affected by acid mine drainage. Environ. Sci. Technol., v. 28, no. 12, pp. 2065-2073.

72. Ford, C.J., Byrd, J.T., Grebmeier, J.M., Harris, R.A., Moore, R.C., Madix, S.E., Newman, K.A., Rash, C.D., 1996. Final project report on arsenic biogeochemistry in the Clinch River and Watts Bar Reservoir, Volume 1 ORNL/ER-206/V1/H3.

73. Smith, S.L., Jaffe, P.R., 1998. Modeling the transport and reactions of trace metal in water saturated soils and sediments. Water Res. Research Vol. 34, No. 11, pp. 3135-3147.

74. Eary, L.E., 1999. Geochemical and equilibrium trends in mine pit lakes. Applied Geochemistry 14(8): 963-987.

75. Brown, J.G., Bassett, R.L., Glynn, P.D., 2000. Reactive transport of metal contaminants in alluvium-model comparison and column simulation. Applied Geochemistry 15(1) 35-49.

76. Prol-Ledesma, R.M., S.I. Hernandez-Lombardini and R. Lozano-Santa Cruz. 1996. Chemical variations in the rocks of the La Primavera geothermal field related with hydrothermal alteration. In Press, University of Mexico, Mexico City.

77. Ramirez-Silva, G.R. 1981. Informe climatologico de la Zona Geotermica La Primavera-San Marcos-Heveres de la Vega, Jalisco. Informe 16-81. Comision Federal de Electridad, Mexico, Suberencia de Estudios Geotermicos, Departmento de Exploracion, May, 1981.

78. Ramirez-Silva, G.R. 1982. Hidrologia superficial y subterranea en las Zonas Geotermicas La Primavera-San Marcos Heveres de la Vega, Jalisco. Informe 19-82. Comision Federal de Electricidad, Mexico, Suberencia de Estudios Geotermicos, Departmento de Exploracion, April, 1982.

79. Yokoyama, I. and M. Mena. 1991. Structure of La Primavera caldera, Jalisco, Mexico, deduced from gravity anomalies and drilling results. Journal of Volcanology and Geothermal Research 47: 183-193.

80. Grossl, P.R., M. Eick, D.L. Sparks, S. Goldberg, and C.C. Ainsworth. 1997. Arsenate and Chromate Retention Mechanisms on Goethite. 2. Kinetic Evaluation Using a Pressure-Jump Relaxation Technique. Environ. Sci. Technol. 31: 321-326.

81. Cherry, J.A., A.U. Shaikh, D.E. Tallman, and R.V. Nicholson. 1979. Arsenic species as an indicator of redox conditions in groundwater. J. Hydrol. 45: 373-392.

82. Brockbank, C.I., G.E. Batley, and G. K-C Low. 1988. Photochemical decomposition of arsenic species in natural water. Environmental Technology Letters 9: 1361-1366.

83. Garland, T.R., R.E. Wildung, and H.P. Harbert. 1983. Influence of irrigation and weathering reactions on the composition of percolates from retorted oil shale in field lysimeters. Pacific Northwest Laboratories. Richland, Washington. October 1983.

84. Onysko, S.J. and R.L. McNearny. 1997. GIBBTEQ: A MINTEQA2 thermodynamic error detection program. Ground Water, Computer Notes 35(5): 912-914.

85. Ficklin, W.H. 1983. Separation of arsenic(III) and arsenic(V) in ground waters by ion exchange. Talanta. 30(5): 371-373.

86. Goldberg, S., 1998. Ion Adsorbtion at the Soil Particle-Solution Interface: Modeling and Mechanisms. in Structure and Surface Reactions of Soil Particles, P.M. Huang ed. pp. 378-408. Wylie and Sons, New York.

87. Wang, F. Chen, J., Forsling, W., 1997. Modeling sorption of trace metals on natural sediments by surface complexation model. Environ. Sci. Technol. 31: 448-453.

88. Westall, J. C. 1999. Personal Communication.

89. Felmy, A.R. and J.R. Rustad. 1998. Molecular statics calculations of proton binding to goethite surfaces: Thermodynamic modeling of the surface charging and protonation of goethite in aqueous solution. Geochimica et Cosmochimica Acta 62(1): 25-31.

90. Manning, B.A., Goldberg, S., 1996b. Modeling Competitive Adsorption of Arsenate with Phosphate and Molybdate on Oxide Minerals. Soil Soc. Am. J. v. 60, p. 121-131.

91. Manning, B.A., Goldberg, S., 1997. Arsenic(III) and Arsenic(V) Adsorbtion on Three California Soils. Soil Science, v. 162(12), p. 886-895.

92. Manning, B.A, Fendorf, S.E., Goldberg, S., 1998. Surface Structures and Stability of Arsenic(III) on Goethite: Spectroscopic Evidence for Inner-Sphere Complexes. Environ. Sci. Technol. v. 32, p. 2383-2388.

93. Lindberg, R.D. Runnels, D.D., 1984. Ground Water Redox Reactions: An analysis of Equilibrium State Applied to Eh Measurements and Geochemical Modeling. Science, Vol. 225, 31 August 1984, p. 925-927.

94. Herbelin, A.L., Westall, J.C., 1999. FITEQL 4.0 - A Computer Program for Determination of Chemical Equilibrium Constants from Experimental Data. Report 99-01, Department of Chemistry, Oregon State University, Corvallis.

95. Goldberg, S., 1985. Chemical Modeling of Anion Competition on Goethite Using the Constant Capacitance Model. Soil Sci. Soc. Am. J. 49: 851-856.

96. Ghosh, M.M., Yuan J.R., 1987. Adsorption of inorganic arsenic and organoarsenicals on hydrous oxides. Environmental Progress 6(3): 150-157.

97. Cox, C.D., Ghosh, M.M., 1994. Surface complexation of methylated arsenates by hydrous oxides. Water Resources 28(5): 1181-1188.

98. Cherry, J.A., Shaikh, A.U., Tallman, D.E., Nicholson, R.V., 1979. Arsenic species as an indicator of redox conditions in groundwater. J. Hydrol. 45: 373-392.

99. Holm, T.R., Curtiss, C.D., 1989. A comparison of oxidation-reduction potentials calculated from the As(V)/As(III) and Fe(III)/Fe(II) couples with measured platinum-electrode potentials in groundwater. J. Contaminant Hydro. 5: 67-81.

100. Wilkie, J.A., Hering, J.G., 1998. Rapid oxidation of geothermal arsenic(III) in streamwaters of the eastern Sierra Nevada. Environ. Sci. Technol. 32: 657-666.

101. Meng, X., Letterman, R.D., 1996. Modeling Cadmium and Sulfate Adsorbtion by $Fe(OH)_3/SiO_2$ Mixed Oxides Water Research, v. 30(9), p. 2148-2154.

102. Sadiq, M., 1997. Arsenic chemistry in soils: an overview of thermodynamic predictions and field observations. Water, Air, and Soil Pollution 93: 117-136.

103. Welch, D.M., Miller, G.P., Norman, D.I., Brandvold, L.A., 2000. Distribution of Arsenic in the Sediments and Water of a Small Geothermally Influenced Watershed, Guadalajara, Mexico. Part 1: Empirical Relationships. Submitted May 2000 to Applied Geochemistry.

104. Manning, B.A. and S. Goldberg. 1996. Modeling competitive Adsorption of Arsenate with Phosphate and Molybdate on Oxide Minerals. Soil Soc. Am. J. v. 60, p. 121-131.

105. Welch, D.M., 1999. Arsenic Geochemistry of Stream Sediments Associated with Geothermal Waters at the La Primavera Geothermal Field, Mexico. Masters Thesis, New Mexico Institute of Mining and Technology, Socorro, New Mexico.

106. Van Geen, A., Robinson, A.P., Leckie, J.O., 1994. Complexation of carbonate species at the goethite surface: Implications for adsorption of metal ions in natural waters. Geochimica Cosmochim. Acta, 58(9): 2073-2086.

107. Mahood, G.A., A.H. Truesdell, and L.A. Templos M. 1983. A reconnaissance geochemical study of La Primavera geothermal area, Jalisco, Mexico. Journal of Volcanology and Geothermal Research. 16: 247-261.

108. Alatorre-Zamora, M.A. and J.O. Campos-Enriquez. 1992. La Primavera Caldera (Mexico): Structure inferred from gravity and hydrogeological considerations. Geofisica International 31(4): 371-382.

109. Santoyo-Gutierrez, S., A. Garcia, M. Morales, J. Perezyera and A. Rosas. 1991. Applied technology in the solution of geothermal drilling problems of deep wells in La Primavera caldera (Mexico). Journal of Volcanology and Geothermal Research. 47: 195-208.

110. U.S. Geological Survey. 1977. National handbook of recommended methods for water quality data acquisition. Office of Water Data Coordination, United States Geological Survey, Reston Virginia.

111. Maiorino, R.M. and H.V. Aposhian. 1985. Dimercaptan metal-binding agents influence the biotransformation of arsenite in the rabbit. Toxicology and Applied Pharmacology. 77: 240-250.

112. Aggett, J. and G.A. O'Brien. 1985. Detailed model for the mobility of arsenic in lacustrine sediments based on measurements in Lake Ohakuri. Environ. Sci. Technol. 19: 231-238.

113. Chen, S.L., S.R Dzeng, M.H. Yang, K.H. Chiu, G.M. Shieh, and C.M. Wal. 1994. Arsenic species in groundwaters of the Blackfoot disease area, Taiwan. Environ. Sci. Technol. 28(5): 877-88.

114. Holm, T.R., M.A. Anderson, R.R. Stanforth, and D.G. Iverson. 1980. The influence of adsorption on the rates of microbial degradation of arsenic species in sediments. Limnol. Oceanogr. 25(1): 23-30.

115. Takamatsu, T., H. Aoki, and T. Yoshida. 1982. Determination of Arsenate, Arsenite, Monomethylarsonate, and Dimethylarsinate in Soil Polluted with Arsenic. Soil Science 133(4): 239-246.

116. Kuwabara, J.S. 1992. Associations between benthic flora and diel changes in dissolved arsenic, phosphorus, and related physico-chemical parameters. Journal of North American Benthological Society 11(2): 218-228.

117. Ghosh, M.M. and J.R. Yuan. 1987. Adsorption of inorganic arsenic and organoarsenicals on hydrous oxides. Environmental Progress 6(3): 150-157.

118. Cox, C.D. and M.M. Ghosh. 1994. Surface complexation of methylated arsenates by hydrous oxides. Water Resources 28(5): 1181-1188.

119. Tessier, A., P.G.C. Campbell, and M. Bission. 1979. Sequential extraction procedure for the speciation of particulate trace metals. Analytical Chemistry. 51(7): 844-851.

120. Chao, T.T. and L. Zhou. 1983. Extraction techniques for selective dissolution of amorphous iron oxides from soils and sediments. Soil Sci. Soc. Am. J. 47: 225-232.

121. Grabinski, A.A. 1981. Determination of arsenic(III), arsenic(V), monomethylarsonate, and dimethylarsinate by ion-exchange chromatography with flameless atomic absorption spectrometric detection. Analytical Chemistry. 53: 966-968.

122. Barranco, F.T., Jr., W.L. Balsam, and B.C. Deaton. 1989. Quantitative reassessment of brick red lutites: evidence from reflectance spectrophotometry. Marine Geology 89: 299-314.

123. Davies, B.E. 1974. Loss-on-ignition as an estimate of soil organic matter. Soil Sci. Soc. Amer. Proc. 38: 150-151.

124. Kheboian, C. and F. Bauer. 1987. Accuracy of selective extraction procedures for metal speciation in model aquatic sediments. Anal. Chem. 59: 1417-1423.

125. Xiao-Quan, S., and C. Bin. 1993. Evaluation of sequential extraction for speciation of trace metals in model soil containing natural minerals and humic acid. Anal. Chem. 65: 802-807.

126. Lawrence, GHM. 1951. Taxonomy of Vascular Plants. MacMillan Publ. Co., New York.

127. McVaugh, R. 1983. Flora Novo-Galiciana: a descriptive account of the vascular plants of Western Mexico. Univ. Mich. Press, Ann Arbor.

128. Pesman, M.W. 1962. Meet Flora Mexicana. Northland Press, Flagstaff.

129. Miller, G.P., D.I. Norman, and P.L. Frisch, 2000. A comment on Arsenic Species Separation Using Ion Exchange. Wat. Res. 34(4): 1397-1400.

130. Borkovec, M., Westall, J., 1983. Solution of the Poisson-Boltzman equation for surface excesses of ions in the diffuse layer at the oxide-electrode interface. Journal of Electroanalytical Chemistry 150: 325-337.

131. Jackson, M.L., and L.W. Zelazny. 1986. Oxides, Hydroxides, and Aluminosilicates. In Methods of Soil Analysis, Part 1. Physical and Mineralogical Methods. Second Edition, Agronomy Monograph No. 9. Arnold Klute, ed. pp. 101-148.

A
APPENDIX A – RIO SALADO FIELD INVESTIGATION

Field Activities

Rio Salado (Salty River), in the Bosque La Primavera (Spring Forest) conservation area
25 km west of Guadalajara, Mexico, was selected for evaluation of some of the processes
controlling arsenic occurrence and transport (Figure A-1). The closest community to the field site
is the village of La Primavera with less than 500 inhabitants. Rio Salado lies within a national
conservation area consisting of bathing, hiking, and camping areas, a private spa, an elder hostel,
hot springs, and the headwaters of the Rio Caliente-Rio Salado drainage. La Primavera was
selected for study due to a number of favorable factors, including that:

- It is a relatively undisturbed watershed with national conservation area protection,
  eliminating anthropogenic influences to the highest degree possible;

- The total arsenic concentration exceeds 1 ppm, allowing reactions to be studied in detail that
  could be below quantification limits for other sites; and,

- General water chemistry and geology of the site is analogous many high-arsenic areas in the
  United States.

The site allows access to arsenic waters at the ground surface. Groundwater is shallow in the
region, so groundwater investigations can be conducted less expensively. Biota can be examined
for arsenic uptake and effect outside of a laboratory. Access to the site is relatively easy.
Universidad Nacional Autonoma de Mexico (UNAM), Comision Federal de Electricidad (CFE)
and the Comision Nacional del Agua (CNA) support and welcome investigative efforts at
Rio Salado. UNAM has a program to investigate in detail the geology and hydrology in the area
providing regional and site-specific supporting data and research to the project. UNAM, CFE
and CNA also provide logistical support when possible. The climate is conducive to year-round
research and provides for experimental stability. Having arsenic waters at the surface allows easy
testing of passive, innovative, or low-cost treatment alternatives. Establishment of the Bosque La
Primavera conservation area has allowed unique, multidisciplinary, research and technology
development to be conducted without fear of the effects of major human encroachment on the
site.

There has been little or no residential, commercial, or industrial activity within the boundaries of
the watershed other than the previously mentioned recreational facilities. The Rio Salado system
provides a temperature and redox gradient along the length of its primary and secondary streams,
forcing changes in surface water and sediment chemistry. Distinct changes in biotic zonation
have been observed. Alluvium along and under the streams allows for shallow groundwater
investigation. The physical and biologic setting is conducive to the examination of the rate of
change between arsenic species. The primary source of arsenic in Rio Salado streams is

geothermally impacted groundwater discharging from springs. Other sources of arsenic can include groundwater infiltrating stream channels or releases from sediments or rocks brought about by changing environmental conditions. Although there are probably some minor man-made sources of arsenic in the Rio Salado system, these sources must be quite small when compared to average concentrations in volcanic rocks and geothermal water, and the total flux of arsenic from the Rio Salado site. The waters of Rio Salado can exceed 1200 ppb total arsenic, a level well above established health thresholds. We have determined that methyl arsenic compounds are present in the Rio Caliente-Rio Salado watershed.

The naturally high arsenic concentrations at Rio Salado reduce the analytical error that occurs when investigating arsenic transformation and attenuation near the limit of quantification. The high concentrations at Rio Salado may result in arsenic availability and detectability over a much greater stream reach than at many other sites, allowing the arsenic transformations to be observed in greater detail. The site naturally releases about 11,000 kg/year of arsenic to the environment.

La Primavera is composed of acidic volcanic rocks (dominantly rhyolitic) and is quite young. Caldera formation started about 150,000 years ago, with the last eruptions occurring 30,000 years ago. It is part of the Trans-Mexican Volcanic Belt, a structure that spans Mexico east to west (Figure A-1). The Trans-Mexican Volcanic Belt is a target for CFE's geothermal power development efforts. The volcanic rocks provide the heat source for geothermal activity and are responsible for the high levels of arsenic present in La Primavera groundwater. The springs of La Primavera surface at the western caldera rim and form Rio Caliente, that drains to the Rio Salado. In this report, "Rio Salado" is used to refer to the study area. The site geomorphology is typical of faulted volcanic terrain. Topographic relief is rolling to steeply sloping in the watershed, with the watershed boundaries formed by mesas and escarpments. Elevations range from 1500 to 1600+ meters above sea level. In the areas with a sediment bottom, vegetation has stabilized sand and gravel bars. Base flow through the alluvium may represent a substantial portion of the total flowin these areas. Generally, the portion occupied by stream flow varies from <1 m to 5 m wide. Small rapids and braided stream sections are common. Air temperatures are moderate (average 20.8°C) with little variation. The area is subject to a dry season and a wet season, with the dry season occurring in late fall through mid winter. The area receives an average of 945 mm of precipitation with evapotranspiration of 658 mm resulting in recharge to shallow groundwater.
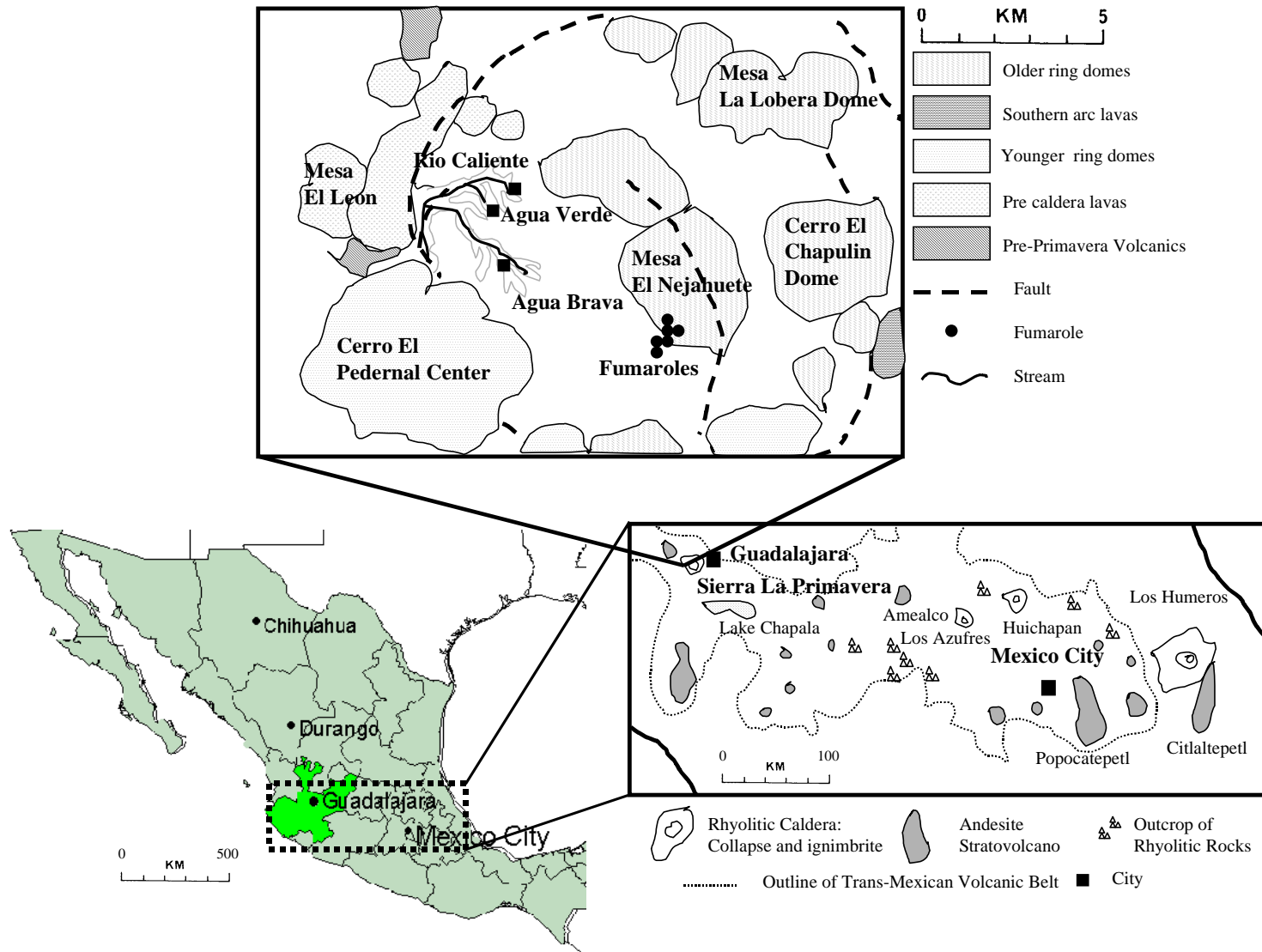
Figure A-1
Location of the La Primavera Watershed and Rio Salado, Mexico

The sodium bicarbonate waters of Rio Salado are discharged from a network of thermal springs associated with a fault at approximate rates of 1-200L/s. There are four dominant point thermal discharges and numerous smaller seeps and springs. The fault is a 5 km north-south trending structure that forms the escarpment to the east of Rio Salado and is collocated with three of the four main springs. The springs discharge mixed geothermal waters that contain about 1 ppm arsenic and 100 ppm chloride versus the 14 ppm arsenic and 900 ppm chloride found in the deeper geothermal reservoir fluids. Silica content is high but precipitates found at spring mouths are carbonate (travertine). Mixing with cool, meteorically derived groundwater has taken place prior to spring discharge. Spring temperatures are variable with some approaching 70°C, and flow from the major springs is fairly constant throughout the year. Flow and chemistry appear to be stable, over time based on review of historical data [77, 78, 79, 80, 110, 111, 112].

Rio Caliente is the local name for the stream that forms the headwaters of Rio Salado. The four primary thermal springs of the headwater area have consistent high-arsenic, and high-temperature discharge. In the early 1980's, CFE began investigating the La Primavera geothermal field for power production. As part of the development, eight surface water flow measurement structures (sharp crested weirs) were constructed on the streams of interest to this study. These stations are numbered RC-1 through RC-8 in Figure A-2 (RC for Rio Caliente). These structures were evaluated for use as part of this project in June and July of 1997, and again in January 1998.
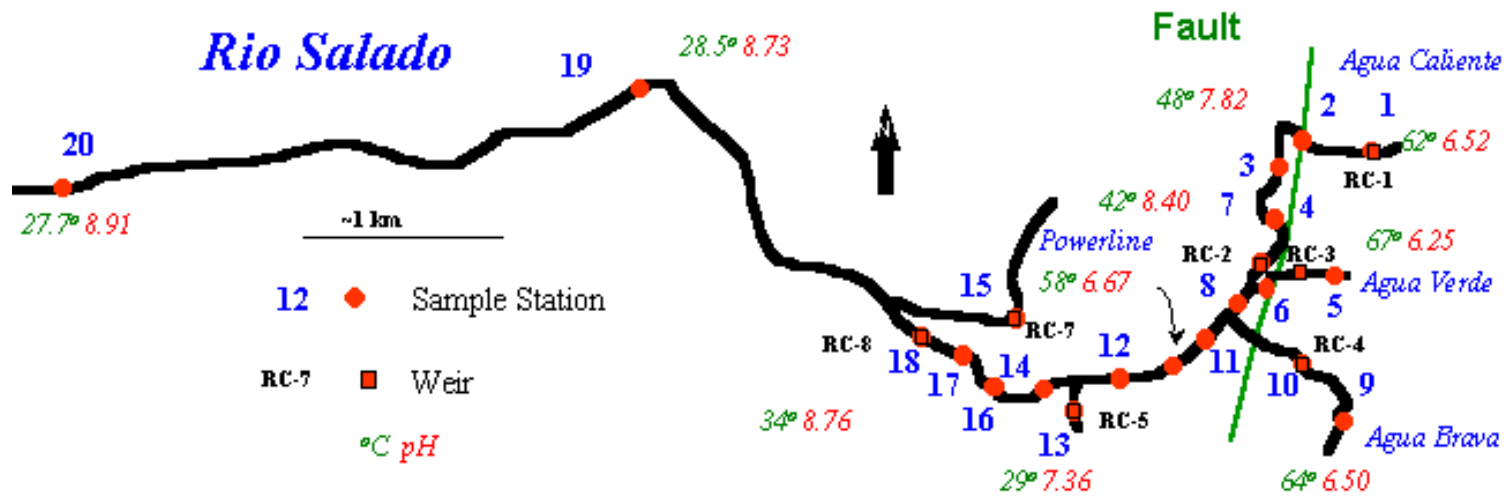
Figure A-2
Rio Salado Sampling Stations, January 1998

Currently, there are seven known flow measurement stations spread over four kilometers of stream reach. RC-6 was not found and is presumed to have been destroyed. Five of the stations are on first order streams, three of which originate from large thermal springs (RC-1, RC-3, and RC-4), two from non-thermal waters (RC-5 and RC-7). Two of the structures are on the main channel of Rio Salado (RC-2 and RC-8), a second order stream. Flow measurements were conducted by CFE during part of 1981 and 1982. The CFE data has been used for this effort when appropriate. The stations have not been maintained since that time. Although these structures require upgrades and rehabilitation, they can be restored to function, if the data would be useful. This would consist primarily of cleaning of upstream pools and fitting of new weir plates and data logging equipment.

The primary location control used for this effort is the 1:50,000 scale Cetenal Carta Geologica, Guadalajara Oeste F-13-D-65, 19 topographic and geologic map produced by Geologia de México, the Mexican equivalent of the US Geological Survey. The scale limited the accuracy of position determinations. Global Positioning System (GPS) equipment was used to resolve these problems with some success. However, steep walled canyons and heavy vegetative cover limited the accuracy of GPS readings. Compass and pace methods were used to locate sample stations when difficulties arose. The subjectively best determinations were used with the base map to estimate the distance between sampling stations. It is estimated that the maximum error in any sample station's location is ±30 m. Stream kilometer was set to zero at the northern most sample location, Station 1, the headwaters of Rio Salado.

Sampling points used for the reconnaissance sampling (Stations 1-20 and Agua Dulce) are described in Table A-1 and depicted in Figure A-2. Some explanation of the nomenclature used here might be useful. The headwaters and upper watershed of Rio Salado lie in the Bosque de La Primavera, a national conservation area. Locally, the headwaters of Rio Salado are known as Rio Caliente and the northernmost spring as Agua Caliente. Three major thermal springs enter Rio Caliente from the east. CFE does not name the northern most spring, and uses Arroyo Agua Brava for the middle spring and Agua Verde for the southern spring. Mahood [110] refers to the northern spring as Rio Caliente, the middle as Agua Brava, and Arroyo Verde to the south. The nomenclature used here is that used locally and by UNAM staff and students. Agua Caliente is used for the headwaters spring, moving south from the headwaters the names used in order are Agua Verde then Agua Brava. Powerline is used for a major thermal spring that is not mentioned in the literature. La Primavera, Rio Salado, and Rio Caliente can be used interchangeably in the current study area.

Table A-1
Rio Salado Sampling and Measurement Station Locations

Station	Description	Use
1	Rio Salado-Rio Caliente headwaters sampling station. Stream kilometer 0.0. Samples taken just below weir. Sand and gravel bottom. Little or no algae or in-stream vegetation. Rio Caliente of Mahood [110].	Water samples. Tracer test injection point.
2	On Rio Salado. Broad sand and gravel bottom. Abundant brown and green algae.	Water samples. Tracer test monitoring.
3	On Rio Salado just upstream of concrete bridge into Rio Caliente Spa. Gravel and cobble bottom. Abundant brown and green algae. Sampled twice, once early morning once in the afternoon.	Water samples. Tracer test monitoring. Flow measurement.
4	On Rio Salado downstream of spa. Broad sand and gravel bottom. Sparse brown and green algae. Stream braided with plants established on sandbars.	Water samples. Tracer test monitoring.
5	Headwaters of Agua Verde. Rock and gravel bottom. Under trees. Sprigs issue from network of rock openings. Sample taken from largest and hottest thermal source. Agua Brava of Mahood, 1983. No algae at sample location.	Water samples. Tracer test injection point.
6	15 meters upstream Agua Verde from confluence with Rio Salado. Rock and gravel bottom. Under trees. Abundant algae at sample location. Downstream of RC-3. Two meter waterfall 35 meters upstream.	Water samples. Tracer test monitoring.
7	On Rio Salado in upstream pool of flow structure RC-2. Rock and boulder bottom with braids, riffles, eddies and rapids upstream. No algae at sample location.	Water samples. Tracer test monitoring.
8	On Rio Salado between Agua Verde and Agua Brava confluence. Gravel bottom. Gentle steady flow. Braided stream upstream of location. Sparse algae at sample location.	Water samples. Tracer test monitoring. Flow measurement.
9	Headwaters of Agua Brava. Rock and gravel bottom. Under trees. Sample taken from well mixed location 20 meters downstream of a cluster of large thermal springs. Arroyo Verde of Mahood, 1983. Thick algae mat on bottom and rapids through entire length of stream.	Water samples. Tracer test injection point.
10	In upstream pool of flow structure RC-4 on Agua Brava. Sand, gravel and boulder bottom with braids, riffles, eddies and rapids upstream. No algae at sample location.	Water samples. Tracer test monitoring. Flow measurement.
11	On Rio Salado below Agua Brava confluence. Gravel bottom. Gentle steady flow. Algae at sample location.	Water samples. Tracer test monitoring. Flow measurement.

Table A-1
Rio Salado Sampling and Measurement Station Locations (Continued)

Station	Description	Use
12	On Rio Salado below Powerline confluence, above RC-5 confluence. Gravel and bolder bottom. Rapid steady flow, riffles, eddies. Algae at sample location.	Water samples. Tracer test monitoring. Flow measurement.
13	First order stream with seep and spring source that enters Rio Salado ~100 m upstream of Station 14. 240 ppb total arsenic. May be representative of less thermal groundwater.	Water samples.
14	On Rio Salado below RC-5 confluence. Gravel bottom. Gentle steady flow, braided upstream with vegetation in sand bars. Under trees. Sparse algae at sample location.	Water samples. Tracer test monitoring.
15	Name for total metals water sample taken at RC-7. Not used otherwise.	Water samples.
16	On Rio Salado. Gravel bottom. Gentle steady flow. Sparse algae at sample location.	Water samples. Tracer test monitoring.
17	On Rio Salado. Gravel bottom. Gentle steady flow. Moderate algae at sample location.	Water samples. Tracer test monitoring.
18	On Rio Salado in pool below RC-8. Sand and gravel bottom. Gentle steady flow. Under trees. Thick black algae on stream edge. Last location for monitoring of tracer tests.	Water samples. Tracer test monitoring. Flow measurement.
19	On Rio Salado. Gravel bottom. Gentle steady flow. Sparse algae at sample location. Near small cattle operation and downstream of a public bathing area. Stream kilometer 6.6.	Water samples. Flow measurement.
20	On Rio Salado below RC-5 confluence. Sand bottom. Gentle steady flow. Near corn and sugar cane fields. Sparse algae at sample location. Stream kilometer 10.2, farthest downstream station.	Water samples. Flow measurement.
RC-1 Weir	One meter concrete sharp crested weir at the most upstream point of Rio Salado. Triangular cross section. Collocated with Station 1, monitors all Agua Caliente flow. Weir and pool are in need of rehabilitation.	Sampled for total metals several times.
RC-2 Weir	Three meter wide concrete sharp crested rectangular weir in Rio Salado rock channel. No low flow provisions. Weir and pool are in need of rehabilitation.	
RC-3 Weir	One meter rectangular weir with steel edge. Can be fitted with weir plate. Monitors all flow from Agua Verde. Pool needs cleaning.	Sampled for total metals several times.
RC-4 Weir	One meter rectangular weir with steel edge. Can be fitted with weir plate. Monitors all flow from Agua Brava. Pool needs cleaning.	Sampled for total metals several times.
RC-5 Weir	One meter rectangular weir with steel edge. Can be fitted with weir plate. Monitors all flow from cool low arsenic spring between Stations 12 and 14. Pool needs cleaning and vegetation removal. Collocated with Station 13.	Water samples.

Table A-1
Rio Salado Sampling and Measurement Station Locations (Continued)

Station	Description	Use
RC-6 Weir	Never located. Probably collocated with Station 14.	
RC-7 Weir	Located in drainage that enters downstream of RC-8 and Station 18. One meter triangular concrete weir. May not be repairable. Located too far upstream to capture full flow contribution to Rio Salado. Stagnant ponded condition. Station 15.	Sampled for total metals once.
RC-8 Weir	Three meter wide concrete sharp crested rectangular weir with wing walls in Rio Salado. No low flow provisions. Weir and pool are in need of serious rehabilitation. Weir undercut by stream channel across entire width. Collocated with Station 18.	
Powerline Spring	Spring that enters main channel of Rio Salado from stream bank. May be submerged in high flow conditions. Lies between Stations 11 and 12.	Sampled for total metals several times.
Agua Dulce	First order stream with seep and spring source that enters Rio Salado ~100 m upstream of Station 19. 115 ppb total arsenic. May be representative of non-thermal groundwater.	Sampled for total metals once.

Stream Flow

The principles of streamflow measurement are well established. Two streamflow measurement techniques were used: tracer tests, to determine average time of travel between sampling points, and a direct measurement velocity-area method that provides point-velocity measurements and calculated discharges.

Tracer Tests

Tracer tests track the movement and concentration of a foreign substance in a fluid to determine chemical and physical properties of the flow system. One use of tracer tests is to determine surface water travel time between two points. This is accomplished by the detection at known time and location of a tracer substance that was introduced upstream. Ideally, a tracer is not chemically reactive with the water or sediments and is easy and inexpensive to detect. Solids, liquids, and gasses have all been successfully employed as tracers. The known ideal behavior of a tracer allows the interpretation of tracer test data.

The tracer is usually dumped into the stream as rapidly as possible to provide a "slug" initial condition (instantaneous introduction of tracer). Tracer tests are subject to the influence of in-stream mixing (dispersion and diffusion components), and physical or chemical reactions (predominantly sorption). Because of these influences, the tracer spreads out from its initial highly concentrated slug into an elongated parcel of water, where tracer concentrations diminish to zero at the upstream and downstream edges, with size constantly increasing as it moves downstream. The concentration tail later can be quite long. Tracer determinations of velocity provide the range of possible stream velocities during the test. The velocity determined from first detection of the tracer approximates the behavior of a small parcel of water that has always taken

the fastest route downstream. The velocity associated with the concentration peak approximates the velocity of the average parcel of water in the stream. Velocities determined from the late-time tail represent parcels of water that were trapped or retarded in their movement downstream. A precise and accurate tracer test can be used to determine a probability distribution of travel times, or quantify diffusion, dispersion, and sorption parameters. These parameters may be necessary for detailed evaluation of in-stream chemical evolution.

Tracer tests were conducted on January 12 and 13, 1998 after all sampling had been completed. The tracer tests were intended to support investigation of arsenic speciation kinetics and provide data for the design of future experiments at Rio Salado. Some questions cannot be answered by velocity-area discharge determination investigations as easily and/or as well as by tracer tests. Specifically:

- What is the general range of streamflow velocities at the site?

- What are the fast, average, and slow travel times between sampling stations?

- Qualitatively, what is the mixing length, time, area, and volume of a slug injection as it moves downstream?

Time and budget constraints would not allow use of sophisticated tracer detection methods, such as quantitative fluorescence, nor were they necessary for the given purposes. Tracer tests were limited to the upper 4 km of the watershed, e.g. upstream of Station 18. Two types of tracers were used, fluorescent dyes and sodium chloride. The detection methods used were qualitative visual detection of fluorescent dyes and detection of changes in specific conductivity caused by introduction of the salt.

Dye Tests

Three individual dye tests were conducted. Agua Brava and Agua Verde were traced from their respective sources to the junctions with Rio Salado on January 12. The main channel test, from Station 1, Agua Caliente, to Station 18, was completed on January 13. The dyes used were 51 wt. % Rhodamine WT and 78 wt. % fluorescine supplied by the Ben Meadows company. Fluorescine was used for Agua Brava and Agua Verde, and Rhodamine WT was used for the main channel test. Permission to conduct the tests was provided verbally by Oscar A. Escolero Fuentes of CNA, Mexico City. The use of two dyes was planned to compare visual effectiveness, and guard against possible interference or misinterpretation. Sufficient dye was used to ensure visual detection for the entire duration of the test, two liters of Rhodamine WT for the main channel and 0.5 liter Fluorescine for each Agua Verde and Agua Brava. Fluorescine was by far the superior dye for visual detection in Rio Salado at base flow. Subjective visual estimation of dye concentration and wristwatches were used to determine travel times between stations for the first dye arrival, approximate dye centroid, and length of the tail. Not all stations had all measurements. The travel times and calculated velocities determined from the dye tracer tests are given in Table A-2.

Sodium Chloride Test

The sodium chloride (salt) tracer test was conducted at the same time as the main channel Rhodamine WT tracer test. The test was conducted by introducing 40 liters of saturated salt

solution (~350 g/L at 20°C) that was prepared from common processed water softener rock salt and Type II water. The need for this amount of salt solution was based on desiring a 30% increase over background conductivity at Station 18, assuming that a dilution of 1:2000 would occur over the stream reach. The salt solution was introduced at the same time as the two liters of Rhodamine WT for the dye tracer test. The travel times and calculated velocities determined from the salt tracer test are given in Table A-2.

Velocity-Area Method

The velocity-area method is a direct measurement of stream velocity taken with a paddle-wheel current meter, and a stopwatch. In combination with cross-sectional area measurements this method can be used to calculate discharge. Velocities determined in this manner are generally not representative of travel times. The ideal stream section in which to use the velocity-area method is a straight stream channel section much longer than wide, with little variation in depth, and no in-stream obstructions. Most Rio Salado locations for measurement required some accommodation from the ideal.

The current meter used was a Model F583 Price-Pygmy vertical-axis rotating element meter, SN# 4887, maintained by the New Mexico Bureau of Mines and Mineral Resources. The meter is factory calibrated with no adjustment necessary unless the meter is damaged or extremely worn. All calibrations and repairs are made by the factory. The meter is rated to a maximum velocity of 0.76 m/s. The discharge equation used is: $V = 0.665 N + 0.04$, where V is velocity in m/s and N is the paddle-wheel revolutions per second. The discharge equation was supplied by the manufacturer and is unique to the meter. Maximum suggested stream depth for this model meter is less than 0.46 m.

The stream channel is divided into equal width segments (generally 10-12) using a fiberglass tape measure. Depth measurements are taken at the midpoint of each segment using the current meter wading rod and/or a plastic ruler. Areas used are the product of the segment width and corresponding segment midpoint depth. The most accurate and recommended method for discharge determination under these conditions is to make the measurement at 0.6 of the stream total depth below the stream surface [113]. This method was used exclusively.

With the following exception, all point discharge measurements were made within the operational range of the equipment. The discharge measurements made at Station 3 are suspect. These measurements exceeded the maximum rated velocity of the meter by over 40%. Discharge and velocity measurements made on June 27-28, 1997 and January 11-13, 1998 are tabulated below (Table A-3) with flows determined in 1981-82 by CFE.

Table A-2
Tracer Test Flow Velocities, Rio Salado, January 1998

Station	Stream Kilometer	Observation	Velocity (km/hr)	First arrival (km/h)	Peak Dye (km/h)	Dye Tail (km/h)	Salt Peak (km/h)	Salt Tail (km/h)
1	0.00	Dropped Dye and Salt						
2	0.48	First Arrival	0.864	0.864				
2	0.48	Peak Dye	0.375		0.375			
3	0.90	First Arrival	0.614	0.614				
3	0.90	Peak Dye	0.587		0.587			
3	0.90	Salt Peak	0.574				0.574	
3	0.90	Salt Tail	0.524					0.524
3	0.90	Dye Tail	0.514			0.514		
4	1.35	First Arrival	0.704	0.704				
4	1.35	Peak Dye	0.669		0.669			
4	1.35	Dye Tail	0.453			0.453		
7	1.73	First Arrival	0.525	0.525				
7	1.73	Salt Peak	0.518				0.518	
7	1.73	Peak Dye	0.512		0.512			
7	1.73	Dye Tail	0.458			0.458		
8	2.01	First Arrival	0.532	0.532				
Agua Brava	2.14	First Arrival	0.553	0.553				
Powerline	2.69	First Arrival	0.527	0.527				
14	3.31	First Arrival	0.595	0.595				
16	3.66	First Arrival	0.561	0.561				

Table A-2
Tracer Test Flow Velocities, Rio Salado, January 1998 (Continued)

Station	Stream Kilometer	Observation	Velocity (km/hr)	First arrival (km/h)	Peak Dye (km/h)	Dye Tail (km/h)	Salt Peak (km/h)	Salt Tail (km/h)
17	3.96	First Arrival	0.587	0.587				
18	4.34	First Arrival	0.618	0.618				
18	4.34	Salt Peak	0.547				0.547	
18	4.34	Peak Dye	0.537		0.537			
18	4.34	Dye Tail	0.510			0.510		
18	4.34	Salt Tail	0.505					0.505
18	4.34	Background	0.499					
Agua Verde				1.421	1.080			
Agua Brava				0.428	0.422	0.363		
Rio Salado Averages				First arrival	Peak Dye	Dye Tail	Salt Peak	Salt Tail
				0.607	0.536	0.484	0.546	0.515

A-13

Table A-3
Point Velocity and Discharge Values

Station	Date	Velocity (km/h)	Discharge(m^3/s)	Comments
RC-4	6/27/97	1.461	0.195	Upstream of weir
RC-4	6/27/97	1.367	0.195	Duplicate test
8	6/27/98	1.741	0.214	~100 m upstream of confluence of Agua Brava and Rio Caliente
6	6/28/98	0.794	0.059	Downstream RC-3
RC-8	1/12/98	1.285	0.543	Below RC-8 weir 50 m, weir washed out
19	1/11/98	1.411	0.569	At intersection of Granjas Road and Rio Salado
20	1/11/98	1.230	0.571	At intersection of El Mirador Road and Rio Salado
12 +	1/12/98	1.356	0.472	40 m downstream of Powerline Spring
11 +	1/12/98	0.959	0.443	30 m upstream of Powerline Spring
11	1/12/98	1.338	0.337	~100 m upstream of sample point 11
8	1/12/98			~100 m upstream of confluence of Agua Brava and Rio Caliente
RC-1	1/2/82	No Value	0.060	CFE
RC-2	1/2/82	No Value	0.133	CFE
RC-3	1/2/82	No Value	0.043	CFE
RC-4	1/2/82	No Value	0.156	CFE
RC-5	1/2/82	No Value	0.010	CFE
RC-6	1/2/82	No Value	0.379	CFE
RC-7	1/2/82	No Value	0.102	CFE
RC-8	1/2/82	No Value	No Value	CFE

Powerline Discharge = 0.029 m^3/s

Field Parameters

Field parameters of pH, specific conductivity, temperature, and oxidation reduction potential (ORP) were measured using calibrated probes. The field parameters data collected in this effort are presented in Table A-4. Measurements were conducted at the time of sampling and during tracer tests. Field measurements were made as close as practical to the stream channel location that was sampled, within several minutes of sample collection. All meters were calibrated and stored according to the manufacture's instructions and cleaned between uses with a Type I water

rinse. Occasional physical cleaning of probe sensors was accomplished with Kim-wipes tissue or cotton swabs. All calibrations, equipment malfunctions, or failures to spot check were recorded in the project logbooks. Over the course of two weeks one pH meter-thermometer and one specific conductivity sensor failed and backups had to be brought into use.

A Cole-Parmer TDSTestr 40 with a temperature compensated range of 0-1999 and 0-199 μS/cm and accuracy of ±2% of full scale was used to monitor conductivity. A conductivity calibration standard of 1333 and 133 μS/cm was used to check instrument response several times a day. The instrument was calibrated to the same standards daily before use.

An OMEGA model PHH-82 meter was used to measure pH and ORP. The glass-bulb gel-filled combination electrode pH meter has a range of 0-14 pH units, resolution of 0.01 pH units, and accuracy of ±0.02 pH units over an automatically temperature compensated range of 0-70°C. Fresh National Institute of Testing and Standards (NITS) traceable pre-mixed buffer solutions of 4.01, 7.00, and 10.01 pH units at 25°C, accurate to ±0.02 pH units (OMEGA), were used for daily calibrations. The true buffer values were calculated using the manufacturer supplied temperature dependent pH corrections appropriate for each buffer. Since Rio Salado waters were found to have a pH range of 6.25 to 8.91, calibration was checked frequently. Very little drift in calibration was noted during these checks. The ORP meter is a platinum electrode type with range of ±1000 mV, resolution of 1 mV, and accuracy of ±15 mV. The ORP meter is factory calibrated at time of manufacture and is not intended for user adjustment. The meter is referenced to the Ag/AgCl electrode in the pH sensor with the meter reading the differential voltage between the Pt and Ag/AgCl electrodes. This reading is corrected to Eh by addition of the standard potential for the Ag/AgCl electrode (200 mV) to the meter reading. The meter was new at project initiation.

Temperature was initially measured using an OMEGA model PHH-3X combination thermometer and pH meter with a range of 0-70°C. This unit has a resolution of 1°C and accuracy of ±1°C. The PHH-3X failed on January 6, 1998. The meter was replaced with a mercury thermometer with resolution of 0.1°C and accuracy of ±0.2°C on January 9, 1998. This resulted in some loss of planned data. Temperature dependent pH meter calibrations were made on the morning of January 7 and 8 using morning temperature values from January 6. No temperature reading was made at Station 14.

Dissolved oxygen was measured only at three cool sample locations (<40°C) using a Yellow Springs Instruments model 53 DO meter. Streamflow was rapid enough that a stirrer was not necessary. The DO probe sensor would be damaged at temperatures above 40°C. The meter was calibrated according to the manufacturer's instructions using water-saturated air as a standard. It was originally intended that other gas measurements would be provided by quadrupole mass spectrometry (QMS). Equipment difficulties were not resolved quickly enough to have confidence in the QMS gas analysis for the majority of samples obtained in January. It was several weeks after return from the field before the samples could have been run. One gas analysis of a spring was completed.

Alkalinity was determined by titrating a 50 ml sample with standardized 0.020 N H_2SO_4 to phenolphthalein (colorless, pH~8.3) and bromcresol green-methyl red (light pink, pH~4.5) endpoints. Titrations were conducted at the end of each field day. Carbonate (CO_3^{2-}) concentrations can be estimated as two times the phenolphthalein alkalinity. The bicarbonate

(HCO_3^-) concentration estimate is the bromcresol green-methyl red alkalinity, minus two times the phenolphthalein alkalinity. Due to the high silica content, and some lesser ions, there is a non-carbonate contribution to the total alkalinity. This correction is performed as part of the modeling effort. The uncorrected alkalinity values and other field data are presented in Table A-4.

Table A-4
Field Parameters

Station	Date	Time (MST)	Temp (°C)	Conductivity (uS/cm)	pH	ORP (mV)	CO_3^{2-} (ppm)	HCO_3^- (ppm)
RC-1 North	1/10/98	830			6.52	273		
RC-1 South	1/10/98	830			6.53	280		
RC-1 West	6/26/97	1300	62.1	1674	7.01			
RC-3	1/6/98	1145	53	1289	7.64	224		
RC-3	1/7/98	919	49	1359	7.87	251		
RC-3	1/12/98	1601	60.5	1412	7.67	240		
AV Source 1	1/5/98	1032	31	1500	7.42	226		
AV Source 2	1/5/98	1035	25	1340	7.85	310		
AV Source 3	1/5/98	1036	61	1475	6.83	275		
AV Source 4	1/5/98	1040	63	1385	6.56	330		
AV Source 5	1/5/98	1045	64	1360	6.49	300	0	328
AV Source 5	1/12/98	1045	67.5					
AV Source 5	6/26/97	1500	67	1566	6.25			
AB Source 1	1/6/98	1320	57	1335	7.7	231		
AB Source 2	1/6/98	1321	64	1329	6.5	219		
AB Source 2	1/12/98	1355	67.5					
AB Source 3	1/6/98	1322	46	1049	7.67	217		
Powerline	1/7/98	1017	51	1182	6.8	187		
Powerline	1/12/98	1242	58.5	1242	6.67	174		
RC Down AV	1/5/98	1457	36	1312	8.46	285		
RC Down Powerline	1/12/98	1140	42.8					
RC Up AV	1/5/98	1457	35	1287	8.45	282		
RC Up Powerline	1/7/98	1039	27	1241	8.3	196		
RC Up Powerline	1/12/98	1330	41.5	1241	8.3	196		
1	1/6/98	756	58	1415	7.16	240	0	416

Table A-4
Field Parameters (Continued)

Station	Date	Time (MST)	Temp (°C)	DO mg/L	Conductivity (uS/cm)	pH	ORP (mV)	CO_3^{2-} (ppm)	HCO_3^- (ppm)
1	1/7/98	724	57		1333	7.29	284		
1	1/10/98	800	61		1406	7.47	290		
2	1/5/98	1703	46		1395	7.75	58	0	392
3	1/8/98	815			1220	7.81	327	0	408
3	1/10/98	1614	48		1291	7.82	280	0	424
4	1/10/98	1210	42.5		1277	8.4	287	80	328
6	1/5/98	1332	48		1310	8.48	280	88	300
7	1/6/98	1002	42		1287	8.4	218	56	320
8	1/9/98	1040			1269	7.89	308	76	334
9	1/6/98	1416			1289	7.64	226	0	368
9	1/12/98	1345	61.5						
10	1/6/98	1601			1188	8.45	226	104	270
10	1/7/98	942	42		1250	8.45	248		
10	1/12/98	1328	51.5		1310	8.53	206		
11	1/7/98	1642			1232	8.67	240	160	236
12	1/7/98	1459			1207	8.44	222	88	308
14	1/7/98	1303			1130	8.45	264	40	336
16	1/8/98	1505			1130	8.51	269	152	252
17	1/8/98	1310			1233	8.76	257	152	256
18	1/8/98	1130			936	266	66	96	280
18	1/12/98	1200	34	5.2					
19	1/11/98	1110	28.5	5.3	1245	275	75	144	220
20	1/11/98	1451	27.7	6.3	1005	295	95	140	284
AD	1/11/98	1238	29		443	267	67		
13	1/7/98	1116		5.2	316	208	8	0	88
13	1/12/98	1334	29						

Surface Water Sampling

The Rio Salado was sampled along ~10 km of stream reach. At most sampling locations, sediments, rocks, soils, and plants were sampled in addition to surface water. There were three water sampling programs during the reconnaissance sampling: 1) Broad sampling, conducted for

all parameters at most all sites; 2) Repeated opportunistic total arsenic source sampling, conducted at the RC-1, RC-3, and RC-4 weirs, and the Powerline Spring, to examine the variability of total arsenic over time; and, 3) Diurnal sampling, conducted at Station 3 to examine arsenic speciation in light and dark conditions and check for variability over time of the broad parameter list.

All water samples were grab samples collected before any sediment, rock, or plant sampling. Every reasonable effort was made not to perturb the stream bottom before and during water sampling. Field parameters (with exception of alkalinity) were measured in-stream following water sample collection. At all sample stations the water sample was collected from the stream position that appeared to be best mixed and most representative of the main flow (thalweg), or directly from a spring source. A pre-washed high-density polyethylene (HDPE) pail was rinsed several times in this flow and used to dipper out a sample. This sample was split with 0.5L being immediately filtered through a 0.45 μm cellulose acetate membrane (Millipore) under hand-pump vacuum, and 0.5 L being retained as an unfiltered aliquot. A 1.0 L Nalgene HDPE graduated cylinder was used to measure water aliquots for filtration. The unpreserved filtered and unfiltered aliquots were subsampled for arsenic speciation, then one aliquot was preserved to pH≤2 with concentrated nitric acid that had been double distilled at the New Mexico Bureau of Mines and Mineral Resources (NMBMMR). Another 1 L aliquot was obtained for an unpreserved sample for anion and alkalinity determination. Speciated arsenic samples did not receive additional acid preservation. For time series sampling a 125 ml container was pre-rinsed with sample a few times, filled, and preserved with nitric acid. At the end of each field day the samples were checked for plastic bag, label, and container integrity and iced. All samples were kept on ice in the custody of the sampling team until return to the laboratory in New Mexico where they were refrigerated at $4 \pm 2°C$ until analysis.

Stream Sediment Sampling

Stream sediment collection was accomplished by David Welch of the New Mexico Institute of Mining and Technology (NMIMT). Welch conducted the sampling and analysis in support of this effort and his evaluation was used as partial completion of his master's degree in Geochemistry at NMIMT [108]. Welch's sampling and analysis procedures and evaluations of the Rio Salado sediments are presented as edited excerpts from his thesis. Due to the complexity of his methodology and the importance of his findings to the modeling effort, they are included in this report generally as excerpts from the thesis rather than by paraphrasing the text. Accurate sediment analytical work is essential to testing of the modeling approach presented later. Welch's effort provided the raw data necessary to define mineral surfaces for the Rio Salado modeling approach.

Samples were collected at 20 sample stations separated by approximately 500 meters along Rio Caliente and its tributaries. Sediments were collected within 20 meters of locations where stream waters were sampled so that direct comparisons could be made between water and sediment chemistry. Where possible, sediments were collected midstream by plastic scoop and contained in one-half gallon plastic buckets and one-liter plastic bottles that were refrigerated to $4 \pm 2°C$ until time of sample preparation. In some locations larger cobbles and algae mats were removed before scooping.

Before sample collection, redox conditions at the sediment-water interface and several inches within the sediments were tested using an OMEGA model PHH-82 meter. Though measured Eh conditions within sediments ranged from +70 to +350 mV, only samples with Eh values greater than +200 mV (corrected for 200 mV difference between standard platinum electrode and Ag/AgCl reference electrode) were used for direct comparison between sample stations. This was done to reduce heterogeneity of samples resulting from different mineral assemblages stable under differing redox conditions. Also, the procedures involved in preservation of reduced sediments are elaborate and were beyond the scope of what could be accomplished on this sampling trip.

Sediments were air-dried and split into manageable portions using the cone and quartering method. With this method, a cone was initially made by pouring the sediments through a plastic funnel. The sediment cone was then quartered on a sheet of plastic. Two of the opposite quarters were then mixed and quartered again. This procedure was repeated several times until a manageable sample size was obtained. Air-drying of the samples was done because it is believed to have a lower possibility of affecting secondary mineral phases and organic matter than heat-drying or freeze-drying.

Plant and Algae Sampling

Algae and plant specimens were also collected at each of the La Primavera sample locations. An attempt was made to collect each type of plant and algae present at sample sites. Algae and plants were stored in separate ziplock bags and refrigerated at $4 \pm 2°C$ until time of sample preparation. Algae samples were first patted dry with a paper towel to remove excess moisture and weighed to obtain a "wet weight" then dried overnight at 105°C. The dried algae was re-weighed to obtain a dry weight and ground to a powder in a ceramic mortar for analysis.

Analytical Methods

Overview

Other than field measurements and separations, all analytical procedures were conducted at New Mexico Institute of Mining and Technology (NMIMT) and New Mexico Bureau of Mines and Mineral Resources (NMBMMR) facilities. Water analysis was conducted by Gregory P. Miller and sediment analysis by David Welch of NMIMT. The principal instruments used for water and sediment extract analyses are an IL Video Model 12 flame atomic adsorption spectrophotometer (FAA), Varian 600 Zeeman, graphite furnace atomic adsorption spectrophotometer (GFAA), and Dionex 4000 ion chromatograph (IC). The determinations and analyses that were performed for this effort are listed in Table A-5. Tabular analytical data for all analyses described here is presented later.

Table A-5
Reconnaissance Sampling Data Collection

Parameter	PQL[1]	Method	Comments
Field Measurements			
pH	± 0.02 units	Field Probes	Calibrated daily and checked frequently through the day.
Conductivity	±10 µS/cm		
Temperature	± 1°C	Field Probes	Calibrated daily against temperature corrected KCl standard.
Eh	± 10 mV	Field Probes	Measured with calibrated probes and mercury thermometer.
Alkalinity	5 mg/L as CaCO$_3$	Field Probes	Platinum electrode values corrected for Ag/AgCl reference electrode (add 200 mV to meter reading).
		Titration	Field titrated alkalinity at pH 8.3 and 4.5 endpoints. Performed in field daily.
Metals			
Aluminum	0.005 mg/L	GFAA	
Arsenic	0.002 mg/L	GFAA	
Barium	0.003 mg/L	GFAA	
Boron	1 mg/L	GFAA	
Cadmium	0.001 mg/L	GFAA	Cadmium not detected.
Calcium	0.2 mg/L	FAA	
Chromium	0.001 mg/L	GFAA	Chromium not detected.
Copper	0.0005 mg/L	GFAA	
Iron	0.003 mg/L	GFAA	
Lithium	0.05 mg/L	GFAA	
Magnesium	0.05 mg/L	FAA	
Manganese	0.005 mg/L	GFAA	
Molybdenum	0.005 mg/L	GFAA	
Potassium	0.1 mg/L	FAA	
Selenium	0.005 mg/L	GFAA	Selenium not detected.
Silica	20 mg/L	FAA	
Sodium	0.2 mg/L	FAA	
Strontium	0.004 mg/L	GFAA	
Vanadium	0.005 mg/L	GFAA	Vanadium not detected.
Zinc	0.03 mg/L	FAA	Zinc not detected.

Table A-5
Reconnaissance Sampling Data Collection (Continued)

Parameter	PQL[1]	Method	Comments
Anions			
Total Bromine	1 mg/L	IC	Samples prefiltered using 0.22 micron cellulose acetate filter (Millipore) and direct injected to the Dionex 4000 IC.
Chloride	1 mg/L	IC	
Fluoride	0.2 mg/L	IC	
Nitrate	0.1 mg/L	IC	
Phosphate	0.1 mg/L	IC	Phosphate not detected.
Sulfate	0.1 mg/L	IC	
Sediments			
Sediment preparation was highly variable and dependent on the analytical method used.	Specific surface area. Trace elements by XRF. Grain size distribution. Trace level carbonate solid phases. Amorphous digestion for Fe, Mn, and Al concentrations. Strong acid digestion for Fe, Mn, and Al concentrations. Hydroxylamine hydrochloride extraction for Fe, Mn, and Al concentrations (Chao reagent). Arsenic speciation by phosphate ion –exchange displacement followed by ion chromatography. Electron microprobe and reflectance spectrophotometry of polished sections. Total organic carbon by loss on ignition.		

[1] Practical Quantification Limit Note: mg/L = parts per million (ppm) and µg/L = parts per billion (ppb)

Data Quality

Reagents and Standards

Trace metal grade reagents were used when available. Fisher Trace Metal HCl and NH_4OH were diluted as necessary. These reagents were used for column preparation and regeneration that does not require very precise molarity, and they were not standardized. HCl and NH_4OH used for ion exchange chromatography eluant were standardized to pH values within ± 0.05 units of optimal. The maximum error from this simplification is less than 10% for HCl and less than 1% for NH_4OH. TCA for elution was made from Sigma ACS reagent solid and could be formulated by dilution to precise molar concentrations. The measured pH of the 0.006 M trichloroacetic acid (TCA) was 2.25 ± 0.05 and the 0.2 M TCA was 1.05 ± 0.05 at 23.2°C. The pH was checked when stock solutions were made.

With the exception of MMAA, all arsenic standards were obtained from Sigma. MMAA could not be located through the normal chemical suppliers. MMAA was obtained from Dr. Dean Carter of the University of Arizona. As^{3+} standards were prepared from American Chemical Society (ACS) certified reagent grade arsenic trioxide. As^{3+} standards were prepared the day of use as a 1.000 g/L arsenic stock solution by dissolution in 100 ml of hot 1.0 M trace metal grade HCl and dilution to 1 liter with Type I (ASTM) water. Complete oxidation of As^{3+} standards to

As^{5+} in two weeks was observed during this effort. Partial oxidation has been observed in less than 12 hours. Attempts were not made to preserve the As^{3+} standards. As^{5+} and DMAA standards were prepared from ACS reagent sodium arsenate and Sigma Ultra cacodylic acid as 1.000 g/L arsenic stock solutions by dissolution in 1 liter of Type I water. Since only ~50 mg of MMAA was made available to this effort, a 52 ppm as arsenic stock solution was prepared by dissolving 0.0201 g of MMAA in 100 ml of Type I water.

Quality Assurance

Design of this project incorporated a data quality objective (DQO) development process early in its inception. It was recognized that this data might be used for risk assessment, risk management, or comment on rulemaking. Balanced with this was the necessity to limit analytical and field costs. Data quality objectives had to be set to meet these competing priorities.

A DQO process was used to define the sampling and analysis program described here. The DQO process was created by the USEPA in the late 1980's for use in the Superfund program as part of a general, and ongoing, revision of their quality assurance and quality control practice, regulation, and guidance. The DQO process borrows heavily from elements of Terzhagi's observational method and other well accepted experimental design principles. USEPA's objective was to create a publicly-acceptable quality framework for environmental data collection that would meet the needs of environmental compliance and risk assessment at lowest cost. The intended purpose of the DQO process is to ensure that:

- The questions to be answered through data collection and analysis are well defined;

- The data collected is of known quality;

- An acceptable level of uncertainty for answers to the questions is specified; and

- The cost, amount, and quality of data necessary to answer questions are critically evaluated.

The DQO process enabled us to establish the following findings and objectives.

- Combining arsenic analysis with surface water flow measurement allows evaluation of the sources and sinks of arsenic, kinetics of arsenic transformations, and the role of other chemicals in arsenic behavior.

- High levels of arsenic may make it easier to inspect the system for processes that are known to occur, but have elusive quantification.

- Speciation of arsenic was required because the species distribution was unknown.

- A broad range of analysis is required to allow detailed evaluation of water-mineral chemistry and mechanistic modeling of system geochemistry.

- Sample aliquots were preserved appropriately and were large enough to allow additional analyses to be conducted if data gaps are identified.

- Analytical techniques should be comparable to a US laboratory protocol or peer reviewed publications.

- Physical and chemical parameters such as temperature, pH, Eh, streamflow needed to be measured.

- Sediment mineralogy, physical properties, and surface chemistry required investigation.

- The density of measurements was selected to arsenic speciation and partitioning at different scales.

- The uncertainty in the data and interpretation was hoped to be comparable to that of a preliminary risk assessment or initial remedial investigation.

Plan review was accomplished before project implementation. The Phase I reconnaissance sampling plan was reviewed and approved by Ishwar Murarka, and the plan for subsequent Phase II modeling of the data was reviewed and approved by Mary McLearn, both of EPRI.

The data set was very broad in terms of the analysis conducted and was found to be of good accuracy and precision. At this point it was determined that exploratory modeling using a thermodynamically based, mechanistic surface complexation approach was possible with the existing data set. Correction of a few data gaps and inclusion of the Rio Salado sediment data [108] was required for modeling. The predictions are made using thermodynamic properties and assume equilibrium conditions.

All data collection met project-specific precision, accuracy, representativeness, completeness, and comparability criteria (PARCC parameters) or it was determined that an out-of-control event had taken place and the data used with caution if used at all. Chemical analyses should meet the precision and accuracy standards of SW-846 in order for the data to be acceptable. Generally, the reconnaissance data met these requirements. However, due to the novel and exploratory use of the data, full SW-846 QA (matrix spikes, matrix spike duplicates, and internal laboratory QA programs) was not invoked. Some methods, such as ion exchange chromatography and sediment partial extraction do not have SW-846 equivalents. All non-SW-846 analytical methods used have been peer reviewed, published in peer reviewed journals, or developed as part of this effort.

Sample types were determined based on the environmentally significant repositories of arsenic at the field site, namely water, geomedia, and plants. The sample locations for the reconnaissance survey were selected based on several factors. The first was to limit the number of sample locations to 20 for the reconnaissance survey so that all locations could be sampled within time and budget constraints. Next was to ensure that all major arsenic sources (thermal springs) be sampled directly. Samples are also desired at each of the existing flow structures and above and below the coalescence between first and second order streams to separate arsenic contributions and effects. An approximate sample spacing of 500 meters within the watershed was selected to enable the study to observe arsenic transformation kinetics on the scale that it had been noted in Hot Creek, California [44]. Additional sample locations were filled in at approximately this spacing. Finally, two sample locations were selected at a distance of 2 and 6 km downstream of RC-8 to examine far-field geochemistry.

All sample containers were new HDPE (Nalgene or equivalent) bottles or pails. All containers were cleaned with Alconox detergent and warm water, triple rinsed with tap water, triple rinsed with Type I water, and allowed to air dry with openings down. Following drying, caps were replaced and sample containers stored in zip-closure plastic bags for transportation to the field.

Any other field sampling equipment was field cleaned immediately following use with 1.0 M Fisher Trace Metal grade HCl, and triple rinsed with Type I water. All field sampling equipment was cleaned nightly with an Alconox wash, triple rinse with Type I water, and air drying. No sampling equipment was exposed to the high-arsenic tap water available at the field site.

All water samples were containerized and preserved according to USEPA SW-846 accepted methods. Samples remained in the sample team custody throughout the sampling event and were transported to the laboratory in the custody of the sampling team. Water and sediment samples were stored at $4 \pm 2°$C until analysis. SW-846 mandated holding times were met. All sample locations are identified alphanumerically. Sample numbers were recorded in the project logbook. These numbers will be used to track the samples until final disposal.

Data was obtained from the analytical laboratory in electronic format to minimize transcription errors. A copy of the raw data was archived along with copies of logbooks and other data that would be difficult to reproduce. Spreadsheets were used for data manipulation and unit conversions. A number of types of exploratory statistical methods were be used to examine the data for trends and outliers, such as box and whisker plots or analysis of distributions using histograms and probability plots.

All data to be collected was used for the evaluation of arsenic environmental chemistry. The initial parameter lists were broad in order to orient the study to a reduced set of analyses for following work. Surface water flow data was needed to evaluate mass balance and determine reaction kinetics and partitioning. Sediment data is needed to evaluate solid-water partitioning coefficients. All of the data obtained, in either raw or reduced form was used to develop the conceptual model and calibrate and validate the numerical model(s). In order to model an environmental system, the mathematical formulation of the model must be capable of accurately representing the physical system that is being modeled. This was accomplished by comparing the model output to an analytical solution for a simple system. This was accomplished for the public domain codes. Models were verified for successful computer installation by running example data sets and by comparison with the supplied test date set outputs. Code modifications were documented. There were no problems in code compiling. After any code modification, a test data set was used to demonstrate that the computer code produces a correct solution to the mathematical model, and that the mathematical model is a valid solution to the physical problem. Once this was accomplished and documented, the code was considered to be verified. Following verification steps input parameters were systematically varied to produce a valid model of the physical system under consideration. Once the calibration target was met or exceeded (Rio Salado model), the model is ready for use for predictions (Florida Model).

Other quality assurance activities included logging of all field and lab data in bound logbooks, noting out of control events and their resolution, written preplanning of all activities, and following standard field and laboratory hygiene and safety practices. All equipment was used and maintained according to manufacturer's instructions. Malfunctioning equipment was removed from service until repairs were made. Backup equipment was available for most needs.

Quality Control

The GFAA and FAA use autocalibration procedures based on standard dilution. FAA methods for the analytes of interest are routinely run at the NMBMMR laboratory and no modification of the standard methods was necessary to achieve accurate reproducible results. This was not true for ion-exchange chromatography samples that were strongly attenuated by matrix and arsenic species effects. Special procedures were implemented in order to meet PARCC parameters for these samples.

In the case of the GFAA arsenic analysis in acidified total metals samples, little or no matrix effect was noted. The calibration curve for these samples was developed using 20 and 50 ppb standard solutions of As^{5+} in Type I water acidified to pH < 2 with ultra pure HNO_3. All analytical methods used a five point calibration curve. A blank and a 20 ppb standard were analyzed at the rate of 1 in 20. Calibration reslope was performed every 20 samples and recalibration every 40. It was noted that there was some negative bias with the mean value of 20 ppb standard (36 measurements) being 17.9 ppb. The GFAA is able to achieve detection at 1.0-1.5 ppb without matrix effects. For this effort a practical quantification limit (PQL) was set to 2.0 ppb, a value greater than the mean of the blank (36 measurements) plus two standard deviations, that gives a reproducible absorbance peak (RMS error <10% for 3 analyses).

The samples from the arsenic speciation exhibited strong matrix effects. In order to correct for this effect, standards were made by spiking eluant from a blank ion exchange separation. The blank eluant did not have detectable arsenic before the spike. This was also a control check for the regeneration process since the columns had been used with arsenic standards before the blank eluant run. The 0-55 ml fraction was used to prepare the standard for As^{3+} and MMAA analysis, the 55-85 ml fraction for As^{5+} analysis, and the 95-140 ml fraction for DMAA analysis. These standards were all spiked from the As^{5+} stock solution to 20 and 50 ppb strength. A NITS traceable standard was tested, providing a result of 56.6 ppb with a true value of 56.02 ± 0.73 μg/L arsenic as As^{5+}. Duplicates were run to spot-check unexpected values, however, there was no systematic use of duplicates. A double peak in the absorbance was also noted for the speciation matrices. The ramp and drying times for the GFAA were adjusted until this was not problematic. Arsenic analysis by GFAA is generally subject to recovery, accuracy, and precision problems. This is evidenced by the USEPA SW-846 acceptable limits for Method 7061 (GFAA) of 60-140% for accuracy (% recovery), precision of 0-40% (reproducibility) at a method detection limit of 1.4 ppb and reporting limit of 2.0 ppb. These problems were also noted in this effort.

Quantification limit studies were not performed for aqueous analytes other than arsenic since they are run routinely at the NMBMMR laboratory and/or the current level of investigation does not require greater accuracy and precision than was available to this study. There is an exception, phosphate as PO_4. Phosphate is known to affect arsenic surface complexation. The NMBMMR IC, as normally configured, has a PQL for phosphate of 100 ppb. The corresponding detection limit is ~60 ppb. It is possible that <60 ppb of phosphate could noticeably affect arsenic speciation when the arsenic level is closer to the phosphate level. This is in an arsenic and phosphate concentration range that may be common. Using the standard IC setup, phosphate was not detected in Rio Salado waters. It would improve the present and future work to lower the PQL for phosphate at the NMBMMR laboratory.

Quality Assessment

Samples are generally representative of the site conditions because deviations were not made from acceptable sampling practice for the media of interest. With the exception of arsenic speciation, chemical data is 'complete' because >90% of all data collected meets PARCC requirements within project standards. The chemical data is comparable to other data collected using SW-846 protocols. The DMAA data obtained is suspect and the achievable phosphate PQL should be lowered for low-arsenic work.

Speciation of Arsenic in Water

Investigation of the speciation of arsenic in the environment requires the ability to preserve the arsenic species before analysis, or to separate the species before transformation takes place. Given the uncertainties in the preservation of arsenic species, field separation was selected. Separation is initiated within minutes of sample collection. Uncertainties associated with sample preservation are eliminated. In order to accomplish this, an existing ion chromatography separation method for As^{3+}, As^{5+}, MMAA, and DMAA was modified for field use [124].

Speciation Method Modification

The published method uses 9 cm of anion exchange resin (100-200 mesh, AG-1X8, Bio-Rad) and 26 cm of cation exchange resin (100-200 mesh, AG50W-X8, Bio-Rad) in a single 1×35 cm nitrogen pressurized glass column to separate these four arsenic species. Since nitrogen pressurization was not practical for field use, gravity flow and 50-100 mesh resin was used to allow separation in a reasonable time. Using gravity, the flow rate was maintainable at about 3 ml/min. Separations were completed roughly one hour after sample introduction.

A second modification was the use of two glass columns in series connected by a capillary tube, a 1×10 cm column for the anion resin at the bottom, and a 1×30 cm upper column for the cation exchange resin, rather than a single column containing both resins in layers. There were several reasons for this modification. Occasionally Grabinski's columns required repacking to remove air bubbles that caused non-ideal flow conditions [124]. The anion and cation exchange resin must not be mixed during this process. Laboratory testing indicated that this would be difficult on a stream bank. By keeping the cation resin separate, it is possible to remove air bubbles by agitating the resin with a pipette. The anion resin is back flushed with a wash bottle to remove air bubbles. Another reason is that capillary connections between columns can provide for peak sharpening by allowing the main mass to catch up with the diffuse peak. All columns were stock borosilicate glass "Econo-Columns" from Bio-Rad. Prior to packing, all columns and connectors were cleaned with Alconox detergent and warm water, triple rinsed with tap water, triple rinsed with 1.0 M Fisher Trace Metal grade HCl, triple rinsed with Type I water, and allowed to air dry with openings down or covered with Kim-Wipe laboratory tissue. The anion column was filled with a 10 cm bed of AG-1X8 resin in the chloride form and capped top and bottom with a porous polymer bed support and Luer fitting. The cation column was filled with 26 cm of AG50W-X8 resin in the hydrogen form using a porous polymer bed support and Luer fitting at the base. The capillary used is a Luer connector. All columns were slurry filled with resin using Type I water and preconditioned before used.

Column conditioning, elution, and regeneration generally followed the method outlined by Grabinski. Following packing, the columns were conditioned by rinsing with 70 ml of Type I water, then two ordered series of 70 ml aliquots each of 1.5 M NH_4OH, 1 M HCl, and 0.48 M HCl. Arsenic species were not used in preconditioning. Grabinski states that "several" of the same series were used for preconditioning in his work, preceded by introduction of 50 µg each of As^{3+}, As^{5+}, MMAA and DMAA. Grabinski and this effort both used a single series to regenerate the columns between elutions. This effort preconditioned the columns with 25 ml of 0.006 M trichloroacetic acid (TCA) following the 1.50 M NH_4OH, 1.00 M HCl, and 0.48 M HCl series (before sample introduction) as suggested by Maiorino and Aposhian [114]. Grabinski did not mention preconditioning with TCA. Columns were also stored overnight, saturated with 0.006 M TCA in the laboratory and field.

Method Performance

Arsenic speciation methods were researched to find a procedure suitable for field use. No organic/inorganic arsenic method was found that was directly transferable to the field. The Grabinski method was selected for modification and testing in the laboratory. The most important factor to evaluate was if gravity flow variable head ion exchange chromatography could be used to resolve the arsenic species of interest. Recovery of arsenic standards was tested and limited optimization of the procedure conducted. There remains considerable room for refinement of the procedure. Time and budget did not allow detailed experimentation with the separation method for this project. Following determination that the gravity flow method would separate the four arsenic species of interest, in the concentration range expected at Rio Salado, the method was taken to the field.

Grabinski indicates good arsenic recovery rates (96-107%) at total arsenic concentrations below 500 ppb. The modifications to the method resulted in lower recoveries than published by Grabinski. The results obtained from the lab and field separations still provide useful data. Grabinski had noted that separation efficiency tailed off at total arsenic concentrations of greater than 500 ppb (1 µg in 2 ml). Sample recoveries tabulated in Table A-6 indicate this problem clearly. We did not try to increase recovery rate prior to field implementation of the modified method. There is also peak overlap for MMAA and As^{3+} at 1.0 ppm concentration that is not apparent in Grabinski's data. Ion exchange chromatographic methods were used to separate the arsenic species into separate aliquots for analysis by graphite furnace atomic absorption quantification.

Table A-6
Ion Exchange Chromatography - GFAA Recovery Rates

Method	As^{3+}	MMAA	As^{5+}	DMAA
Grabinski	104%	100%	97%	99%
Modified 250 ppb	90%	85%	116%	77%
Modified 1000 ppb	92%	75%	63%	43%

The ion chromatography method depends on the property of arsenic species to change charge depending on pH. Referring to the table of weak acid disassociation constants (pKa) below it is clearly seen that pH has a strong influence on the ionic charge of arsenic species. As^{3+}, as $HAsO_2$, As^{5+} as H_3AsO_4, and MMAA are either neutral or negatively charged oxyanions at pH values from 1-12. DMAA can act as an anion, neutrally charged, or a cation dependent on pH.

Table A-7
Acid Disassociation Constants for Arsenic Compounds

Species	Below pK$_1$	pK$_1$	pK$_1$ ⇔ pK$_2$	pK$_2$	Above pK$_2$	pK$_3$
As^{3+}	neutral	9.18	anion			
As^{5+}	neutral	2.22	anion	6.98	anion	11.60
MMAA	neutral	3.41	anion	8.18		
DMAA	cation	2.60	neutral	6.27	anion	

It is this principle that allows separation of these four arsenic species by ion exchange chromatography. Below a pH of 9.18, As^{3+} is a neutral species, above that pH it is an anion. For As^{5+} below pH 2.22, As^{5+} is neutral, above that pH it is negatively charged. Below a pH of 3.41, MMAA is a neutral species, above that pH it is an anion. DMAA below a pH of 2.60 is in the cation form, between 2.6 and 6.27 it is neutral and above pH 6.27 it is an anion. By selective use of eluant, it is possible to take advantage of these differences and separate the four species.

The elution process is as follows. The sample is gently introduced to the top of the cation exchange column using a 2 ml class A pipette (±0.006 ml). The stopcock on the base of the column is opened and 2 ml of the 0.006 M TCA is wasted. As in the Grabinski method, the sample is then eluted using 55 ml of 0.006 M TCA, 8 ml of 0.2 M TCA, 55 ml of 1.5 M NH_4OH, and 50 ml of 0.2 M TCA that are gently decanted into a gravity fed reservoir. Since gravity flow is used, flow rates are variable as the head on the column changes.

The arsenic species separations work in the following manner. In 0.006 M trichloroacetic acid, pH < 2.5, the As^{3+} and MMAA exist in solution as uncharged species, the As^{5+} exists primarily as an anionic species, and DMAA is dominantly a cation. Most of the DMAA is retained at this pH on the cation exchange column. Elution of the neutral As^{3+} is not retarded by cation and anion exchange resins and elutes the first 25 ml. The second fraction of the eluted solution (25 to 55 ml) contains the MMAA. Although the MMAA is also predominantly uncharged, it elutes behind the As^{3+}. The literature did not contain any detailed, plausible explanations of this behavior. It is probable that the MMAA is weakly retained due to non-polar interactions or other processes that are not well understood at this time. The retardation of the MMAA is consistent. The resin column now contains the As^{5+} species strongly bound on the anion exchange resin and the DMAA species strongly bound on the cation exchange resin. The addition of 8 ml of 0.2 M TCA lowers the pH to less than 1.0. The DMAA is retained strongly on the cation exchange resin. As the more concentrated TCA enters the anion resin, As^{5+} is converted into its neutral form and is collected in the 55 to 85 ml fraction. The only arsenic species left in the chromatographic column is the DMAA on the cation resin. Addition of the solution of

1.5 M NH$_4$OH (pH~12) converts the DMAA into its anionic form, strips it from the cation exchange and carries it into the anion exchange resin at the bottom of the column where it is strongly retained. Finally, the addition of 0.2 M TCA strips the DMAA species by converting it to its neutral and cationic forms to be collected in the 85 to 140 ml fraction.

Referring to the validation run arsenic elution points, Figure A-3, it can be seen that there is definite separation between the arsenic species. The right figure depicts the elution curve of 1000 ppb standards. The graph on the left depicts the separate arsenic species eluting when a mixed standard with 250 ppb of As^{3+}, As^{5+}, MMAA and DMAA is used. Based on these and other validation runs, the 0-25 ml aliquot was collected as As^{3+}, the 25-55 ml aliquot as MMAA, the 55-85 ml aliquot as As^{5+}, and DMAA in the 85-140 ml fraction. The overlap in the As^{3+} and MMAA peaks is of some concern at higher concentrations. As evidenced in Figure A-3 the As^{3+}-MMAA peak separation is good at a concentration of 250 ppb.

Problems with DMAA Quantification

There are some problems with the separation of DMAA using the method as employed in January 1998. The method used here quantified significant amounts of DMAA (20-200 ppb). Two other researchers (Eric Crecelius, Battelle Marine Sciences Laboratories and Walter Goessler, University of Austria-Graz), did not find DMAA in sub-samples of the Rio Salado water samples. Crecelius and Goessler did not find DMAA in either the filtered HNO$_3$ preserved samples or unfiltered unpreserved samples that were sent to them in July, 1998. Ion exchange laboratory validation had shown successful separation of DMAA from other arsenic species.

A - Mixed Standards 250 ppb

B - Individual Standards 1000 ppb
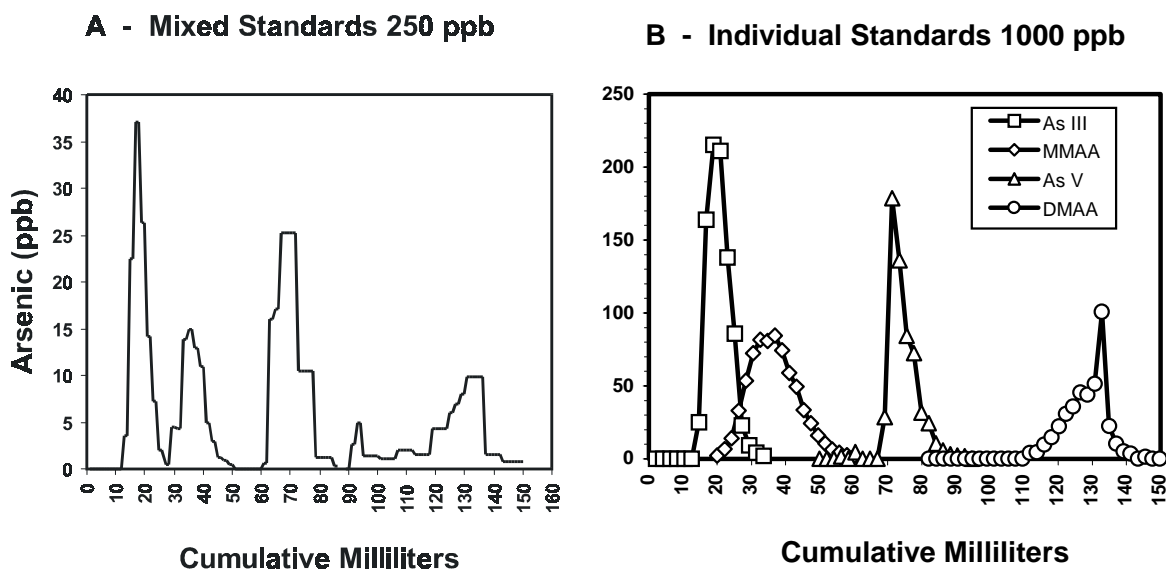
Figure A-3
Examples of Early Validation Runs for Ion Exchange Separation of Arsenic Species

During the laboratory testing conducted before the January 1998 sampling event, analysis of the eluant in the 110-160 ml range was not done when only As^{5+} standards were used. Testing after the January sampling did examine this area of the As^{5+} elution. The problem lies in that the

peaks at 115 and 135 ml points create a false positive for DMAA. A confounding factor for this being an explanation of DMAA false positives is that the mass of As present in the 'late' As^{5+} eluant is far less than the mass of As found in the field collected DMAA eluant fractions. This is shown in Figure A-4. The triangles are the amounts of late arsenic that show up in the eluant at >110 ml after As^{5+} standards have been run through the column. The dark diamonds and squares are DMAA values for the field samples. Only a few samples fall below the 1000 ppb As^{5+} 'late peak' mass line. This would appear to indicate that the DMAA seen could not be a result of the As^{5+} bleeding through to the DMAA eluant. If the 'DMAA' seen in the field samples is indeed As^{5+}, a constant ratio would be expected, since the 'late' eluted As^{5+} (filled triangles Figure A-4) concentrations are quite linear with respect to the concentration of the As^{5+} standard introduced to the column. We also evaluated DMAA/As^{5+}, DMAA/Total As, and As^{5+}/Total As ratios for the different sample stations and DMAA vs. As^{5+} concentration.
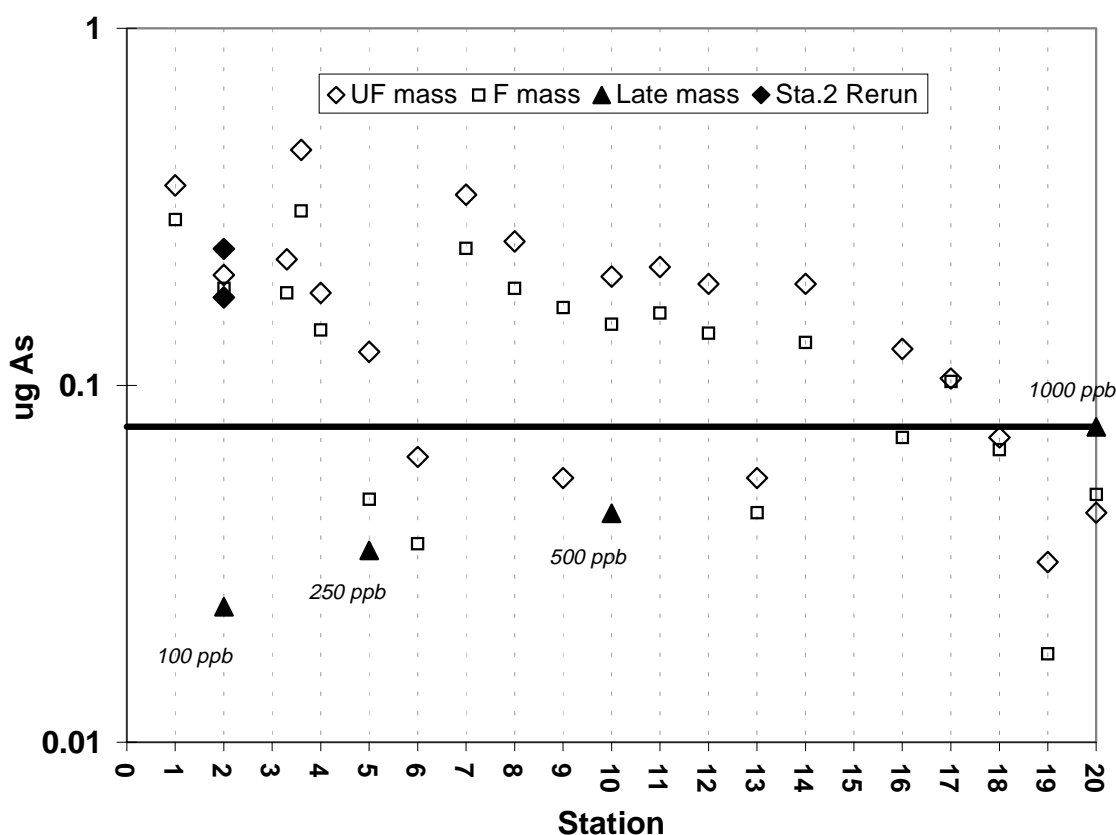
Figure A-4
Comparison of the Late Mass Peaks Produced by As^{5+} and the Mass of 'DMAA' Detected at Rio Salado

We found that the ratio of DMAA to As^{5+} or Total As is not constant, implying that they are not proportional and are not correlated. As^{5+} and Total As ratios are relatively constant, implying a relationship. When taken all together, the column evidence indicates the presence of DMAA in substantial concentrations, not related to As^{5+} concentration, but only if other evidence to the contrary is ignored. A 2 ml aliquot of the unpreserved Station 2 sample (anion) from January 1998 was run through the column twice in October 1998. The eluted 'DMAA' mass is

plotted as light diamonds in the figure. These 'DMAA' values are almost identical to the values determined from field elution. It is difficult to explain the amount of 'late' arsenic showing up in Station 2 based on the bleed through of As^{5+} observed during the DI water tests (triangles). Subsequent testing using the Grabinski method as published, and as modified here, failed to replicate the published finding that 8 ml of 0.2 M TCA is sufficient to elute all As^{5+} from the column. These methods result in a late peak for As^{5+} in the DMAA elution range. It was found that 40 ml of 0.2 M TCA was required to cleanly elute the As^{5+} peak and eliminate the late peak.

In summary, DMAA is a common constituent in surface waters. The detected 'DMAA' is suspect given the number of confounding factors. The observation of MMAA in absence of As^{3+} (no possibility of peak overlap) and Welch's observation of MMAA and DMAA in sediments and algae is definitive evidence that there is organic As in the Rio Salado system. DMAA is more likely to be present in natural waters than MMAA [46, 47, 48, 71, 115, 116, 117, 118, 119, 120, 121]. There should be DMAA in Rio Salado waters but quantification was prevented due to problems with the speciation method.

Sediment Extractions

The sediment extraction text presented below has been excerpted from Welch, 1999. Welch's text has been annotated, modified, or reorganized as necessary to ensure nomenclature and organizational compatibility with this report. All excerpts, graphics, and text modifications have been used or made with permission of the author. Data is presented in the Tabular Data section of this appendix.

Sediments were dry-sieved using U.S. Standard sieves to characterize the grain size distribution. Initially, in order to reduce sample heterogeneity, the >2 mm size fraction was sieved out and archived and is not used in the grain size distribution or chemical extractions. About 100 grams of dried sediment was weighed for separation into the following size fractions: 1.0-2.0 mm (very coarse sand), 0.5-1.0 mm (coarse sand), 0.25-0.5 mm (medium sand), 0.125-0.25 mm (fine sand), 0.0625-0.125 mm (very fine sand) and <0.0625 mm (silt-clay). The different sieves were stacked in sequence with fining mesh sizes towards the bottom and placed on the Ro-Tap machine to be shaken 15 minutes. After shaking, sediments from each of the size fractions were weighed to obtain the grain size distribution. A small portion of split sediments was ground to -80 mesh in a ball crusher to reduce the heterogeneity present in un-sieved material for some of the analyses. A grinding time of only 10 to 20 seconds was used to prevent the sample from heating up as well as to cut down on possible contamination by metal from the grinder itself.

Selective Extraction

A combination of partial extraction techniques developed by Tessier et al. [122] and Chao and Zhou [123] was performed on the sediments to determine relative proportions of exchangeable arsenic (water soluble and affected by adsorption-desorption processes), arsenic associated with carbonates, amorphous iron and manganese oxides, and organic matter. The procedure used is as follows: about one gram of sediment, ground to -80 mesh, is agitated in 8 ml of 1 M NaOAc adjusted to pH 8.2 for 1 h to remove exchangeable arsenic. Next, the residue from the exchangeable extraction is agitated in 8 ml of 1 M NaOAc adjusted to pH 5 for 4 hours to remove arsenic associated with carbonates. The resulting residue is then digested in 20 ml of

0.25 M NH_2OH-HCl in 0.25 M HCl heated to 50°C for 30 minutes to extract arsenic associated with amorphous iron and manganese oxides. Extraction of arsenic bound to organic matter is achieved by adding the residue from the iron-manganese oxide digestion to 3 ml of 0.02 M HNO_3 and 5 ml of 30% H_2O_2 adjusted to pH 2 with HNO_3. This mixture is heated to 85°C for 2 h after which an additional 3 ml aliquot of 30% H_2O_2 is added with continued heating for an additional 3 h. The use of 0.25 M NH_2OH-HCl (hydroxylamine hydrochloride) in 0.25 M HCl, described by Chao and Zhou [123], was used instead of the 0.04 M NH_2OH-HCl in 25% v/v HOAc suggested by Tessier et al. [122] because of its greater selectivity for amorphous Fe and Mn oxides and reduced matrix effects.

All extractions were conducted in plastic centrifuge tubes to avoid loss of sample and cross contamination. Between each successive extraction samples were centrifuged at 10,000 rpm for 30 minutes and the supernatant pipetted off for analysis. Afterwards, 8 ml of distilled water was added and the residue again centrifuged for 30 minutes. The second supernatant was removed and discarded before addition of the next extracting reagent.

HNO$_3$ Digestions

Nitric acid extractions were conducted on each of the size fractions and on whole sediment samples. About 1 gram of sediment was added to 10 ml of 8 M HNO_3, (1:1 HNO_3 and distilled water) and microwave-heated under pressure in sealed Teflon containers. This mixture was heated 12 minutes at 50 psi and followed by 30 minutes at 100 psi, about 180°C. After cooling, extracts were filtered and diluted for analysis on the GFAA.

The HNO_3 procedure dissolves many of the secondary minerals and organic matter, but not residual minerals and glasses. It also provides an estimate of the "total" acid leachable arsenic in the sediments, and represents arsenic that could be remobilized with changes in environmental conditions such as pH or Eh. USEPA indicates that the analysis provides a measure of the total amount of environmentally available metals.

Speciation of Arsenic in Sediments

Speciation of As^{3+}, As^{5+}, MMAA and DMAA in sediments was achieved by using an ion-exchange chromatography method modified after Grabinski [124]. The apparatus consisted of a 10 cm glass column, 1 cm diameter, filled with AG-1X8 anion resin in the chloride form connected by a capillary to a 26 cm glass column, also 1 cm diameter, filled with AG50W-X8 cation resin in the hydrogen form. Resins were 50-100 mesh allowing gravity flow rates of about 3 ml/min. The top and bottom of the anion column and the bottom of the cation column were capped with a porous polymer bed support, and a Luer fitting for flow control was used at the base.

Before use, the ion exchange columns were first conditioned and regenerated as described by Grabinski [124]. Initially, resin was packed into the columns with distilled water, then washed twice with successive elutions of 1.5 M NH_4OH (70 ml), 1.0 M HCl (70 ml), 0.48 M HCl (70 ml) and 0.006 M (25 ml) trichloroacetic acid (TCA). After the first sample had been run, columns were regenerated by washing with the same successive elutions only once after each additional use.

Validation of the ion-exchange method was done using the sediment extracting reagent (0.1 M H_3PO_4) before running samples. This was carried out with prepared standard solutions of 250 ppb As^{3+}, As^{5+}, MMAA and DMAA in 0.1 M H_3PO_4. Initially, each arsenic species was run separately to determine sample collection ranges and to validate separation. After sample collection ranges were determined, mixed standards containing known amounts of all 4 arsenic species were run to determine sample recoveries. Average recoveries for each of the species ranged as follows: As^{3+} (84%), MMAA (96%), As^{5+} (79%) and DMAA (79%). This extraction procedure provides semi-quantitative results for comparison between arsenic species and for comparison of the same species between different sample stations.

The effect of the H_3PO_4 extract on arsenic species was also investigated before sample analysis. Three sets of mixed standards in H_3PO_4 were run through the ion-exchange columns immediately after preparation, and an additional 3 sets run 1.5 h after preparation. No significant difference was observed between samples indicating no oxidation of As^{3+} during the time required for sediment extraction and centrifuging.

Samples were run through the columns by using successive additions of 0.006 M TCA (55 ml), 0.2 M TCA (8 ml), 1.5 M NH_4OH (55 ml) and 0.2 M TCA (50 ml). The first 29 ml of sample collected from the column contained As^{3+}, 29 to 60 ml MMAA, 60 to 90 ml As^{5+} and 90 to 140 DMAA. A description of the elution process is as follows: during the first elution with 0.006 M TCA (pH~2.5) As^{3+} is present as a neutral species and travels through the column to be collected in the first 29 ml. MMAA is also a neutral species under these conditions and is eluted after the As^{3+} and collected in the 29 to 60 ml fraction. While As^{3+} and MMAA are being eluted As^{5+} and DMAA retain a charge and stick to the anion and cation resins. $Arsenic^{5+}$ is converted to its neutral form when the 0.2 M TCA reaches it in the anion resin and is collected in the 60 to 90 ml fraction while DMAA is strongly retained on the cation exchange resin. The DMAA is converted to its anionic form and moves from the cation resin to the bottom anion resin with the addition of 1.5 M NH_4OH. The final elution with 0.2 M TCA converts the DMAA to a positively charged species removing it from the anion resin to be collected in the 90 to 140 ml fraction.

The procedure used in sediment analysis is as follows: about 1 gram of sediment, ground to <80 mesh, was added to 10 ml of 0.1 M H_3PO_4 and shaken for 1 h in a plastic centrifuge tube. Samples were centrifuged for 30 minutes at 10,000 rpm, then 5 ml of sediment extract was pipetted on to the top of the ion-exchange column. The column was eluted until the sample was level with the resin bed, after which the first elution with 55 ml of 0.006 M TCA was begun. The first 5 ml of eluant, collected while leveling the sample with the resin, was discarded and the As^{3+} fraction was collected from 5 to 29 ml. The other As species were collected in the ranges described previously. Analyses were conducted by GFAAS with calibration of the instrument in the same matrix as the sample (H_3PO_4).

Sediment Mineralogy

Sediment Petrology and Mineralogy

In addition to the sediment examinations presented below, Welch also conducted petrographic analysis of sediments to classify the rock and or mineral type present. This included thin section

analysis and modal analysis or rock or mineral type comprising the sediments at all sampling stations.

Sediments were air dried and split into manageable portions using the cone and quartering method. With this method, a cone was initially made by pouring the sediments through a plastic funnel. The sediment cone was then quartered on a sheet of plastic. Two of the opposite quarters were then mixed and quartered again. This procedure was repeated several times until a manageable sample size was obtained. Air-drying of the samples was done because it is believed to have a lower possibility of affecting secondary mineral phases and organic matter than heat-drying or freeze-drying.

Carbonate Analysis

Carbonate was present in very small amounts and was measured by pressure difference, due to acid evolved CO_2, and gas analysis using a quadrupole mass spectrometer. A glass vacuum reaction vessel was used that had a glass partition at the bottom creating two open, but separated chambers. The reaction vessel fit into a glass neck with a Teflon valve allowing the vessel to be sealed. This apparatus was fitted to a system of vacuum lines in contact with a capacitance manometer for pressure measurements. The system of vacuum lines is also set up to send a gas sample directly to a Balzers model QMG 125 quadrupole mass spectrometer.

Initially, sediment ground -80 mesh was oven dried at 105°C for about 10 minutes to remove excess moisture. Afterwards, about 1.5 g of sediment was placed in one chamber of the reaction vessel and 4 ml of concentrated H_3PO_4 was pipetted into the other. The apparatus was sealed with vacuum grease and attached to the vacuum lines. Low and hi-vacuum pumps were used to create a vacuum in the reaction vessel and were allowed to pump down overnight to remove adsorbed water and gas from the sample. The following day a downward extension on the vacuum line, filled with glass beads, was immersed in a cold trap of dry-ice in ethanol for removal of water. When the pressure in the vacuum line reached about 0.0000 mbar the initial pressure was recorded and the reaction vessel sealed off and tipped, allowing the acid to react with the sediment. The reaction was allowed to proceed for two hours, during which time the vacuum lines were pumped down to about 0.0000 mbar. Next, the vacuum pumps were sealed off and the reaction vessel opened allowing the evolved gas to fill a known volume of vacuum line connected to a capacitance manometer and cold trap. After two minutes the reaction vessel was sealed off to prevent possible leakage of air into the system. About 30 to 45 minutes were required for the pressure to equilibrate, due to removal of water from the vacuum lines by the cold trap. The final pressure and temperature was then recorded and the sample sent to the quadrupole mass spectrometer for gas analysis.

Before analysis, background intensities of H_2O, N_2, O_2, Ar and CO_2 gasses were measured when the pressure in the mass spectrometer was less than 2×10^{-7} mbar. Next, a valve was opened allowing the sample to enter the mass spectrometer. A leak valve was used to maintain a pressure in the spectrometer of 2E 10^{-6} mbar. After a few moments, the intensities of H_2O, N_2, O_2, Ar and CO_2 gasses from the sample were recorded. Mole percentages of each of the gasses were calculated and corrected from the sample intensities.

Determination of the time required for reaction was made by recording pressure increases with time after reacting a sample with acid. After two hours, in a sample containing the largest amount of carbonate, 97% of the total gas had been evolved. The largest possible sample size, about 1.5 to 2 g was used to obtain the maximum precision possible. One sample, done in triplicate, was used to provide a detection limit of 0.05% carbonate which was calculated as two times the relative standard deviation. A second sample, containing less carbonate, was also done in duplicate with reproducibility better than 0.05%. Although, the amount of evolved CO_2 could be measured very precisely, the exact proportions of CO_2 resulting from dissolution of $CaCO_3$, $MnCO_3$, $MgCO_3$ can not be determined. As a result, values are reported as % carbonate not as % $CaCO_3$.

Electron Microprobe Analysis

Polished one-inch round sections were examined by a Comica SX-100 electron microprobe. An accelerating voltage of 15 kV and a probe current of 20 nA was used. Iron oxides were visible as discrete grains and as oxidized mafic grains that still retained relict textures. No manganese minerals were detected with the microprobe. The distribution of arsenic within iron oxides was examined by conducting line scans on two different grains. Scans began in the center and proceeded in a line towards the outer edge of the grain. Output data from the line scans consisted of the number of counts of Fe and As at points along the traverse. The microprobe was also used to make point-count measurements of arsenic contents in iron-oxides relative to background glasses. Point count measurements do not provide a concentration of arsenic, only the number of counts of arsenic in one phase relative to another allowing comparison between the two.

Reflectance Spectrophotometry

A method of visible light reflectance spectrophotometry, outlined by Barranco et al., [125], was used to identify the types of iron oxides present in sediments. About 5 drops of water were added to 0.1 to 0.15 g of ground sediment, which was then mixed to make a thin slurry on a petrographic slide and dried. Samples were run on a Perkin-Elmer Lambda 6 spectrophotometer relative to a barium sulfate standard for the wavelength range 250 to 850 nm. Output data consisted of percent total reflectance vs. wavelength. Data was processed and enhanced by taking the first derivative of % reflectance and plotting it against wavelength.

Surface Area Measurements

Surface area measurements were conducted on a Monosorb direct-reading surface area analyzer (Quantachrome) using 30 mole % N_2 with 70 mole % H_2 carrier gas. Before analysis, whole sediments were heated overnight in a muffle furnace at 430°C for removal of organic matter. The Monosorb was calibrated following factory recommended procedures. About 1 to 1.5 g of sample was placed in a u-shaped glass sample tube with holder, leaving space above the sample so that gas flow was not impeded. The sample tube was then placed in an "out-gassing" station and heated with a heat gun for about 2 minutes to drive off excess moisture. After cooling, the sample tube and holder is moved to a "sample" receptacle and immersed in a liquid nitrogen bath, during which time the Monosorb records an adsorption signal. When the adsorption signal is completed the sample tube is removed from the bath and the desorption signal begins. When

the desorption signal is completed the Monosorb displays the surface area in square meters. This number is divided by the sample weight to determine m^2/gm of sediment. Though no standard reference material was available for determination of accuracy, triplicate measurements were made on 60-100 mesh Silicar silica gel produced by Mallinckrodt, which reported a surface area of 480 m^2/g. Triplicate measurements conducted on the silica gel were 598 $m^2/g \pm 7.8$. Triplicate measurements on La Primavera samples, were 1.52 ± 0.09.

Determination of Total Organic Carbon (TOC)

Percent TOC was determined by loss-on-ignition. About 10 g of un-sieved sediments were oven dried at 105°C for 3 to 4 h and weighed, then placed in a muffle furnace and heated at 430°C for 24 h. After cooling, sediments were re-weighed to determine the amount lost-on-ignition, representing TOC. Contribution to the sediment weight loss by structural water expelled from clays is insignificant due to the fact that clays were present in non-detectable amounts. Also, carbonates do not to affect the loss-on-ignition value at temperatures of 430°C [126].

X-Ray Diffraction

An attempt was made to separate clays for identification by X-Ray diffraction (XRD). Removal of organic matter was done by addition of 5 to 6 g of >63 μm sediments to 10 ml of Clorox (NaOCl) adjusted to pH 9 with HCl. This mixture is heated 15 minutes in a boiling water bath, then centrifuged for 5 minutes and decanted. This procedure is repeated several times until the decanted liquid is clear and shows no brown coloration indicating oxidized organic matter. Afterwards, the >63 μm sample is placed in a beaker with distilled water and several drops of Calgon to keep the clays dispersed. This mixture is stirred, and after 10 minutes settling time 2 ml is pipetted on to a petrographic slide for XRD on a Rigaku DMAX/2 X-Ray diffractometer. Dissolution of the organic matter with 0.02 M HNO_3 and 30 % H_2O_2 following the procedure of Tessier et al. [122], described previously, was also tried. The same technique of clay dispersion and slide preparation was used on these samples as well.

X-Ray Fluorescence

Values of total As, Fe and Mn were determined by X-ray fluorescence (XRF) on a Phillips PW 2400 instrument at the New Mexico Bureau of Mines and Mineral Resources lab. Ground un-sieved sediments were used to make pressed powder pellets that were analyzed using standard procedures.

Barium Arsenate

Barium arsenate $Ba_3(AsO_4)_2$, and the monohydrate $Ba_3(AsO_4)_2 \cdot H_2O$, have a very low solubility in water. It has been postulated that barium or calcium arsenate may exert a strong control on available arsenic by its precipitation. Barium arsenate and the monohydrate have not been observed in nature. Following the determination that quantifiable barium is introduced to Rio Salado at the Powerline spring, an investigation was conducted to determine if barium was precipitating arsenate downstream of that point. Air dried sediment aliquots of ~500 g were

sieved and the –200 mesh fraction discarded and the remainder placed in Nalgene 1L bottles and mechanically rolled for several hours to abrade the outer grain surfaces. The abraded samples were sieved again and the –200 mesh fraction retained. XRD was used on this fraction to evaluate the presence of barium arsenates. All sample tested did not indicate the presence of insoluble arsenates. In order to increase the sensitivity of the XRD method, portions of the –200 mesh retained fraction were placed in lithium polytungstate solution with a density >3.0 g/ml and centrifuged. In theory, barium arsenate with a density of 5.1 g/cc should be separated by this method. The monohydrate, with a density of 1.93 would not be concentrated by this method. The heavy liquid separation was successful in separating heavy minerals as was evidence by a strong hematite peak in the XRD scan (hematite's density is 5.24) and the large volume reduction of the sample. Barium arsenate was not detected in any of the heavy liquid separates. Although thermodynamically stable, barium arsenate was not found in Rio Salado.

Algae Digestions and Arsenic Speciation

About 0.5 g of ground, dried algae was added to 10 ml of concentrated HNO_3 in a capped Teflon microwave vessel. Samples were microwave heated at 55% power under 40 psi for 10 minutes allowing 5 minutes to reach pressure, followed by 55% power at 85 psi for 10 minutes allowing 5 minutes to reach pressure and finished with heating at 55% power and 100 psi for 10 minutes allowing 5 minutes to reach pressure. After cooling, 30% H_2O_2 was added until the effervescence ceased, then an additional 2 ml 30% H_2O_2 was added and allowed to digest overnight. Digestion overnight was done to give the solution time for the H_2O_2 to dissipate, otherwise the 30% H_2O_2 will oxidize the graphite tube in the GFAA. Samples were then filtered and diluted for analysis by GFAA.

Speciation of arsenic present in the algae was done using the same technique as described previously for stream sediments. Digestion by HNO_3 and 30% H_2O_2 (USEPA SW-846 Method 3050) gave results for total arsenic in algae, leaving no visible trace of algae afterwards. The digestion procedure for speciation is less destructive and provides qualitative data on relative amounts of each species present. The method does not completely digest the algae nor does it liberate all the arsenic present.

Plant Digestions

Plant samples were removed from frozen storage and thawed at room temperature. The samples were classified roughly according to plant type (e.g. Grass 1, Grass 2) and segregated by station. From 2-15 g of wet-weight plants were cut up using medical grade stainless steel scissors into pre-weighed aluminum foil boats and dried at 95-105ºC for 24 hours. The samples were weighed again then digested according to USEPA Method SW-846 3050 (concentrated nitric acid and 30% hydrogen peroxide reflux). Samples were filtered using 0.45 μm Millipore cellulose acetate then diluted to a known volume (100 ml). Arsenic analysis, as total arsenic, was conducted using the GFAA and data reduced to mg/kg dry weight. A portion of the plant samples were retained for classification by a botanist (John D. Vitti) possessing familiarity with North American vegetation.

Tabular Data

Table A-8
In-Stream Arsenic Species: Unfiltered Samples (µg/L)

Station	As^{3+}	MMAA	As^{5+}	DMAA	Sum of Species	Total As	MMAA (%)	DMAA (%)	MMAA+DMAA (%)
1	0	0	1095	182	1290	1109	0%	14%	14%
2	64	0	1088	102	1267	1189	0%	8%	8%
3.3 (PM)	0	0	1171	113	1296	1042	0%	9%	9%
3.6 (AM)	0	41	973	228	1248	1073	3%	18%	22%
4	0	13	1178	91	1287	1142	1%	7%	8%
5	0	0	1076	62	1146	937	0%	5%	5%
6	0	0	1014	32	1052	985	0%	3%	3%
7	0	25	1048	171	1246	1119	2%	14%	16%
8	11	18	986	127	1141	1065	2%	11%	13%
9	0	24	827	28	883	909	3%	3%	6%
10	0	16	889	101	1005	897	2%	10%	12%
11	0	16	1038	107	1162	1002	1%	9%	11%
12	145	27	888	96	1156	983	2%	8%	11%
13	0	0	235	28	274	242	0%	10%	10%
14	26	16	968	96	1106	949	1%	9%	10%
16	13	13	1055	63	1144	909	1%	6%	7%
17	0	13	911	52	981	935	1%	5%	7%
18	0	20	956	36	1011	903	2%	4%	6%
19	0	0	867	16	892	848	0%	2%	2%
20	0	11	878	22	911	804	1%	2%	4%

Table A-9
In-Stream Arsenic Species: Filtered Samples (μg/L)

Station	As^{3+}	MMAA	As^{5+}	DMAA	Sum of Species	Total As	MMAA (%)	DMAA (%)	MMAA+DMAA (%)
1	0	18	1130	146	1293	1065	1%	11%	13%
2	69	23	1085	94	1269	1121	2%	7%	9%
3.3 (PM)	0	11	1178	91	1284	1126	1%	7%	8%
3.6 (AM)	0	34	998	154	1193	1088	3%	13%	16%
4	0	18	1188	72	1281	1109	1%	6%	7%
5	0	0	1044	24	1077	970	0%	2%	2%
6	0	148	962	18	1130	964	13%	2%	15%
7	0	20	918	121	1060	1119	2%	11%	13%
8	16	50	896	94	1055	1046	5%	9%	14%
9	0	23	827	83	932	893	2%	9%	11%
10	0	16	750	74	840	888	2%	9%	11%
11	0	23	951	80	1058	722	2%	8%	10%
12	133	27	815	70	1044	983	3%	7%	9%
13	0	0	218	22	254	227	0%	9%	9%
14	28	23	756	66	872	911	3%	8%	10%
16	15	45	1006	36	1102	918	4%	3%	7%
17	0	0	957	51	1023	918	0%	5%	5%
18	0	18	956	33	1006	890	2%	3%	5%
19	0	0	1083	9	1098	821	0%	1%	1%
20	0	11	981	25	1017	756	1%	2%	4%

Table A-10
Unfiltered Water Samples

Station	Ca ppm	Na ppm	Mg ppm	K ppm	SiO$_2$ ppm	Ba ppb	Al ppb	Mn ppb	Fe ppb	Li ppm	Sr ppb	Mo ppb	Cu ppb	As ppb
1	3.2	296	0.19	13.6	531	ND	7	56.83	88.2	1.02	10.0	40.7	1.30	1109
2	3.8	312	0.20	13.7	533	ND	7	79.2	14.0	1.04	10.1	37.4	1.28	1189
3.3 (PM)	3.4	280	0.27	13.5	504	ND	9	77.6	28.2	1.02	9.1	39.8	1.38	1042
3.6 (AM)	3.6	280	0.28	13.3	518	ND	10	117.2	26.7	1.01	9.7	40.5	1.65	1073
4	3.4	306	0.26	13.5	522	ND	9	28.9	50.1	1.04	10.4	41.7	1.34	1142
5	3.7	276	0.28	13.6	496	ND	10	148.9	2.0	0.95	10.2	35.6	1.47	937
6	2.7	270	0.20	14	514	ND	7	10.4	0.6	0.97	6.9	42.9	0.12	985
7	3.8	300	0.30	13.6	513	ND	11	28.7	42.0	1.04	9.5	35.2	2.11	1119
8	3.7	298	0.29	14.1	505	ND	10	40.0	23.2	1.02	9.0	38.6	1.68	1065
9	4.2	275	0.33	13.7	452	ND	12	90.4	5.2	0.94	8.1	31.8	2.18	909
10	4.1	275	0.32	13.7	454	ND	9	43.2	4.0	0.91	8.4	37.2	2.53	897
11	3.7	287	0.32	13.9	482	ND	17	32.5	14.0	0.94	9.9	36.3	1.12	1002
12	3.8	280	0.60	13.8	488	6.4	24	63.5	32.0	0.91	9.9	37.2	1.29	983
13	2.5	64	1.38	3.7	254	ND	9	1.3	4.4	0.23	5.6	24.0	1.23	242
14	3.7	270	0.63	13.4	478	5.6	19	39.6	30.3	0.91	9.7	35.9	1.34	949
16	3.7	266	0.63	13.7	488	5.1	17	29.3	23.5	0.9	9.05	38.5	2.63	909
17	3.7	265	0.63	13.6	469	5.4	19	35.3	20.3	0.9	9.4	37.9	1.45	935
18	3.5	266	0.65	12.9	459	5.0	17	20.4	18.3	0.9	8.6	37.9	1.42	903
19	3.7	255	0.94	12.6	442	4.9	42	12.7	26.7	0.83	10.5	36.1	1.31	848
20	3.4	244	0.93	12.2	421	3.9	56	10.9	52.5	0.77	9.9	35.4	1.43	804
Powerline		280		22.6			103	74.9	0.8					
Agua Dulce		68		4.5			8	273.4	0.2					

Table A-11
Filtered Water Samples (0.45 µm)

Station	Ca ppm	Na ppm	Mg ppm	K ppm	SiO$_2$ ppm	Ba ppb F	Al ppb	Mn ppb	Fe ppb	Li ppm	Sr ppb	Mo ppb	Cu ppb	As ppb
1	3.8	292	0.19	12.7	486	ND	12	64.0	10.9	1.01	10.5	36.4	1.40	1065
2	3.8	306	0.19	13.2	511	ND	8	66.5	14.2	1.02	10.9	34.0	1.26	1121
3.3 (PM)	3.1	307	0.25	13	504	ND	11	90.2	26.4	1	9.2	35.5	1.36	1126
3.6 (AM)	3.5	297	0.28	13	494	ND	22	104.9	41.5	0.98	11.0	35.9	2.19	1088
4	3	295	0.25	13.3	513	ND	7	26.3	21.8	0.98	8.7	36.3	1.15	1109
5	3.7	290	0.3	13.5	476	ND	55	165.1	5.9	0.98	11.5	29.0	1.27	970
6	2.8	267	0.21	13.5	519	ND	7	61.1	3.9	0.93	9.7	39.8	0.55	964
7	3.8	294	0.3	13.5	507	ND	9	18.5	36.8	0.99	10.4	29.7	1.00	1119
8	3.8	285	0.32	13.6	500	ND	5	37.5	19.2	0.95	9.0	31.9	1.00	1046
9	4.2	268	0.34	13.6	446	ND	9	53.2	7.6	0.87	8.1	25.9	1.14	893
10	4.2	269	0.34	13.6	465	ND	13	38.2	2.1	0.86	8.5	24.9	1.12	888
11	3.8	289	0.32	14.2	488	ND	10	26.6	10.8	1	9.6	29.4	1.10	722
12	3.8	271	0.62	13.8	477	6.2	12	50.0	20.6	0.96	9.4	20.1	3.24	983
13	2.6	68	1.41	ND	251	ND	8	1.8	1.0	0.22	5.4	31.1	1.16	227
14	3.7	254	0.65	13.4	462	4.5	5	30.8	28.7	0.92	9.4	31.1	1.36	911
16	3.8	265	0.64	13.4	458	5.9	11	23.9	178.3	0.93	10.6	28.7	1.29	918
17	3.7	260	0.61	13.4	471	5.4	8	21.9	148.3	0.91	9.5	28.9	1.32	918
18	3.6	262	0.63	12.9	476	4.6	7	22.1	25.7	0.92	9.7	28.2	1.11	890
19	3.7	242	0.91	12.7	440	3.7	5	7.2	16.4	0.84	11.7	27.9	1.88	821
20	3.5	226	0.91	12.4	412	3.5	6	7.1	31.6	0.75	10.2	23.5	2.74	756

Table A-12
Anions and Uncorrected Alkalinity

Station	Cl ppm	F ppm	Br ppm	B ppm	SO$_4$ ppm	CO$_3$ ppm	HCO$_3$ ppm	NO$_3$ ppm
1	93.1	14.8	0.81	7.3	26.8	ND	416	0.3
2	92.6	14.9	0.46	8.7	27.8	ND	392	ND
3.3 (PM)	92.6	15.7	0.37	7.1	28.5	ND	424	ND
3.6 (AM)	91.7	15.5	0.37	4.3	27.8	ND	408	ND
4	89.9	15.9	0.39	7.3	28.8	80	328	0.1
5	73.6	13.7	0.06	6.8	20.1	ND	328	0.1
6	79.2	15.0	0.50	9.4	20.3	88	300	0.1
7	92.0	16.0	0.42	8.9	28.5	56	320	ND
8	86.5	15.5	0.36	7.8	25.8	76	334	0.1
9	73.8	13.3	0.42	8.8	18.6	ND	368	0.2
10	75.4	14.0	0.25	9.3	19.1	104	270	0.1
11	82.5	15.1	0.33	5.7	22.9	160	236	ND
12	77.1	14.6	0.27	6.6	21.8	88	308	ND
13	16.9	6.1	ND	4.1	6.5	ND	88	ND
14	74.2	15.1	0.29	6.5	22.1	40	336	ND
16	75.9	14.7	ND	5.2	21.7	152	252	0.3
17	76.1	14.5	0.23	5.1	21.8	152	256	0.1
18	74.5	14.6	0.32	5.0	21.3	96	280	ND
19	70.9	13.8	0.27	4.7	20.3	144	220	ND
20	63.9	12.5	0.05	4.3	18.2	140	284	ND

Table A-13
Arsenic Concentrations of Time Series Samples

Station	Date	As (ppb)	Station	Date	As (ppb)
RC-1	1/6/98	1284	RC-4	1/7/98	931
RC-1	1/6/98	1245	RC-4	1/7/98	976
RC-1	1/7/98	1120	RC-4	1/12/98	1019
RC-1	1/7/98	1164	RC-4	1/12/98	972
RC-1	1/13/98	1069	RC-4	1/13/98	931
RC-1	1/13/98	1211	RC-4	1/13/98	924
RC-3	1/6/98	1044	RC-7	1/12/98	654
RC-3	1/6/98	992	RC-7	1/12/98	718
RC-3	1/7/98	1044	RC-8	1/13/98	990
RC-3	1/7/98	1034	Powerline	1/7/98	906
RC-3	1/12/98	1006	Powerline	1/7/98	942
RC-3	1/12/98	997	Powerline	1/12/98	843
RC-3	1/13/98	1072	Powerline	1/12/98	938
RC-3	1/13/98	1037	Powerline	1/13/98	805
RC-3	1/13/98	981	Powerline	1/13/98	933
			Agua Dulce	1/11/98	186

Table A-14
Sediment Eh, Organic Carbon (TOC), and Grain Size Distribution

Location	Eh	TOC wt.%	<63 um	63-125 um	125-250 um	250 um -0.5 mm	0.5-1.0 mm	1-2 mm
1	280	1.5	1.1	2.1	16.0	23.5	33.3	24.0
2	200	1.8	0.9	2.9	18.4	21.4	28.6	27.7
3 a.m.	80	2.0	0.3	1.8	18.0	18.8	29.4	35.6
3 p.m.	325	1.9						
4	310	1.7	0.4	3.2	16.9	23.5	31.2	24.8
5	200	2.5	2.0	9.2	25.4	26.1	20.8	16.5
6	267	3.0	2.4	6.1	17.2	27.4	30.5	16.4
7	220	2.6	1.7	6.9	22.2	27.1	29.6	12.6
8	230	1.6	0.2	1.9	15.8	25.6	27.4	29.1
9	212	1.9	1.9	1.9	6.2	16.6	37.0	36.4
10	250	1.8	1.6	2.4	6.1	16.9	35.8	37.3
11	210	3.0	1.7	5.2	18.0	30.4	28.0	15.0
12	225	1.8	2.1	5.9	16.4	18.9	29.9	26.9
13	200	3.1	1.8	4.8	14.2	26.0	33.2	20.0
14	70	2.3	2.8	6.4	18.1	29.3	30.2	13.2
16	280	3.1	14.8	14.4	53.1	15.0	1.8	0.9
17	290	3.7	1.3	5.2	27.3	40.8	19.0	6.4
18	280	1.3	0.1	1.9	13.1	23.0	34.5	27.3
19	350	1.3	0.8	3.1	11.3	17.3	33.5	34.1
20	340	1.2	0.0	0.2	1.7	11.8	47.0	39.3
Agua Dulce		1.5	0.3	1.1	8.2	25.5	32.6	32.2
Average		2.1	1.9	4.3	17.2	23.2	29.7	23.8
Standard Deviation		0.7	3.2	3.3	10.5	6.5	8.7	10.8

Table A-15
Arsenic Bound in Each Size Fraction as % of Total Arsenic and BET Surface Area

Location	BET Surface Area (m²/g)	<63 um	63-125 um	125-250 um	250 um - 0.5 mm	0.5-1.0 mm	1-2 mm
1	0.7	3.9	3.0	10.4	12.9	52.0	17.8
2	0.8	1.3	3.6	16.9	20.5	31.9	25.8
3 a.m.		1.1	2.3	15.5	20.0	28.2	32.8
3 p.m.	1.2						
4	1.0	1.2	5.4	22.5	26.6	18.5	25.8
5	1.4	6.2	9.7	20.1	24.5	22.4	17.0
6	2.0	3.3	5.3	11.7	22.0	35.1	22.7
7	1.4	2.8	7.4	18.7	16.6	24.8	29.7
8	1.0	0.5	2.7	19.9	24.5	27.4	25.1
9	1.5	5.6	2.1	8.1	15.8	33.3	35.1
10	1.4	2.7	3.2	5.1	14.1	32.3	42.6
11	2.1	7.8	10.8	23.7	21.2	16.7	19.7
12	1.3	3.7	6.2	19.1	19.0	22.1	29.8
13	1.8	5.7	6.9	17.4	23.0	29.6	17.4
14	1.5	7.5	10.7	34.5	18.5	17.2	11.6
16	2.7	27.2	13.7	44.2	12.6	1.5	0.8
17	2.5	1.3	4.4	23.9	43.0	23.5	3.9
18	1.0	0.3	2.4	12.7	25.8	33.0	25.9
19	1.4	1.4	3.2	10.1	16.9	41.1	27.2
20	1.3	0.1	0.2	1.5	11.2	36.1	51.0
Agua Dulce	2.3	1.1	2.1	9.3	26.3	32.9	28.4
Average		3.0	4.8	15.8	21.2	29.4	25.8
Standard Deviation		2.5	3.1	7.8	7.0	8.7	10.6

Table A-16
Counts of As Measured for Iron Oxide and Glasses by Electron Microprobe

Sample ID	Mineral	Counts (As)	Sample ID	Mineral	Counts (As)
1	FeOx	2389	1	glass	1536
1	FeOx	2375	1	glass	1421
1	FeOx	2257	1	glass	1558
1	FeOx	3273	1	glass	1657
1	FeOx	2598	1	glass	1572
1	FeOx	2667	1	glass	1626
1	FeOx	2135	5	glass	1510
1	FeOx	2927	5	glass	1560
5	FeOx	4695	5	glass	1576
5	FeOx	6688	5	pyroxene	1966
5	FeOx	4398	8	glass	1582
5	FeOx	3226	8	glass	1628
5	FeOx	3059	9	glass	1518
8	FeOx	2407			
8	FeOx	2162			
8	FeOx	3231			
9	FeOx	3005			
Average	FeOx	3140	Average	glass	1593

Table A-17
Description of Sediment >2 mm

Location	Petrologic Description
1	75% pumice, 20% welded tuff fragments, 5% obsidian, <1% grains coated with FeOx's, minor plant fragments and some algae coatings on larger grains
2	58% welded tuff fragments, 30% pumice, 10% obsidian, 2% grains coated w/FeOx's, trace organic matter
3.6 (AM)	70% pumice, 20% welded tuff fragments, 8% obsidian, 2% grains coated w/FeOx's, <1% organic matter as twig and leaf fragments and algae coatings
3.3 (PM)	70% pumice, 20% welded tuff fragments, 8% obsidian, 2% grains coated w/FeOx's, <1% organic matter as twig and leaf fragments and algae coatings
4	50% welded tuff fragments, 33% pumice, 15% obsidian, 2% grains coated w/FeOx's, <1% organic matter as leaf and twig fragments
5	65% pumice, 20% welded tuff fragments, 12% obsidian, 3% grains coated w/FeOx's, <1% organic matter as leaf and twig fragments
6	80% pumice, 15% welded tuff fragments, 2% obsidian, 2% grains coated w/FeOx's, 1% organics-twigs, some algae coatings (sample has relatively less >2mm sed)
7	80% pumice, 13% welded tuff fragments, 6% obsidian, 1% grains coated w/FeOx's, <1% organic matter as leaf and twig fragments
8	80% welded tuff fragments, 10% pumice, 8% obsidian, 2% grains coated w/FeOx's, <1% organic matter as twig and leaf fragments
9	60% welded tuff fragments, 15% obsidian, 12% pumice, 2% grains coated w/FeOx's, <1% organic matter as leaf and twig fragments
10	60% welded tuff fragments, 25% pumice, 12% obsidian, 3% grains coated w/FeOx's, trace organic matter present
11	45% welded tuff fragments, 45% pumice, 10% obsidian, 2% grains coated w/FeOx's, <1% organic matter as leaf and twig frags and algae coatings on larger grains
12	15% obsidian, 50% welded tuff fragments, 32% pumice, 3% grains coated with FeOx's, <1% as leaf and twig fragments
13	70% obsidian, 20% pumice, 6% welded fragments, 2% grains coated w/ FeOx's, 2% organic matter as leaves and twigs
14	50% welded tuff fragments, 40% pumice, 8% obsidian, 2% grains coated w/FeOx's, <1% organic matter as leaf and twig fragments
16	69% pumice, 25% welded tuff fragments, 5% obsidian, 1% grains coated w/FeOx's, Trace organics (almost no sediment >2 mm represented ~ 1-2% of total at that site)
17	80% pumice, 12% welded tuff fragments, 4% organic matter as leaf and twigs, 3% obsidian, 1% grains coated w/FeOx's
18	45% pumice, 33% welded tuff fragments, 20% obsidian, 2% grains coated w/FeOx's, <1% organic matter as leaf and twig fragments
19	75% welded tuff fragments, 17% pumice, 6% obsidian, 2% grains coated w/FeOx's, <1% organic matter as twig and leaf fragments
20	43% pumice fragments, 30% obsidian, 25% welded tuff fragments, 2% grains coated w/FeOx's, <1% organic matter as twig and leaf fragments and algae coatings
Agua Dulce	50% welded tuff fragments, 45% pumice, 4% grains coated w/FeOx's, 1% obsidian, trace organic matter

Table A-18
Fe, Mn and As Extracted by HNO$_3$ from Whole Sediment

Location	Sample mass (g)	Fe (mg/kg)	Mn mg/kg	As (mg/kg)
1	1.280	1798	102	3.7
2	1.120	2342	33	4.4
3.6 (AM)	1.120	2236	45	4.1
3.3 (PM)	1.010	1699	225	5.9
4	1.050	1721	201	5.1
5	1.020	1276	147	12.8
6	1.150	3484	1045	15.3
7	1.090	2110	257	6.3
8	1.340	2910	179	5.3
9	1.020	2941	304	7.1
10	1.090	2752	183	5.2
11	1.160	3886	294	10.4
12	1.340	1644	149	5.0
13	1.060	1896	23	2.9
14	1.110	1838	184	6.8
16	1.100	2005	593	11.1
17	1.160	2236	679	7.3
18	1.100	1821	510	6.6
19	1.210	2397	107	7.0
20	1.240	1852	129	3.0
Agua Dulce	1.390	4095	101	2.9

Table A-19
Fe, Mn, Al, Si, and As Extracted by HNO₃ from –80 Mesh Sediment

Location	Sample mass (g)	Fe (mg/kg)	Mn (mg/kg)	Al (mg/kg)	Si (mg/kg)	As (mg/kg)
1	0.956	2908	103	2166	492	8.0
2	0.931	3602	18	2621	227	4.5
3.6 (AM)	0.899	3713	55	2916	379	11.8
3.3 (PM)	0.992	3428	316	2127	343	9.7
4	1.202	2830	258	2263	310	6.1
5	0.907	2595	232	3452	269	11.8
6	0.820	3848	770	3402	297	16.6
7	1.000	2713	319	3470	405	6.8
8	1.017	3601	356	2968	335	7.1
9	0.983	3478	276	4610	215	6.1
10	1.372	3984	228	4482	178	5.5
11	0.829	3788	554	4597	138	11.0
12	1.088	3383	347	3006	343	8.6
13	1.008	2611	0	6957	306	7.7
14	0.993	3078	230	2990	310	8.8
16	0.877	2981	634	4139	352	10.5
17	1.130	3024	800	4406	216	11.6
18	0.900	2923	526	2055	307	7.6
19	1.150	3642	120	3808	128	5.2
20	0.891	3415	189	3043	346	6.8
Agua Dulce	0.885	4569	56	8785	276	3.5

Table A-20
Fe, Mn, Al, Si, and As Extracted by Chao Reagent with Ground –80 Mesh Sediment

Sample ID	Sample mass (g)	Fe (mg/kg)	Mn (mg/kg)	Al (mg/kg)	Si (mg/kg)	As (mg/kg)
1	0.967	511	76	155	259	0.7
2	1.038	602	0	183	273	0.5
3.6 (AM)	1.123	560	24	223	252	1.3
3.3 (PM)	1.012	484	280	153	344	2.1
4	1.100	635	244	182	272	1.2
5	0.983	515	302	254	272	1.5
6	0.977	556	907	256	357	1.4
7	0.910	146	316	181	240	1.3
8	0.832	633	377	192	301	1.1
9	0.955	534	357	325	365	1.0
10	0.913	568	221	307	346	1.0
11	1.000	814	613	345	349	2.0
12	1.045	798	375	206	334	1.3
13	0.847	719	0	514	411	1.1
14	0.931	623	225	204	304	1.2
16	1.013	690	746	252	360	5.1
17	1.007	706	948	243	411	7.2
18	0.969	730	498	160	242	1.3
19	1.012	767	104	277	328	0.7
20	0.926	741	182	232	359	0.9
Agua Dulce	1.042	722	67	408	428	0.5

A-50

Table A-21
As Species, Fe, and Mn Extracted by 0.1 M H$_3$PO$_4$ with Ground —80 Mesh Sediment

Location	Sample mass (g)	As3+ (mg/kg)	As5+ (mg/kg)	DMAA (mg/kg)	MMAA (mg/kg)	Fe (mg/kg)	Mn (mg/kg)
1	0.980	0.3	1.5	ND	ND	333	71
2	1.200	0.3	0.6	ND	ND	415	9
3.6 (AM)	1.170	0.7	2.6	ND	0.3	383	35
3.3 (PM)	0.970	0.6	2.4	ND	0.3	106	106
4	1.000	0.5	1.4	ND	ND	449	224
5	0.930	0.8	2.7	ND	0.4		
6	0.940	0.4	2.2	ND	ND	307	420
7	1.110	0.5	2.0	ND	0.2	70	115
8	1.060	0.5	1.6	ND	ND	345	246
9	1.090	0.4	1.7	ND	ND	324	263
9 b	0.950	0.5	2.0	ND	ND		
10	1.110	0.6	2.5	ND	ND	286	158
10 b	1.050	0.3	1.1	ND	ND		
11	0.990	0.8	4.1	ND	0.4	456	377
12	1.040	0.5	2.9	ND	ND	484	238
13	1.020	0.8	2.4	ND	0.3	434	16
14	1.000	0.7	2.3	ND	ND	327	183
16	0.990	0.8	4.8	ND	0.3	434	462
17	1.010	1.3	7.1	0.5	0.7	347	456
18	1.030	0.6	2.0	ND	0.3	421	345
19	0.990	0.4	1.4	ND	ND	524	87
20	1.120	0.4	1.4	ND	ND	447	138
Agua Dulce	1.060	0.4	1.7	ND	ND	534	54

Table A-22
Results of Tessier Partial Extractions: As in Sediment Components (mg/kg)

Location	Exchangeable	Carbonate	Fe/Mn Oxide	Organic
3.3 (PM) (a)	0.47	0.54	1.54	0.81
3.3 (PM) (b)	0.54	0.47	1.55	1.02
11	0.69	0.99	2.17	1.49
17	0.88	1.17	4.05	2.67
7	0.49	0.6	0.8	1.01
13	0.32	0.57	0.4	2.14
19 (a)	0.27	0.24	0.3	0.74
19 (b)	0.31	0.26	0.2	0.67

Mn in Sediment Components (mg/kg)

Location	Exchangeable	Carbonate	Fe/Mn Oxide	Organic
3.3 (PM) (a)	0	32.9	265	0
3.3 (PM) (b)	0	22.1	255.1	0
11	0	36.5	566.6	42.20
17	0	123.6	701	78.20
7	0	33.6	298.7	14.4
13	7.9	7.9	0	0
19 (a)	0	30.8	79.6	12.50
19 (b)	0	36.8	56.6	13.40

Fe in Sediment Components (mg/kg)

Location	Exchangeable	Carbonate	Fe/Mn Oxide	Organic
3.3 (PM) (a)	0	0	525.5	406.7
3.3 (PM) (b)	0	0	493.2	472.6
7	0	0	204.6	286.1
11	0	0	690.6	396
13	0	0	530.1	0
17	0	0	506	347.8
19 (a)	0	9	566.6	437.6
19 (b)	0	14	463.2	355.4

A-52

Table A-23
XRF Determinations of Elemental Concentrations in Whole Sediment (mg/kg Unless Noted)

Sample	Sr	Rb	Th	Pb	Ga	Zn	Cu	Ni	Fe	Mn	Cr	Ba	V	As	U	Y	Zr	Nb	Mo	Fe$_2$O$_3$ (wt.%)	MnO (wt.%)	TiO$_2$ (wt.%)
1	14	134	16	14	22	89	28	40	16017	387	340	56	4	6	6	47	540	50	4	2.29	0.05	0.16
1 b	14	134	16	14	22	88	5	7	15178	387	60	57	4	6	5	48	539	49	3	2.17	0.05	0.16
1 c	14	134	16	15	21	97	12	14	15458	387	131	53	3	6	6	47	540	50	4	2.21	0.05	0.16
1 d	14	131	15	14	22	88	5	6	15248	387	62	58	ND	6	5	47	537	49	4	2.18	0.05	0.16
2	28	137	17	14	23	91	5	7	16787	387	58	98	11	6	5	46	515	50	3	2.4	0.05	0.29
3.6 (AM)	23	140	16	15	23	91	5	7	15807	387	75	83	9	9	6	48	526	51	3	2.26	0.05	0.19
3.3 (PM)	25	140	17	16	23	98	5	6	18186	697	65	90	10	10	6	49	532	52	4	2.6	0.09	0.25
4	26	140	17	15	23	89	5	6	14968	542	63	94	ND	7	7	47	512	49	3	2.14	0.07	0.17
5	6	166	20	22	24	113	7	6	14199	465	60	24	ND	13	8	63	442	63	4	2.03	0.06	0.11
6	21	159	18	20	23	110	5	6	16227	1239	47	58	5	20	7	56	442	58	5	2.32	0.16	0.14
7	16	144	17	17	23	93	5	4	14339	697	10	69	ND	10	6	50	499	52	3	2.05	0.09	0.15
8	26	136	16	15	22	96	5	5	15458	774	63	93	5	8	6	44	499	49	4	2.21	0.1	0.18
9	27	147	18	20	24	101	15	6	15528	620	49	88	7	9	6	51	499	56	4	2.22	0.08	0.19
10	41	143	17	17	23	100	6	7	16577	542	67	149	10	8	6	51	491	54	4	2.37	0.07	0.21
11	15	145	17	18	23	104	10	6	15528	852	55	70	4	13	7	53	491	54	4	2.22	0.11	0.15
12	24	139	15	15	23	95	6	6	15598	697	69	112	5	10	6	47	502	51	3	2.23	0.09	0.18
13	13	151	18	20	24	104	5	7	15038	310	88	52	ND	9	7	54	507	60	3	2.15	0.04	0.15
14	18	139	17	16	22	97	7	6	15458	542	52	73	7	10	6	47	416	51	3	2.21	0.07	0.17
16 a	18	139	17	17	22	96	9	12	14409	929	102	84	ND	13	5	48	477	51	3	2.06	0.12	0.15
16 b	18	137	17	16	23	95	7	9	14129	929	72	82	6	13	5	49	478	51	3	2.02	0.12	0.14
17	11	145	18	17	23	102	6	8	14828	1239	76	78	4	16	6	52	479	53	3	2.12	0.16	0.13
18	27	134	16	15	22	93	8	5	14548	774	55	117	4	9	5	45	499	47	3	2.08	0.1	0.17
19	27	168	19	17	24	102	6	7	16017	387	70	98	8	9	7	59	559	63	3	2.29	0.05	0.18
20	23	156	17	16	23	99	6	6	15388	465	58	95	5	7	7	53	557	57	4	2.2	0.06	0.17
Agua Dulce	31	231	22	24	29	140	10	8	16787	310	55	80	7	6	8	77	688	95	2	2.4	0.04	0.17

Table A-24
Mineral Surface Sorbing Sites Determined by HNO₃ Digestion on −80 Mesh Sediment

Station	Fe mg/kg	HFO Strong Sites/kg Water	HFO Weak Sites/kg Water	Goethite Sites/kg Water	Gibbsite Sites/kg Water
1	2908	9.5E-04	3.8E-02	2.8E-03	2.2E-03
2	3602	1.2E-03	4.7E-02	3.5E-03	2.6E-03
3 a.m.	3713	1.2E-03	4.9E-02	3.6E-03	2.9E-03
3 p.m.	3428	1.1E-03	4.5E-02	3.4E-03	2.1E-03
4	2830	9.3E-04	3.7E-02	2.8E-03	2.3E-03
5	2595	8.5E-04	3.4E-02	2.5E-03	3.5E-03
6	3848	1.3E-03	5.0E-02	3.8E-03	3.4E-03
7	2713	8.9E-04	3.6E-02	2.7E-03	3.5E-03
8	3601	1.2E-03	4.7E-02	3.5E-03	3.0E-03
9	3478	1.1E-03	4.6E-02	3.4E-03	4.6E-03
10	3984	1.3E-03	5.2E-02	3.9E-03	4.5E-03
11	3788	1.2E-03	5.0E-02	3.7E-03	4.6E-03
12	3383	1.1E-03	4.4E-02	3.3E-03	3.0E-03
13	2611	8.5E-04	3.4E-02	2.6E-03	7.0E-03
14	3078	1.0E-03	4.0E-02	3.0E-03	3.0E-03
16	2981	9.8E-04	3.9E-02	2.9E-03	4.2E-03
17	3024	9.9E-04	4.0E-02	3.0E-03	4.4E-03
18	2923	9.6E-04	3.8E-02	2.9E-03	2.1E-03
19	3642	1.2E-03	4.8E-02	3.6E-03	3.8E-03
20	3415	1.1E-03	4.5E-02	3.3E-03	3.1E-03

Table A-25
Mineral Surface Sorbing Sites Determined by HNO_3 Digestion on Whole Sediment

Station	Fe mg/kg	HFO Strong Sites/kg Water	HFO Weak Sites/kg Water	Goethite Sites/kg Water	Gibbsite Sites/kg Water
1	1798	5.9E-04	2.4E-02	1.8E-03	2.2E-03
2	2342	7.7E-04	3.1E-02	2.3E-03	2.6E-03
3 a.m.	2236	7.3E-04	2.9E-02	2.2E-03	2.9E-03
3 p.m.	1699	5.6E-04	2.2E-02	1.7E-03	2.1E-03
4	1721	5.6E-04	2.3E-02	1.7E-03	2.3E-03
5	1276	4.2E-04	1.7E-02	1.2E-03	3.5E-03
6	3484	1.1E-03	4.6E-02	3.4E-03	3.4E-03
7	2110	6.9E-04	2.8E-02	2.1E-03	3.5E-03
8	2910	9.5E-04	3.8E-02	2.8E-03	3.0E-03
9	2941	9.6E-04	3.8E-02	2.9E-03	4.6E-03
10	2752	9.0E-04	3.6E-02	2.7E-03	4.5E-03
11	3886	1.3E-03	5.1E-02	3.8E-03	4.6E-03
12	1644	5.4E-04	2.2E-02	1.6E-03	3.0E-03
13	1896	6.2E-04	2.5E-02	1.9E-03	7.0E-03
14	1838	6.0E-04	2.4E-02	1.8E-03	3.0E-03
16	2005	6.6E-04	2.6E-02	2.0E-03	4.2E-03
17	2236	7.3E-04	2.9E-02	2.2E-03	4.4E-03
18	1821	6.0E-04	2.4E-02	1.8E-03	2.1E-03
19	2397	7.8E-04	3.1E-02	2.3E-03	3.8E-03
20	1852	6.1E-04	2.4E-02	1.8E-03	3.1E-03

Table A-26
Mineral Surface Sorbing Sites Determined by H_3PO_4 Digestion on –80 Mesh Sediment

Station	Fe mg/kg	HFO Strong Sites/kg Water	HFO Weak Sites/kg Water	Goethite Sites/kg Water	Gibbsite Sites/kg Water
1	333.2	1.1E-04	4.4E-03	3.3E-04	1.6E-04
2	415.1	1.4E-04	5.4E-03	4.1E-04	1.8E-04
3 a.m.	383.3	1.3E-04	5.0E-03	3.7E-04	2.2E-04
3 p.m.	105.8	3.5E-05	1.4E-03	1.0E-04	1.5E-04
4	449.2	1.5E-04	5.9E-03	4.4E-04	1.8E-04
5	324.0	1.1E-04	4.2E-03	3.2E-04	2.6E-04
6	307.3	1.0E-04	4.0E-03	3.0E-04	2.6E-04
7	69.9	2.3E-05	9.2E-04	6.8E-05	1.8E-04
8	345.1	1.1E-04	4.5E-03	3.4E-04	1.9E-04
9	323.8	1.1E-04	4.2E-03	3.2E-04	3.3E-04
10	285.7	9.3E-05	3.7E-03	2.8E-04	3.1E-04
11	455.6	1.5E-04	6.0E-03	4.5E-04	3.5E-04
12	484.1	1.6E-04	6.3E-03	4.7E-04	2.1E-04
13	433.7	1.4E-04	5.7E-03	4.2E-04	5.2E-04
14	326.5	1.1E-04	4.3E-03	3.2E-04	2.1E-04
16	434.1	1.4E-04	5.7E-03	4.2E-04	2.5E-04
17	346.5	1.1E-04	4.5E-03	3.4E-04	2.4E-04
18	420.6	1.4E-04	5.5E-03	4.1E-04	1.6E-04
19	523.8	1.7E-04	6.9E-03	5.1E-04	2.8E-04
20	446.5	1.5E-04	5.8E-03	4.4E-04	2.3E-04

Table A-27
Mineral Surface Sorbing Sites Determined by Chao Reagent Digestion on ─80 Mesh Sediment

Station	Fe mg/kg	HFO strong Sites/kg water	HFO weak Sites/kg water	Goethite Sites/kg water	Gibbsite Sites/kg water
1	511	1.7E-04	6.7E-03	5.0E-04	1.6E-04
2	602	2.0E-04	7.9E-03	5.9E-04	1.8E-04
3 a.m.	560	1.8E-04	7.3E-03	5.5E-04	2.2E-04
3 p.m.	484	1.6E-04	6.3E-03	4.7E-04	1.5E-04
4	635	2.1E-04	8.3E-03	6.2E-04	1.8E-04
5	515	1.7E-04	6.7E-03	5.0E-04	2.6E-04
6	556	1.8E-04	7.3E-03	5.4E-04	2.6E-04
7	146	4.8E-05	1.9E-03	1.4E-04	1.8E-04
8	633	2.1E-04	8.3E-03	6.2E-04	1.9E-04
9	534	1.7E-04	7.0E-03	5.2E-04	3.3E-04
10	568	1.9E-04	7.4E-03	5.6E-04	3.1E-04
11	814	2.7E-04	1.1E-02	8.0E-04	3.5E-04
12	798	2.6E-04	1.0E-02	7.8E-04	2.1E-04
13	719	2.4E-04	9.4E-03	7.0E-04	5.2E-04
14	623	2.0E-04	8.2E-03	6.1E-04	2.1E-04
16	690	2.3E-04	9.0E-03	6.7E-04	2.5E-04
17	706	2.3E-04	9.2E-03	6.9E-04	2.4E-04
18	730	2.4E-04	9.6E-03	7.1E-04	1.6E-04
19	767	2.5E-04	1.0E-02	7.5E-04	2.8E-04
20	741	2.4E-04	9.7E-03	7.2E-04	2.3E-04

Data Analysis

Aqueous Geochemistry

Field Parameters

There are some general relationships that are discernible from the field parameters. First, the hotter the water the lower the pH and higher the specific conductance. It follows that acidic waters are more representative of the deeper geothermal waters. All the thermal springs are

supplied by the same fault system but the available evidence indicates that the springs vary in the degree of mixing with shallow groundwater. There is a rapid change of almost 2 pH units as the water cools from about 65 to 45°C in short distances from the springs with less change at lower temperatures as the water moves downstream. The waters are all generally oxidizing.

Overall, the field parameters indicate that Agua Brava and Powerline springs have undergone different geochemical processes than Agua Caliente and Agua Verde. All systems are highly buffered with respect to pH by carbonate-silica equilibria. On the surface, the spring waters degas CO_2 and the pH increases. In general, the springs at the north end of the fault system (Agua Caliente and Agua Verde) are hotter, more oxidizing, and more acidic than the springs at the southern end of the fault (Agua Brava and Powerline). The waters of Agua Dulce and RC-5 have a completely different chemistry as evidenced by all parameters. This water may be representative of local groundwater that has seen relatively little geothermal influence.

As the water moves downstream the alkalinity and pH change systematically. Because of the high silica content, field alkalinity cannot be used directly to evaluate changes in carbonate equilibrium. Carbonate equilibria generally is the greatest pH buffer in aqueous systems, and so the observed pH changes should be explainable on this basis. PHREEQC was used to correct the field alkalinity for the effect of acid consuming species, such as silica, and calculate a carbonate distribution, as presented in Figure A-5.

Although direct evidence was not collected, deep thermal waters at La Primavera are charged with CO_2 and it is to be expected that springs would also be high in CO_2. As the CO_2 degasses and the waters cool, pH in the stream increases. There is direct evidence for this pH change being controlled in the presence of carbonate. Welch's carbonate measurements and field checks of carbonate reaction with dilute acid compare well with the modeled relationship in Figure A-5 and Table A-28. It is notable that the model also predicts the change in chemistry due to the mixing of waters from high CO_2 first order streams.

Table A-28
Saturation Indices Predicted by MINTEQU

Sample ID	Calcite	Dolomite	Rhodochrosite	Carbonate
1	0.16	-1.20	-0.83	0.07 wt.%
4	0.38	0.17	-0.11	0.05 wt.%
7	-0.41	-1.55	-0.62	ND
11	0.56	0.62	-0.09	0.09 wt.%
13	-1.35	-2.60	-2.14	ND
17	0.67	1.01	-1.84	0.25 wt.%
19	0.60	0.99	-1.44	0.08 wt.%

Detection Limit (2 x Relative Standard Deviation) = 0.05 wt%

A-58

Filtered and Unfiltered Analysis

Ratios of aluminum and iron concentrations in filtered and unfiltered water samples indicates that these elements may be precipitating out of the water at some sample stations. Filtered aluminum concentrations are almost monotonic downstream. From stream kilometer 2-10, the unfiltered aluminum concentration rises to five times that of the filtered. It is probable that colloidal aluminum compounds are forming in the water as it cools and the pH rises. A similar, but smaller, trend is noted for iron downstream of kilometer 4. Given that a similar small trend in lower concentrations of arsenic in filtered samples it is not an unreasonable assumption that some of the arsenic in Rio Salado is adsorbing on to Fe and Al colloids. The effect is small with respect to arsenic concentrations. In general, the unfiltered samples provided the most consistent arsenic data with the most reasonable trends. Unfiltered analysis was used for all modeling efforts.
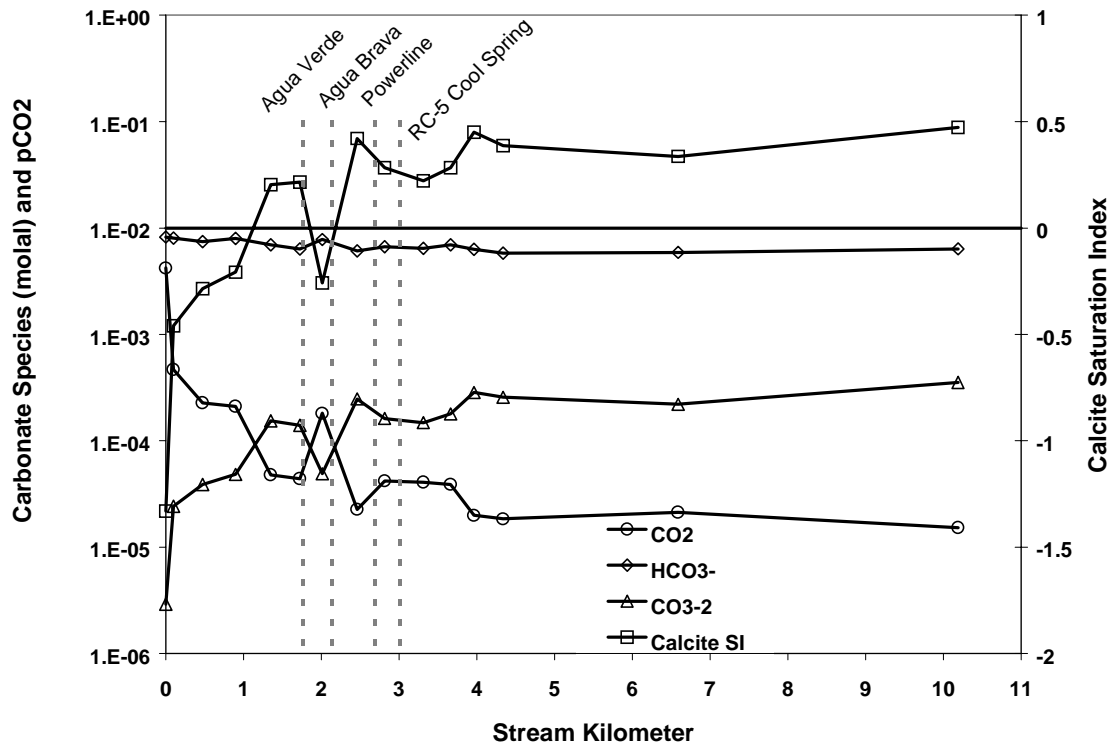
Figure A-5
Modeled Alkalinity and Calcite Saturation Index for the Main Channel of Rio Salado by PHREEQC

Thermal and Non-Thermal Waters

Agua Dulce and RC-5 are assumed to be representative of shallow groundwater at Rio Salado that is relatively free of the impact of geothermal waters or processes. These waters have approximately ¼ of the potassium, sodium, lithium, chloride, sulfate and fluoride found in Rio Salado. If the assumption that Agua Dulce and RC-5 represent shallow groundwater is correct, significant cool groundwater infiltration of Rio Salado can be detected by dilution. Using

lithium, sodium, sulfate, chloride, boron, bromine, and fluoride as tracers and calculating their mass flow it is noted that the flux of these elements decreases as the discharge of Rio Salado increases by about 10% in the stream reach below kilometer 4. Even though RC-5 enters the main channel above kilometer 4 its cool water discharge is not readily discernible except for an increase in manganese concentration. This being the case the chemistry of Rio Salado is dominated by thermal waters above kilometer 4 and is influenced by shallow, cooler, groundwater downstream.

Arsenic Source Variability

It was unknown if the spring discharge chemistry was highly variable prior to the reconnaissance sampling. There are north-south trends in water chemistry revealed by the field parameters. There are also trends in total arsenic concentration. The highest arsenic concentrations were found at Agua Caliente and the lowest at Powerline. Figure A-6 and the summary statistics in Table A-29 display these trends clearly. The arsenic mean concentration decreases by 24% from the north to the south. The arsenic concentrations also varied in time, with RC-1 varying by 184 µg/L (about 16%) over seven days time. This is not to suggest evaluating temporal trends with such a small data set is appropriate. The variation presented herein is felt to be real.

Figure A-6
Replicate Arsenic Sampling at Spring Sources to Determine Variability

Table A-29
Arsenic Source Variation Summary Statistics
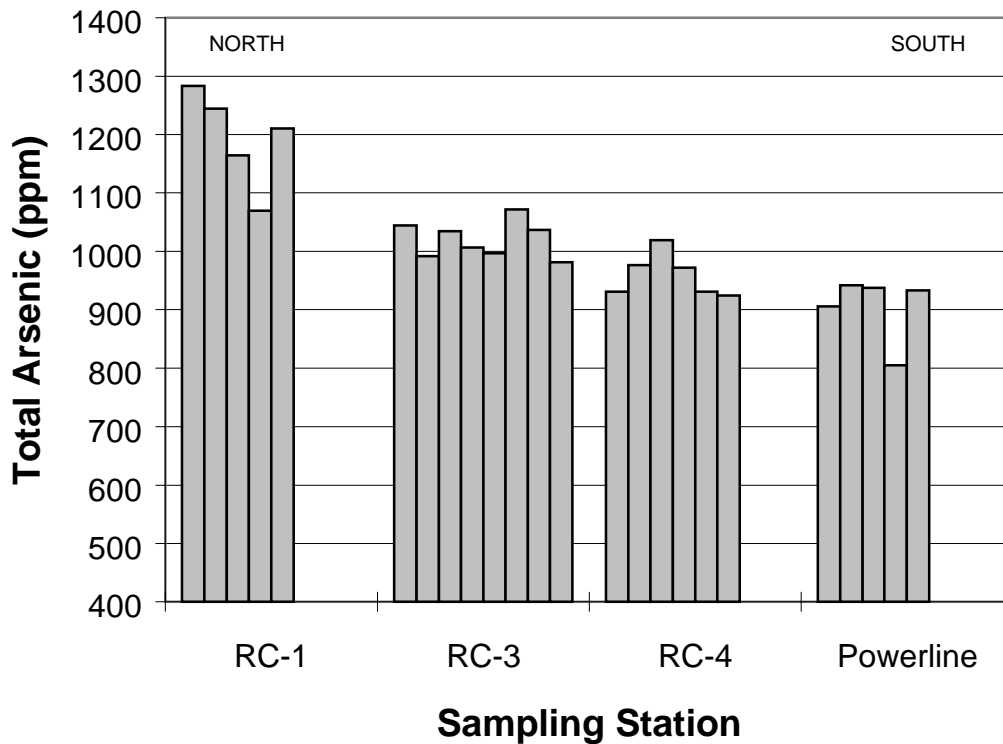
Measure (ppb)	RC-1	RC-3	RC-4	Powerline
Mean	1182	1023	959	894
95% Confidence Interval About the Mean	84	23	39	60
Median	1188	1034	951	919
Range	214	90	95	137
Standard Deviation	80	30	37	57

Arsenic Diurnal Variation – Replicate Sampling

Station 3 was sampled on January 8 and 10 with the intent of determining if there is change in arsenic speciation between light and dark conditions. The sampling effort also served as replicate to evaluate other metal and anion day-to-day variability. To maximize the possibility of detecting a difference in arsenic speciation, a sample should be taken in a full sun location as possible late in the day, and again at or before the dawn twilight. This provides the maximum sun without shadows and as long a dark period as possible. Station 3 was selected because of its proximity to the camp, full sun location, and single spring and channel source without tributaries. The location is proximal to the spa, but is probably not impacted by runoff or groundwater flow from the spa facilities (septic system and laundry). The data for this station contained elsewhere is repeated here for ease of reference.

All data from the replicate sampling is in very close agreement with exception of conductivity, ORP, manganese, and arsenic speciation. Higher levels of manganese are found in the morning, under more oxidizing conditions, in the absence of As^{3+}. There is an increase in As^{5+} and As^{3+} in the afternoon that is approximately equal to the increase in MMAA and DMAA overnight. The average of three direct determinations of total arsenic for Station 3 varied less than 15 ppb between January 8 and 10 indicating that the source concentration was consistent at these two times. Since the sampling was separated by another full day it is not possible to estimate the kinetics of the diurnal variation in arsenic speciation for these data. The diurnal variation in chemistry for filtered and unfiltered samples is depicted in Figure A-7. A separate scale is not provided for ORP.

Table A-30
Arsenic Analytical Values for Diurnal Sampling (ppb)

Unfiltered	Date	Time	As3+	MMAA	As5+	DMAA	Species Total	Total As
3-Afternoon (3.3)	1/10/98	1621	0	0	1171	113	1296	1042
3-Morning (3.6)	1/8/98	0815	0	41	973	228	1248	1073
Filtered								
3-Afternoon (3.3)	1/10/98	1621	0	11	1178	91	1284	1126
3-Morning (3.6)	1/8/98	0815	0	34	998	154	1193	1088

Table A-31
Metals and Anion Analytical Values for Diurnal Sampling (ppm Unless Indicated)

Unfiltered	Ca	K	Na	Li	Mg	Si	Fe (ppb)	Mn (ppb)	Cl	SO$_4$	F
3-Afternoon (3.3)	3.4	13.5	280	1.02	0.27	236	28	78	93	28	16
3-Morning (3.6)	3.6	13.3	280	1.01	0.28	242	27	117	92	28	16
Filtered											
3-Afternoon (3.3)	3.1	13	307	1.00	0.25	236	26	90			
3-Morning (3.6)	3.5	13	297	0.98	0.28	231	41	105			

Table A-32
Diurnal Field Measurements

Station	Date	Time	°C	Conductivity (µS/cm)	PH	ORP	CO$_3^{2-}$ (ppm)	HCO$_3^-$ (ppm)
3-Afternoon (3.3)	1/10/98	1614	48	1291	7.82	80	0	424
3-Morning (3.6)	1/8/98	0815		1220	7.81	127	0	408
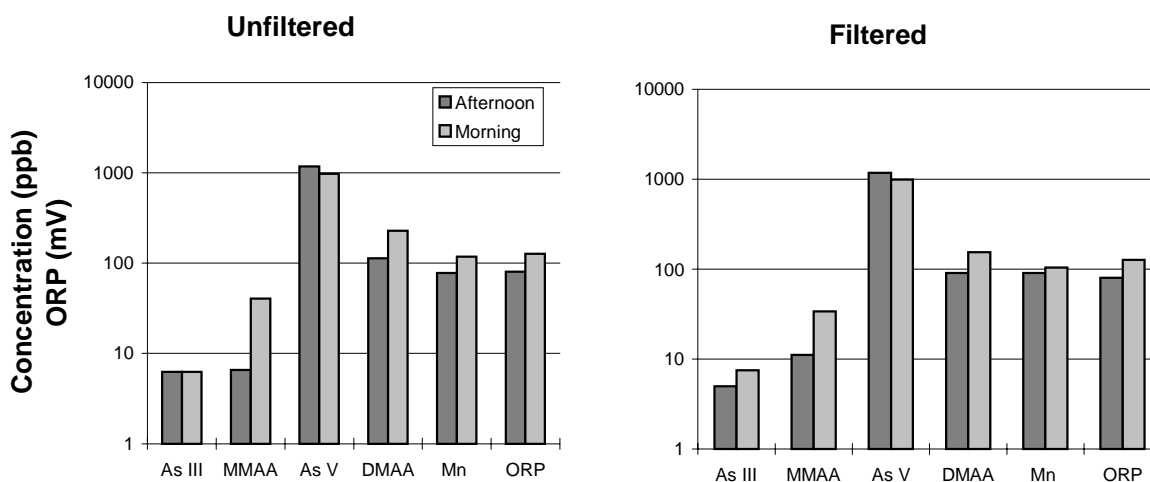
Figure A-7
Diurnal Variation in Arsenic Speciation and Redox Parameters for Station 3

Sediment Geochemistry

Very little variation was seen in local geology and sediment mineralogy over the 10 km of stream reach. Study of the >2 mm fraction showed sediments to be composed of varying proportions of pumice, welded rhyolite tuff fragments and obsidian with Fe-oxides coating some grains. No quartz, feldspar or mafic grains were seen in the >2 mm fraction. The study of 6 thin sections revealed a similar composition with approximately 80% volcanic glass, consisting of

obsidian, welded rhyolite tuff and pumice fragments, 12% quartz, 7-8% sanidine and generally <1% magnetite and iron oxides. The thin sections showed more primary minerals as a result of being made up from the <2 mm size fraction. Many grains showed little evidence of transport with sharp edges still present on much of the glasses.

Iron oxides, present as mineral coatings, discrete grains, and as partially oxidized mafic minerals were identified as hematite and goethite by reflectance spectrophotometry. Reflectance spectra show characteristic first derivative peaks for hematite at 555 nm and goethite at 435 nm. These spectra are qualitative in the sense that they only confirm the presence of hematite and goethite. Quantification of the amount of oxides requires preparation of standard calibration curves for each oxide in a representative sediment matrix. The presence of manganese oxides was confirmed through several different selective dissolution procedures and occurred as thin dark coatings on some of the grains.

Sediment size fraction analysis conducted for each sample station showed the sediments to be dominated by coarse-grained material with over 50% coarser than 0.5 mm. On average less than 2% of the sediments fell into the <63 μm size fraction (silt-clay). Although the size fraction analysis is somewhat biased in regards to the total range of sizes with the >2 mm fraction excluded, it is intended to characterize the most active portion of sediments. The coarse nature of La Primavera sediments is also apparent in surface area measurements with an average value of only 1.5 m^2/gm.

TOC in the sediments consisted of leaf, twig and algae fragments as well as thin algae coatings on some of the larger grains. Measured % TOC ranged from 1.2 to a relatively high value of 3.7. The effect of interstitial water from clays on measured % TOC is believed to be insignificant due to the vary small amount of clays present in sediments.

Point-counts using the electron microprobe showed Fe-oxide grains to contain As at levels 2-3 times above background glasses and minerals. This method is semi-quantitative, but does confirm the enrichment of As in Fe-oxides over background. However, line scans traversing across Fe-oxide grains show no direct relationship between the amount of Fe and As.

Carbonates were present as thick laminated deposits of travertine at the spring sources and were also apparent in stream bank sediments as an effervescence due to acid reaction. Although carbonates were not visible in sediment thin sections, their presence was confirmed by carbonate analysis using the system of vacuum lines and quadrupole mass spectrometer. Percent carbonate ranged from non-detectable to 0.27 wt. % with a detection limit of 0.05 wt. % calculated as two times the relative standard deviation of a sample run in triplicate. Measured carbonate in sediments also showed some agreement with calculated saturation indices for calcite, dolomite and aragonite. The presence of rhodochrosite ($MnCO_3$) in these waters is unlikely with negative saturation indices. Comparison of initial modeling results, done with the older MINTEQA2 (version 3.11) database, to those of the MINTEQU [85] database revealed significant differences in predicted saturation indices for carbonate minerals (Table A-28). In the case of La Primavera, the calcium carbonate minerals calcite, dolomite and aragonite were under-predicted while rhodochrosite was over-predicted.

XRD analyses revealed the predominance of amorphous phases representing glasses and could only positively identify quartz. Attempts to isolate and concentrate clays were unsuccessful due to the very small amounts present relative to the large amounts of amorphous matter.

Total As in sediments is not much higher than normal crustal abundance averaging about 8 ppm which is surprising given the high As concentrations of these waters. Analysis of the size fractions showed the <63 μ fraction to contain the highest relative concentrations of As; however, some samples showed a bimodal distribution with high concentrations in the coarser size fractions that may be related to Fe and Mn which also show similar distributions. Although the silt-clay fraction has the highest relative concentration, it only amounts to a small percent of the whole sediment which results in most of the arsenic in a sample being contributed by the coarser size fractions.

Results of the sequential extraction show As to be dominantly associated with organic matter and Fe/Mn-oxides with smaller amounts associated with the carbonate and exchangeable fractions. About 80% of the Mn and 60 % of the Fe occurs in the Fe/Mn-oxide fraction indicating that most of the Mn and Fe is present as amorphous oxides. These results also show some association of Mn with carbonate and a significant fraction of the Fe with organic matter.

Results of the sequential extraction procedure are intended to provide additional information that may be used to make inferences about mineral phases and possible associations with As. They are not to be regarded as absolute values as there is evidence that some re-adsorption and non-selective dissolution may occur [127, 128]. However, it is believed that the sequential extraction procedure can provide useful, valid information particularly when similar or supporting results can be obtained through alternate methods.

Arsenic Speciation of Sediments and Algae

Results of speciation of sediments for As^{3+}, As^{5+}, MMAA and DMAA show As^{5+} to be the dominant species present in La Primavera sediments. As^{3+} is also present in all samples and is proportional to As^{5+} with a positive correlation coefficient of 0.86. Qualitatively, MMAA is also proportional to As^{3+} and As^{5+}, but was below detection limits in many cases. DMAA was found at only one sample site.

Algae contain between 18 and 68 ppm total arsenic on a dry weight basis which is predominantly As^{5+}, but also contain measurable As^{3+}, MMAA and DMAA. The two different morphological types of algae recognized at La Primavera also seemed to have differing capacities to uptake As. The algae types containing the highest concentrations of arsenic were those present as dense mats covering the rocks and stream bottom near the source where waters are the hottest. The filamentous algae that generally occurred in cooler waters contained lower total As.

Numerical Modeling of Geochemistry

PHREEQC was used to evaluate the saturation indices of many mineral phases in order to determine if the potential for any gross precipitation reactions were possible due to mixing or changes in chemical condition. The only major change observed was that for carbonate

saturation previously mentioned. Some care should be exercised in use of saturation indices to predict solid phases present due to inconsistencies in thermodynamic databases, metastable phases, and nucleation or oversaturation requirements. The pH, Eh, and concentration conditions very near the grain boundaries and mineral surfaces can be very different than that measured in the bulk solution.

The Rio Salado system is oversaturated with respect to amorphous silica phases, slightly undersaturated with respect to amorphous hydrous aluminum oxides, saturated for diaspore, and oversaturated for closely related kaolinite. The system is strongly oversaturated for the iron oxides goethite, magnetite, and hematite, and often amorphous FeOOH. PHREEQC predicts that the sorbing mineral phases of interest are thermodynamically stable over all modeled sample stations, and that HFO is below but near saturation in the upper reaches and above saturation in the lower reaches.

Table A-33
Mineral Saturation Indices Evaluated

Mineral Family	Mineral
Aluminosilicates	Adularia Albite Analcime Annite Beidellite Laumontite Phillipsite
Other Silicates	Chalcedony Cristobalite Magadiite Quartz Sepiolite Sepiolite(d) Silica Gel Talc
Arsenic Minerals	Arsenolite Scorodite $AlAsO_4:2H_2O$ As_2O_5 $Ba_3(AsO_4)_2$ $Ca_3(AsO4)_2:4H_2O$ $Mn_3(AsO_4):8H_2O$
Clay Minerals – Micas	Chlorite14A Chlorite7A Kaolinite K-Mica Montmorillonite-Aberdeen Montmorillonite-Belle Fourche Montmorillonite-Ca Phlogopite
Zeolites	Halloysite
Aluminum Oxides	Boehmite Diaspore Gibbsite $Al(OH)_3(a)$
Manganese Oxides	Hausmannite Manganite Pyrochroite Pyrolusite
Iron Oxides	Goethite Magnetite Hematite $Fe_3(OH)_8$ $Fe(OH)_{2.7}Cl._3$
Other Metal Oxides	Cuprite Tenorite
Carbonates	Aragonite Bixbyite Calcite Dolomite Dolomite(d) Huntite Rhodochrosite Rhodochrosite(d) Siderite Siderite(d) Witherite
Sulfates	Melanterite Barite $CuSO_4$ Celestite

Rio Salado Flow and Chemical Flux

Flow

Simple inspection of the tracer test velocities and point velocities (Tables A-2 and A-3) shows that these values are not in agreement. This is not unexpected. The tracer tests measure the way that a chemical disperses and moves in Rio Salado. The point measurements are really a measure of stream energy; the mass of water that is pushed at a point, over time, by the energy gradient of

stream. Therefore, it is appropriate to use the tracer test numbers for chemical calculations such as kinetics, and the point measurements for discharge volume. Figure A-8 depicts the range of travel times for a parcel of water moving down Rio Salado as determined from the dye and salt tracer tests. The velocity-area method measurements were used to construct the base flow (steady state) profile for Rio Salado, with exception of Stations 1 and 3 that were estimated from values reported by CFE. The location of flow contributions from first order streams is also plotted. Most of the discharge of Rio Salado on the measured reach (stream kilometer 0-10) was contributed prior to stream kilometer 4. Generally, all of the observed flow can be accounted for by the known first order springs and streams (Figure A-9). There appears to be a groundwater component (gaining stream) past stream kilometer 5 (RC-8 and Station 18).
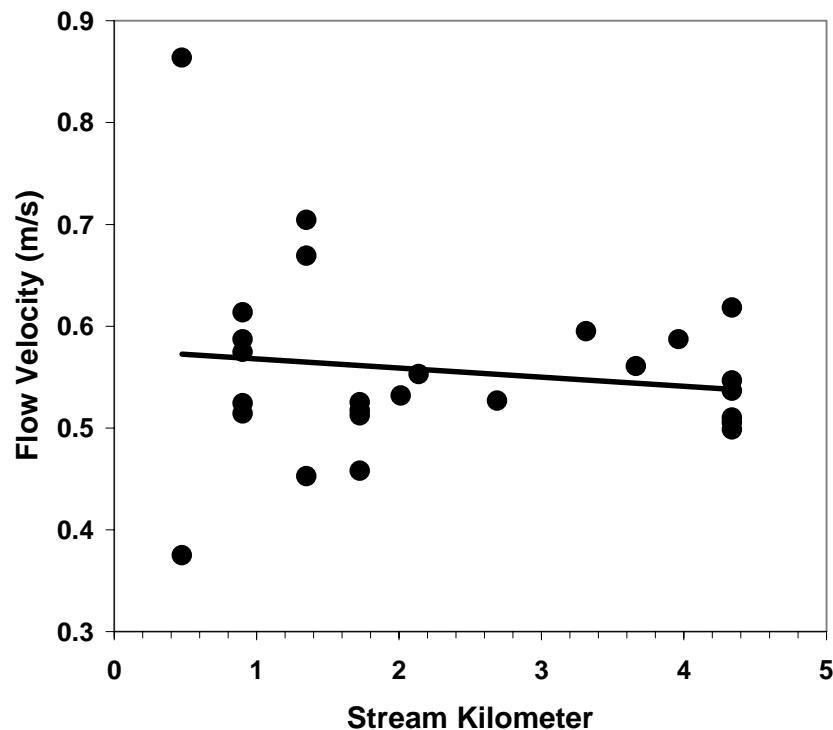
Figure A-8
Rio Salado Flow Velocities Determined from Tracer Tests
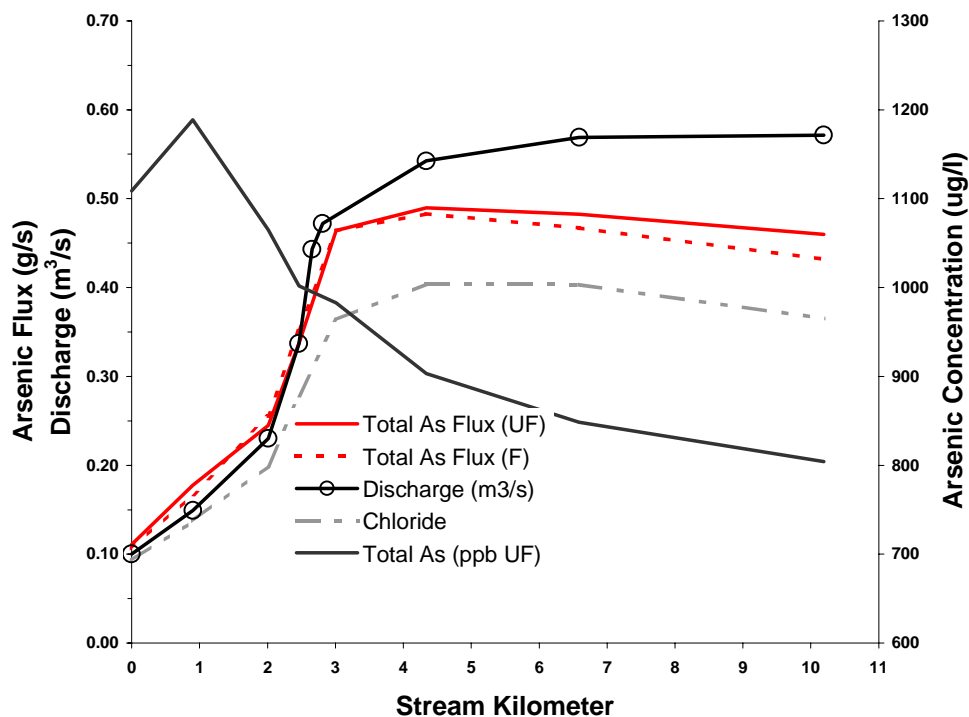
Figure A-9
Rio Salado Discharge and Chemical Flux

The possible range of velocities decreases as the parcel of water moves downstream. This occurs because over short distances small variations in measured travel time have a large effect on calculated velocity. A best-fit line tends to indicate that the velocity tends to decrease downstream as do the point measurements in Table A-3. The maximum and minimum average travel times were recorded by the dye first arrival and tail time (0.607-0.484 km/h). Conductivity was not as reliable an indicator of early and late travel times because of detection difficulties. However, there is good agreement between dye average peak velocity and salt average peak velocity with the dye faster by 1.8%, indicating that the dye tended to behave in an ideal manner. Summary statistics and a frequency histogram of the flow provide a modal velocity of 0.55 km/h and standard deviation of 0.092 km/h. This is quite close to the dye peak velocity. The distribution is somewhat skewed towards lower values. For kinetics calculations, the modal flow velocity value of 0.55 km/h is used.

Flux

Flux is the product of a concentration and a rate. In the case of Rio Salado it is the product of the dissolved constituents and the streamflow discharge. Other than a few perturbations by input from first-order streams and groundwater contributions, the dissolved phase concentration of compounds decreases rather uneventfully downstream. Figure A-9 depicts the total arsenic concentration profile for the main channel of Rio Salado. The stream discharge curve shows gaining discharge while the arsenic flux decreases. The total arsenic curve mimics that for chloride. Given the previously presented evidence for dilution, total arsenic concentration decreases in Rio Salado due to dilution rather than chemisorption. Other than dilution, the flux of

total arsenic in Rio Salado at baseflow is conservative, as are most other compounds. This would not be discernable from concentration alone. The divergence of the filtered from the unfiltered results may indicate some colloidal sorption of arsenic.

Arsenic Speciation and Kinetics

The arsenic speciation in Rio Salado is dominantly inorganic as As^{5+}, with As^{3+} present at Station 2, 3 and downstream of the Powerline spring. Organic arsenic as MMAA is present at 1-5% in for the majority of sample stations. A MMAA high of 13% was found in the early morning at Station 3. DMAA data is suspect. Although organic arsenic kinetics were not discernible in the data, the As^{3+} point discharge into Rio Salado at Powerline spring was ideal for observing the disappearance kinetics of As^{3+}. Based on the As^{3+} concentrations in the main channel below Powerline, and a flow velocity of 0.55 m/s a $t_{1/2}$ of 0.13 hours was calculated. Wilkie and Hering found a $t_{1/2}$ of 0.3 hours for As^{3+} in Hot Creek, CA that was attributed to biologic reductive pathways [103].

Rio Salado Plants

Arsenic in Plants

Rio Salado plants were collected and analyzed for arsenic to:

- Look for trends in plant concentrations that could provide insight into arsenic pathways at Rio Salado.

- Provide data to estimate what arsenic levels would be expected in organic stream detritus.

- Identify plant types that have elevated arsenic levels and might be candidates for phytoremediation.

The arsenic analysis reveals a few trends. Other than Station 1, with anomalously high values, no distinct trend in arsenic content was observed. Figure A-9 depicts arsenic concentrations in plants for all sample stations. There is good correlation between 10 sediment values and arsenic in plants, a relationship not unexpected. A proportionality to water concentrations is much more tenuous, but there is a trend. The mean concentration of arsenic (censoring values from Station 1) in most of the plants lies below 3 (mg/kg) dry weight with SEDGE 1 slightly higher at 4.5 mg/kg and CRESS and TALL GRASS 2 substantially higher at 8.2 and 8.9 mg/kg, respectively. This is graphically depicted in Figure A-11.
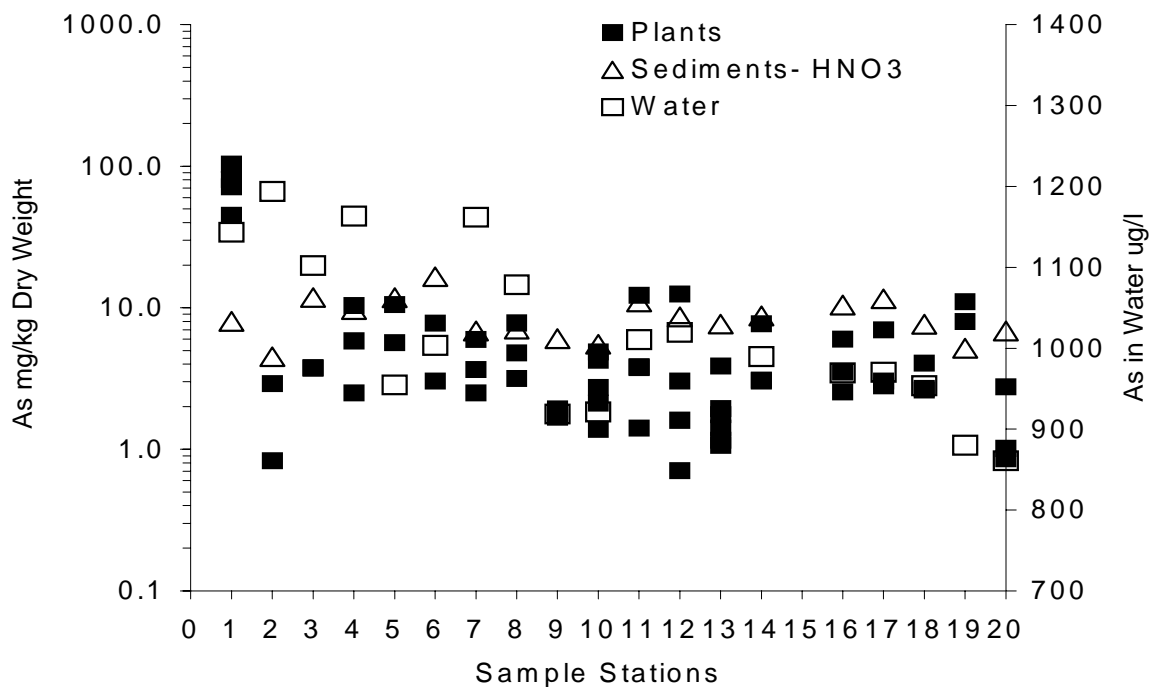
Figure A-10
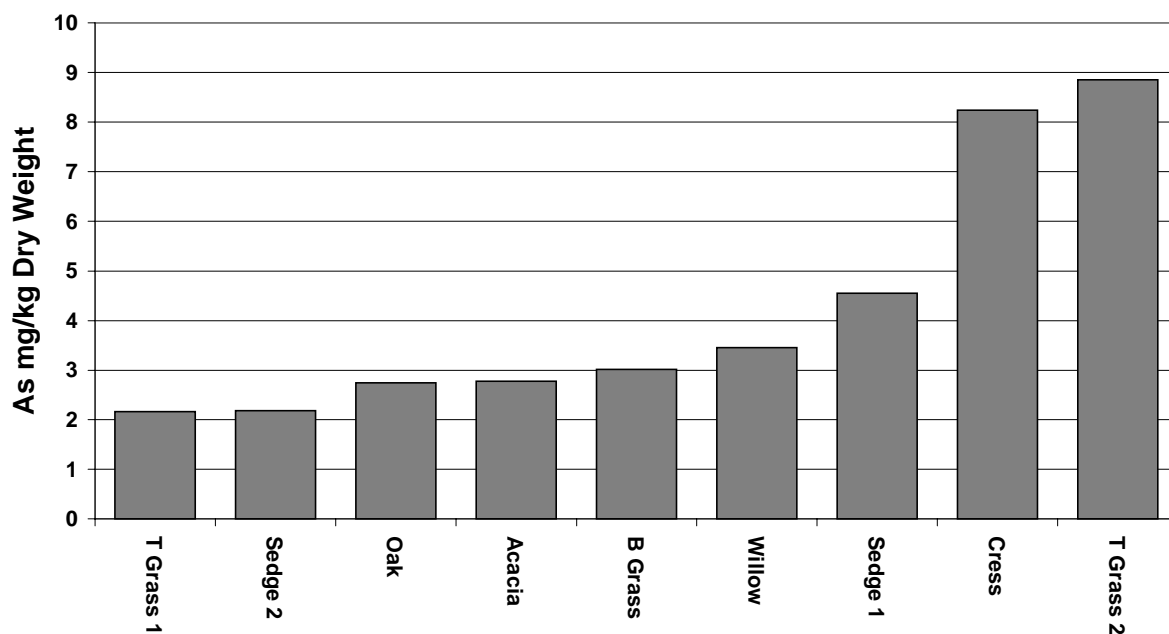**Extraction of Arsenic from Plants, Sediments, and Water**

Figure A-11
Arsenic in Plants by Field Name

Plant Descriptions and Taxonomy

Plants have been identified by John D. Vitti as well as the partial specimens allowed. Eight specimens are identified here. Seven are identified to the genus level; four of these seven include probable species level identification and two include possible species level identification. The remaining three of the ten specimens are identified to the family level only; two include probable genus level identification. Generally accepted common names are also listed [171,172,173]. The identification nomenclature follows current botanical convention:

- Family level identification = Family.

- Genus level identification = *Genus* Authority. [Family].

- Species level identification = *Genus species* Authority. [Family].

Citations in the broader literature are given as found, or either without the Authority or without the Family listed (i.e., *Genus* [Family] or *Genus* Authority).

LOCAL OAK. A species of Oak, *Quercus* L. [Fagaceae]. Hardwood trees or shrubs of the temperate and tropical Northern Hemisphere. Worldwide: 450-500 species. Approximately 250 species occur in the Americas with Mexico as the center of distribution. Probably Netleaf Oak, *Quercus rugosa* Nee. [Fagaceae], the distinguishing characteristic being elaborately netted leaf venation.

TALL GRASS 1. A species of Fingergrass or Windmill Grass, *Chloris* Swartz. [Graminae]. Perennial or annual grasses of tropical and subtropical regions. Worldwide: 60-70 species. At least 10 species common in Mexico. Possibly *Chloris virgata* Sw. [Graminae], the distinguishing characteristic being racemes densely floriferous from tip to base.

BERMUDA GRASS. A species of *Hilaria* HBK. [Graminae]. Perennial grasses mostly with rhizomes or stolons. The genus consists of nine species, mainly distributed in southern North America. Possibly *Hilaria ciliata* (Scribn.) Nash. [Graminae], the distinguishing characteristic being bearded nodes.

TALL GRASS 2. A member of the Rush Family, Juncaceae. Perennial or annual grass-like herbs of temperate regions. Worldwide: 8 or 9 genera and 300-350 species. Two genera occur in the northern hemisphere: *Juncus* and *Luzula* accounting for approximately 300 species. Distinguished by culms filled with sponge-like pith. Probably a species of *Juncus* L. [Juncaceae].

CRESS. A species of False Loosestrife, *Ludwigia*, [Onagraceae]. Perennial herbs, mostly, of moist, warm regions. Worldwide: 70-80 species. Many common to Mexico. Probably Water Purslane, *Ludwigia palustris* (L.) Elliott. [Onagraceae], the distinguishing characteristics being elliptic-ovate leaves and rooting at nodes.

ACACIA. A species of *Lysiloma* Benth. [Leguminosae]. Shrubs or trees of tropical and subtropical regions. The genus consists of 30-35 species of tropical America. Probably Watson Borderpod Acacia, *Lysiloma watsonii* J.N.Rose. [Fabaceae], the distinguishing characteristics being densely pubescent leaves and twigs and long, flat, cordlike-margined fruit.

WILLOW. A species of *Pluchea* Cass.[Compositae]. Malodorous, willowlike herbs or shrubs of warm or tropical regions. Worldwide: 40 species, mostly New World. Probably *Pluchea salicifolia* (Mill.) Blake. [Compositae], the distinguishing characteristic being the dentate, conspicuously decurrent leaves terminating as foliaceous stem wings.

SEDGE 1. A member of the Sedge Family, Cyperaceae. Mostly perennial grass-like herbs widely dispersed around the globe. Worldwide: 75-80 genera and about 3200 species. Distinguished by solid, three-sided culms.

SEDGE 2. A member of the Rush Family, Juncaceae. Perennial or annual grass-like herbs with small regular persistent flowers. Worldwide: 8 or 9 genera and 300-350 species of temperate regions. Two genera occur in the northern hemisphere: *Juncus* and *Luzula* accounting for approximately 300 species. Distinguished by culms filled with sponge-like pith. Probably a species of *Juncus* L. [Juncaceae].

B
APPENDIX B – FLORIDA FIELD INVESTIGATION

Water and Sediment Sampling

A review of data on arsenic-contaminated sites was conducted with the assistance of Southern Company Services. The objective of the review was to identify sites that are suitable for investigation of the transferability of the model used at Rio Salado. The mechanistic surface complexation model used for Rio Salado was successful. However, it was unknown if it could be used at other sites by collecting only the data necessary to constrain the model. This is in contrast to Rio Salado where the conceptual model was developed through detailed examination of the site. Two sites were identified that had characteristics that made them suitable for evaluation of the transferability of the model. Analysis of the sediments and water allow a determination of the accuracy of the surface complexation approach in predicting the sorbed arsenic concentration on the sediments. Tyndall Air Force Base (AFB) and Fort Walton, Florida have shallow groundwater plumes that contain elevated levels of arsenic. Ditches are groundwater discharge points at Tyndall AFB and Fort Walton. Where the arsenic plume crosses a ditch contaminated surface water is found. Contaminated ditches represent ideal sampling points to collect sediment-water pairs for the purpose of this effort because:

- It is relatively easy to collect high quality samples using only hand equipment;

- The depth of penetrations can be minimized; and,

- Water samples can be collected without use of wells or penetrometers.

At Tyndall AFB all paved roads have adjacent drainage swales. Ditch Reach 4 crosses groundwater known to be arsenic-contaminated. Arsenic has been detected in surface water in the swale. This swale was sampled at three locations. The original intent was to be near both endpoints and the midpoint of the ditch. Field relocation of two sample locations was necessary to meet sampling objectives. At each sample location, a sediment-water pair was collected.

The Fort Walton plume is proximal to a ditch on the east and south sides. The open ditch was sampled near the headwall east of Jet Stadium and in the open section southwest of Robinwood Drive SW. It was planned to take a sample west of Bass Avenue, but this location was not suitable for sample collection in support of model testing. Sample locations in the open reaches were set based on field conditions and the discretion of the sampling team. The sample locations for Tyndall AFB and Fort Walton Beach are described in Table B-1.

Table B-1
Florida Sampling Station Locations

Station	Description	Use
FW-1	Fort Walton Beach downstream sample. Robinwood Drive SW location. Open drainage channel with natural bottom. Sample location at the end of point bar ~5 m from headwall on downstream side of Robinwood Drive. Flow rate ~0.1 m^3/s. Sediments are medium to fine sands with orange staining.	Sediment-water pair
FW-2	Fort Walton Beach upstream sample. Jet Stadium sample location. Sample location from middle of submerged section ~10 m north of Hollywood Blvd. Sediments are medium to fine sands with orange staining.	Sediment-water pair
T-1	Tyndall AFB 'upstream' sample. 10 m NW of Reach 4 upstream headwall. Sample collected using wide diameter shallow piezometer.	Sediment-water pair
T-2	Tyndall AFB 'center' sample. 15 m NW of Reach 4 upstream headwall. Sample collected using wide diameter shallow piezometer.	Sediment-water pair
T-3	Tyndall AFB 'downstream' sample. 20 m NW of Reach 4 upstream headwall. Sample collected using wide diameter shallow piezometer.	Sediment-water pair

Other than field measurements, separations, and the X-ray fluorescence (XRF) analysis conducted at the University of New Mexico, all analytical procedures were conducted at New Mexico Institute of Mining and Technology (NMIMT) and New Mexico Bureau of Mines and Mineral Resources (NMBMMR) facilities. The principal instruments used for water and sediment extract analyses are an IL Video Model 12 flame atomic adsorption spectrophotometer (FAA), Varian 600 Zeeman graphite furnace atomic adsorption spectrophotometer (GFAA), and Dionex 4000 ion chromatograph (IC). The determinations and analyses that were performed for this effort are listed in Table B-2. Tabular analytical data for all analyses described here are found in a following section of this appendix.

Table B-2
Data Collection

Parameter	PQL[1]	Method	Comments
Field Measurements			
pH	± 0.02 units	Field Probes	Calibrated daily and checked frequently through the day.
Conductivity	± 10 µS/cm	Field Probes	Calibrated daily against temperature corrected KCl standard.
Temperature	± 1°C	Field Probes	Measured with calibrated probes and mercury thermometer.
Eh	± 10 mV	Field Probes	Platinum electrode values corrected for Ag/AgCl reference electrode (add 200 mV to meter reading).
Alkalinity	5 mg/L as CaCO$_3$	Titration	Field titrated alkalinity at pH 8.3 and 4.5 endpoints. Performed in the field daily.
Metals			
Aluminum	0.5 mg/L	FAA	
Antimony	0.5 µg/L	GFAA	
Arsenic	0.001 mg/L	GFAA	
Barium	0.003 mg/L	GFAA	
Boron	0.5 mg/L	GFAA	Boron not detected
Cadmium	0.01 µg/L	GFAA	
Calcium	0.1 mg/L	FAA	
Chromium	0.4 µg/L	GFAA	
Cobalt	0.3 µg/L	GFAA	
Copper	0.8 µg/L	GFAA	
Iron	0.2 µg/L	GFAA	
Lithium	0.05 mg/L	GFAA	Lithium not detected
Lead	0.4 µg/L	GFAA	
Magnesium	0.05 mg/L	FAA	
Manganese	0.4 µg/L	GFAA	
Molybdenum	1.5 µg/L	GFAA	
Nickel	0.2 µg/L	GFAA	
Potassium	0.1 mg/L	FAA	Selenium not detected.
Selenium	0.9 µg/L	GFAA	
Silica	15 µg/L	GFAA	
Silver	0.02 µg/L	GFAA	
Sodium	0.2 mg/L	FAA	
Strontium	0.1 µg/L	GFAA	
Vanadium	2.4 µg/L	GFAA	
Zinc	0.2 µg/L	GFAA	

Table B-2
Data Collection (Continued)

Parameter	PQL[1]	Method	Comments
Anions			
Total Bromine	1 mg/L	IC	Bromine not detected
Chloride	1 mg/L	IC	
Fluoride	0.2 mg/L	IC	
Nitrate	0.1 mg/L	IC	
Phosphate	0.025 mg/L	Colorometric	
Sulfate	0.1 mg/L	IC	
Sediment Determinations			
Sediment preparation was highly variable and dependent on the analytical method used.	Sequential Extraction (Tessier Method) for Fe, Mn, and Al concentrations Strong acid (USEPA SW-846 Method 3051) digestion for Fe, Mn, and Al concentrations Hydroxylamine hydrochloride extraction for Fe, Mn, and Al concentrations (Chao reagent) Trace elements by XRF Total organic carbon by loss on ignition		

[1] Practical Quantification Limit
Note: mg/L = parts per million (ppm) and μg/L = parts per billion (ppb)

Sampling Method

Tyndall AFB

A reconnaissance of Tyndall AFB was not conducted before sampling. Photographs and drawings of the site were examined for planning. It was apparent that the ditches contain a shallow layer of organic muck. This was not the material desirable to sample for the purpose of validation. In order to collect a representative sediment-water pair the muck layer was removed and a temporary 6" PVC casing with screened perforations installed through the layer to the cleaner sands below. Casing installation was started the morning of January 7, 2000 after obtaining the necessary permit from the Base Engineer's office. Casings were advanced using a bucket hand-auger to remove sediments through the casing while driving with hammer taps from the top. This was continued until the casing was advanced into the sediments 0.3-0.5 meters. The operation was repeated until the casing was installed in the originally planned configuration of one casing near each headwall of Reach 4 with one casing located approximately in the center. We created a caisson that would allow upward groundwater flow from the bottom and discharge through the screened perforations driven by the natural hydraulic gradient. The caisson sequested

1-2 liters of water from the muck. The intent was to be able to collect a water sample of a liter or more in as representative a manner as practical. The water should have very recently been in equilibrium with the sediments. Following collection of the water sample, a disturbed sample of the sediment formerly in equilibrium with the water was collected.

Inspection several hours after installation revealed that the center and downstream casings were not installed in locations with groundwater up flow. The field decision was made to relocate those casings closer to the upstream headwall where up flow conditions were observed. Relocation was accomplished on the morning of January 8, 2000. The casings were moved to straddle location T-2 that had indicated good hydraulic connection. T-2 was purged several times while T-1 and T-3 were installed. Following installation of T-1 and T-3, these casings were purged of 10-20 liters of water by frequent removal of a liter or two of water over the course of a few hours. Sampling was initiated with T-2 with all sampling finished the same day. Water samples were collected by evacuating the caisson, collecting field parameters and collecting samples after the caisson has refilled, filtering one 500 ml sample (metals), and two 500 ml unfiltered samples (metals and anions). The filtered and unfiltered aliquots were subsampled and the arsenic in the subsamples speciated in the field using ion exchange chromatography. Separation was conducted using the modified Grabinski method described in Appendix A and the modified Ficklin [87] method described by Miller et al. [132]. Disturbed sediment samples were collected from the sediments at the base of the in-place casing using a hand auger immediately following collection of water samples. All sample containers and preservation (other than arsenic speciation) were according to USEPA SW-846 protocol.

Fort Walton Beach

A reconnaissance of the Fort Walton drainage was not conducted before sampling. Photographs and drawings of the site were examined to plan the sampling. Fort Walton site sediment-water pairs were collected from a drainage ditch that bounds the plume on the southern and eastern sides a distance of ~300 m from the application area of the herbicide. The drainage is typical of an urbanized small stream, with steeply incised banks and a narrow riparian boundary between the channel and built up areas. Much of the stream channel in the plume area is routed through buried drains. The sampled sections were open channels. The stream bottom was composed of loose sediments with submerged point bars and other fluvial structures. The channel was surprisingly free of refuse given the location and setting. Water depth varied from 0-50 cm with most of the water ~20 cm deep. Sediment water pairs were collected from the upstream faces of submerged point bars in the drainage at two locations, FW-1 and FW-2. Water and sediment samples were collected on January 9, 2000 in the manner described in Appendix A for Rio Salado sediment-water pairs. Sample preservation and analysis was identical to that used at Tyndall AFB. Sampling was completed January 9, 2000.

FW-1 was located farthest downstream of the substation. The sample was taken on the downstream side of the culvert that crosses under Robinwood Drive SW. The drainage is about 10 meters wide at this point. Approximately half the width of the drainage was flowing water at the time of sampling. A large point bar, located just downstream of the headwall was sampled on its submerged upstream face.

FW-2 was located adjacent to Jet Stadium (a city recreational area) ~300 m due east of the substation. The drainage is about 5 meters wide at this location. The channel is deeply incised with the stream water level approximately three meters below ground surface. A small point bar with a broad upstream face was selected for sampling.

Field Parameters

Field parameters of pH, specific conductivity, temperature, and oxidation-reduction potential (ORP) were measured using calibrated probes. Field measurements, with exception of alkalinity, were made within several minutes of sample collection. All meters were calibrated and stored according to the manufacture's instructions and cleaned between uses with a Type I water rinse. Occasional physical cleaning of probe sensors was accomplished with Kim-Wipes® tissue or cotton swabs. All calibrations, equipment malfunctions, or failures to spot check were recorded in the project logbooks.

A Cole-Parmer TDSTestr 40 with a temperature compensated range of 0-1999 and 0-199 μS/cm and accuracy of $\pm$ 2% of full scale was used to monitor conductivity. A conductivity calibration standard of 1333 and 133 μS/cm was used to check instrument response several times a day. The instrument was calibrated to the same standards daily before use. An OMEGA model PHH-82 meter was used to measure pH and ORP. The glass-bulb gel-filled combination electrode pH meter has a range of 0-14 pH units, resolution of 0.01 pH units, and accuracy of $\pm$ 0.02 pH units over an automatically temperature compensated range of 0-70ºC. Fresh National Institute of Testing and Standards (NITS) traceable pre-mixed buffer solutions of 4.01, 7.00, and 10.01 pH units at 25ºC, accurate to $\pm$ 0.02 pH units (OMEGA), were used for daily calibrations. The true buffer values were calculated using the manufacturer supplied temperature dependent pH corrections appropriate for each buffer.

The ORP meter is a platinum electrode type with range of $\pm$ 1000 mV, resolution of 1 mV, and accuracy of $\pm$ 15 mV. The ORP meter is factory calibrated at time of manufacture and is not intended for user adjustment. The meter is referenced to the Ag/AgCl electrode in the pH sensor with the meter reading the differential voltage between the Pt and Ag/AgCl electrodes. This reading is corrected to Eh by addition of the standard potential for the Ag/AgCl electrode (200 mV) to the meter reading. Temperature was measured with a mercury thermometer with resolution of 0.1ºC and accuracy of $\pm$ 0.2ºC.

Alkalinity was determined by titrating a 50 ml sample with standardized 0.020 N H_2SO_4 to phenolphthalein (colorless, pH~8.3) and bromcresol green-methyl red (light pink, pH~4.5) endpoints. Titrations were conducted at the end of each field day. Carbonate (CO_3^{2-}) concentrations can be estimated as two times the phenolphthalein alkalinity. The bicarbonate (HCO_3^-) concentration estimate is the bromcresol green-methyl red alkalinity, minus two times the phenolphthalein alkalinity. The Tyndall alkalinity values are low enough that a substantial portion of the alkalinity is probably non-carbonate. The alkalinity values and other field data are presented in Table B-3.

Table B-3
Field Parameters

Station	Date	Time (CST)	Temp(°C)	Conductivity (µS/cm)	pH	ORP (mV)	CO_3^{2-} (ppm)	HCO_3^- (ppm)
T-1	1/8/00	1401	15.6	103	5.07	97	0	10.1
T-2	1/8/00	1050	15.5	128	4.85	111	0	13.0
T-3	1/8/00	1613	15.6	105	5.00	60	0	19.1
FW-1	1/9/00	938	17.3	354	6.95	284	0	118.3
FW-2	1/9/00	1224	20.5	327	6.74	264	0	127.2

Speciation of Arsenic in Water

Investigation of the speciation of arsenic in the environment requires the ability to preserve the arsenic species prior to analysis, or to separate the species before transformation takes place. Given the uncertainties in the preservation of arsenic species, field separation was selected. Separation is initiated within minutes of sample collection. Uncertainties associated with sample preservation are eliminated. In order to accomplish this, two existing ion chromatography separation methods were modified for field use [87, 124]. The first method was the four species method previously used at Rio Salado for As^{3+}, As^{5+}, MMAA, and DMAA. The second method is designed primarily for the separation of As^{3+} and As^{5+} and has been shown to yield false positives for As^{3+} when MMAA and/or DMAA are present.

As presented in Appendix A, the four species arsenic separation method exhibited some problems with DMAA, providing false positives. This was rectified before employing the method in Florida. In addition, a two species method modified from that published by Fickin [87, 132] was used in parallel with the four species method.

Sediment Extractions

Sediment extractions on the Florida samples repeated the selective extractions and microwave assisted HNO_3 digestion used on the Rio Salado samples by Welch [108]. Manganese was not evaluated in the Florida extractions. Manganese oxides were not included in the Rio Salado model as sorbing phases and therefore it was not necessary to analyze the Florida extracts for comparison purposes. An additional extraction method often used by soil scientists for evaluation of iron hydroxides and oxides, citrate-bicarbonate-dithionate, was also employed.

Selective Extraction

A combination of partial extraction techniques developed by Tessier et al. [122] and Chao and Zhou [123] was performed on the sediments to determine relative proportions of exchangeable arsenic (water soluble and affected by adsorption-desorption processes), arsenic associated with

carbonates, amorphous iron and manganese oxides, and organic matter. The procedure used is as follows: about one gram of sediment, coned and quartered from air dried field samples, is agitated in 8 ml of 1 M NaOAc adjusted to pH 8.2 for 1 h to remove exchangeable arsenic. Next, the residue from the exchangeable extraction is agitated in 8 ml of 1 M NaOAc adjusted to pH 5 for 4 hours to remove arsenic associated with carbonates. The resulting residue is then digested in 20 ml of 0.25 M NH_2OH-HCl in 0.25 M HCl heated to 50°C for 30 minutes to extract arsenic associated with amorphous iron and manganese oxides. Extraction of arsenic bound to organic matter and crystalline oxides is achieved by adding the residue from the iron-manganese oxide digestion to 3 ml of 0.02 M HNO_3 and 5 ml of 30% H_2O_2 adjusted to pH 2 with HNO_3. This mixture is heated to 85°C for 2 h after which an additional 3 ml aliquot of 30% H_2O_2 is added with continued heating for an additional 3 h. The use of 0.25 M NH_2OH-HCl (hydroxylamine hydrochloride) in 0.25 M HCl, described by Chao and Zhou [123], was used instead of the 0.04 M NH_2OH-HCl in 25% v/v HOAc suggested by Tessier et al. [122] because of its greater selectivity for amorphous Fe and Mn oxides and reduced matrix effects.

All extractions were conducted in plastic centrifuge tubes to avoid loss of sample and cross contamination. Between each successive extraction, samples were centrifuged at 10,000 rpm for 30 minutes and the supernatant pipetted off for analysis. Afterwards, 8-12 ml of Type I water was added and the residue again centrifuged for 30 minutes. The second supernatant was removed and discarded before addition of the next extracting reagent.

HNO_3 Digestions

Nitric acid extractions were conducted on whole sediment samples. About 1 gram of sediment was added to 10 ml of 8 M HNO_3, (1:1 HNO_3 and distilled water) and microwave-heated under pressure in sealed Teflon containers. This is equivalent to USEPA SW-846 Method 3051. This mixture was heated 12 minutes at 50 psi and followed by 30 minutes at 100 psi, about 180°C. After cooling, extracts were filtered (0.45 μm) and diluted for analysis.

The HNO_3 procedure dissolves many of the secondary minerals and organic matter, but not residual minerals and glasses. It also provides an estimate of the "total" acid leachable arsenic in the sediments, and represents arsenic that could be remobilized with changes in environmental conditions such as pH or Eh. USEPA indicates that the analysis provides a measure of the total amount of environmentally available metals.

Citrate-Bicarbonate-Dithionate Extractions

The citrate-bicarbonate-dithionate (CBD) extraction method was used only on the Florida samples. The CBD method [134] is designed to remove amorphous coatings and crystals of iron oxide from soil. With time and testing, it is now considered appropriate for this use and determination of extractable aluminum, silica and manganese. The CBD extraction is not very effective on highly crystalline oxides of aluminum, silica and manganese. The extraction is conducted on approximately 1.0 g of air dried sediment. Sediments are then combined with 40 ml of 0.3 M sodium citrate and 5 ml of 1 M $NaHCO_3$ solution in a 100 ml centrifuge tube. The contents are mixed by shaking and the tube placed in a 75 to 80°C water bath. The sediments are stirred with a glass rod until they reach 75 to 80°C. At that point, about 1 g of $Na_2S_2O_4$

(dithionate) powder is added, the solution stirred thoroughly for 1 minute and intermittently for 5 additional minutes. Then an additional 1 g portion of $Na_2S_2O_4$ is added and the digestion continued for 10 more minutes, stirring occasionally. The use of various flocculating agents to the extract to assist in separating the supernatant from the residue is often suggested for the CBD method. Rather than using that method the sample was centrifuged at 10,000 rpm for 15 minutes and the supernatant decanted for analysis.

Speciation of Arsenic in Sediments

The phosphoric acid (H_3PO_4) extraction and speciation method used on the Rio Salado samples was repeated using Florida samples. The results were very poor. Very little arsenic was recovered from these extractions. Spikes were not recovered. After several attempts, exhibiting similar results, the effort to speciate the arsenic on the Florida sediments by phosphate extraction were abandoned. Welch had difficulty with the method on the Rio Salado samples, but satisfactory results were obtained. A laboratory artifact is suspected rather than an issue with the method's utility. The source of the difficulty with the Florida sediments was not investigated.

Sediment Properties

Sediment Petrology and Mineralogy

The Florida sediments are a relatively simple system from a mineralogical perspective. At both sites the dominant (>99%) mineral present is quartz. Sediments are dominantly sand sized. Non-quartz grains are composed of shell fragments, urban debris, residual minerals, organic fragments, and unidentifiable material. These non-sand components comprise 1% or less of the total sediment volume. The following classification is used: 1.0-2.0 mm (very coarse sand), 0.5-1.0 mm (coarse sand), 0.25-0.5 mm (medium sand), 0.125-0.25 mm (fine sand), 0.0625-0.125 mm (very fine sand) and <0.0625 mm (silt-clay).

At Fort Walton Beach the sediments are very coarse to very fine quartz sand with occasional grains to 3 mm, very poorly sorted, with subangular to subrounded grains. FW-2 has a distinct orange staining on the grain surface absent at FW-1. Tyndall AFB Reach 4 sediments are fine to medium quartz sand very poorly sorted, with subangular to subrounded grains. The sediments have a gray cast that may be related to the overlying muck layer.

Determination of Total Organic Carbon (TOC)

Percent TOC was determined by loss-on-ignition. About 10 g of un-sieved sediments were oven dried at 105ºC for 3 to 4 h and weighed, then placed in a muffle furnace and heated at 430ºC for 24 h. After cooling, sediments were re-weighed to determine the amount lost-on-ignition, representing TOC. Contribution to the sediment weight loss by structural water expelled from clays is insignificant due to the fact that clays were present in non-detectable amounts. Also, carbonates do not to affect the loss-on-ignition value at temperatures of 430ºC [126].

X-Ray Fluorescence

Values of total metals were determined by X-ray fluorescence (XRF) on the instrument at the University of New Mexico geology laboratory. Ground whole sediments were used to make pressed powder pellets that were analyzed using standard procedures. This instrument does not have the required sensitivity for arsenic. Total arsenic was determined by reflux digestion with perchloric-nitric-hydrofluoric acids.

Tabular Data

Table B-4
Arsenic Concentration in Water (ppb)

Station	Total Unfiltered	Total Filtered	As III by Two Species Method	As V by Two Species Method	As III by Four Species Method	As V by Four Species Method	MMAA by Four Species Method	DMAA by Four Species Method
FW-1	10.7	9.5	4.6	5.2	6.3	7.5	0.0	0.0
FW-2	10.2	9.7	4.0	4.6	5.0	7.5	0.0	0.0
T-1	210.7	189.9	123.2	19.4	137.5	24.4	4.5	8.1
T-2	524.2	474.7	214.0	160.0	207.5	150.0	43.5	33.0
T-3	107.2	71.1	42.0	6.2	34.4	15.0	4.5	8.7

Table B-5
Arsenic Species as Percentage of Total Filtered Arsenic Concentration in Water and Method Recovery as Compared to the Total (ppb)

Station	As III by Two Species Method	As V by Two Species Method	Two Species Method % Recovery	As III by Four Species Method	As V by Four Species Method	MMAA by Four Species Method	DMAA by Four Species Method	Four Species Method % Recovery
FW-1	48%	55%	103%	66%	66%	0%	0%	131%
FW-2	41%	47%	89%	52%	52%	0%	0%	103%
T-1	65%	10%	75%	72%	72%	2%	4%	151%
T-2	45%	34%	79%	44%	44%	9%	7%	104%
T-3	59%	9%	68%	48%	48%	6%	12%	115%
Average FW	45%	51%	96%	59%	59%	0%	0%	117%
Average Tyndall	50%	31%	81%	50%	50%	5%	6%	112%

Table B-6
Unfiltered Water Sample Analytical Results

Station	Ag (ppb)	Al (ppb)	Ba (ppb)	Ca	Cd (ppb)	Co (ppb)	Cr (ppb)	Cu (ppb)	Fe (ppb)	K	Mg	Mn (ppb)	Mo (ppb)	Na	Ni (ppb)	Pb (ppb)	Sb (ppb)	Si (ppb)	Sr (ppb)	V (ppb)	Zn (ppb)
FW-1	0.06	1.27	82	34.6	0.02	0.6	0.8	11.5	68.0	9.3	1.98	6.7	3.9	21	2	ND	7.9	799	311	2.8	39
FW-2	0.04	1.43	125	34	0.04	0.1	0.7	6.6	27.0	10	1.50	5.2	2.6	18	1.9	ND	3.6	2272	420	ND	30
T-1	0.13	3.66	ND	7.5	0.23	0.4	0.5	8.9	11.1	1.8	3.03	2.1	ND	6	1.5	1.1	0.9	1605	11	5.7	13
T-2	0.22	1.98	ND	8.5	0.19	0.8	1.2	12.6	26.0	1	1.74	2.0	ND	10	3	3.7	2.2	3299	20	ND	26
T-3	0.24	2.32	ND	7.8	0.03	0.2	1	5.3	36.0	2.1	1.26	3.4	ND	4	4	2.5	2.7	2197	72	ND	20

Table B-7
Filtered Water Sample Analytical Results

Station	Ag (ppb)	Al	Ba (ppb)	Ca	Cd (ppb)	Co (ppb)	Cr (ppb)	Cu (ppb)	Fe (ppb)	K	Mg	Mn (ppb)	Mo (ppb)	Na	Ni (ppb)	Pb (ppb)	Sb (ppb)	Si (ppb)	Sr (ppb)	V (ppb)	Zn (ppb)
FW-1	ND	1.95	68	34	0.02	0	0.7	1.9	23.0	8	1.99	12.0	2.7	21	0.7	ND	6.9	801	304	ND	124
FW-2	ND	1.98	110	34	0.02	0	0.9	3.3	23.0	8.1	1.52	9.6	1.6	18	1.2	ND	6.8	1849	372	2.5	93
T-1	ND	2.44	ND	7.3	0.04	0.2	0.5	3.7	2.1	0.5	2.40	2.3	ND	6	0.5	0.7	3	646	17	ND	12
T-2	ND	2.55	ND	7.9	ND	0.2	0.9	7.4	21.0	1.2	1.71	15.7	ND	13	0.4	2.7	ND	1542	17	ND	30
T-3	ND	2.57	ND	4.1	ND	0.3	ND	4.5	1.0	2.1	0.81	2.0	ND	6	0	1.1	ND	1001	44	ND	20

Table B-8
Anions in Water

Station	Cl ppm	SO$_4$ ppm	F ppm	NO$_3$ ppm	PO$_4$ ppm
T-1	19.9	43.8	0.28	0.95	100
T-2	16.9	13.5	0.26	0.81	50
T-3	8.6	13.4	0	0.44	100
FW-1	14.8	5.1	0	0.92	225
FW-2	12.4	4.5	0	1.39	350

Table B-9
Concentration of As, Fe, Al, Si by Sediment Extraction Method

HNO$_3$	As (mg/kg)	Fe (mg/kg)	Al (mg/kg)	Si (mg/kg)
FW-1	2.718	642.9	1338.6	ND[1]
FW-2	3.712	1240.1	3716.3	ND[1]
T-1	0.431	18.9	212.1	ND[1]
T-2	0.637	13.1	106.3	ND[1]
T-3	3.410	14.8	142.1	ND[1]
T-1 Dup	0.689	23.8	241.2	ND[1]
CBD	**As (mg/kg)**	**Fe (mg/kg)**	**Al (mg/kg)**	**Si (mg/kg)**
FW-1	0.569	32.4	342.1	570.7
FW-2	0.421	96.3	570.5	623.8
T-1	0.936	2.4	680.3	777.9
T-2	0.438	5.2	235.2	521.2
T-3	0.492	2.9	260.4	600.6
T-1 Dup	0.747	1.5	546.9	703.1
Tessier Extractions				
Exchangeable NaOAc pH 8.3	**As (mg/kg)**	**Fe (mg/kg)**	**Al (mg/kg)**	**Si (mg/kg)**
FW-1	0.364	0.8	13.2	73.1
FW-2	0.306	0.8	15.1	91.9
T-1	0.188	0.7	17.8	91.9
T-2	0.238	0.4	7.5	75.0
T-3	0.191	0.3	12.2	68.6
T-1 Dup	0.209	0.5	12.5	88.0

Table B-9
Concentration of As, Fe, Al, Si by Sediment Extraction Method (Continued)

Carbonate NaOAc pH 8.3	As (mg/kg)	Fe (mg/kg)	Al (mg/kg)	Si (mg/kg)
FW-1	0.768	21.7	39.0	52.2
FW-2	1.012	28.7	29.4	24.0
T-1	2.430	7.1	772.3	762.9
T-2	5.484	6.5	109.5	617.1
T-3	1.777	8.6	119.4	649.0
T-1 Dup	1.368	7.6	502.8	966.2
Amorphous Oxides Chao Reagent	**As (mg/kg)**	**Fe (mg/kg)**	**Al (mg/kg)**	**Si (mg/kg)**
FW-1	0.339	18.1	63.2	8.1
FW-2	0.244	28.2	104.7	52.2
T-1	0.126	1.2	129.1	0.0
T-2	0.001	2.4	19.0	0.0
T-3	0.001	2.9	16.3	0.0
T-1 Dup	0.139	2.1	93.1	0.0
Organic and Crystalline Oxides	**As (mg/kg)**	**Fe (mg/kg)**	**Al (mg/kg)**	**Si (mg/kg)**
FW-1	0.125	131.3	373.9	155.1
FW-2	0.197	180.8	632.2	209.4
T-1	0.103	9.2	79.5	115.3
T-2	0.156	3.3	9.2	2.8
T-3	2.216	2.6	15.4	3.1
T-1 Dup	0.160	24.5	91.6	107.2
Total by XRF or Digestion (mg/kg)	**As (mg/kg)**	**Fe (mg/kg)**	**Al (mg/kg)**	**Si (mg/kg)**
FW-1	14.7	552	4160	457202
FW-2	44.4	795	5796	447807
T-1	14.2	379	3880	458091
T-2	13.6	365	2758	459025
T-3	32.0	252	2945	457623
T-1Dup	10.8	355	3132	457156

[1] Strong matrix interference prevented quantification, value near 50-100 mg/kg.

Table B-10
Arsenic by Partial Extraction Methods as Compared to Arsenic by Total Digestion

Sample	HNO$_3$	CBD	Exchangeable	Carbonate	Amorphous Oxides	Organic and Crystalline Oxides	Tessier Total	Digestion
FW-1	18%	4%	2%	5%	26%	1%	34%	100%
FW-2	8%	1%	1%	2%	1%	0%	4%	100%
T-1	3%	7%	1%	17%	1%	1%	20%	100%
T-2	5%	3%	2%	40%	0%	1%	43%	100%
T-3	11%	2%	1%	6%	0%	7%	13%	100%
T-1 Dup	6%	7%	2%	13%	1%	1%	17%	100%

Table B-11
Mineral Surface Sorbing Sites Determined by HNO$_3$ Digestion

Station	Fe (mg/kg)	HFO Strong Sites/kg Water	HFO Weak Sites/kg Water	Goethite Sites/kg Water	Al (mg/kg)	Gibbsite Sites/kg Water
FW-1	643	2.6E-04	1.0E-02	7.8E-04	1339	3.0E-03
FW-2	1240	4.6E-04	1.8E-02	1.4E-03	3716	7.7E-03
T-1	19	7.2E-06	2.9E-04	2.1E-05	212	4.5E-04
T-2	13	4.8E-06	1.9E-04	1.4E-05	106	2.2E-04
T-3	15	5.3E-06	2.1E-04	1.6E-05	142	2.8E-04
T-1Dup	24	8.9E-06	3.5E-04	2.6E-05	241	5.0E-04

Table B-12
Mineral Surface Sorbing Sites Determined by Citrate-Bicarbonate-Dithionate (CBD) Digestion

Station	Fe (mg/kg)	HFO Strong Sites/kg Water	HFO Weak Sites/kg Water	Goethite Sites/kg Water	Al (mg/kg)	Gibbsite Sites/kg Water
FW-1	32	1.3E-05	5.2E-04	3.9E-05	342	7.7E-04
FW-2	96	3.6E-05	1.4E-03	1.1E-04	571	1.2E-03
T-1	2	9.2E-07	3.7E-05	2.8E-06	680	1.4E-03
T-2	5	1.9E-06	7.7E-05	5.7E-06	235	4.8E-04
T-3	3	1.0E-06	4.1E-05	3.1E-06	260	5.2E-04
T-1D	1.5	5.6E-07	2.3E-05	1.7E-06	547	1.1E-03

Table B-13
Mineral Surface Sorbing Sites Determined as the Sum of All Tessier Sequential Extraction Steps

Station	Fe (mg/kg)	HFO Strong Sites/kg Water	HFO Weak Sites/kg Water	Goethite Sites/kg Water	Al (mg/kg)	Gibbsite Sites/kg Water
FW-1	172	7.0E-05	2.8E-03	2.1E-04	489	1.1E-03
FW-2	238	8.9E-05	3.6E-03	2.6E-04	781	1.6E-03
T-1	18	6.9E-06	2.8E-04	2.1E-05	999	2.1E-03
T-2	13	4.6E-06	1.8E-04	1.4E-05	145	3.0E-04
T-3	14	5.2E-06	2.1E-04	1.5E-05	163	3.3E-04
T-1D	35	1.3E-05	5.2E-04	3.8E-05	700	1.5E-03

Table B-14
Mineral Surface Sorbing Sites Determined by the Chao Reagent Step of the Tessier Sequential Extraction

Station	Fe (mg/kg)	HFO Strong Sites/kg Water	HFO Weak Sites/kg Water	Goethite Sites/kg Water	Al (mg/kg)	Gibbsite Sites/kg Water
FW-1	18	7.3E-06	2.9E-04	2.2E-05	63.2	1.4E-04
FW-2	28	1.1E-05	4.2E-04	3.1E-05	104.7	2.2E-04
T-1	1	4.6E-07	1.8E-05	1.4E-06	129.1	2.7E-04
T-2	2	8.7E-07	3.5E-05	2.6E-06	19.0	3.9E-05
T-3	3	1.1E-06	4.2E-05	3.2E-06	16.3	3.3E-05
T-1D	2	7.8E-07	3.1E-05	2.3E-06	93.1	1.9E-04

Table B-15
Porosity, Density, and Organic Carbon Content

Station	Bulk Density (g/cc)	Porosity	Calculated Particle Density (g/cc)	Solids to Water Ratio (kg/kg)	% TOC[1]	% TOC[2]
FW-1	1.60	0.354	2.480	4.53	0.41%	0.48%
FW-2	1.58	0.380	2.550	4.16	0.54%	0.74%
T-1	1.50	0.355	2.331	4.23	0.61%	0.64%
T-2	1.53	0.376	2.452	4.08	0.25%	0.16%
T-3	1.54	0.383	2.489	4.01	0.25%	0.28%
T-1D	1.50	0.360	2.338	4.15	0.54%	0.53%

[1] Analysis by Loss on Ignition conducted at New Mexico Institute of Mining and Technology.
[2] Analysis by Loss on Ignition conducted at University of New Mexico.

Data Quality

Reagents and Standards

Trace metal grade reagents were used whenever available. Fisher Trace Metal HCl and NH_4OH were diluted as necessary. These reagents are used for column preparation and regeneration that does not require very precise molarity and they were not standardized. The maximum pH error from this simplification is less than 10% for HCl and less than 1% for NH_4OH. HCl and NH_4OH used for ion exchange chromatography eluant were standardized to pH values within ± 0.05 units of optimal. TCA for elution was made from Sigma ACS reagent solid and could be formulated by dilution to precise molar concentrations. The measured pH of the 0.006 M TCA was 2.25 ± 0.05 and the 0.2 M TCA was 1.05 ± 0.05 at 23.2°C. The pH was checked when stock solutions were made and periodically thereafter.

With the exception of MMAA, all arsenic standards were obtained from Sigma. MMAA could not be located through the normal chemical suppliers. MMAA was obtained from Dr. Dean Carter of the University of Arizona. As^{3+} standards were prepared from American Chemical Society (ACS) certified reagent grade arsenic trioxide. As^{3+} standards were prepared the day of use as a 1.000 g/L arsenic stock solution by dissolution in 100 ml of hot 1.0 M trace metal grade HCl and dilution to 1 liter with Type I (ASTM) water. Complete oxidation of As^{3+} standards to As^{5+} in two weeks was observed during this effort. Partial oxidation has been observed in less than 12 hours. Attempts were not made to preserve the As^{3+} standards. As^{5+} and DMAA standards were prepared from ACS reagent sodium arsenate and Sigma Ultra cacodylic acid as 1.000 g/L arsenic stock solutions by dissolution in 1 liter of Type I water. Since only ~50 mg of MMAA was made available to this effort a 52 ppm as arsenic stock solution was prepared by dissolving 0.0201 g of MMAA in 100 ml of Type I water.

Quality Assurance

Design of this project incorporated a data quality objectives development process early in its inception. It was felt that this data might eventually be used for risk assessment, risk management, or comment on rulemaking. Balanced with this was the necessity to limit analytical and field costs. Data quality objectives had to be set to meet these competing priorities.

A Data Quality Objectives (DQO) process was used to define the sampling and analysis program described here. The DQO process was created by the USEPA in the late 1980's for use in the Superfund program as part of a general, and ongoing, revision of their quality assurance and quality control practice, regulation, and guidance. The DQO process borrows heavily from elements of Terzhagi's observational method and other well accepted experimental design principles. USEPA's objective was to create a publicly acceptable quality framework for environmental data collection that would meet the needs of environmental compliance and risk assessment at lowest cost. The intended purpose of the DQO process is to ensure that:

- The questions to be answered through data collection and analysis are well defined;
- The data collected is of known quality;

- An acceptable level of uncertainty for answers to the questions is specified; and,

- The cost, amount, and quality of data necessary to answer questions are critically evaluated.

The DQO process enabled us to establish the following findings and objectives.

The primary objective was to obtain samples from a location other than Rio Salado to test the transferability of the modeling process to other locations. This being the case, sampling and analysis should be as comparable to that conducted at Rio Salado as is reasonably possible. Only the data necessary to support model testing should be collected. Plan review was accomplished before project implementation by Mary McLearn of EPRI.

All data collection met project-specific precision, accuracy, representativeness, completeness, and comparability criteria (PARCC parameters) or it was determined that an out-of-control event had taken place and the data used with caution if used at all. Chemical analyses should meet the precision and accuracy standards of SW-846 in order for the data to be acceptable. Generally, the reconnaissance data met these requirements. However, due to the novel and exploratory use of the data, full SW-846 QA (matrix spikes, matrix spike duplicates, and internal laboratory QA programs) was not invoked. Some methods, such as ion exchange chromatography and sediment partial extraction do not have SW-846 equivalents. All non-SW-846 analytical methods used have been peer reviewed, published in peer reviewed journals, or developed as part of this effort.

The sample locations for the Florida effort were selected based on several factors. The first was to identify sites where the limit and extent of arsenic contamination was known. Sampling of sediment-water pairs needed to be accomplished without the use of drilling equipment or expansive effort. The number of sites to be investigated was limited to two and the samples to be collected were limited to a total of six.

All sample containers were new high-density polyethylene (Nalgene or equivalent) bottles. All containers were cleaned with Alconox detergent and warm water, triple rinsed with tap water, triple rinsed with Type I water, and allowed to air dry with openings down. Following drying, caps were replaced and sample containers stored in zip-closure plastic bags for transportation to the field. Any other field sampling equipment was field cleaned immediately following use with 1.0 M Fisher Trace Metal grade HCl, and triple rinsed with Type I water. All field sampling equipment was cleaned nightly with an Alconox wash, triple rinse with Type I water, and air drying.

All water samples were containerized and preserved according to USEPA SW-846 accepted methods with exception of arsenic speciation samples. Samples remained in sample team custody throughout the sampling events and during transportation to the laboratory. Water and sediment samples were stored at 4°C ± 2°C until analysis. SW-846 mandated holding times were met. All sample locations are identified alphanumerically. Sample numbers were recorded in the project logbook. These numbers will be used to track the samples until final disposal.

Whenever possible, data was obtained from the analytical laboratory in electronic format to minimize transcription errors. A copy of the raw data was archived along with copies of logbooks and other data that would be difficult to reproduce. Spreadsheets were used for data manipulation and unit conversions. The parameter lists are broad in order to emulate the

sampling and analysis conducted at Rio Salado. Sediment data is needed to evaluate solid-water partitioning coefficients. All of the data obtained, in either raw or reduced form was used to calibrate and validate the numerical model.

Other quality assurance activities included logging of all field and lab data in bound logbooks, noting out of control events and their resolution, written preplanning of all activities, and following standard field and laboratory hygiene and safety practices. All equipment was used and maintained according to manufacturer instructions. Malfunctioning equipment was removed from service until repairs were made. Backup equipment was available for most needs.

Quality Control

The GFAA and FAA use autocalibration procedures based on standard dilution. FAA methods for the analytes of interest are routinely run at the NMBMMR laboratory and no modification of the standard methods was necessary to achieve accurate reproducible results. This was not true for ion-exchange chromatography samples that were strongly attenuated by matrix and arsenic species effects. Special procedures were implemented in order to meet PARCC parameters for these samples. The arsenic methods outlined in Appendix A were used for the Florida samples. Arsenic quantification has improved at the NMBMMR laboratory since the analysis of the Rio Salado samples. Routine quantification on natural waters is below 1ppb with reproducibility within 10-15%. Using multiple injection techniques on the GFAA detection can be lowered to 0.2 ppb in many matrices.

Detailed quantification limit studies were not performed for aqueous analytes other than arsenic. This does not preclude the standard procedure of assigning practical quantification limits (PQL's) based on two standard deviations of the blank signal achieved during analysis. This is for routine analysis without significant matrix effects and is reflected by the PQL's in Table B-1.

Quality Assessment

Samples are generally representative of the site conditions because deviations were not made from acceptable sampling practice for the media of interest. The chemical data is comparable to other data collected using SW-846 protocols. There is an exception, phosphate as PO_4. The NMBMMR IC, as normally configured, has a PQL for phosphate of 100 ppb. The corresponding detection limit is ~60 ppb. Phosphate is known to affect arsenic surface complexation. It is possible that <60 ppb of phosphate could noticeably affect arsenic surface complexation when the arsenic level is close to the phosphate level. Using the standard IC configuration phosphate was not detected in Rio Salado waters (Appendix A). Therefore, a molybdate blue colorometric method sensitive to 10 ppb and quantifiable in 25 ppb increments to 500 ppb was used to evaluate phosphate in the Florida samples.

Target:

Transmission and Distribution Soil and Water
Issues

1000547